

**Synthesis and Properties of Bridged  
Nitrogen Heterocycles**

**Thesis submitted for the degree of  
Doctor of Philosophy  
at the University of Leicester**

**by**

**Waleed Alkhuraiji  
Department of Chemistry  
University of Leicester**

**June 2007**

UMI Number: U491043

All rights reserved

INFORMATION TO ALL USERS

The quality of this reproduction is dependent upon the quality of the copy submitted.

In the unlikely event that the author did not send a complete manuscript and there are missing pages, these will be noted. Also, if material had to be removed, a note will indicate the deletion.



UMI U491043

Published by ProQuest LLC 2013. Copyright in the Dissertation held by the Author.  
Microform Edition © ProQuest LLC.

All rights reserved. This work is protected against  
unauthorized copying under Title 17, United States Code.



ProQuest LLC  
789 East Eisenhower Parkway  
P.O. Box 1346  
Ann Arbor, MI 48106-1346

**To**  
**My Parents, My Wife & My Daughters**

## Statement

The accompany thesis submitted for the degree of Ph.D. entitled 'Synthesis and Properties of Bridged Nitrogen Heterocycles' is based on work conducted by the author in the Department of Chemistry at the University of Leicester mainly during the period between October 2002 and September 2006. All the work in this thesis is original unless indicated otherwise in the text or references. None of the work has been submitted for another degree in this or any other university.

Signed..........

Date.....29/8/07.....

## **Acknowledgements**

I would like to express my gratitude to my supervisor Dr John Malpass for his guidance, encouragement, enthusiasm and advice through my stay at Leicester. Thanks to my co-supervisor Prof Paul Cullis and Dr Sandeep Handa who were always ready with helpful suggestions.

I am grateful to the following people. Dr Gerry Griffith for NMR, Dr Graham Eaton for mass spectrometry, Dr John Fawcett and Kuldip Singh for X-ray crystallography, Mick Lee for his technical expertise and Dr Mark Edgar for the high field NMR experiment conducted at Loughborough University.

I would also to thank my colleagues for their support and friendship especially Dr Anup Patel and Dr Richard White.

I would like to further acknowledge King Khalid Military Academy (National Guard) for the financial support.

Mum and Dad, sister and brothers for their love and support.

Last, but not least I dedicate this thesis to my wife (Amsha) for her love and patience and to my daughters (Norah and Sarah) to whom I express my love and best wishes.

## Abstract

### Synthesis and Properties of Bridged Nitrogen Heterocycles

By Waleed Alkhuraiji

The synthesis of derivatives of the parent 7-azabicyclo[2.2.1]heptyl system was achieved. The synthesis of the novel 1-methyl-7-azabicyclo[2.2.1]hepta-2,5-diene was accomplished. The carbonyl group at position C2 of the 7-azabicyclo[2.2.1]heptyl system was synthesized. The work was extended to include the synthesis of derivatives of the 1,4-dimethyl-7-azabicyclo[2.2.1]heptyl system. Investigation of the synthesis of epibatidine was not successful.

The work was extended to include a wide range of urethanes and amines of 7-azabicyclo[2.2.1]heptyl system where no  $^{15}\text{N}$  NMR studies had been reported. The  $^{15}\text{N}$  NMR spectra were recorded, in all cases, at natural abundance. The effect of the unsaturation and the substituted carbonyl at position C2 on the  $^{15}\text{N}$  chemical shifts was addressed.  $^{14}\text{N}$  NMR spectra were measured in some cases where the  $^{15}\text{N}$  chemical shifts were difficult to obtain.

The barriers to nitrogen inversion were determined for several 1-methyl-7-azabicyclo[2.2.1]heptyl systems. The effect of unsaturation, the influence of carbonyl substitution at position C2 and the presence of substituted 1,4-dimethyl were assessed on the nitrogen inversion barrier. Direct measurement of invertomer ratios and preferences was possible using low temperature NMR methods for some cases where the population is not 50:50. A good correlation was found between the nitrogen inversion barrier and  $^{15}\text{N}$  NMR chemical shifts. The high barrier is associated with the more downfield nitrogen NMR shift.

X-Ray crystallographic studies showed that urethanes of the bicyclic 7-azabicyclo[2.2.1]heptane are nitrogen-pyramidal. The CNC bond angles,  $\theta$  angles and  $\alpha$  angles for 7-azabicyclic urethane derivatives were measured. The CNC bond angles,  $\theta$  angles and  $\alpha$  angles for 7-azabicyclic urethane derivatives were calculated for the parent urethanes where x-ray data could not be obtained. Increased planarity at nitrogen correlated with upfield  $^{15}\text{N}$  NMR shifts. The calculated CNC bond angles correlated well with the nitrogen NMR shifts.

## Abbreviations

°	Degrees
BTMSA	Bis(trimethylsilyl)acetylene
COSY	Correlation spectroscopy
°C	Degrees Celsius
DCM	Dichloromethane
DEPT	Distortionless enhancement by polarisation transfer
DMAP	4-Dimethylaminopyridine
DMF	Dimethyl formamide
D-NMR	Dynamic nuclear magnetic resonance
EI	Electron impact
FAB	Fast atom bombardment
FT NMR	Fourier transform nuclear magnetic resonance
g	Grams
GS	Ground state
h	Hours
HCl	Hydrochloric acid
Hz	Hertz
IR	Infra-red
INDOR	Internuclear Double Resonance
J	Joule
k	Kilo
M	Molar
M <sup>+</sup>	Molecular ion
MHz	Megahertz
ml	Millilitre
mol	Moles
mol <sup>-1</sup>	Per mole
MS	Mass spectrometry
NBO	Natural bond orbital
NBS	<i>N</i> -Bromosuccinimide
NMR	Nuclear magnetic resonance
ppm	Parts per million
rt	Room temperature

TFA	Trifluoroacetic acid
THF	Tetrahydrofuran
TLC	Thin layer chromatography
TS	Transition state

## Contents

<b>Statement</b>	i
<b>Acknowledgements</b>	ii
<b>Abstract</b>	iii
<b>Abbreviations</b>	iv
<b>Chapter 1: Introduction</b>	1
1.1 Statement of Purpose	1
1.2 Inversion at nitrogen	2
1.3 Factors influencing the inversion barriers	4
1.3.1 Steric effects	4
1.3.1.a Non-bonded interactions	4
1.3.1.b Ring strain	5
1.3.1.c The bicyclic effect	6
1.3.2 Electronic effect	8
1.3.2.a Conjugation effects	8
1.3.2.b Heteroatom effects	8
1.4 The determination of inversion barriers and invertomer ratios	9
1.4.1 Inversion barriers	9
1.4.2 Invertomer ratios	11
1.4.2.a Low temperature <sup>1</sup> H NMR spectroscopy method	11
1.4.2.b Low temperature <sup>13</sup> C NMR spectroscopy method	12
1.4.2.c Quaternisation (kinetic protonation)	13
1.4.2.d X-ray crystallography	14
1.5 Azabicyclic systems having unusually high barriers to inversion at nitrogen	14
1.6 <sup>15</sup> N NMR chemical shifts of 7-azabicyclo[2.2.1]heptane, hepta-5-ene, and hepta-2,5-diene	19
<b>Chapter 2: Synthesis of 7-azabicyclo[2.2.1]heptane derivatives</b>	23
2.1 Synthesis of 7-azanorbornadiene derivatives	23
2.1.1 Synthesis of ethynyl <i>p</i> -tolyl sulfone ( <b>25</b> )	24
2.1.2 Synthesis of 7-azabicyclo[2.2.1]heptadiene derivative ( <b>23b</b> )	25
2.1.3 Synthesis of <i>N</i> -protected 7-azanorbornadiene ( <b>26b</b> )	25
2.1.4 Synthesis of <i>N</i> -methyl-7-azanorbornadiene ( <b>3a</b> )	26

2.1.5	NMR spectroscopic data for the free amine ( <b>3a</b> ) and quaternary salt ( <b>3a:HCl</b> )	26
2.1.6	Synthesis of the secondary amine 7-azanorbornadiene ( <b>3b</b> )	28
2.1.7	<sup>1</sup> H NMR spectroscopic data for the free amine ( <b>3b</b> ) and quaternary salt ( <b>3b:HCl</b> )	31
2.2	Routes to <i>N</i> -methyl-7-azanorbornene ( <b>2a</b> )	32
2.2.1	Synthesis of 7-azabicyclo[2.2.1]hept-2-ene sulfone ( <b>36</b> )	32
2.2.2	Synthesis of 7-azabicyclo[2.2.1]hept-2-ene sulfone ( <b>37</b> )	33
2.2.3	Synthesis of 7-azanorbornene ( <b>38</b> )	33
2.2.4	Synthesis of <i>N</i> -methyl-7-azanorbornene ( <b>2a</b> )	34
2.2.5	NMR spectroscopic data for the free amine ( <b>2a</b> ) and quaternary salt ( <b>2a:HCl</b> )	35
2.2.6	Synthesis of the secondary amine 7-azanorbornene ( <b>2b</b> )	37
2.2.7	NMR spectroscopic data for the free amine ( <b>2b</b> ) and quaternary salt ( <b>2b:HCl</b> )	38
2.3	Synthesis of <i>N</i> -methyl-7-azanorbornane ( <b>1a</b> )	39
2.3.1	NMR spectroscopic data for amine ( <b>1a</b> ) and the quaternary salt ( <b>1a:HCl</b> )	41
2.3.2	Synthesis of the secondary amine 7-azanorbornane ( <b>1b</b> )	42
<b>Chapter 3: Synthesis of novel 1,4-dimethyl-7-azabicyclo[2.2.1]heptane derivatives</b>		44
3.1	Introduction	44
3.2	Synthesis of 1,4-dimethyl-7-azanorbornadiene derivatives	44
3.3	Attempted synthesis of 1,4-dimethyl-7-azanorbornane	46
3.4	Attempted reduction of ( <b>49</b> ) with sodium amalgam	47
3.5	Synthesis of alternatives compounds of ( <b>3a</b> ) and ( <b>52</b> )	48
3.6	Synthesis of 1,4-dimethyl-7-azanorbornane derivative ( <b>55</b> )	53
3.7	Synthesis of <i>N</i> -chloroamine derivatives	56
<b>Chapter 4: Synthesis of 7-azabicyclo[2.2.1]heptan-2-one derivatives</b>		59
4.1	Routes to the synthesis of 7-methyl-7-azabicyclo[2.2.1]heptan-2-one ( <b>4a</b> )	59
4.2	Synthesis of 2-bromoethynyl <i>p</i> -tolyl sulfone ( <b>62</b> )	59
4.3	Synthesis of 2-bromo-7-azabicyclo[2.2.1]hept-2,5-diene sulfone ( <b>63</b> )	60
4.4	Synthesis of 7-azabicyclo[2.2.1]heptan-2-one sulfone derivative ( <b>65</b> )	60

4.5	Synthesis of 7-azanorbornanone derivative ( <b>66</b> )	61
4.6	Synthesis of 7-methylazabicyclo[2.2.1]heptan-2-one ( <b>4a</b> )	62
4.7	Attempted synthesis of 7-methyl-7-azabicyclo[2.2.1]hept-5-en-2-one ( <b>5a</b> )	64
4.8	Synthesis of 7-azanorbornenone derivative ( <b>71</b> )	64
4.9	Attempted synthesis of epibatidine	68
<b>Chapter 5: Nitrogen NMR spectroscopy of 7-azabicyclo[2.2.1]heptane derivatives</b>		<b>75</b>
5.1	Nitrogen NMR spectroscopy	75
5.2	Referencing nitrogen NMR spectra	76
5.3	Influence of protonation on <sup>15</sup> N chemical shifts	78
5.4	<sup>15</sup> N chemical shifts of urethane derivatives of 7-azabicyclic systems	80
5.4.1	<i>N</i> -Alkoxy carbonyl-7-azanorbornane derivatives	80
5.4.2	<i>N</i> -Alkoxy carbonyl-7-azanorbornene derivatives	80
5.4.3	<i>N</i> -Alkoxy carbonyl-7-azanorbornadiene derivatives	81
5.5	<sup>15</sup> N NMR spectra of tertiary amine derivatives of 7-azabicyclic systems (and the derived HCl salts)	82
5.6	<sup>15</sup> N NMR spectra of secondary amine derivatives 7-azabicyclic systems (and the derived HCl salts)	83
5.7	<sup>15</sup> N shifts of urethane derivatives of 7-azabicyclic systems containing different substituents in the 2-carbon bridges	84
5.8	<sup>15</sup> N shifts of the tertiary amine (HCl salts) derivatives of 7-azabicyclic systems containing different substituents in the 2-carbon bridges	85
5.9	Discussion	87
<b>Chapter 6: Inversion barriers</b>		<b>90</b>
6.1	Inversion barriers in 7-azabicyclo[2.2.1]heptyl derivatives	90
6.2	7-azanorbornadiene derivatives	91
6.3	Nitrogen inversion barriers of 7-azabicyclo[2.2.1]heptane systems containing different substituent in the 2-carbon bridges	93
6.4	Nitrogen inversion barriers in 1,4-dimethyl-7-azabicyclo[2.2.1]heptane systems	94
6.5	Invertomer preferences of <i>N</i> -Me derivatives	95
6.6	A more refined treatment of $\Delta G^{\ddagger}_{inv}$ measurements for systems having unequal invertomer populations	99

6.7	Protonation experiments	100
6.8	Investigation of correlations between nitrogen inversion barriers and $^{15}\text{N}$ chemical shifts	102
<b>Chapter 7:</b>		
7.1	Nitrogen-pyramidalization	107
7.2	Results and discussion	110
7.3	Overall summary and conclusions	114
<b>Chapter 8: Experimental</b>		117
<b>Appendix: Crystal structure data</b>		155
<b>References</b>		171

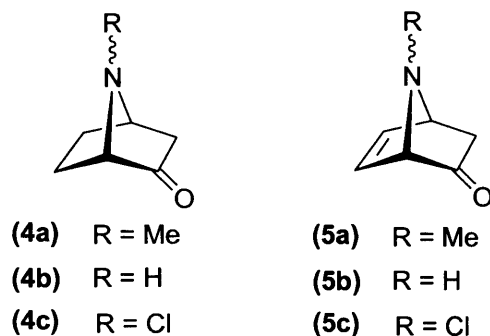
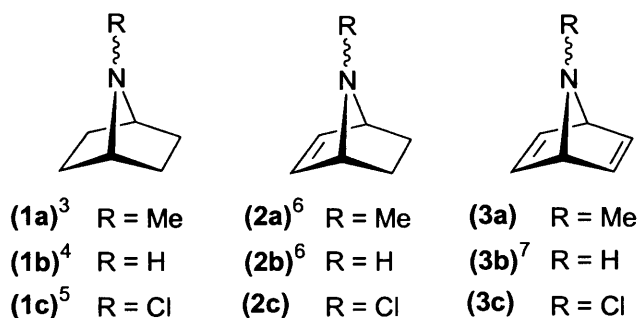
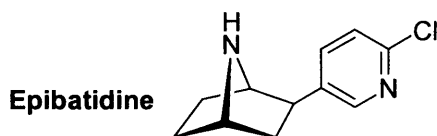
**Chapter 1**  
**Introduction**

# Chapter 1

## Introduction

### 1.1 Statement of Purpose

Epibatidine, one of the most important alkaloids, is based on the 7-azabicyclo[2.2.1]heptane skeleton. It was first isolated in 1992;<sup>1</sup> it was extracted from the skin of the Ecuadorian poison frog *Epipedobates tricolour*. Thus, a number of different targets that are derivatives from this unique 7-azabicyclo[2.2.1]heptane system (**1-3**) were under investigation to complete the measurement of nitrogen inversion barriers in this ring system. It has been known that nitrogen inversion barriers in 7-azanorbornane systems are unusually high<sup>2</sup> and there has been much discussion of the possible reasons for this which will be considered in detail in this thesis. The goal of this investigation is to synthesize (**1-3**), to measure nitrogen inversion barriers of these amines and also to extend the measurement of <sup>15</sup>N chemical shift in the 7-azanorbornane system in order to explore the hybridization of the bridging nitrogen. This synthetic work and the spectroscopic data will also provide a reason to synthesize and study other substituted azabicyclo[2.2.1]heptane (**4-5**) which will be the focus of future investigations.



## 1.2 Inversion at nitrogen

The nitrogen atom in simple primary, secondary, or tertiary amines is approximately  $sp^3$  hybridized. The three  $sp^3$  orbitals form  $\sigma$ -bonds to other atoms; the fourth  $sp^3$  orbital contains the unshared electron pair which is known as the lone pair. Therefore, the geometry of the three groups that form  $\sigma$ -bonds with nitrogen is considered as being trigonal pyramidal. However, if the lone pair is considered as being a group, the geometry of the amine is described as tetrahedral.

When the nitrogen atom is linked to three different substituents, the amine becomes a chiral centre and two enantiomers exist. The conversion between these two enantiomers is rapid and they cannot usually be isolated. This process of converting (a) to (b) is known as pyramidal inversion<sup>2,8,9,10</sup> that occurs from  $sp^3$  hybridized geometry via a  $sp^2$ -hybridized transition state (ab) (Figure 1.1).

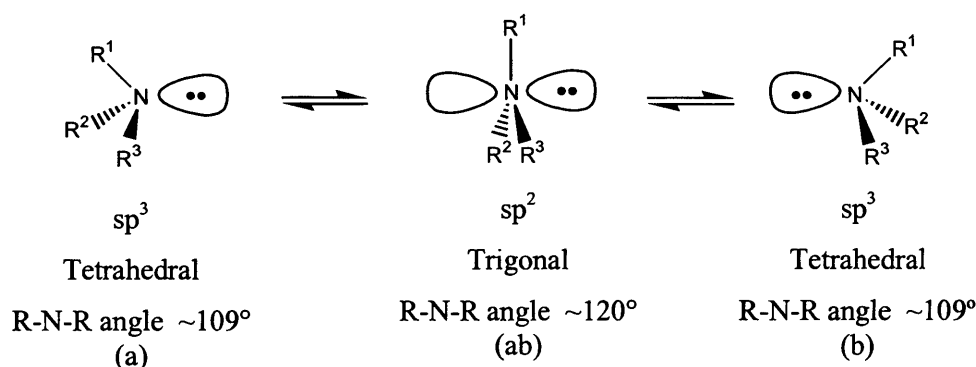


**Figure 1.1**

The energy which is required to rehybridize the tetrahedral  $sp^3$  form to the approximately planar  $sp^2$  form is known as the free energy of activation ( $\Delta G_{inv}^\ddagger$ ) (Figure 1.2). The nitrogen atom and the three substituents bonded to it lie roughly in the same plane and the lone pair occupies a p-orbital whose axis is perpendicular to this plane.

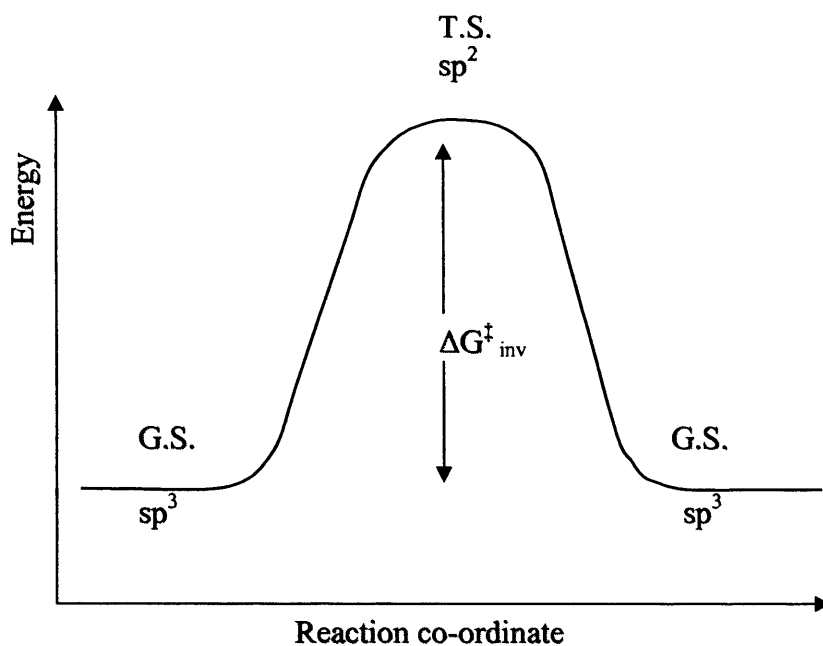


**Figure 1.2**

Resolution of enantiomers is not possible for the majority of amines since they are rapidly interconverted by nitrogen inversion. However, there have been examples of resolution of certain *N*-Cl amines due to the unusually high inversion barriers.<sup>11,12</sup>

The two invertomers do not necessarily have an enantiomeric relationship. The equilibrating forms (a) and (b) may not be isoenergetic and then become diastereoisomers and as such possess different physical and chemical properties.

Separation of diastereoisomers is not possible for the majority of amines since they are rapidly interconverted by nitrogen inversion. Such separation has been achieved in some compounds that do have high inversion barriers.<sup>11,12</sup> Compounds with such high barriers are of special interest for two reasons. The study of these compounds may increase our knowledge of the effect of the structural features on the inversion barriers in order to increase our understanding of nitrogen inversion generally. Moreover, compounds with sufficiently high barriers for the configuration at nitrogen to be stable may allow observation of separate and different chemical reactivity for each of the two invertomers. This has commonly been observed in carbon chemistry and has more recently been investigated successfully in nitrogen chemistry.<sup>8,13</sup>

The nitrogen inversion barrier is influenced by various factors, which fall into two main categories, being steric and electronic.

### 1.3 Factors influencing the inversion barriers

#### 1.3.1 Steric effects

##### 1.3.1.a Non-bonded interactions

The increase of the congestion in pyramidal ground states (a) and (b), which occurs when there are bulky substituents on nitrogen, destabilizes the ground state. Therefore, the barrier to inversion is lowered when a small substituent on nitrogen, such as methyl, is replaced by a large group, such as *t*-butyl and the change of CNC bond angle required to reach ca.  $120^\circ$  is reduced (Table 1.1). In certain other cases, where the substituents are distant from nitrogen, the steric congestion in the ground state is increased, the ground state is once more destabilized with respect to the transition state, and so the barrier is lowered. An example of this is the *N*-Me azetidines where dimethyl substitution at C2 of the azetidine ring causes a destabilization of the ground state and thus lowers the inversion barrier (Table 1.1).

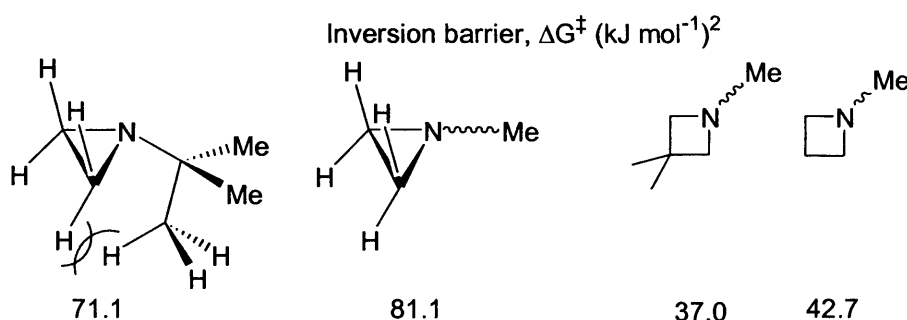
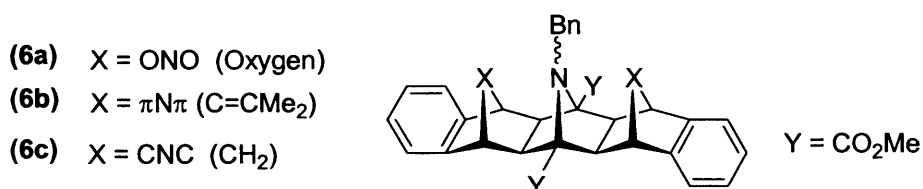


Table 1.1

This effect has not been commonly observed but has assumed new relevance following a later study<sup>14</sup> which investigated the pressure effects through space from a pair of flanking groups (X) on the central tertiary amine bridge in the poly-aza-bridged systems (**6**) (Figure 1.3). The presence of the two flanking bridges in the compounds of interest (**6a-c**) led to flattening at the central nitrogen i.e. an increase in  $\alpha$  angle (which is defined as the average of the sum of the bond angles around the nitrogen of the central bridge). This presents a suitable measure of the pyramidalization at the central nitrogen bridge. The geometric changes at the central nitrogen bridge can be correlated with the nitrogen inversion barriers. The nitrogen inversion barriers for compounds (**6a-c**) were measured using VT <sup>1</sup>H NMR spectroscopic data and compared with simple *N*-benzyl-7-azanorbornanes (**7-9**)<sup>15,16</sup> (Table 1.2). The result of this is a progressive reduction in  $\Delta G^\ddagger_{\text{inv}}$  values along the series X – Y as the bulk of the flanking bridge substituents is

increased. This is caused by progressive destabilization of the ground state in the compounds (**6a-c**). Table 1.2 demonstrates that the inversion barrier for ONO (**6a**) is already substantially decreased when compared with the simple examples (**7-9**). However, the presence of bulky demanding methylene bridges in CNC (**6c**) further decreases the inversion barrier dramatically when compared with the reference compounds.



**Figure 1.3**

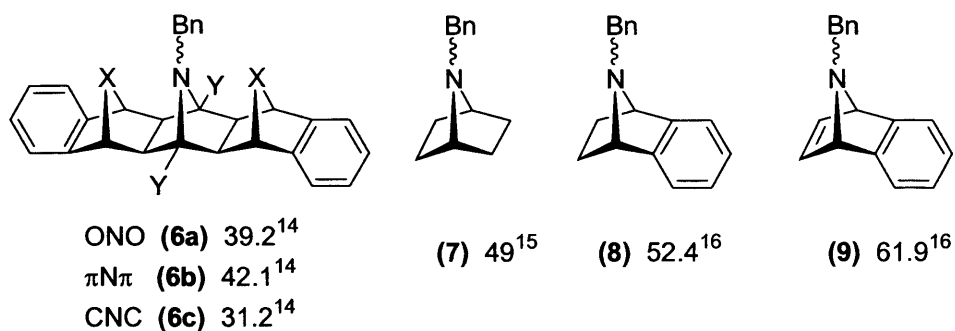


**Table 1.2** Inversion barriers at nitrogen,  $\Delta G^\ddagger_{\text{inv}}$  (kJ mol<sup>-1</sup>).

### 1.3.1.b Ring strain

The transition state for inversion, when the geometry of the transition state is sp<sup>2</sup> hybridized, requires a CNC bond angle of ca.120°. The energy required to expand the CNC bond angle of the ground state as it reaches the transition state increases in the cyclic systems because it is more difficult for the ring CNC bond angle to reach 120°. The ring bond angle in the ground state is reduced from ca. 109° to a smaller CNC angle in azetidines (ca. 96°) and aziridines (ca. 60°). The difficulty in reaching the normal sp<sup>2</sup> bond angle (ca. 120°) of the transition state raises the inversion barrier greatly with respect to unstrained amines.

The nitrogen inversion barrier in aziridines, which is very high, was predicted<sup>17</sup> before the first two invertomers of an aziridine were separated.<sup>18</sup> Table 1.3 shows the effect of the ring CNC bond angle changes on the inversion barrier for rings of different sizes. For example, the inversion barrier increases on going from azetidine to aziridine as

the lone pair in aziridines has more s-orbital character than that of a normal tetrahedral  $sp^3$  lone pair. This is a ground state stabilization which contributes to the increase in the energy required to approach the pure p-orbital character of the lone pair at the transition state.

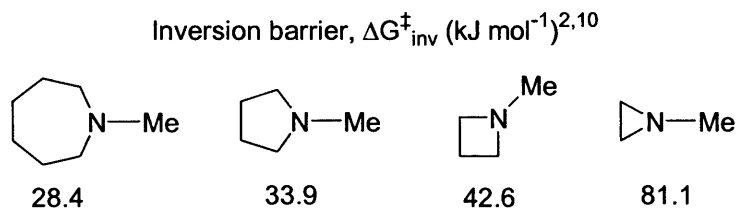


Table 1.3

### 1.3.1.c The bicyclic effect<sup>1</sup>

The inversion barrier of the aza-monocyclic system is increased further when the nitrogen is part of a bicyclic system (Table 1.4).

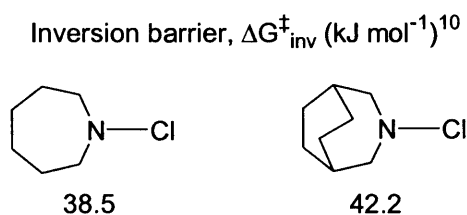


Table 1.4

This bicyclic effect may be to some extent due to increased molecular rigidity imparted by the additional carbon bridge which also increases the difficulty in attaining the planar transition state. Again, the energy of the transition state is increased if there is increased s-character of the lone pair in the ground state. The consequences of the 'bicyclic effect' can be illustrated by the 2-azabicyclo[2.2.2]octane and 2-azabicyclo[2.2.1]heptane systems in which the degree of flexibility is reduced as the carbon bridge sizes are reduced and as the C-C distances are reduced by replacing C-C single bonds by C=C double bonds (Table 1.5).<sup>19</sup> So, the inversion barrier at nitrogen is increased when the rigidity of the bicyclic skeleton is raised.

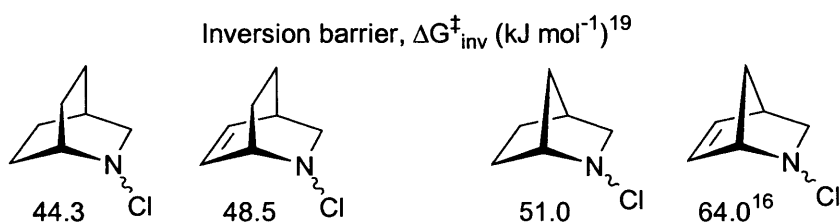
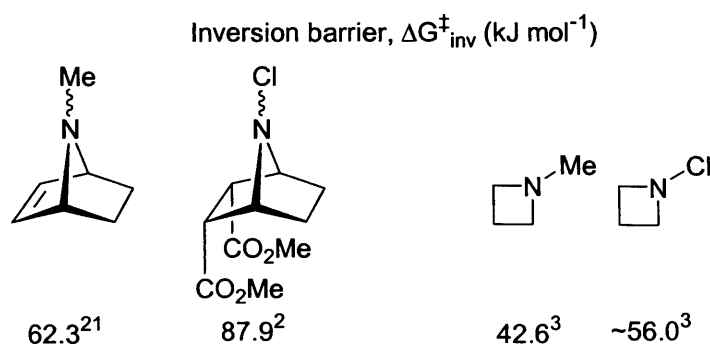


Table 1.5

However, the most significant ‘bicyclic’ effect is discovered in 7-azabicyclo[2.2.1]heptanes and similar system. Here, the inversion barrier is almost as high as those recorded in aziridines. The CNC bond angle in the 7-azabicyclo[2.2.1]heptyl system is ca.  $96^\circ$ ,<sup>20</sup> which is close to that in azetidines, however the free energy of inversion is much higher than azetidines, (Table 1.6). The reason for this unusual effect on the inversion barrier at nitrogen in the 7-azabicyclic system is not yet fully understood and this question will form a major part of this investigation.



**Table 1.6**

The unusually high barrier to inversion in 7-azabicyclo[2.2.1]heptanes (7-azanorbomanes) was reported in 1970 when Lehn referred to the ‘bicyclic effect’ but without a complete explanation.<sup>2</sup> It has been reported that the high inversion barrier in 7-azanorbomanes is due to simple ring strain at the transition state for N-inversion.<sup>15</sup> However, Malpass *et al.*<sup>22,23</sup> believe that TS effects do not explain the whole idea of the high barrier at nitrogen and proposed that ground state stabilization in this rigid bicyclic system is likely to play a substantial part in raising the barrier to inversion at nitrogen. Significant additional evidence of the unusual nature of the bridging N in 7-azanorbomanes came from the first <sup>15</sup>N chemical shift data<sup>24,25</sup> which demonstrated that the bridging N is deshielded by up to 100 ppm in comparison with nitrogen in other cyclic and acyclic environments. The downfield shifts are indicative of the delocalization of N electron density into the bicyclic framework leaving the nitrogen significantly less shielded. This delocalization was associated with stabilization of the ground state and hence an increase in the inversion barrier.

### 1.3.2 Electronic effect

#### 1.3.2.a Conjugation effects

When a substituent bonded to nitrogen has  $\pi$ -orbitals which are available for conjugation with the lone pair on the nitrogen, the delocalization of electrons is greater in the transition state than in the ground state. In the transition state the lone pair occupies a pure p-orbital which is able to overlap more effectively than when it is in a normal  $sp^3$ -orbital in the ground state. So, the presence of a conjugating substituent on nitrogen lowers the barrier of the nitrogen inversion primarily by stabilization of the transition state (Table 1.7). In some cases such as amides, there may be a substantial flattening of the nitrogen pyramid hence lowering the inversion barriers. The inversion barrier of the 7-azabicyclo[2.2.1]heptane system in which the N is part of an amide group is expected to be low but the amide is expected to be planar. However, there have been reports that the amide in the 7-azabicyclo[2.2.1]heptane system is not completely planar.<sup>26,27</sup> Nevertheless, the inversion barrier is low, the process which can be observed by VT NMR is actually N-CO rotation. This will be addressed in more detail later in the thesis.

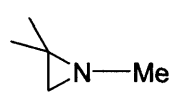
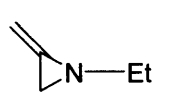
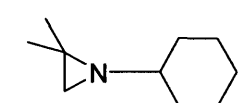
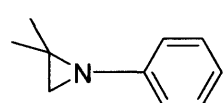
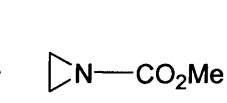
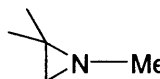
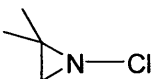
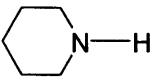
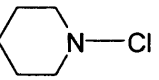
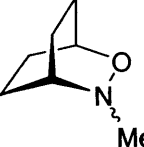
Inversion barrier, $\Delta G_{inv}^\ddagger$ (kJ mol <sup>-1</sup> ) <sup>2</sup>				
				
78.2	43.1	73.2	46.8	29.7

Table 1.7

#### 1.3.2.b Heteroatom effects

When an electronegative atom such as a halogen (F, Cl, Br) or oxygen is bonded to nitrogen, it withdraws electron density from the nitrogen atom. Since the electron density is more readily pulled from the nitrogen atom, the s-character of the lone pair on the nitrogen becomes greater. This effect is a ground state stabilization and hence increases the barrier since the lone pairs required to be in a pure p-orbital in the transition state (Table 1.8).

The heteroatom is often the exocyclic inverting atom but may also be endocyclic as in the bicyclic oxazine in Table 1.8.

Inversion barrier, $\Delta G_{\text{inv}}^{\ddagger}$ (kJ mol <sup>-1</sup> )			
78.2 <sup>2</sup>			>98 <sup>24</sup>
25.5 <sup>28</sup>			42.6 <sup>29</sup>
27.6 <sup>30</sup>			62.3 <sup>31</sup>

**Table 1.8**

Moreover, the repulsive interaction between the nitrogen lone pair and the lone pair on a substituent bonded to it is greater in the transition state than in the ground state. Therefore, the inversion barriers may increase (Figure 1.4).

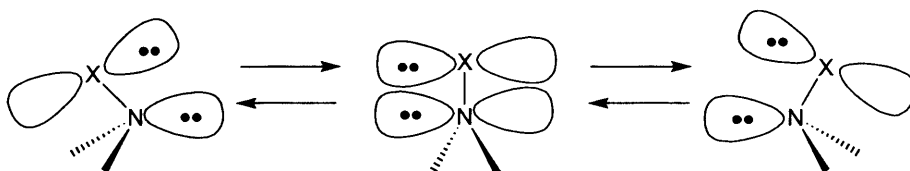


**Figure 1.4**

It is not easy to distinguish between the influences of the electronegative effect and the lone pair-lone pair interactions, since most atoms are electronegative and possess lone pairs of electrons.

## 1.4 The determination of inversion barriers and invertomer ratios

### 1.4.1 Inversion barriers

Inversion barriers in amines may be measured using several methods. Each technique is appropriate for a different range of energies. The selection of the most suitable technique for the barrier measurement depends on the magnitude of the barrier measured and the structure of the compound. Inversion barriers are usually measured by microwave spectroscopy and, to a lesser extent, by IR spectroscopy when the energy range is between 0 – 20 kJ mol<sup>-1</sup>. This barrier range is normally for low molecular weight amines such as ammonia and methylamine.

For molecules whose inversion barriers lie in the range 20 – 100 kJ mol<sup>-1</sup>, where the measurement by microwave or IR spectroscopy is limited, the most rapid and

amenable method of choice is dynamic nuclear magnetic resonance spectroscopy (DNMR). The measurement of the inversion barriers requires the rate of inversion to be slow on the NMR time scale<sup>9</sup> and two magnetically non-equivalent sites should exchange. The NMR signals due to a special group in each diastereoisomer should be suitably separated for temperature coalescence to be observed. When the temperature is raised, the rate of inversion is increased so that the two signals broaden and merge. Peak coalescence is monitored when the rate of inversion is similar to the frequency difference at slow exchange. As a result of raising the temperature, the inversion becomes too rapid on the NMR time scale to be observed. Therefore, the sites become difficult to distinguish and a single sharp peak is seen, located at the average (the weighted average if the invertomer populations are unequal) of the slow exchange frequencies.

This temperature is known as the coalescence temperature  $T_c$ , when the two signals just become incoherent. The rate constant for inversion at  $T_c$  may be obtained from equation (1).

$$k_c = \pi\Delta\nu/\sqrt{2} \quad (1)$$

where  $\Delta\nu$  is the frequency separation at slow exchange.

$\Delta G^\ddagger$  (the free energy of inversion) at coalescence can be calculated by using the Eyring equation (2).<sup>9</sup>

$$k_c = K_B/h T \exp(-\Delta G^\ddagger/RT) \quad (2)$$

where  $K_B$  is Boltzman's constant,  $h$  is Planck's constant,  $R$  is gas constant and,  $T$  is absolute temperature. This equation may be re-expressed to equation (3).

$$\Delta G^\ddagger = 19.12 T_c (10.32 + \log_{10} T_c/K_c) \quad (3)$$

This technique is only strictly appropriate to systems with identical<sup>32</sup> invertomer populations at equilibrium. However, with modification, its use can be extended to other systems.<sup>33</sup> The coalescence method is not suitable for calculating the free enthalpy ( $\Delta H^\ddagger$ ) and entropy ( $\Delta S^\ddagger$ ) for inversion, but  $\Delta G^\ddagger$  can be verified to a high degree of accuracy.<sup>9</sup> It is now possible by computer-based lineshape analysis of spectra to employ all the data included therein and achieve accurate values for all the activation parameters linked with inversion.

Historically, the estimation of inversion barriers were most commonly determined using <sup>1</sup>H NMR spectroscopy. More recently, the development of sensitive FT NMR spectrometers, the inversion barrier measurements have been extended using other nuclei such as <sup>13</sup>C, <sup>15</sup>N and <sup>19</sup>F where appropriate. <sup>13</sup>C NMR spectra are often much less

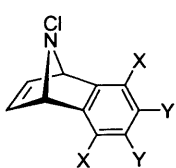
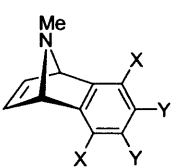
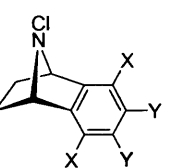
complicated than  $^1\text{H}$  NMR spectra due to the lack of coupling and the wider range of chemical shifts. It is usually possible to use  $^{13}\text{C}$  NMR to study coalescence for more than one set of peaks although the slow relaxation of the  $^{13}\text{C}$  nucleus has a disadvantage which affects the accuracy of integration of absorptions. The use of  $^{15}\text{N}$  NMR was limited due to the low natural abundance of this nucleus and its low sensitivity. However, with the development of more sensitive, higher-field NMR spectrometers the study of this nucleus at natural abundance has become possible.

## 1.4.2 Invertomer ratios

The ratio of invertomers in many cyclic amines can be measured and invertomer structures can be assigned by various methods. The most used methods are as follows.

### 1.4.2.a Low temperature $^1\text{H}$ NMR spectroscopy method

$^1\text{H}$  NMR chemical shift correlations are usually used for assigning the signals that correspond to each invertomer. Each invertomer in such cases can be assigned by a direct  $^1\text{H}$  integration of NMR spectra when the conversions of the two invertomers are slow on the NMR timescale and the corresponding signals of an atom at each of the exchanging site give rise to different chemical shifts. Overlapping signals have, in the past, been resolved using various techniques at low field including selective spin-decoupling and INDOR spectroscopy<sup>34</sup> but, nowadays, can usually be resolved at high field. Table 1.9 shows selected compounds in which the  $^1\text{H}$  NMR signals were sufficiently separated to allow integration at low temperature.<sup>22</sup>

			
	<i>syn : anti</i>	<i>syn : anti</i>	<i>syn : anti</i>
<b>a: X = Y = Me</b>	63 : 37	70 : 30	
<b>b: X = Y = H</b>	60 : 40	71 : 29	53 : 47
<b>c: X = OMe; Y = H</b>	67 : 33	80 : 20	54 : 46
<b>d: X = Y = Cl</b>	82 : 18	82 : 18	71 : 21
<b>e: X = Y = F</b>	84 : 16	88 : 12	80 : 20

*syn-anti-* methyl and chloro- substituents with respect to the aryl ring.

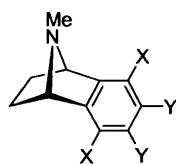
**Table 1.9** Invertomer ratios for N-methyl and N-chloro compounds measured by  $^1\text{H}$  NMR spectroscopy.<sup>22</sup>

Steric influences seem to be the predominant factor in determining invertomer preferences, but there are also systems where electronic factors appear to be significant. This encouraged direct measurement of invertomer preferences for a range of tertiary amines in order to assess the relative importance of electronic effects (Table 1.9).<sup>22</sup> Variation of the substituents in the aryl ring of these compounds allowed alteration of the electronic environment with minimal steric change. This therefore, provided a simple empirical test of the relative importance of  $\pi$ -lone pair interactions in this ring system. There are two important observations to be drawn from these invertomer ratios.

Firstly, there is a clear preference for the *syn* configuration in both the *N*-Cl and *N*-Me series and the proportion increases with increasing electronegativity of the substituents in the aryl ring. Secondly, there seems to be little dependence of the invertomer ratio whether the substituent at nitrogen is a chlorine or methyl group with the same substituents in the aromatic ring which are summarized in Table 1.9.<sup>22</sup>

#### 1.4.2.b Low temperature <sup>13</sup>C NMR spectroscopy method

<sup>13</sup>C NMR spectra often show two different signals of each carbon in unsymmetrical molecules when the inversion at nitrogen is slow, usually at low temperature. When the populations of the two invertomers are not equal, there will be major and minor peak corresponding to each carbon. The invertomer ratios in <sup>13</sup>C NMR are directly calculated since signal overlap is less likely to occur. Only signals of similar carbons can be integrated with any confidence using <sup>13</sup>C NMR spectroscopy since accurate integration requires that relaxation of both carbons occurs at a similar rate. Table 1.10 shows the invertomer ratios of selected compounds according to the integration of the <sup>13</sup>C signals at low-temperature.<sup>22</sup> The invertomer ratios of the same selected compounds could not be resolved accurately using <sup>1</sup>H NMR integration due to the difficult assignment of the minor invertomer signals. The variation of the aryl substituents leads to very little difference in the ratio.

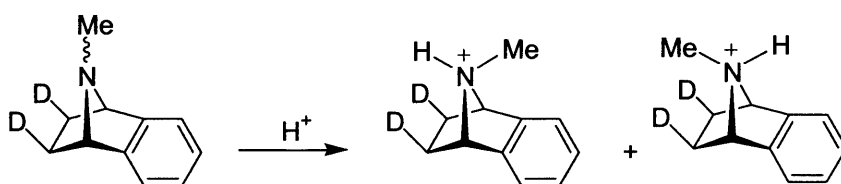
	<b>a: X = Y = Me</b>	<b><i>syn</i> : <i>anti</i></b>
	<b>b: X = Y = H</b>	95 : 5
	<b>c: X = OMe; Y = H</b>	94 : 6
	<b>d: X = Y = Cl</b>	97 : 3
	<b>e: X = Y = F</b>	97 : 3
	<b>e: X = Y = F</b>	98 : 2

*syn*-/*anti*- methyl and chloro-substituents with respect to the aryl ring.

**Table 1.10** Invertomer ratios for tertiary amines by <sup>13</sup>C NMR.<sup>22</sup>

### 1.4.2.c Quaternisation (kinetic protonation)

Low temperature NMR spectroscopy techniques are not always applicable for measuring barriers and ratios due to the very low inversion barriers. An alternative method is the addition of the amine to a large excess of strong acid leading to protonation at the nitrogen atom. This chemical reaction is considered to be very rapid (diffusion controlled) and irreversible protonation of the two amine invertomers occurs to give a mixture of diastereoisomeric quaternary ammonium ions (Scheme 1.1).<sup>21,35</sup> Integration of the appropriate signals in the <sup>1</sup>H or <sup>13</sup>C NMR spectrum provides the ratio.<sup>22</sup> Marchand<sup>21</sup> has reported that the invertomer ratio (Scheme 1.1) from kinetic protonation studies is in good agreement when compared with the values obtained using dynamic <sup>1</sup>H NMR experiments at low temperature. Marchand<sup>21</sup> and Malpass<sup>22</sup> in recent studies reported the invertomer ratios of the free base (Scheme 1.1) (94% *syn*-methyl with respect to the aryl ring) via <sup>1</sup>H NMR studies at low-temperature. These results are in good agreement with the kinetic protonation studies (ca. 93% *syn*-methyl with respect to the aryl ring).<sup>21</sup>



**Scheme 1.1**

In addition, the effectiveness of kinetic protonation experiments has also been assessed in 2-azabicyclo[2.2.1]heptyl and -[2.2.2]octyl ring systems where comparisons with DNMR methods have been made.<sup>9</sup> Table 1.11 shows the ratios of stereoisomeric quaternary salts using <sup>1</sup>H and <sup>13</sup>C NMR values which are in good agreement. Also, Table 1.11 shows the invertomer ratios data for the corresponding *N*-Cl amines which were obtained by direct integration of signals at low-temperature;<sup>19</sup> the signals due to the minor invertomers were identified with the aid of homonuclear INDOR spectroscopy. The ratios in Table 1.11 show close similarities between the ratios for the *N*-methyl amines and those observed directly for the corresponding *N*-Cl amines.

Amine	R = Me (ratios from kinetic protonation)		R = Cl (ratios from kinetic protonation)	
	<i>endo-exo</i> -ratio		<i>endo-exo</i> -ratio	
	<sup>1</sup> H NMR	<sup>13</sup> C NMR	<sup>1</sup> H NMR	
	77 : 23	76 : 24	88 : 12 (at -54°C)	81 : 19 (at 41°C)
	24 : 76	24 : 76	25 : 75 (at -84°C)	35 : 65 (at 24°C)
	88 : 12	89 : 11	91 : 9 (at -87°C)	85 : 15 (at 20°C)

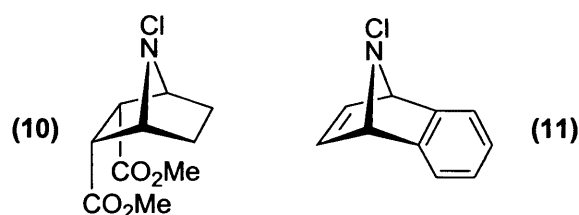
**Table 1.11** Invertomer ratios.

#### 1.4.2.d X-ray crystallography

X-ray crystallography is the most useful method for determining molecular structures and, in particular, for determining bond angles at nitrogen. Its drawbacks are that it can only be applied to well grown crystal structures, the relative long time and effort to produce a structure, and the potential differences in molecular shape in solution compared to the solid state. Structures of some non-crystalline amines can be determined using their crystalline quaternary salts.

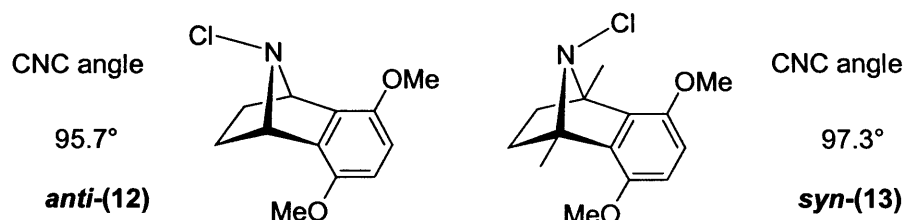
### 1.5 Azabicyclic systems having unusually high barriers to inversion at nitrogen

Usual values of nitrogen inversion barriers for alicyclic amines lie in the 20-38 kJmol<sup>-1</sup> range.<sup>2</sup> However, as discussed above, 7-azabicyclo[2.2.1]heptane, 7-azabicyclo[2.2.1]hept-5-ene, and 7-azabicyclo[2.2.1]-hepta-2,5-diene systems have abnormally high barriers for nitrogen inversion. Lehn<sup>2</sup> reported the inversion barrier ( $\Delta G_{inv}^\ddagger$ ) of ca. 87.9 kJ mol<sup>-1</sup> for *N*-Cl amine (**10**) that was measured by dynamic NMR spectroscopy. Moreover, Rautenstrauch<sup>36</sup> has verified a higher  $\Delta G_{inv}^\ddagger$  of ca. 98.3 kJ mol<sup>-1</sup> for molecule (**11**) by direct equilibration. Later work by Nelsen<sup>3</sup> and other work cited by Nelsen contained similar high barriers in a wider range of compounds.

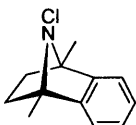
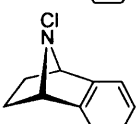


The effect of angle strain of the C-N-C bond at the 7-position does not appear to explain these barriers completely. Malpass *et al.*<sup>37</sup> reported the isolation and X-ray crystallographic structure determination of single invertomers of *N*-Cl amines (**12**) and (**13**). The CNC bond angle for (**12**) is 95.7° for the *anti*-invertomer and 97.3° for the *syn*-invertomer (**13**). However, the invertomers inversion barriers are significantly higher than might be expected from CNC bond angles of this magnitude imposed by the bicyclic skeleton.

For example, the inversion barrier of *N*-chloroazetidine was measured to be ca. 56 kJ mol<sup>-1</sup>,<sup>3</sup> although the *endo* cyclic CNC bond angle is smaller than that of the 7-azabicyclo[2.2.1]heptyl derivatives.



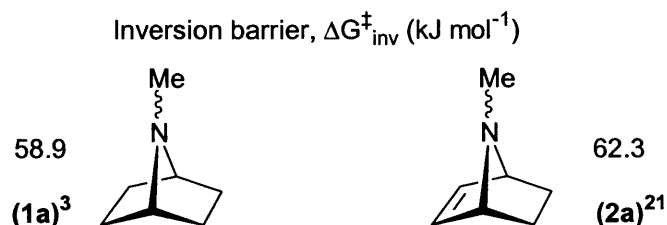
Moreover, Malpass *et al.* reported the inversion barrier for (**14**) which is lower than (**15**).<sup>23</sup> The lower barrier for (**14**) is consistent with the wider CNC bond angle [95.7° for (**12**) c.f. 97.3° for (**13**)<sup>37</sup>]. This perhaps results from the effect of the two bridgehead methyl substituents which raise the electron density in the bridgehead orbitals leading to increased mutual repulsion (Table 1.12).<sup>23</sup>

	$\Delta G^\ddagger_{anti \rightarrow syn}$ (kJmol <sup>-1</sup> )	$\Delta G^\ddagger_{syn \rightarrow anti}$ (kJmol <sup>-1</sup> )
( <b>14</b> )	77.6	77.9
	94.5	94.8

**Table 1.12** Nitrogen inversion barriers for (**14**) and (**15**).<sup>23</sup>

The barrier to nitrogen inversion in saturated 7-azanorbornane (**1a**) was measured<sup>3</sup> to be 58.9 kJ mol<sup>-1</sup> which is not very different from the inversion barrier of unsaturated 7-azanorbornene (**2a**) (62.3<sup>21</sup> kJ mol<sup>-1</sup>). This tends to suggest that the interaction between the bridging  $\pi$ -system and the N p-orbital does not have a very large effect on the nitrogen inversion barrier in the ground state (the shorter C=C double bond is likely to be the

major factor, as discussed below). However, the original proposal by Lehn<sup>2</sup> when first discussing the ‘bicyclic effect’ was that  $\pi$ - $\pi$  interactions *at the transition state* are important in raising the barrier to nitrogen inversion.



Malpass *et al.*<sup>22</sup> investigated the effects of the electronic and steric factors on the inversion barriers in the 7-azabicyclo[2.2.1]heptyl derivatives. A reduction in  $\Delta G^\ddagger_{\text{inv}}$  of 10.1 kJmol<sup>-1</sup> is seen on replacement of the etheno- bridge by a tetrafluoroaryl ring, which is consistent with a reduction of  $\pi$ -electron density (Table 1.13).

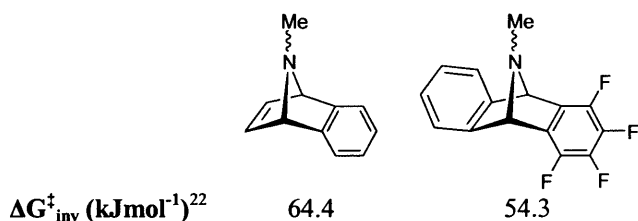


**Table 1.13**

An interesting comparison between  $\Delta G^\ddagger_{\text{inv}}$  values can be made by alteration of the electronic character in the benzene ring.<sup>22</sup> The most electronic-rich aryl ring is associated with the highest inversion barrier, the all-hydrogen analogue is lower by 2.1 kJmol<sup>-1</sup>, and the dimethoxy ring sits between these two. There is a substantial change for the electron-deficient systems, which show barriers that are lower by >6 kJ mol<sup>-1</sup> (Table 1.14).

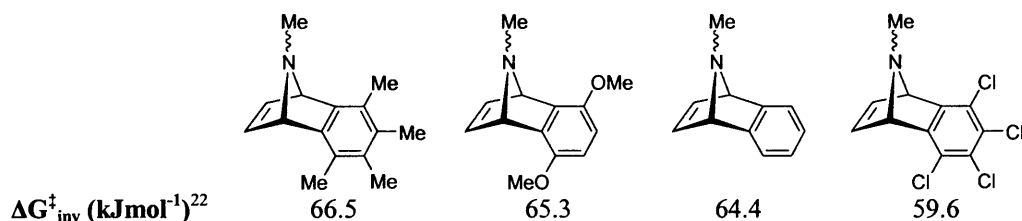
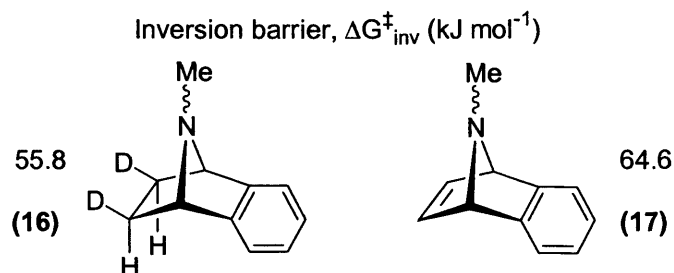


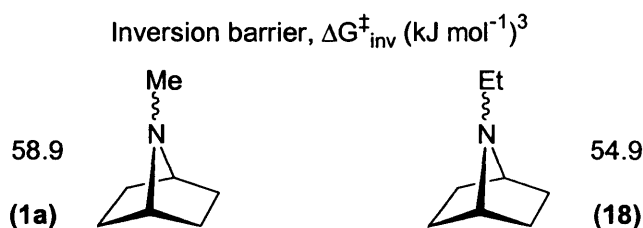
**Table 1.14**

Malpass *et al.*<sup>22</sup> suggested that the inversion barrier is lowered by saturation of the bridging  $\pi$ -bond (which increases the C-C distance and hence reduces bicyclic ring strain)

but also introduced the involvement of another major effect which is the ground state destabilization. The inversion barrier of **(16)** was found to be 55.8 kJ mol<sup>-1</sup> with a large difference (8.8 kJ mol<sup>-1</sup>) compared with unsaturated **(17)** (64.6 kJ mol<sup>-1</sup>).



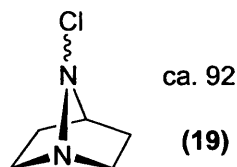
If the interaction between bridging  $\pi$ -systems and the nitrogen p-orbital were important at the transition state for N inversion, we would expect to see changes as the unsaturated bridges are saturated sequentially. The inversion barrier is lowered by saturation of one or more of the bridging  $\pi$ -bonds. However, a major factor here is ground state destabilization of the *anti* N-Me invertomer (with respect to the aryl ring), explained by steric repulsion between the 7-methyl and the *exo*-hydrogens in the two-carbon bridge. This is supported by the further reduction in the barrier of 7-methyl-azanorbornane on replacement of the N-Me by the slightly more bulky ethyl group **(18)**.<sup>3,22</sup>



Moreover, in order to consider more factors that might influence the ‘bicyclic effect’,<sup>1</sup> Malpass *et al.*<sup>38</sup> reported a high inversion barrier for the diazabicyclic system **(19)** (ca. 92 kJ mol<sup>-1</sup>) and emphasized that neither the nitrogen in position one nor the chlorine substitution was the principal source of this high barrier and supported Lehn’s suggestion of a ‘bicyclic effect’. The effect of the extra nitrogen on the inversion barriers is small in the bicyclo[2.2.2]octane systems. The increase in the inversion barrier of **(20a)**<sup>38</sup> is only 3.3 kJmol<sup>-1</sup> over the value for **(21a)**<sup>39</sup> of 44.2 kJmol<sup>-1</sup>. Similar, small effects of a second nitrogen are observed in the corresponding N-Me analogues **(20b)** and **(21b)** where the difference is ca. 4.8 kJmol<sup>-1</sup>.<sup>30</sup> The Cl substituent effect on raising the

inversion barrier is clearly greater than the Me substituent in these systems but the chlorine is not the primary cause of very high barriers.

Inversion barrier,  $\Delta G^\ddagger_{\text{inv}}$  (kJ mol<sup>-1</sup>)

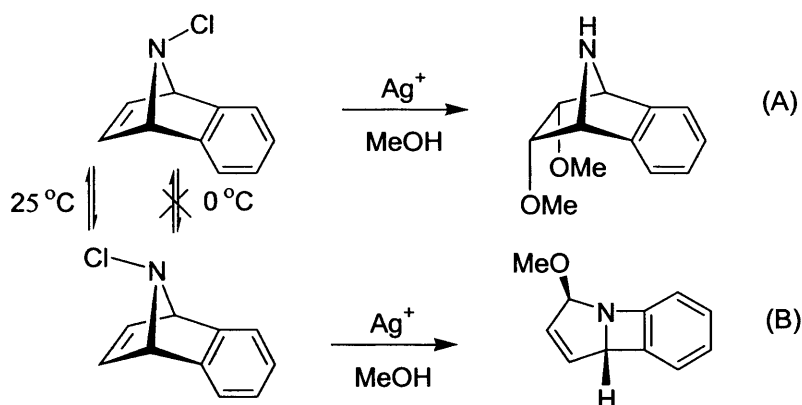


Inversion barrier,  $\Delta G^\ddagger_{\text{inv}}$  (kJ mol<sup>-1</sup>)



The high inversion barriers in **(1a)** and **(19)** due to the ‘bicyclic effect’ occur in compounds having no  $\pi$ -bonds in the 2C bridges. Thus, the ‘bicyclic effect’ must be a fundamental property of the 7-azabicyclo[2.2.1]heptane system. The inversion barrier is also further increased by incorporation of  $\pi$ -bonds and/or attachment of Cl (or other heteroatoms) to the nitrogen.

Moreover, the control of the invertomer ratio can demonstrate different reaction pathways for each invertomer when the reactions are performed at low temperature. Malpass *et al.*<sup>40</sup> reported the solvolysis of *N*-Cl derivatives of the 7-azabenzonorbornadiene ring systems which undergo silver (I)-assisted rearrangement with participation of etheno- (*syn*-Cl- series) or benzo- (*anti*-Cl- series)  $\pi$ -electrons (Scheme 1.2). When the reaction was performed at 0 °C, inversion was very slow and each invertomer gave a different product. In contrast, at 25 °C, inversion was rapid and (A) only was observed, formed from the more reactive *syn*-invertomer by participation of the  $\pi$ -bond.



**Scheme 1.2**

### 1.6 $^{15}\text{N}$ NMR chemical shifts of 7-azabicyclo[2.2.1]heptane, -hept-5-ene, and -hepta-2,5-diene

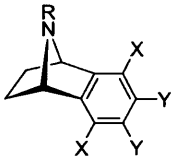
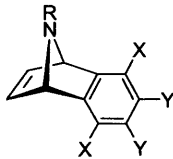
It has already been established that the inversion barriers of the 7-azabicyclo[2.2.1]heptane derivatives approach the high values observed in aziridines.<sup>2</sup> Investigations of the origins of the unusual high barriers at nitrogen,<sup>2,3,7,9,37,41</sup> the question of invertomer preferences at nitrogen,<sup>37,42</sup> and the different chemistry of the two invertomers (reactions)<sup>40</sup> are an open area for chemists to develop. Also, the bridging nitrogen atoms in the 7-azabicyclo[2.2.1]heptyl systems exhibit unusually downfield chemical shift in their NMR spectra.<sup>24,25</sup>

Significantly, the chemical shifts of the bridging atoms such as  $^{13}\text{C}$ ,  $^{17}\text{O}$ ,  $^{31}\text{P}$ , and  $^{29}\text{Si}$  in bicyclo[2.2.1]heptyl systems also have unusually downfield signals (large deshielding) in their NMR spectra (Table 1.15), and different suggestions have been introduced for this effect which will be discussed later with nitrogen NMR studies.

<p><math>\delta^{13}\text{C}</math> NMR data (downfield from TMS = 0)<sup>43</sup></p> <p>38.7      48.5      75.4</p>	<p><math>\delta^{31}\text{P}</math> NMR data (downfield from <math>\text{H}_3\text{PO}_4 = 0</math>)<sup>45</sup></p> <p>22.0      137.0      147.0</p>
<p><math>\delta^{17}\text{O}</math> NMR data (downfield from TMS = 0)<sup>44</sup></p> <p>85.5      110.0      192.5</p>	<p><math>\delta^{29}\text{Si}</math> NMR data (downfield from TMS = 0)<sup>46</sup></p> <p>58.5      76.9</p>

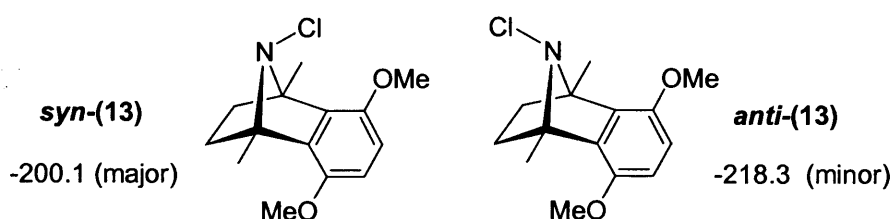
**Table 1.15**

The  $^{15}\text{N}$  NMR spectra of the few 7-azabicylo[2.2.1]heptyl systems which have been reported showed significant downfield shifts compared to other cyclic secondary and tertiary amines (Table 1.16).<sup>24,25</sup> It seems that the angle strain at the 7-position is not the only effect responsible for deshielding effects. It must be significant that nitrogen atoms in other strained ring systems having high inversion barriers are actually highly *shielded*; an example is provided by aziridine ( $-339.3$  ppm) which has a nitrogen shift *upfield* from normal amines<sup>47</sup> in contrast to the *downfield* shifts shown by the azabicyclic compounds discussed above.

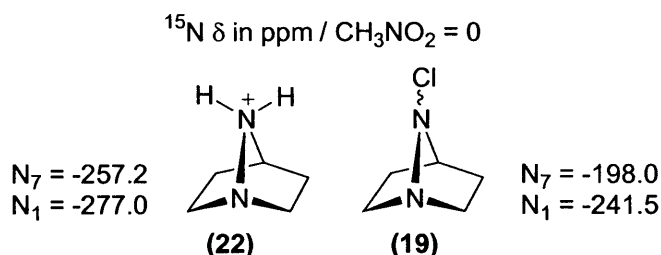
R	X	Y		
H	Me	Me	-279.3	-244.7
H	H	H	-277.5	-239.6
H	OMe	H	-276.9	-236.3
Me	Me	Me	<i>syn</i> -291.0 (95%) <i>anti</i> -300.0 (5%)	<i>syn</i> -259.3 (70%) <i>anti</i> -260.6 (30%)
Me	H	H	<i>syn</i> -287.5 (94%) <i>anti</i> -298.1 (6%)	<i>syn</i> -254.1 (71%) <i>anti</i> -257.5 (29%)

**Table 1.16** Some examples of  $^{15}\text{N}$  chemical shift values for secondary and tertiary amines.<sup>24, 25</sup>

Compound (13) shows significantly different  $^{15}\text{N}$  NMR shifts for the major *syn* and minor *anti* invertomers (ratio of 71:29 respectively, measured by  $^1\text{H}$  NMR spectroscopy).<sup>24</sup>



In the bicyclic hydrazinium salt (22), the chemical shift of N-1 is within the normal range for hydrazines ( $-270$  to  $-330$  ppm /  $\text{CH}_3\text{NO}_2 = 0$ );<sup>47</sup> but, in contrast, N-7 is substantially deshielded. The *N*-Cl derivative of hydrazine (19) shows a significant downfield shift of both nitrogens which suggests that the inductive effect of Cl is a factor.<sup>24</sup>



Clearly, the picture is complicated by the addition of benzo- substituents and by different substitution patterns within aryl rings and the subtle differences in inversion barriers and  $^{15}\text{N}$  shifts have not all been explained satisfactorily. Therefore, it has been decided that investigation of a range of simpler 7-azabicyclo[2.2.1]heptyl derivatives was justified, looking for the effect of unsaturation and change of substituents at nitrogen without the complications introduced in more complex systems.  $^{15}\text{N}$  NMR spectroscopy was expected to be of significance in looking for possible empirical correlations between the  $^{15}\text{N}$  chemical shift and substitution at nitrogen ( $\text{R} = \text{H}, \text{CH}_3, \text{Cl}$ ), together with possible interactions involving etheno ( $\text{HC}=\text{CH}$ ) or ethano ( $\text{H}_2\text{C}-\text{CH}_2$ ) bonds and, in addition, possible correlations with the varying, high inversion barriers.

The inversion barrier investigations will be extended to include 7-azanorbornane derivatives substituted in the 2-carbon bridges (4-5). In relation to this system, a nucleophilic displacement at the C-7 position of a norbornane compound is difficult to achieve due to angle constraints and steric factors.<sup>48</sup> The transition state for  $\text{S}_{\text{N}}2$  reaction requires  $120^\circ$  bond angle but the rigid bicycle in norbornane (Figure 1.5) prevents this bond angle being achieved at the 7-position ( $\text{C}_1\text{C}_7\text{C}_4 = 93^\circ$ ). The *exo*-hydrogens at C5 and C6 hinder the approach of the incoming nucleophile. However, when the norbornane is substituted with a carbonyl group at the C2 position, the carbonyl group aids the displacement reaction with complete inversion of configuration at C7 (Figure 1.6).<sup>49</sup> Moreover, Morrison *et al.* reported an enhancement in the displacement reactivity in the diketone.<sup>48</sup> Therefore, the inversion barriers will be investigated in the 7-azanorbornan-2-one derivatives in view of the clear similarity between the T.S. for  $\text{S}_{\text{N}}2$  substitution and the T.S. for nitrogen inversion in 7-azanorbornane (Figure 1.5).

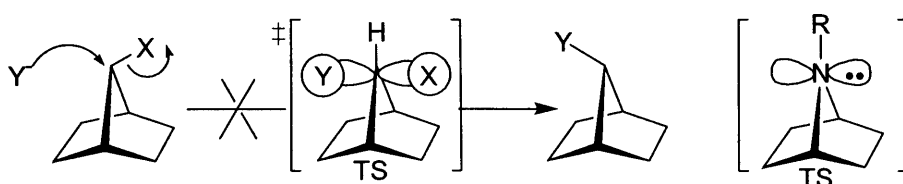


**Figure 1.5**

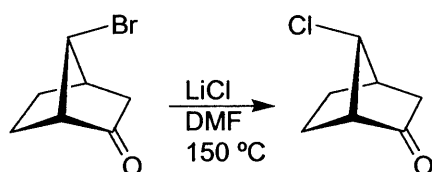


**Figure 1.6**

Furthermore, molecular mechanics calculations were performed to address the phenomenon of the ‘bicyclic effect’. Nelsen *et. al.* suggested that the degree of  $\alpha$ -branching was an important factor raising the barrier in bicyclic systems, perhaps due to increased ground state stabilization caused by lone pair, alkyl group  $\sigma^*$  orbital mixing.<sup>3</sup> However, on inclusion of monocyclic systems into the comparison, the  $\alpha$ -branching hypothesis did not seem appropriate. In the most recent study, Belostotskii *et. al.* reported the determination of the nitrogen inversion barriers of different bicyclic amines using dynamic NMR and MP2/6-31G\* level of theory.<sup>50</sup> The inversion barriers were found to vary from 26 to 54 kJmol<sup>-1</sup>. A number of interesting points can be drawn from this study<sup>50</sup> on the nitrogen inversion and ‘bicyclic effect’ in cyclic amines. The inversion barriers increase with decreasing of the ring size in azabicycles. Also, the presence of a five-membered ring as a part of a rigid nitrogen-bridge bicyclic framework raises the inversion barrier by ca. 12 kJmol<sup>-1</sup> per ring. The inversion barrier of the ring inversion in six-membered ring is lowered as a double bond introduced to the system. Moreover, the high barriers in most of these azabicycles were determined by the energy of the  $\sigma$ -orbitals of the  $C_\alpha$ - $C_\beta$  bonds as well as the nitrogen lone pair using the natural bond orbital (NBO) analysis.<sup>50</sup> No experimental evidence has been found so far to support the suggestion that observed high barriers in the 7-azabicyclic derivatives is caused by the delocalization of the nitrogen lone pair.

The aim of this study was to synthesize new and known members of a series of simple 7-azanorbornane derivatives and to investigate these using spectroscopy (variable temperature <sup>1</sup>H NMR and <sup>15</sup>N NMR) of the compounds (1-3). Variation of the N-substituents in the bridged molecules (1-3) will also be used to study the relative effects on the dynamics of N-inversion where applicable. Further, this study will be extended to bridged 7-azabicyclic system (4-5), substituted elsewhere in the bicyclic framework and their possible effects on the nitrogen inversion barriers and <sup>15</sup>N chemical shifts.

## **Chapter 2**

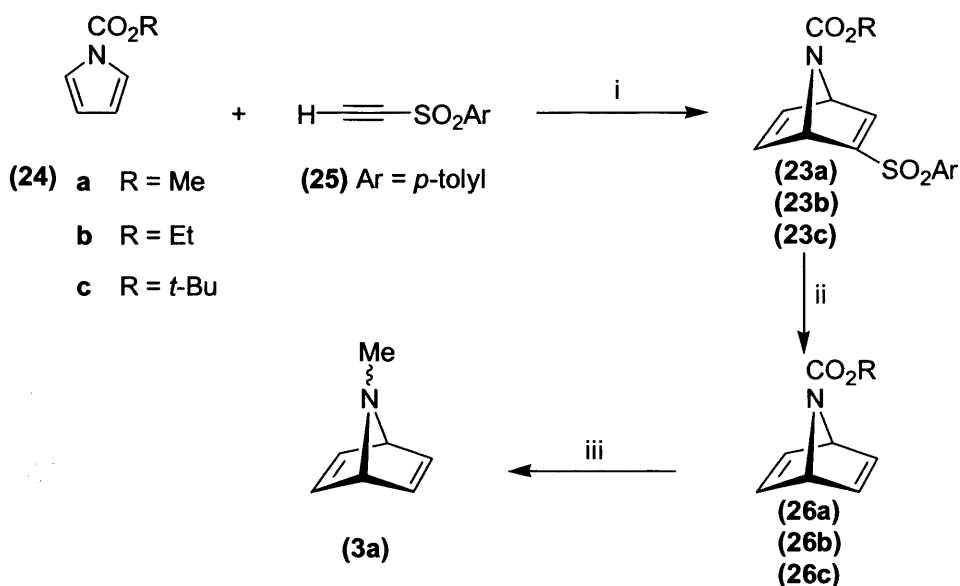
### **Synthesis of 7-azabicyclo[2.2.1]heptane derivatives**

## Chapter 2

### Synthesis of 7-azabicyclo[2.2.1]heptane derivatives

#### 2.1 Synthesis of 7-azanorbornadiene derivatives

The major challenge was to synthesize the novel *N*-methyl amine (**3a**) which has not been reported in the literature and to complete the synthesis of the series of the parent compounds of the 7-azabicyclic system (**1-2**). Comparison of the properties of compound (**3**) with the mono-ene (**2**) and the fully saturated analogue (**1**) has the potential to further our understanding of the 'bicyclic effect'. Therefore, some of the interest in this compound lies in the measurement of the inversion barrier and  $^{15}\text{N}$  chemical shift. In addition, appropriate reductive methods should provide the series of compounds (**2**) and (**1**) from (**23**) (Scheme 2.1). The route used to synthesize the desired *N*-protected 7-azanorbornadiene (**23**) [the precursor to the range of compounds including *N*-methyl-7-azanorbornadiene (**3a**)] is outlined in Scheme 2.1.



**Scheme 2.1** Reagents and conditions: (i) 80-85 °C, 48 h; (ii) 6% Na/Hg,  $\text{Na}_2\text{HPO}_4$  in THF/ $\text{CH}_3\text{OH}$  (1:1), -78 °C, 4 h; (iii) (*i*-Bu) $_2\text{AlH}$ , Toluene, RT, 8 h.

The [4+2] cycloaddition reaction of *N*-acylpyrrole (**24**) (R = Me, Et and Bu<sup>t</sup>) substrates and an electron-deficient arylsulfonyl-substituted acetylene (**25**) has proven to be a useful method for one-step construction of the 7-azabicyclo[2.2.1]heptadiene ring system.<sup>4,7</sup> Desulfonation of (**23**) with 6% sodium amalgam afforded *N*-carboalkoxy derivative (**26**), which was further reduced to (**3a**). Taking into consideration that the *N*-acylpyrrole substrates contain  $^{15}\text{N}$  at natural abundance (0.37 %), these methods will only

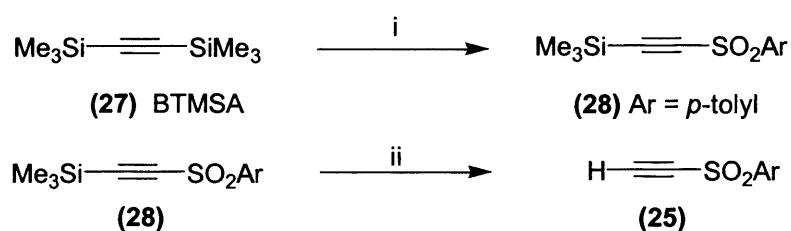
produce azabicyclic targets which have the same low levels of  $^{15}\text{N}$ . Of course, work with enriched material would be difficult and very expensive.<sup>25</sup> However, it was expected that modern spectrometers would be able to produce  $^{15}\text{N}$  signals at natural abundance;  $^{14}\text{N}$  NMR spectra should also be measurable.

The methods that were used will be described as follows.

### 2.1.1 Synthesis of ethynyl *p*-tolyl sulfone (25)

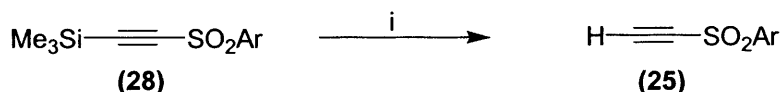
The acetylenic sulfone, ethynyl *p*-tolyl sulfone (25) has been used as an acetylene equivalent in organic synthesis and acts as an activated dienophile in Diels-Alder reactions for the construction of bicyclic systems.<sup>4,7</sup>

The route to the formation of ethynyl *p*-tolyl sulfone (25) is illustrated in Scheme 2.2, using Paquette's method.<sup>51</sup> This method employs a two-step reaction sequence which uses commercially available bis(trimethylsilyl)acetylene (BTMSA) (27) as the starting material. The first step was the treatment of (BTMSA) (27) in dichloromethane with a solution of *p*-toluenesulfonyl chloride-aluminium chloride in dichloromethane to afford the *p*-tolyl-2-(trimethylsilyl)ethynyl sulfone (28) in 70% yield after purification. The ethynyl *p*-tolyl sulfone (25) was then formed in 70 % yield by hydrolysis of the trimethylsilyl group of (28) in basic buffered solution. The temperature of the hydrolysis reaction must be maintained at 30 °C, otherwise the reaction is not completed (below 30 °C) or resinous material is obtained (above 30 °C). The  $^1\text{H}$  NMR spectroscopic data were identical to those described in Paquette's work.



**Scheme 2.2** Reagents and conditions: (i)  $\text{ArSO}_2\text{Cl}-\text{AlCl}_3$ ,  $\text{CH}_2\text{Cl}_2$ , 0 °C. (ii)  $\text{K}_2\text{CO}_3$ ,  $\text{KHCO}_3$ ,  $\text{CH}_3\text{OH}$ ,  $\text{H}_2\text{O}$ .

Moreover, in order to avoid the hydrolysis step in Paquette's method,<sup>51</sup> Eisch *et al.* reported the conversion of (28) using NaF to afford (25) in a high yield (90 %) of reasonably pure material (Scheme 2.3).<sup>52</sup> Therefore, to avoid the hydrolysis reaction described by Paquette, the alternative Eisch's method was followed here for the removal of the TMS group.



**Scheme 2.3** Reagents and conditions: (i) 95% EtOH, NaF/water, 0 °C.

### 2.1.2 Synthesis of 7-azabicyclo[2.2.1]heptadiene derivative (23b)

The synthesis of (23a) (Scheme 2.1) by the cycloaddition reaction of *N*-methoxycarbonylpyrrole (24a) with ethynyl *p*-tolyl sulfone (25) was first reported by Vogel.<sup>7</sup> The azabicyclic derivative (23b) was synthesized by using the method of Muchowski.<sup>53</sup> Treatment of the *N*-ethoxycarbonylpyrrole (24b) (prepared using the method of Ciamician and Denstedt)<sup>54</sup> with the dienophile (25) in a 2:1 molar ratio respectively and without solvent at 80-85 °C for 48 h resulted in a highly satisfactory 74% yield of the 7-azabicyclo[2.2.1] heptadiene derivative (23b) (Scheme 2.1). The excess of the *N*-substituted pyrrole can be removed and recovered easily by using column chromatography on silica gel.

The <sup>1</sup>H NMR spectrum of the *N*-ethoxycarbonyl-7-azanorbornadiene (23b) shows a singlet at 7.37 ppm with an integration of one olefinic proton which corresponds to the H<sub>3</sub> proton. H<sub>5</sub> and H<sub>6</sub> olefinic protons appear at 6.90 and 6.95 ppm respectively. The two bridgehead protons appear at positions C1 and C4 with 5.43 and 5.23 ppm confirming the formation of the cycloadduct. The CH<sub>3</sub> and CH<sub>2</sub> protons on the ethoxy group are broad peaks due to slow, restricted rotation about the N-C-O bond at room temperature. The aromatic protons appear at 7.75 and 7.36 ppm as an AA'BB' pattern (*J* = 8.3 Hz).

### 2.1.3 Synthesis of *N*-protected 7-azanorbornadiene (26b)

Vogel *et al.* reported the removal of the arylsulphonyl group in 42% yield.<sup>4</sup> Using this method, treatment of the 7-azabicyclo[2.2.1]heptadiene (23b) with 1.7 equivalents of freshly prepared 6% Na/Hg (sodium amalgam) afforded 7-azabicyclo[2.2.1]hepta-2,5-diene (26b) as a colorless liquid after column chromatography on silica gel (Scheme 2.1). The desulfonation step gave only a low yield of the cycloadduct (26b) (23%) which was reported here for the first time with the ethoxy carbonyl protection group. This was a serious problem given the proposed use of this key cycloadduct as a precursor for a wider range of compounds.

The <sup>1</sup>H NMR spectrum of the 7-azanorbornene (26b) illustrates the absence of the aromatic protons which demonstrates the successful cleavage of the phenyl sulfone group after purification. The <sup>1</sup>H NMR spectrum of (26b) exhibits a broad singlet at 7.01 ppm

with an integration of four olefinic protons. Also, H<sub>1</sub> and H<sub>4</sub> appear as a broad singlet at 5.25 ppm with an integration of two protons. The broadness is probably a result of the slow rotation about the N-C=O bond at room temperature. However, measurement of a <sup>15</sup>N NMR spectrum at natural abundance was straightforward using a concentrated solution (ca. 0.4 g of **(26b)** in ca. 0.25 ml of CDCl<sub>3</sub>). The <sup>15</sup>N NMR spectrum of the urethane **(26b)** shows a single peak at -203.6 ppm and is reported for the first time. This value was compared with other reported <sup>15</sup>N shifts for 7-azabicyclo[2.2.1]heptyl derivatives<sup>55</sup> **(29)** and **(30)** (Figure 2.1) which will be discussed later.

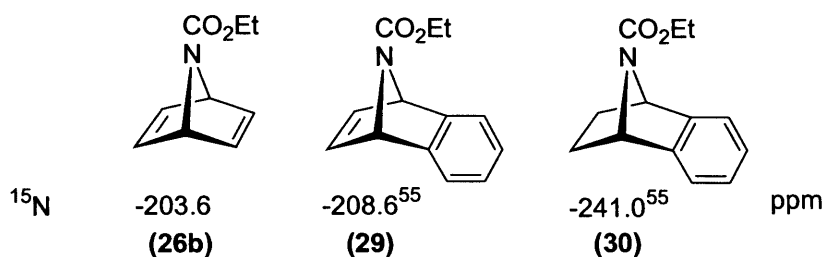


**Figure 2.1** <sup>15</sup>N chemical shift values for urethanes relative to neat CH<sub>3</sub>NO<sub>2</sub>.

#### 2.1.4 Synthesis of *N*-methyl-7-azanorbornadiene (**3a**)

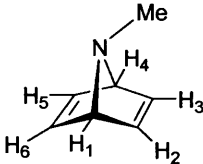
The procedure of Marchand<sup>6</sup> was used to synthesize the previously unreported tertiary amine **(3a)**. The *N*-carbethoxy-7-azanorbornadiene **(26b)** was treated with diisobutylaluminum hydride to reduce the *N*-protecting group to the free amine **(3a)**. The yield was low (11%) but was acceptable (Scheme 2.1). The major concern was the volatility of **(3a)** as the free amine. Therefore, compound **(3a)** was isolated and handled as a salt. When the free amine was required, it was extracted from a basified aqueous solution into an appropriate organic solvent.

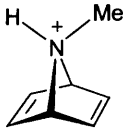
The inversion barrier of **(3a)** was measured using high temperature NMR spectroscopy and the nitrogen chemical shift of the free amine was also measured. The results of the inversion barrier and nitrogen NMR measurements will be discussed later.

#### 2.1.5 NMR spectroscopic data for the free amine (**3a**) and quaternary salt (**3a**:HCl)

<sup>1</sup>H and <sup>13</sup>C NMR spectra for **(3a)** were measured and analyzed in detail. The <sup>1</sup>H NMR spectrum of the free amine **(3a)** includes a singlet at 2.18 ppm with an integration of three protons (*N*-Me protons). Because compound **(3a)** is symmetrical, only one singlet peak is expected for the olefinic protons if inversion at N is rapid. However, two broad singlet signals were observed at 6.69 and 7.00 for the alkene protons. Thus, slow

inversion at nitrogen must be the cause of the different electronic environment for each alkene. Therefore, two invertomers of (**3a**) are present in solution at room temperature on the NMR timescale. Clearly the invertomers are isoenergetic (identical). A protonation experiment was performed using strong acid (HCl). The NMR spectroscopic data are summarized in Table 2.1.



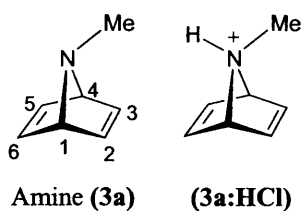


Protons	Amine ( <b>3a</b> )		<b>(3a:HCl)</b>	
	Mult.	ppm	Mult.	ppm
H <sub>1</sub> , H <sub>4</sub>	brm	4.25	brs	4.99
H <sub>2</sub> , H <sub>3</sub>	brs	7.00	brs	7.18
H <sub>5</sub> , H <sub>6</sub>	brs	6.68	brs	6.99
N-Me	s	2.19	d $J_{\text{NH,Me}} = 4.7 \text{ Hz}$	2.77

**Table 2.1** <sup>1</sup>H NMR data for amine (**3a**) and its protonated quaternary salt (**3a:HCl**).

The first thing to be noticed when looking at Table 2.1 is that each signal in the salt has been shifted downfield compared to its counterpart in the free amine (this is caused by the electron deficiency caused by the protonation at nitrogen). The fixing of the configuration at nitrogen is clearly observed in the change of multiplicity. The *N*-Me singlet in (**3a:HCl**) becomes a doublet ( $J_{\text{NH,Me}} = 4.7 \text{ Hz}$ ) in the protonated form (**3a:HCl**) as a result of vicinal coupling.

The <sup>13</sup>C NMR assignments for the free amine (**3a**) were measured at room temperature. Carbons C<sub>1</sub> and C<sub>4</sub> are α to the nitrogen atom and therefore they are shifted downfield most. Two sets of signals of the alkene carbons C<sub>2</sub>-C<sub>3</sub> and C<sub>5</sub>-C<sub>6</sub> were observed due to the slow inversion at room temperature although (**3a**) is symmetrical under conditions of rapid inversion. In the protonated form, <sup>13</sup>C chemical shifts for (**3a:HCl**) are downfield from the corresponding signals in the free amine (**3a**) due to the electron-withdrawal by the protonation at nitrogen (Table 2.2).



	Amine ( <b>3a</b> )	( <b>3a</b> :HCl)
	ppm	ppm
C <sub>1</sub> , C <sub>4</sub>	72.2	78.1
C <sub>2</sub> , C <sub>3</sub>	139.4	144.1
C <sub>5</sub> , C <sub>6</sub>	144.6	148.4
N-Me	36.2	40.4

**Table 2.2** <sup>13</sup>C NMR data for amine (**3a**) and its protonated quaternary salt (**3a**:HCl).

The assignment of the two alkene signals in both (**3a**) and (**3a**:HCl) was facilitated by the application of the  $\gamma$ -effect of carbon substitution.<sup>56</sup> The  $\gamma$ -effect is demonstrated by the <sup>13</sup>C chemical shifts of C<sub>2</sub> and C<sub>6</sub> of *syn*- and *anti*-7-methylbicyclo[2.2.1]hept-2-ene, (**31**) and (**32**) (Figure 2.2). When a carbon atom is eclipsed by another methyl group (or carbon atom) in the  $\gamma$ -position to it, the <sup>13</sup>C NMR chemical shift of that carbon atom occurs at higher field than the shift of the same carbon when the  $\gamma$ -substituent is *anti*- to it. Thus, the alkene carbon atom C<sub>2</sub> in (**31**) (the Me group is *syn* to the double bond) was observed to resonate at 132.4 ppm, 5.4 ppm upfield of the same carbon atom when the Me group is *anti* to the double bond) (**32**). Similarly, C<sub>6</sub> in (**32**) was observed to resonate upfield of its counterpart in (**31**). This is also known as a Compression Shift (induced by an eclipsing carbon atom). The concept of the  $\gamma$ -compression shift was used in the assignments of major and minor signals in the protonation experiments carried out through this work.

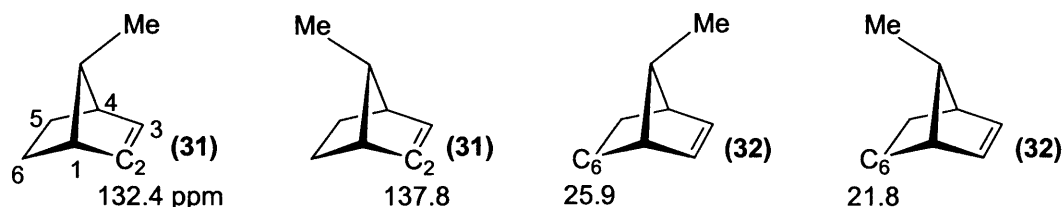
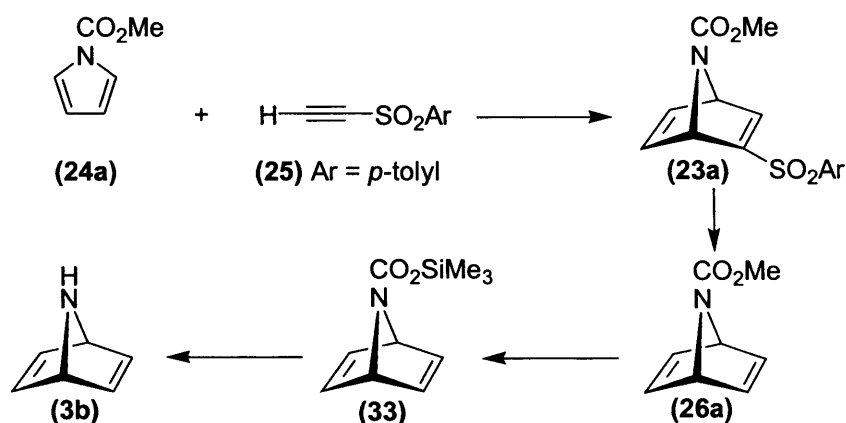


**Figure 2.2**

### 2.1.6 Synthesis of the secondary amine 7-azanorbornadiene (**3b**)

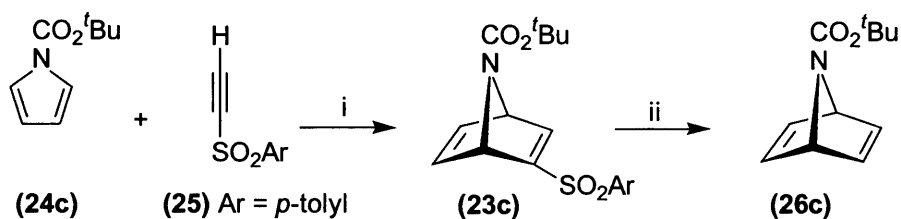
Vogel *et al.* reported the first route toward the synthesis of the parent compound (**3b**) of 7-azanorbornadiene derivatives on a preparative scale.<sup>7</sup> It is the only procedure that describes the synthesis of (**3b**) in the literature. The general overview of this

synthesis is shown in Scheme 2.4. A cycloaddition reaction of *N*-methoxycarbonylpyrrole (**24a**) and the acetylene equivalent ethynyl-*p*-tolyl sulfone (**25**) afforded adduct (**23a**). The reductive removal of the *p*-toluenesulfonyl group was performed with 6% sodium amalgam to afford (**26a**) which was then treated with trimethylsilyl iodide to give (**33**). The silyl ester (**33**) reacted with methanol via the carbamic acid to give the desired secondary amine (**3b**).<sup>7</sup>



**Scheme 2.4**

An alternative method for the synthesis of the secondary amine (**3b**) was developed by us. The *N*-*tert*-butyloxycarbonyl protecting group, which could be removed under milder conditions, was chosen in place of the *N*-methoxycarbonyl group used by Vogel.<sup>7</sup> Thus, heating a solution of *p*-tolylsulfonyl acetylene (**25**) and the commercially available *N*-(*tert*-butyloxycarbonyl)pyrrole (**24c**) provided the [4+2] cycloaddition adduct (**23c**) in 70% yield.<sup>57</sup> Desulfonation of (**23c**) using the same conditions described in Scheme 2.1 afforded a low yield (22%) of the desired compound (**26c**) (Scheme 2.5). The <sup>15</sup>N NMR spectrum of urethane (**26c**) was also measured and showed a single peak at -202.6 ppm which will be discussed later in context.



**Scheme 2.5** Reagents and conditions: (i) 80-85 °C, 48 h; (ii) 6% Na/Hg, Na<sub>2</sub>HPO<sub>4</sub> in THF/CH<sub>3</sub>OH (1:1), -78 °C, 4 h.

The reduction reaction of **(23c)** with 6% sodium amalgam afforded a major byproduct containing the sulfonyl moiety, which warranted further investigation. Indeed, it might be the cause of the low yield of **(26c)**. It was thought to be the consequence of methanol adding across the functionalized ethano- bridge since a 3-proton singlet appeared in the  $^1\text{H}$  NMR spectrum of the product. However, there is unfortunately no evidence to suggest that avoidance of methanol could enhance the yield since when the reaction was attempted in the absence of methanol; the result was simply a low yield of **(26c)**.

The byproduct was identified and characterized as the novel 5-methoxy-6-tosyl-7-azabicyclo[2.2.1]hept-2-ene derivatives **(34)** (Figure 2.3). The mass spectral data confirmed the overall addition of methanol to the azabicyclic system. The  $^1\text{H}$  NMR spectroscopic data also were examined and the methoxy and tosyl groups were assigned as *exo*- and *endo*- respectively with the aid of a  $^1\text{H}$  NMR COSY experiment. It was obvious that  $\text{H}_6$  is coupled to  $\text{H}_1$  which indicates that  $\text{H}_6$  is in the *exo*- position. On the other hand, no coupling was noticed between  $\text{H}_5$  and  $\text{H}_4$ . Two olefinic protons ( $\text{H}_2$  and  $\text{H}_3$ ) were observed at 6.56 and 6.39 ppm. The methoxy protons integrated for three protons and appear as broad singlet at 3.35 ppm. The bridgehead protons ( $\text{H}_1$  and  $\text{H}_4$ ) appear at 4.60 and 4.76 ppm respectively. Moreover, the stereochemistry of **(34)** obtained from the reduction reaction was confirmed by X-ray crystallographic analysis (Figure 2.3).

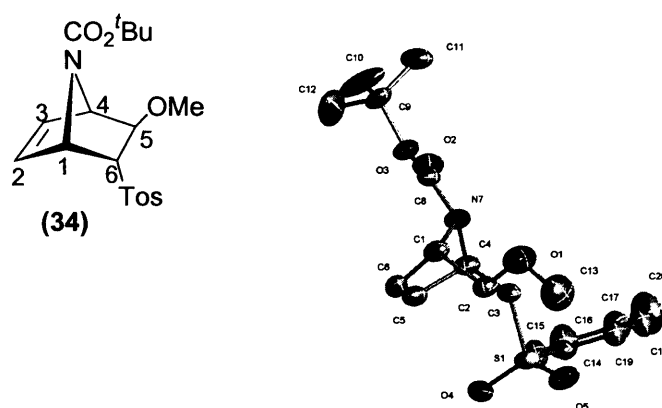
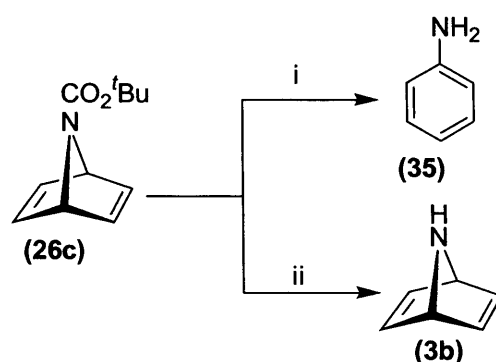


**Figure 2.3** X-ray structure of **(34)**.

There was an attempt to remove the Boc group in **(26c)** using 3M HCl (formed *in situ* at 0 °C from ethanol (2.7 ml), ethyl acetate (7.2 ml) and acetyl chloride (2.7 ml)) which unfortunately led to the formation of aniline **(35)** *via* opening of the azabicyclic ring system. On the other hand, using MeOH saturated with HCl at 0 °C led to removal of the

Boc protecting group without rearrangement to afford the desired product (**3b**). This was repeated successfully on a preparative scale (Scheme 2.6). Great care was necessary during the reaction and work-up since the ring-opening side reaction was noticeable when the reaction mixture was left to warm up to room temperature or left for a longer time. However, the secondary amine (**3b**) itself is not acid sensitive and reacts with hydrogen chloride in dichloromethane to give the hydrochloride salt (**3b:HCl**) which is stable when stored in the fridge for long time. Vogel reported that the free amine (**3b**) undergoes fragmentation into pyrrole and acetylene *via* retro Diels-Alder reaction when heated above 80 °C.<sup>7</sup>



**Scheme 2.6** Reagents and conditions: (i) 3M HCl *in situ* (ethanol (2.7 ml), ethyl acetate (7.2 ml) and acetyl chloride (2.7 ml), 0 °C; (ii) MeOH, HCl, 0 °C.

### 2.1.7 <sup>1</sup>H NMR spectroscopic data for the free amine (**3b**) and quaternary salt (**3b:HCl**)

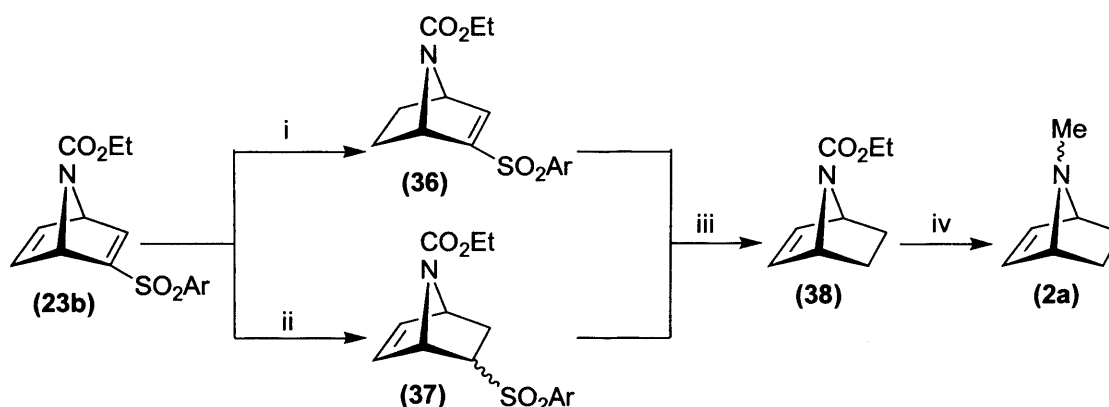
Our samples of the secondary amine (**3b**) and its salt (**3b:HCl**) had spectral data in accord with those described previously.<sup>7</sup> The <sup>1</sup>H NMR spectrum of the free amine (**3b**) consists of a signal at 7.03 ppm which corresponds to four olefinic protons and a signal at 4.73 ppm for the two bridgeheads protons. A protonation experiment was performed using strong acid (HCl) to form the salt (**3b:HCl**). Similar protonation shifts to those described for (**3a:HCl**) were observed. The spectroscopic data are summarized in Table 2.3.

Protons	Amine ( <b>3b</b> ) ppm	( <b>3b</b> :HCl) ppm
H <sub>1</sub> , H <sub>4</sub>	4.73	5.21
H <sub>2</sub> , H <sub>3</sub> , H <sub>5</sub> , H <sub>6</sub>	7.03	7.18
N-H	1.68	

**Table 2.3** <sup>1</sup>H NMR data for amine (**3b**) and its protonated quaternary salt (**3b**:HCl).

## 2.2 Routes to *N*-methyl-7-azanorbornene (**2a**)

The routes used to synthesize the *N*-methyl-7-azanorbornene (**2a**) are outlined in Scheme 2.7 using 7-azabicyclo[2.2.1]heptadiene (**23b**) as starting material. Two slightly different approaches (*via* (**36**) or (**37**)) are possible as illustrated in Scheme 2.7.



**Scheme 2.7** Reagents and conditions: (i) H<sub>2</sub>, Pd/C in CH<sub>3</sub>CN; (ii) NaBH<sub>4</sub>, CH<sub>3</sub>OH, RT, (iii) 6% Na/Hg, Na<sub>2</sub>HPO<sub>4</sub> in CH<sub>3</sub>OH; (iv) (*i*-Bu)<sub>2</sub>AlH, Toluene, RT, 8 h.

### 2.2.1 Synthesis of 7-azabicyclo[2.2.1]hept-2-ene sulfone (**36**)

The 7-azabicyclo[2.2.1]hept-2-ene sulfone (**36**) can be obtained by a selective reduction of the 5,6 carbon-carbon double bond of (**23b**) using the method of Vogel.<sup>4</sup> The reaction here was carried out with one equivalent of hydrogen and Pd/C as catalyst to yield 93% of (**36**) which has not been reported in the literature with the ethoxycarbonyl *N*-protecting group (Scheme 2.7).

The <sup>1</sup>H NMR spectrum of (**36**) shows only one alkene proton signal at δ 7.04 which is assigned to H<sub>3</sub>. The CH<sub>3</sub> and CH<sub>2</sub> protons of the ethoxy group are broad peaks due to restricted rotation about the N-C=O bond at room temperature.

### 2.2.2 Synthesis of 7-azabicyclo[2.2.1]hept-2-ene sulfone (37)

Selective reduction of the 2,3-double bond conjugated with the sulfone moiety can be achieved. Thus, reaction of (23b) with excess sodium borohydride<sup>57</sup> in methanol gave the product (37) of conjugate reduction as a mixture of *endo*- and *exo*- sulfone isomers (7:3 respectively). The yield of the isomers mixture was high (96%) and there was no need for separation before the next desulfonation step.

The <sup>1</sup>H NMR chemical shifts of the protons bonded to the same carbon that linked to the tosyl group are shifted downfield (3.73 and 3.04 ppm) for *endo*- and *exo*-sulfone respectively. The <sup>1</sup>H NMR spectrum for *endo*-(37) shows alkene proton signals at 6.53 and 6.43 ppm for H<sub>3</sub> and H<sub>2</sub> respectively.

### 2.2.3 Synthesis of 7-azanorbornene (38)

The first practical route for the synthesis of the key intermediate (38) was described by Marchand.<sup>6</sup> The disadvantage of this synthesis was the low yield of the starting material which is obtained in 15 – 20% by the cycloaddition reaction of acetylenedicarboxylic acid to *N*-benzylpyrrole.

As alternative methods, 7-azanorbornene (38) can be synthesized by two routes from either compound (36) or (37). The two routes are different according to the status of the carbon atom that bonds to the sulfone group. In compounds (36) and (37), the sulfone is bonded to sp<sup>2</sup> or sp<sup>3</sup> carbon atom respectively which may affect the desulfonation reaction. Because compounds (36) and (37) give identical compound (38), it is important to investigate which route is more efficient and reliable.

Desulfonation of (36) with 1.7 equivalents of 6% sodium amalgam in MeOH-THF (1:1) at -78 °C gave the *N*-ethoxycarbonyl protected 7-azanorbornene (38) in low yield (20%) (Scheme 2.7). The use of an excess of the Na(Hg) amalgam led to further reduction of the double bond of (36) to give a mixture of (38) and saturated protected 7-azanorbornane derivatives (1) judged by the <sup>1</sup>H NMR spectra. Thin-layer chromatography (TLC) shows a difficult separation between the two compounds (38) and the saturated protected 7-azanorbornane derivatives (1). Therefore, it has been concluded that this route is not efficient.

On the other hand, desulfonation of (37) with 9 equivalents of 6% sodium amalgam at -78 °C affords (38) in low yield (18%) as a colorless liquid after chromatography on silica gel. Hodgson, *et al.*<sup>58</sup> reported the desulfonation of a similar system by using the same conditions except that the reaction temperature range employed

was at -10 °C to room temperature (Scheme 2.7). By using the latter method, which was the more reliable method in our hands, the reductive removal of the sulfone group of (37) afforded the desired alkene (38) as major product (44% yield) as a colorless liquid after chromatography on silica gel. Moreover, Carroll *et. al.* reported an alternative method to prepare a similar system of (38) with different protecting groups in high yield by adding tributyltin hydride to a similar system to (36) (with different protecting groups) in benzene containing 2,2'-azobisisobutyronitrile (AIBN) followed by treatment of the resulting addition product with tetrabutylammonium fluoride in tetrahydrofuran.<sup>59</sup>

The <sup>1</sup>H NMR spectrum of (38) exhibits a broad singlet at 6.23 ppm with a relative integration of two olefinic protons. Also, H<sub>1</sub> and H<sub>4</sub> appear as a broad singlet at 4.73 ppm with an integration of two protons. The two *exo* protons (1.86 ppm) are shifted downfield compared to the two *endo* protons (1.12 ppm). The two *exo* protons which were assigned using a <sup>1</sup>H COSY experiment coupled to the bridgehead protons H<sub>1</sub> and H<sub>4</sub>. On the other hand, the two *endo* protons do not couple to the bridgehead protons H<sub>1</sub> and H<sub>4</sub> in agreement with the Karplus relationship. The broadness is probably a result of the slow rotation about the N-C=O bond at room temperature. However, measurement of a <sup>15</sup>N NMR spectrum at natural abundance was straightforward using a concentrated solution (ca. 0.25 g of (38) in ca. 0.25 ml of CDCl<sub>3</sub>). The <sup>15</sup>N NMR spectrum of the urethane (38) shows a single peak at -247.3 ppm and is reported for the first time. This value was compared with other reported <sup>15</sup>N shifts for 7-azabicyclo[2.2.1]heptyl derivatives<sup>55</sup> (Figure 2.4) and with (26b) which will be discussed later.

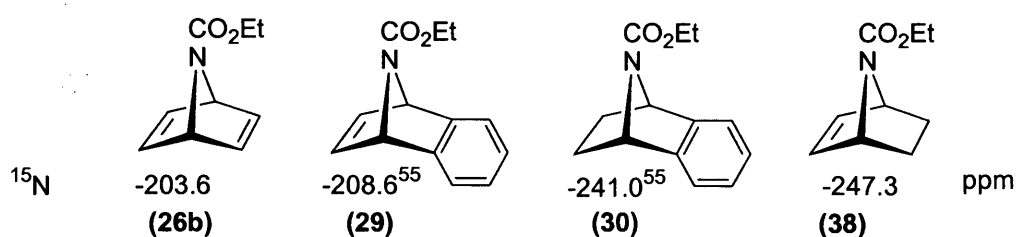


**Figure 2.4** <sup>15</sup>N chemical shift values for urethanes relative to neat CH<sub>3</sub>NO<sub>2</sub>.

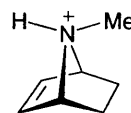
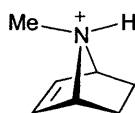
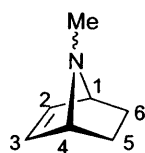
#### 2.2.4 Synthesis of *N*-methyl-7-azanorbornene (2a)

Marchand reported in 1975 the first and only synthesis in the literature of *N*-methyl-7-azanorbornene (2a).<sup>6</sup> In our approach to (2a), a slightly different route was followed using methodology established in other work, as described above (Scheme 2.7). Reduction of the *N*-protecting group of the key intermediate (38) with lithium aluminium hydride afforded the desired compound (2a) in high yield (84%).

In addition, the  $^{15}\text{N}$  chemical shift for the salt (**2a:HCl**) and  $^{14}\text{N}$  chemical shift for (**2a**) were measured and reported for the first time. There was an attempt to measure  $^{15}\text{N}$  shift for the free amine (**2a**) at room temperature, but no result was obtained after thousands of scans, possibly as a result of rapid inversion at nitrogen. Moreover, the inversion barrier was measured here for (**2a**) and the result will be compared with Marchand's result that was reported in 1975.<sup>6</sup> The nitrogen chemical shifts and the inversion barrier results will be discussed later.

### 2.2.5 NMR spectroscopic data for the free amine (**2a**) and quaternary salt (**2a:HCl**)

$^1\text{H}$  and  $^{13}\text{C}$  NMR spectra for (**2a**) were measured and analyzed in detail. The assignment of the  $^1\text{H}$  NMR peaks of the free amine (**2a**) was previously made by Marchand.<sup>6</sup> His assignment is consistent with this work, although our use of higher field naturally led to changes in the appearance of the spectrum of the mixture of invertomers.  $^1\text{H}$  NMR chemical shifts in our results demonstrate a broad singlet at 5.92 ppm which corresponds to two olefinic protons at room temperature. The bridgehead protons ( $\text{H}_1$  and  $\text{H}_4$ ) appear as broad singlet at 3.69 ppm. The *exo*- protons signal ( $\text{H}_{5\text{-exo}}$  and  $\text{H}_{6\text{-exo}}$ ) (1.81 ppm) is shifted downfield compared with that for the *endo*- protons ( $\text{H}_{5\text{-endo}}$  and  $\text{H}_{6\text{-endo}}$ ) (0.97 ppm) as observed for (**38**).  $^{13}\text{C}$  NMR spectroscopic data are reported here for the first time. The  $^{13}\text{C}$  NMR assignment for (**2a**) was made easily by using DEPT experiments which simplified the spectrum and differentiated between CH,  $\text{CH}_2$  and  $\text{CH}_3$ . The  $^{13}\text{C}$  NMR spectrum shows 4 signals which correspond to alkene (130.3 ppm), bridgehead (66.4 ppm), ethano- ( $\text{H}_2\text{C}-\text{CH}_2$ ) (24.7 ppm) and *N*-Me (34.6 ppm). A protonation experiment was performed using strong acid (HCl). The spectroscopic data for (**2a:HCl**) are summarized in Tables 2.4 and 2.5 together with comparison data for the (rapidly inverting) free amine (**2a**).



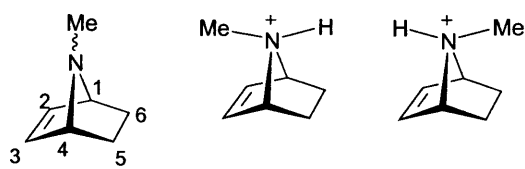
Amine ( <b>2a</b> )			<i>syn</i> -( <b>2a:HCl</b> )			<i>anti</i> -( <b>2a:HCl</b> )		
Protons	Mult.	ppm	Mult.	ppm	ppm	Mult.	ppm	ppm
H <sub>2</sub> , H <sub>3</sub>	brs	5.92	brs	6.29	6.46			
H <sub>1</sub> , H <sub>4</sub>	brs	3.69	brs	4.46	4.46			
H <sub>5</sub> , H <sub>6</sub>	brd	<i>exo</i> - 1.81	brd	<i>exo</i> - overlapped	<i>exo</i> - 2.17			
	brd	<i>endo</i> - 0.97	brd	<i>endo</i> - 1.40	<i>endo</i> - 1.56			
N-Me	s	2.05	d	2.66	2.66			

$$J_{\text{NH,Me}} = 4.8 \text{ Hz}$$

**Table 2.4** <sup>1</sup>H NMR data for amine (**2a**) and its protonated quaternary salt (**2a:HCl**).

As observed earlier, the proton chemical shifts of the salt (**2a:HCl**) have been shifted downfield compared to their counterparts in the free amine (**2a**) Table 2.4. The fixing of the configuration at nitrogen is clearly observed in the change of the *N*-Me multiplicity which becomes a doublet ( $J_{\text{NH,Me}} = 4.8 \text{ Hz}$ ) in the protonated form (**2a:HCl**). Moreover, two diastereoisomeric salts of (**2a:HCl**) were observed. Therefore, two sets of signals of (**2a:HCl**) were recognized for the etheno- and ethano- protons due to the position of the *N*-Me group (*syn* or *anti* to the alkene group).

Two sets of peaks were also seen in the <sup>13</sup>C NMR spectrum of the protonated form of (**2a:HCl**) (Table 2.5). The <sup>13</sup>C NMR assignment of C<sub>5</sub> and C<sub>6</sub> fits with the  $\gamma$ -effect phenomenon where C<sub>6</sub> in the *anti*- isomer is 2.4 ppm upfield from the same carbon in the *syn*- isomer. A similar effect is observed on the alkene carbon C<sub>2</sub> and C<sub>3</sub> in the *syn*- isomer (3.4 ppm upfield) compared to C<sub>2</sub> in the *anti*- isomer. Based on this assignment, the average ratio calculated by <sup>13</sup>C NMR was 74% *syn*-methyl to 26% *anti*-methyl. This ratio is in good agreement with the ratio of the quaternary salts measured by <sup>1</sup>H NMR. Two <sup>15</sup>N NMR signals were also observed for the two diastereoisomeric salts of (**2a:HCl**) at -290.8 and -292.8 ppm.

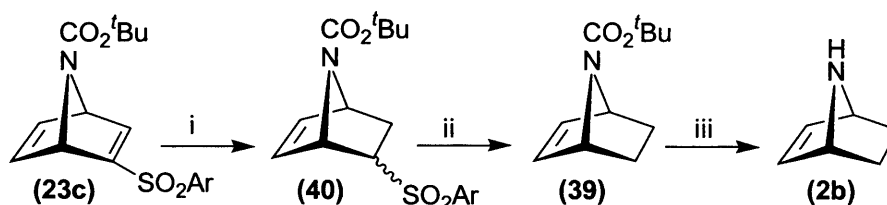


	Amine ( <b>2a</b> )	<i>syn</i> -( <b>2a</b> :HCl)	<i>anti</i> -( <b>2a</b> :HCl)
	ppm	ppm	ppm
C <sub>1</sub> , C <sub>4</sub>	66.4	67.3	65.7
C <sub>2</sub> , C <sub>3</sub>	130.3	130.4	133.8
C <sub>5</sub> , C <sub>6</sub>	24.7	21.9	19.5
N-Me	34.6	32.4	34.5

**Table 2.5** <sup>13</sup>C NMR data for amine (**2a**) and its protonated quaternary salt (**2a**:HCl).

### 2.2.6 Synthesis of the secondary amine 7-azanorbornene (**2b**)

A five-step synthesis of 7-azanorbornene (**2b**) which was developed by Marchand<sup>6</sup> has already been in the literature for some time. However, this method has not been widely taken up in the literature because it is not suitable for the preparation of (**2b**) in sufficient yield. Vogel has developed a synthetic route starting from (**23a**) (Scheme 2.1) to obtain (**2b**) in pure form.<sup>4</sup> Most recently, Hodgson *et. al.* reported the synthesis of (**2b**) in quantitative yield from the known *N*-Boc-azanorbornene (**39**) key intermediate (Scheme 2.8).<sup>60</sup> Thus, deprotection of (**39**) with TFA gave the desired 7-azanorbornene (**2b**). Scheme 2.8 describes the synthetic route that was followed by us to synthesize the target compound (**2b**) with a small variation involving the use of 3M HCl generated *in situ* at 0 °C from ethanol (2.7 ml), ethyl acetate (7.2 ml) and acetyl chloride (2.7 ml) for the deprotection step. Compound (**2b**) is not acid sensitive but needs to be handled carefully because it is a volatile compound. Therefore, it was isolated as a salt (**2b**:HCl).



**Scheme 2.8** Reagents and conditions: (i) NaBH<sub>4</sub>, CH<sub>3</sub>OH, RT, (ii) 6% Na/Hg, Na<sub>2</sub>HPO<sub>4</sub> in THF/CH<sub>3</sub>OH (2:1); (iii) 3M HCl generated *in situ* (ethanol (2.7 ml), ethyl acetate (7.2 ml) and acetyl chloride (2.7 ml), 0 °C, 4h, RT.

Through the synthetic steps of (**2b**), it was of interest to measure the <sup>15</sup>N chemical shift for the simple key intermediate (**39**). The <sup>15</sup>N chemical shift for (**39**) is -248.1 ppm

which is similar to that measured for **(38)** (Scheme 2.7) and the results will be discussed later.

### 2.2.7 NMR spectroscopic data for the free amine (**2b**) and quaternary salt (**2b:HCl**)

$^1\text{H}$  and  $^{13}\text{C}$  NMR spectra for **(2b)** were measured and analyzed in detail. The  $^1\text{H}$  NMR spectroscopic data for the free amine (**2b**) are similar to those reported earlier.<sup>6</sup> The signals at  $\delta$  6.16 ppm are due to the alkene protons ( $\text{H}_2$  and  $\text{H}_3$ ) and appear as a broad singlet. The bridgehead protons ( $\text{H}_1$  and  $\text{H}_4$ ) also appear as a broad singlet at  $\delta$  4.06. The chemical shift for the *exo* protons ( $\text{H}_5$  and  $\text{H}_6$ ) (1.67 ppm) are shifted downfield compared to those *endo* protons of ( $\text{H}_5$  and  $\text{H}_6$ ) (0.95 ppm) as observed for the similar system (**2a**). The  $^{13}\text{C}$  NMR spectrum shows three signals which correspond to the alkene group ( $\text{C}_2$  and  $\text{C}_3$ ) (136.0 ppm), bridgehead ( $\text{C}_1$  and  $\text{C}_4$ ) (58.8 ppm) and ethano- ( $\text{C}_5$  and  $\text{C}_6$ ) (26.6 ppm). There was an attempt to measure the  $^{15}\text{N}$  chemical shift at room temperature for the free amine (**2b**), but no result could be obtained from the small sample available, even after thousands of scans. A protonation experiment was performed using strong acid (HCl). The spectroscopic data are summarized in Table 2.6.

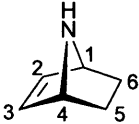
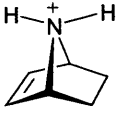
Protons	Amine ( <b>2b</b> )		( <b>2b:HCl</b> )	
	Mult.	ppm	Mult.	ppm
$\text{H}_2, \text{H}_3$	brs	6.16	s	6.57
$\text{H}_1, \text{H}_4$	brs	4.06	brs	4.95
$\text{H}_5, \text{H}_6$	m	<i>exo</i> - 1.67	brd	<i>exo</i> - 2.29
	brd	<i>endo</i> - 0.95	brd	<i>endo</i> - 1.61
NH	brs	1.92		

**Table 2.6**  $^1\text{H}$  NMR data for amine (**2b**) and its protonated quaternary salt (**2b:HCl**).

As noticed earlier, every proton in the protonated form of the salt (**2b:HCl**) is downfield from its counterpart in the free amine (**2b**) due to the electron withdrawal by the protonation at nitrogen (Table 2.6).

The  $^{13}\text{C}$  NMR assignments for the free amine (**2b**) and (**2b:HCl**) were made easily by using the same method described for (**3a**). In the protonated form, two  $^{13}\text{C}$  chemical signals for (**2b:HCl**) are shifted upfield from their counterparts in the free amine (**2b**) which was unexpected. Only, the bridgehead carbons ( $\text{C}_1$  and  $\text{C}_4$ ) are shifted downfield

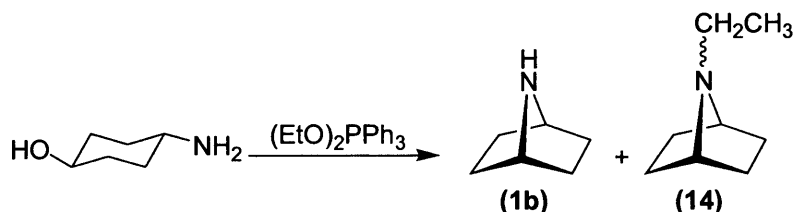
for **(2b:HCl)** compared to the free amine **(2b)** Table 2.7. Similar observation was observed with different azabicyclic systems such as 2-azabicyclo[2.2.1]heptyl and -[2.2.2]octyl derivatives where the  $^{13}\text{C}$  NMR shifts of the protonated forms are not always shifted downfield from its free amine.<sup>61</sup>

		
	<b>Amine (2b)</b>	<b>(2b:HCl)</b>
	ppm	ppm
C <sub>1</sub> , C <sub>4</sub>	58.8	61.2
C <sub>2</sub> , C <sub>3</sub>	136.0	133.5
C <sub>5</sub> , C <sub>6</sub>	26.6	22.0

**Table 2.7**  $^{13}\text{C}$  NMR data for amine **(2b)** and its protonated quaternary salt **(2b:HCl)**.

### 2.3 Synthesis of *N*-methyl-7-azanorbornane (**1a**)

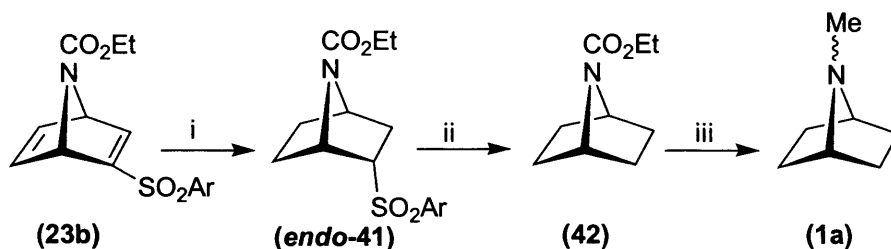
To date, there are few reports describing the synthesis of *N*-methyl-7-azanorbornane (**1a**). *N*-Methyl-7-azanorbornane (**1a**) was first prepared by Fraser and Swingle in 1970 in five steps using a Leuckart reduction of the parent 7-azabicyclo[2.2.1]heptane (**1b**) in 53% yield.<sup>62</sup> In a later study in 1989, Nelsen *et al.*<sup>3</sup> reported a modification of Fraser and Swingle's method to synthesize (**1b**) in a one-step reaction by cyclization of *trans*-4-hydroxycyclohexylamine with diethoxytriphenylphosphorane affording a mixture of (**1b**) and 7-ethyl-azabicyclo[2.2.1]heptane (**18**) (18%) (Scheme 2.9). (**1b**) was then converted easily with ethyl chloroformate into (**42**).<sup>3</sup> Reduction of (**42**) with LAH gave the desired methyl derivative (**1a**) (Scheme 2.10).



**Scheme 2.9**

As illustrated in Scheme 2.10, our synthetic approach to the 7-azanorbornane derivative (**1a**) was developed using earlier methods, starting from (**23b**). Thus, reduction of the double bonds using hydrogen over Pd/C gave 98% of the novel *endo*-(**41**). Reductive cleavage of the sulfonyl group of *endo*-(**41**) using 6% sodium amalgam in

methanol-THF gave the *N*-ethoxycarbonyl-protected 7-azanobornane (**42**) in reasonable yield (50%). Similar reduction of the *N*-ethoxycarbonyl-protected 7-azanobornane (**42**) with LAH afforded the desired *N*-methyl derivative (**1a**) in high yield (95%). The free amine (**1a**) is not acid sensitive and was isolated as a salt (**1a**:HCl) because of its high volatility.



**Scheme 2.10** Reagents and conditions: (i) H<sub>2</sub>, Pd/C in CH<sub>3</sub>CN; (ii) 6% Na/Hg, Na<sub>2</sub>HPO<sub>4</sub> in THF:CH<sub>3</sub>OH (2:1), -10 °C 10 min. to RT, 3h; (iii) LiAlH<sub>4</sub>, diethyl ether, reflux, 8 h.

In the *endo*-tosyl compound (**41**), the <sup>1</sup>H NMR signal due to H<sub>2</sub> is shifted downfield (3.55 ppm) by the tosyl group. The assignment of the <sup>1</sup>H NMR signals of (**42**) was previously reported by Nelsen.<sup>3</sup> His assignment is consistent with this work. The <sup>13</sup>C NMR spectrum has not been described in the literature. The assignments of the <sup>13</sup>C chemical shifts were 56.0 and 29.6 ppm for (C<sub>1</sub> and C<sub>4</sub>) and (C<sub>2</sub>, C<sub>3</sub>, C<sub>5</sub> and C<sub>6</sub>) respectively. Duplication of signals were observed for apparently equivalent carbons in the symmetrical heterocycle framework as a result of slow rotation around the N-C=O bond. The measurement of the <sup>15</sup>N chemical shift of (**42**) was considered important to this investigation; the <sup>15</sup>N signal was observed at -259.5 ppm and the comparisons with other *N*-protected 7-azabicyclic systems (Figure 2.5) will be discussed later in more detail.

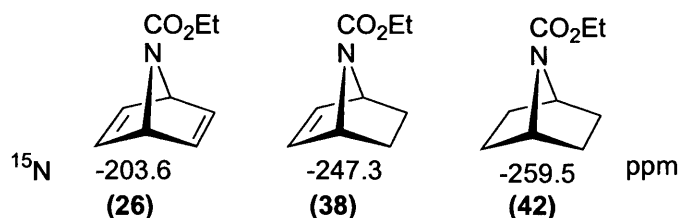


**Figure 2.5** <sup>15</sup>N chemical shift values for urethanes relative to neat CH<sub>3</sub>NO<sub>2</sub>.

### 2.3.1 NMR spectroscopic data for amine (1a) and the quaternary salt (1a:HCl)

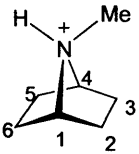
$^1\text{H}$  and  $^{13}\text{C}$  NMR spectra for (1a) were measured and analyzed in detail as done previously. The  $^1\text{H}$  NMR chemical shifts for the free amine (1a) were similar to the literature values.<sup>3</sup> The bridgehead protons ( $\text{H}_1$  and  $\text{H}_4$ ) appear at 3.17 ppm which are shifted upfield compared with (2a) and (3a). The *exo*- protons are shifted downfield compared with the *endo*- protons (1.77 and 1.27 ppm respectively). The *exo*- protons can be easily distinguished from the *endo*- protons using  $^1\text{H}$  COSY experiment. The *exo*- protons couple to the bridgehead protons  $\text{H}_1$  and  $\text{H}_4$ . On the other hand, the two *endo* protons do not couple to the bridgehead protons  $\text{H}_1$  and  $\text{H}_4$  (Karplus relationship). A protonation experiment was performed using strong acid (HCl). The spectroscopic data are summarized in Table 2.8.

Amine (1a)			(1a:HCl)		
Protons	Mult.	$\delta$ (ppm)	Protons	Mult.	$\delta$ (ppm)
$\text{H}_1, \text{H}_4$	brm	3.17	$\text{H}_1, \text{H}_4$	brs	3.93
$\text{H}_2, \text{H}_3, \text{H}_5, \text{H}_6$	brs	<i>exo</i> - 1.77	$\text{H}_2, \text{H}_3$	brd	<i>exo</i> - 2.55
	brd	<i>endo</i> - 1.27	$\text{H}_5, \text{H}_6$	brd	<i>exo</i> - 2.13
N-Me	s	2.24	$\text{H}_2, \text{H}_3$	brd	<i>endo</i> - 1.71
			$\text{H}_5, \text{H}_6$	brd	<i>endo</i> - 1.69
			N-Me	d $J_{\text{NH},\text{Me}} = 5.1$ Hz	2.77

**Table 2.8**  $^1\text{H}$  NMR data for amine (1a) and its protonated quaternary salt (1a:HCl).

Table 2.8 shows the usual downfield shifts for the salt compared to the corresponding signals for the free amine because of the electron deficiency induced by the protonated nitrogen. The fixing of the configuration at nitrogen is clearly observed in the changes of multiplicity. The *N*-Me singlet in (1a:HCl) becomes a doublet ( $J_{\text{NH},\text{Me}} = 5.1$  Hz) in the protonated form as a result of vicinal coupling. Moreover, two sets of signals for both *exo*- and *endo*- protons were observed as a result of the fixing of the *N*-Me group. The  $^{13}\text{C}$  NMR assignment for the free amine (1a) was made easily by using DEPT experiment which simplified the spectrum and distinguished between  $\text{CH}$ ,  $\text{CH}_2$  and  $\text{CH}_3$  (Table 2.9). Only one  $\text{CH}_2$   $^{13}\text{C}$  signal of the free amine (1a) was observed as a result of the symmetry. On the other hand, two  $\text{CH}_2$   $^{13}\text{C}$  signals of the protonated form (1a:HCl) were observed as a result of having two different electronic environments cause by the *N*-

Me group. The  $^{13}\text{C}$  NMR assignment of  $\text{C}_2$  and  $\text{C}_6$  fits again with the  $\gamma$ -effect phenomenon where  $\text{C}_2$  in the *syn*- stereoisomer (according to the *N*-Me group) is upfield from the  $\text{C}_6$  carbon where it is *anti*- to the *N*-Me group (Table 2.9).

			
Amine ( <b>1a</b> )	( <b>1a:HCl</b> )		
	$\delta$ (ppm)		
$\text{C}_1, \text{C}_4$	61.2	$\text{C}_1, \text{C}_4$	64.4
$\text{C}_2, \text{C}_3, \text{C}_5, \text{C}_6$	br 28.6	$\text{C}_2, \text{C}_3$	25.8
		$\text{C}_5, \text{C}_6$	27.9
<i>N</i> -Me	34.8	<i>N</i> -Me	32.6

**Table 2.9**  $^{13}\text{C}$  NMR data for amine (**1a**) and its quaternary salt (**1a:HCl**).

The structure of the free amine (**1a**) was confirmed indirectly by the X-ray crystal structure of its salt (**1a:HCl**) as shown in Figure 2.6. This new result is reported here for the first time as the simplest structure of the 7-azanorbornane derivatives. The CNC bond angle of (**1a:HCl**) is  $95.4^\circ$  which is close to the value for norbornane<sup>20</sup> and other reported 7-azanorbornane derivatives.<sup>37</sup> The effect of the CNC bond angle on the inversion barrier will be discussed in more detail in Chapter 6.

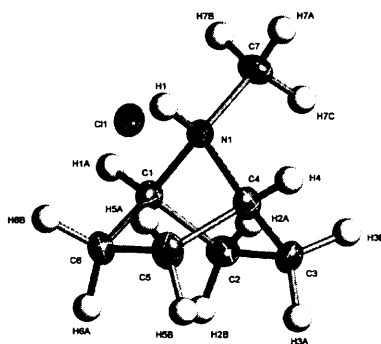


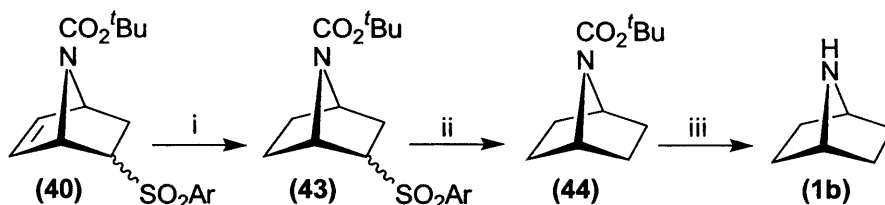
**Figure 2.6** Crystal structure of (**1a:HCl**).

### 2.3.2 Synthesis of the secondary amine 7-azanorbornane (**1b**)

The first synthesis of 7-azabicyclo[2.2.1]heptane (**1b**) was reported by Braun and Schwarz in 1930 with less than 1% overall yield.<sup>63</sup> An improved synthesis of (**1b**) was later reported by Fraser and Swingle in 1970 which increased the overall yield of (**1b**) to

38%.<sup>62</sup> Moreover, Nelsen *et al.* as mentioned above, showed that *trans*-4-hydroxycyclohexylamine could be directly converted into the 7-azabicyclo[2.2.1]heptane (**1b**) (26%) and 7-ethyl-azabicyclo[2.2.1]heptane (**18**) (Scheme 2.9).<sup>3</sup> The disadvantage of Nelsen's method is that the separation between (**1b**) and (**18**) is difficult to achieve unless (**1b**) is converted to (**42**) as described above. Both of these syntheses of (**1b**) depend on the transannular ring-closure reactions of cyclohexylamine derivatives.

Vogel *et al.* reported the synthesis of (**1b**) by hydrogenation of (**3b**).<sup>4</sup> Our synthetic approach to (**1b**) is shown in Scheme 2.11 and constitutes a new route to the target compound making use of methods and intermediates described earlier in Chapters 2 and 3.



**Scheme 2.11** Reagents and conditions: (i) H<sub>2</sub>, Pd/C in CH<sub>3</sub>CN; (ii) 6% Na/Hg, Na<sub>2</sub>HPO<sub>4</sub> in THF:CH<sub>3</sub>OH (2:1), -10 °C 10 min. to RT, 3h; (iii) 3M HCl generated *in situ* (ethanol (2.7 ml), ethyl acetate (7.2 ml) and acetyl chloride (2.7 ml), 0 °C, 4h, RT).

The 7-azabicyclo[2.2.1]hept-2-ene derivatives (**40**) was hydrogenated to give (**43**) in high yield (97%). The key intermediate (**44**) was prepared in similar fashion from (**43**) in good yield (55%) using 6% sodium amalgam and was then converted into (**1b**) with 3M HCl generated *in situ* at 0 °C from ethanol (2.7 ml), ethyl acetate (7.2 ml) and acetyl chloride (2.7 ml).

The <sup>1</sup>H and <sup>13</sup>C NMR spectroscopic data for (**43**) and (**44**) are similar to those reported in the literature.<sup>64</sup> The <sup>15</sup>N NMR shift for the key intermediate (**44**) (-257.5 ppm) was measured for the first time and it will be compared with the other urethane data in the <sup>15</sup>N NMR spectroscopic chapter.

The <sup>1</sup>H and <sup>13</sup>C NMR spectroscopic analysis for (**1b**) and its salt (**1b:HCl**) are assigned similarly to (**2b**) and (**3b**). The <sup>15</sup>N NMR chemical shifts of the free amine (**1b**) and the counterpart (**1b:HCl**) were measured to be -304.4 and -309.5 ppm respectively. These new results will be discussed later in Chapter 5.

## **Chapter 3**

### **Synthesis of novel 1,4-dimethyl-7-azabicyclo[2.2.1]heptane derivatives**

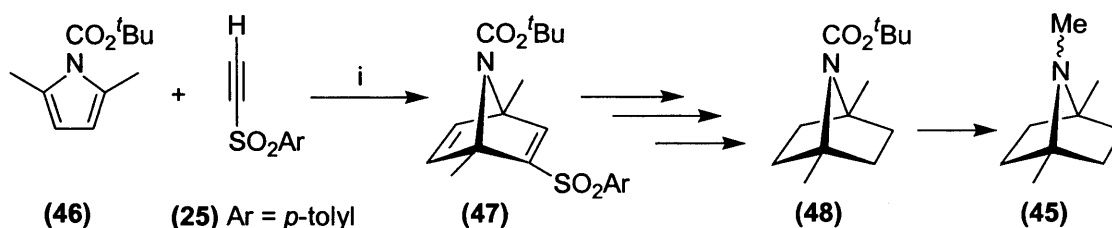
## Chapter 3

### Synthesis of novel 1,4-dimethyl-7-azabicyclo[2.2.1]heptane derivatives

#### 3.1 Introduction

As indicated in the previous chapter, 7-azabicyclo[2.2.1]heptyl systems have attracted substantial interest due to their anomalously high barriers to nitrogen inversion. It was decided to investigate the basic structure of the 1,4-dimethyl-7-azabicyclo[2.2.1]heptane system in order to study the additional effects of dimethyl substituents on inversion barriers and  $^{15}\text{N}$  NMR chemical shifts. This chapter therefore covers the synthesis of some novel 1,4-dimethyl-7-azanorbornane derivatives. The consequences of substitution at the bridgehead positions on inversion and NMR chemical shifts will be explored in detail in Chapter 6 where comparisons will be made with the simplest 7-azanorbornane derivatives (1-3).

Scheme 3.1 demonstrates the proposed route to synthesize the target compound (45) using a similar approach that used in Chapter 2.



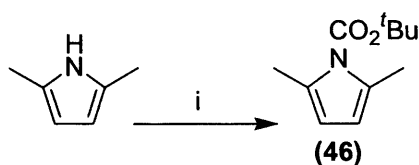
**Scheme 3.1** Reagents and conditions: (i) 80-85 °C, Toluene, 48 h.

#### 3.2 Synthesis of 1,4-dimethyl-7-azanorbornadiene derivatives

The preparation of 1,4-dimethyl-7-azanorbornadiene derivative (47) (Scheme 3.1) was accomplished using the cycloaddition approach described in the previous chapter. 2,5-Dimethylpyrrole derivative (46) was used as the diene for the construction of the 1,4-dimethyl substituted azabicyclic system. The Boc-protected 2,5-dimethylpyrrole (46) is not commercially available, thus it was prepared from the commercially available 2,5-dimethylpyrrole in this laboratory.

Kaiser and Muchowski reported the first synthesis of (46) from 2,5-dimethylpyrrole which was treated with di-*tert*-butyl dicarbonate and potassium *tert*-butoxide; the reaction mixture was refluxed for 4 days but the authors did not quote the yield.<sup>65</sup> Most recently, Hodgson *et al.* reported the protection of different pyrrole derivatives such as 3-ethylpyrrole and 2,4-dimethylpyrrole using an alternative method

(Boc<sub>2</sub>O and DMAP in acetonitrile) with reasonable yield (54-55%).<sup>66</sup> In our synthetic approach to **(46)**, the *tert*-butoxycarbonyl protected group was chosen as it could be readily introduced and removed under mild conditions from the corresponding 1,4-dimethyl-7-azanorbornane systems. Therefore, **(46)** was prepared using Hodgson's procedure<sup>66</sup> by treating a mixture of 2,5-dimethylpyrrole and Boc<sub>2</sub>O with DMAP in acetonitrile. The reaction mixture then was stirred at 25 °C for 24 h under argon to yield 57% of **(46)** (Scheme 3.2). The <sup>1</sup>H NMR spectroscopic data were similar to those reported previously.<sup>65</sup>



**Scheme 3.2** Reagents and conditions: (i) Boc<sub>2</sub>O, DMAP, MeCN, 25 °C, 24h.

The Diels-Alder cycloaddition of this pyrrole derivative **(46)** with the dienophile **(25)** afforded the 1,4-dimethyl-7-azanorbornadiene **(47)** in good yield (72%). Compound **(47)** has not been described previously and it was purified and fully characterized (Scheme 3.1).

The assignment of the <sup>1</sup>H NMR spectrum of **(47)** was completed by making comparisons with the analogous compounds having protons at the bridgehead positions **(23b)** and **(23c)**. The <sup>1</sup>H NMR spectrum of **(47)** contained two sharp, three-proton singlets at 1.97 and 1.84 ppm corresponding to the two methyl groups at the bridgehead positions. The olefinic proton H<sub>3</sub> appears at 7.50 ppm as singlet. The other olefinic protons H<sub>5</sub> and H<sub>6</sub> appear at 6.71 and 6.60 ppm as doublets (*J* = 5.3 Hz).

The <sup>13</sup>C NMR spectrum also indicated the presence of the two methyl groups at 17.2 and 16.1 ppm and three olefinic carbon atoms (159.3 (C<sub>3</sub>) and 149.0, 146.7 (C<sub>5</sub> and C<sub>6</sub>) ppm). Moreover, an X-ray crystal structure was obtained for **(47)** to confirm the structure (Figure 3.1). The two bridgehead methyl groups from the X-ray structure are in different environments as a result of the slow rotation around the N-CO bond in the urethane. The X-ray data also indicate a deviation from planarity at the bridgehead nitrogen. A discussion of planarity at amide and urethane nitrogen will be introduced later.

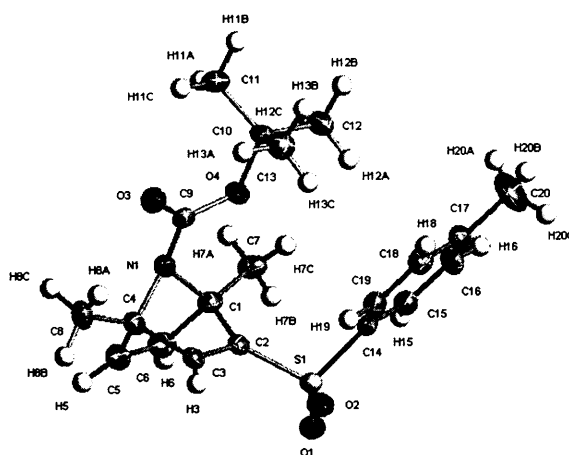
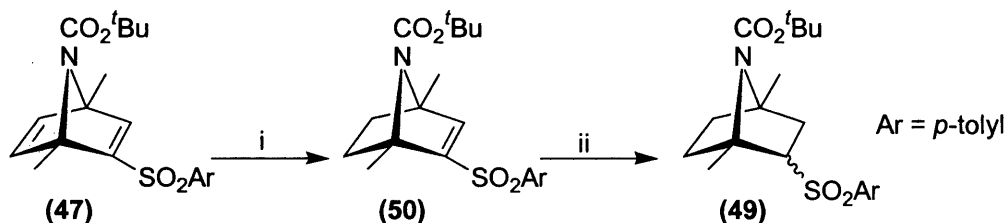


**Figure 3.1** X-ray structure of (47).

### 3.3 Attempted synthesis of 1,4-dimethyl-7-azanorbornane

Attempted preparation of the key intermediate 7-azabicyclo (48) closely followed the methodology previously described in chapter 2. The conversion of (47) to the saturated (49) was achieved by the use of established reductive procedures (Scheme 3.3). In a large scale reaction, (47) dissolved in dry acetonitrile was reduced to (50) in high yield (97%) by hydrogenation at atmospheric pressure. Only the less-substituted double bond was reduced even though the reaction was carried out over two days. The alkenyl sulfone (50) was further reduced with excess sodium borohydride to furnish the saturated (49) in good yield (64%) (Scheme 3.3).

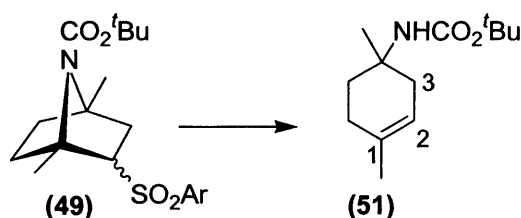


**Scheme 3.3** Reagents and conditions: (i) H<sub>2</sub>, Pd/C in CH<sub>3</sub>CN; (ii) NaBH<sub>4</sub>, CH<sub>3</sub>OH, RT.

Assignment of the <sup>1</sup>H and <sup>13</sup>C NMR spectroscopic data for both (50) and (49) was straightforward. The <sup>1</sup>H NMR spectrum of (50) shows only one alkene proton (H<sub>3</sub>) at 6.95 ppm as a singlet. The <sup>1</sup>H NMR spectrum of (49) illustrates a mixture of *endo*- and *exo*- tosyl isomers which will be assigned in more detail in the next section. The <sup>13</sup>C NMR spectrum of (50) shows two CH<sub>2</sub> carbons (C<sub>5</sub> and C<sub>6</sub>) at 34.6 and 33.4 ppm which indicates the reduction of the double bond; analysis of the signal due to *endo*- and *exo*-(49) will be discussed in the next section.

### 3.4 Attempted reduction of (49) with sodium amalgam

Reductive cleavage of the tosyl group of the mixture of *endo*- and *exo*-(49) using 6% sodium amalgam in methanol-THF was performed at  $-10\text{ }^{\circ}\text{C}$ . Unfortunately, a major byproduct was isolated (20% overall yield) as a mixture with the desired compound (48) (Scheme 3.1). The reaction was also performed at  $-78\text{ }^{\circ}\text{C}$  and a similar result was obtained. Attempted separation of the two compounds using column chromatography was not possible because they have identical  $R_f$  values. The mass spectrum of the mixture shows only one molecular ion peak indicating that the two compounds are isomeric. The ratio of the major byproduct and (48) was 4:1 respectively (determined by  $^1\text{H}$  NMR integration) indicating the low yield of the desired compound (48). The structure of the major byproduct was proposed to be (51), resulting from ring-opening of the 7-azabicyclic system.



The  $^1\text{H}$  and  $^{13}\text{C}$  NMR spectra were consistent with the proposed structure; selected data are discussed as follows. The  $^1\text{H}$  NMR spectrum of the mixture shows a broad doublet signal at 5.15 ppm which corresponds to the olefinic proton at  $\text{C}_2$ . The COSY NMR experiment shows that  $\text{C}_2$  proton couples to the neighboring protons  $\text{H}_{3\text{-eq}}$  and  $\text{H}_{3\text{-ax}}$ . The coupling constant of the olefinic proton could not be resolved due to the broadness. The NH proton appears at 4.38 ppm as a broad signal which was exchangeable by adding  $\text{D}_2\text{O}$ . A DEPT experiment was performed on the mixture of (48) and (51) to help in the assignment of carbons. The  $^{13}\text{C}$  chemical shifts of the olefinic CH and C of (51) are 134.0 and 117.9 ppm respectively. These chemical shifts were also compared with similar structures such as 2-carene and 3-carene<sup>67</sup> which showed a similar pattern of chemical shifts (Table 3.1).

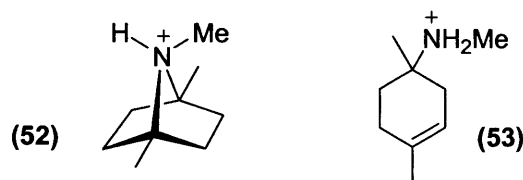
Olefinic carbons				
CH	$\delta$ (ppm)	117.9	119.4	119.4
C	$\delta$ (ppm)	134.0	133.5	131.4

**Table 3.1**

The presence of the olefinic H and two alkene C signals (CH and C) means that there must have been a bond cleavage to form the monocyclic system (**51**) from the bicyclic system.

The  $^{13}\text{C}$  NMR spectrum shows two signals of the  $\text{NC}=\text{O}$  group (155.0 and 156.3 ppm) of the mixture (**48**) and (**51**) respectively and also two similar chemical shifts of the quaternary carbon in  $\text{OC}(\text{CH}_3)_3$  (78.7 and 79.2 ppm) are assigned for the mixture confirming the presence of the two compounds (**48**) and (**51**) respectively.

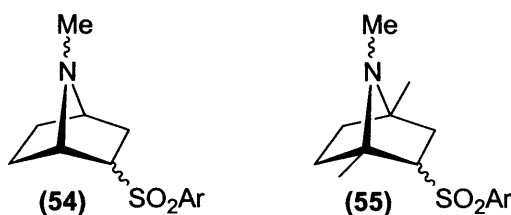
Further reduction of the mixture of compounds (**48**) and (**51**) was performed with  $\text{LiAlH}_4$  in diethyl ether producing the tertiary amines (**52**) and (**53**) which were isolated as salts. Two *N*-Me signals were assigned (2.57 and 2.55 ppm) using  $^1\text{H}$  NMR which confirms the presence of the two compounds (**52**) and (**53**) as a mixture. The olefinic H for (**53**) is seen at 5.27 ppm. The assignments of the other protons are not easy because of severe overlap. The separation of the mixture of the free amines (**52**) and (**53**) could not be achieved. The free amines (**52**) and (**53**) are expected to be highly volatile, therefore the risk of losing (**52**) and (**53**) by using column chromatography is high. Attempts to crystallize (**52**) and (**53**) salts also failed. Thus, no further work was investigated.



### 3.5 Synthesis of alternative compounds of (3a) and (52)

As a result of the difficulty in isolating the key intermediate (**48**), we decided to try to investigate an alternative pair of *N*-methyl compounds that would allow us to compare the effect of bridgehead methyl groups on the properties of the bicyclic nitrogen but should be easier to synthesize. The novel amines (**54**) and (**55**) were chosen. An

additional advantage of these compounds is that **(54)** and **(55)** are not volatile because of the presence of the arylsulfonyl group and so, would not need to be handled as salts. Another advantage is that these compounds are fully saturated which may eliminate the possible formation of side products by involvement of the double bonds. The question of *exo-* / *endo-* stereoisomers was a possible complication but it was hoped that separation would be possible and that both isomers might be isolable.



The amine **(54)** could be synthesized in one step from the reduction of the *N*-Boc protected compound **(43)** which was prepared in chapter 2. Compound **(43)** was isolated as a mixture of *endo-* and *exo-* isomers (8:2 respectively) which were separated easily by column chromatography. The  $^1\text{H}$  NMR spectrum of *endo*-**(43)** (Table 3.2) shows a downfield signal at 3.55 ppm ( $\text{H}_2$ ), shifted downfield due to the tosyl group bonded to the same carbon. Proton  $\text{H}_2$  appears as a multiplet indicating that the tosyl group is in the *endo* position because  $\text{H}_2$  couples to  $\text{H}_1$ ,  $\text{H}_{3\text{-endo}}$  and  $\text{H}_{3\text{-exo}}$  as seen from the  $^1\text{H}$  NMR COSY experiment. This assignment of the stereochemistry of *endo*-**(43)** was confirmed by X-ray crystallography (Figure 3.2). In contrast to the multiplicity of  $\text{H}_2$  in the *endo*-isomer, the  $^1\text{H}$  NMR spectrum of *exo*-**(43)** shows  $\text{H}_2$  as a doublet of doublets (dd) at 3.21 ppm. The proton  $\text{H}_2$  couples to both  $\text{H}_{3\text{-endo}}$  and  $\text{H}_{3\text{-exo}}$ , but not with  $\text{H}_1$  which, according to the Karplus relationship, indicates that  $\text{H}_1$  and  $\text{H}_2$  are orthogonal and thus the tosyl group is in the *exo* position. Table 3.2 summarizes the  $^1\text{H}$  NMR chemical shifts, multiplicity and the measurement of  $J$  values for *endo*-**(43)** and *exo*-**(43)**.

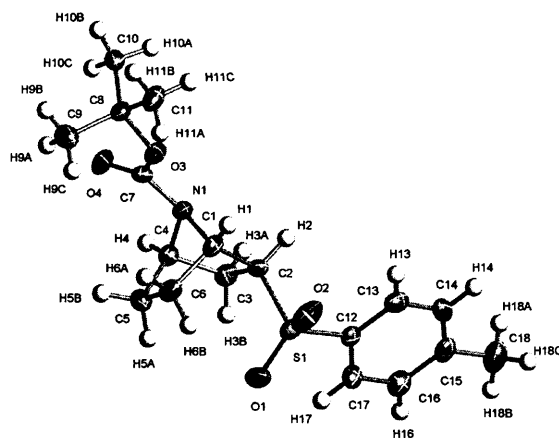
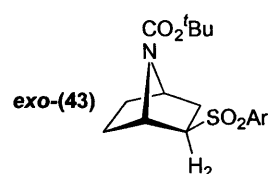
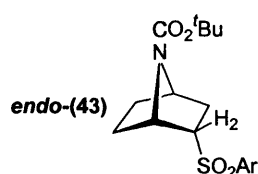


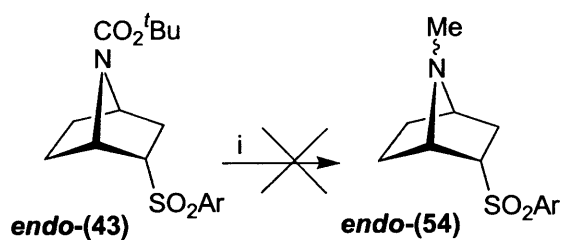
Figure 3.2 X-ray structure of *endo*-(43).



Protons	Multipl.	J (Hz)	$\delta$ (ppm)	Protons	Multipl.	J (Hz)	$\delta$ (ppm)
OC(CH <sub>3</sub> ) <sub>3</sub>	s		1.41	OC(CH <sub>3</sub> ) <sub>3</sub>	s		1.41
H <sub>6-exo</sub> , (H <sub>5-endo</sub> or H <sub>6-endo</sub> )	m		1.64-1.78	H <sub>3-exo</sub> , H <sub>3-endo</sub> , H <sub>5-exo</sub> , H <sub>6-exo</sub> , (H <sub>5-endo</sub> or H <sub>6-endo</sub> )	m		1.42-1.84
H <sub>5-exo</sub>	m		1.88	H <sub>5-endo</sub> or H <sub>6-endo</sub>	br		2.21
H <sub>3-endo</sub>	dd	$J_{2,3-endo}$ 5.7 $J_{3-exo,3-endo}$ 12.6	1.95	overlapping			
H <sub>3-exo</sub>	m		2.03	overlapping			
aryl CH <sub>3</sub>	s		2.45	aryl CH <sub>3</sub>	s		2.43
H <sub>5-endo</sub> or H <sub>6-endo</sub>	m		2.54				
H <sub>2</sub>	m		3.55	H <sub>2</sub>	dd	$J_{2,3-endo}$ 8.8 $J_{2,3-exo}$ 5.5	3.21
H <sub>4</sub>	br t		4.29	H <sub>4</sub>	br		4.25
H <sub>1</sub>	br s		4.33	H <sub>1</sub>	br d		4.55
4 x aryl CH	d	$J$ 8.3	7.37 and 7.76	4 x aryl CH	d	$J$ 8.0	7.34 and 7.79

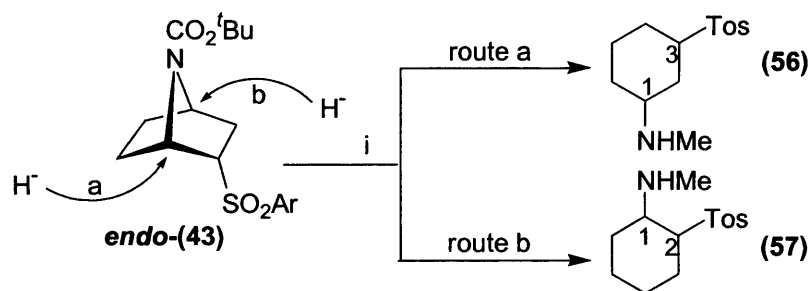
Table 3.2 <sup>1</sup>H NMR spectroscopic data for *endo*-(43) and *exo*-(43).

*Endo*-(43) was then reduced with LiAlH<sub>4</sub> in diethyl ether at reflux. Unfortunately, an unexpected product was isolated from the reduction reaction with none of the desired compound *endo*-(54) (Scheme 3.4). So, another problematic synthetic outcome was observed.



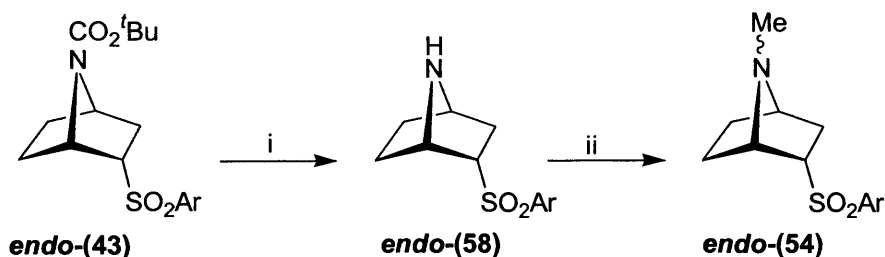
**Scheme 3.4** Reagents and conditions: (i) LiAlH<sub>4</sub>, diethyl ether, reflux, 8 h.

Before moving to investigate other routes to synthesize the desired compounds **(54)** and **(55)**, it was necessary to identify the byproduct that was obtained from the above reaction. Purification of the crude material was carried out successfully using column chromatography. The mass spectrometric analysis of the pure byproduct indicated the addition of two hydrogens to the structure compared with molecular weight of *endo*-(54). The <sup>13</sup>C DEPT experiment of the pure byproduct showed four CH<sub>2</sub> signals which do not fit with *endo*-(54) (three CH<sub>2</sub> signals expected). As a result of this, two possible structures **(56)** and **(57)** were proposed resulting from the formal addition of hydride to the 7-azabicyclic system *endo*-(43) (Scheme 3.5). A COSY experiment confirmed the **(56)** structure which was resulted from route (a) as a result of the absence of correlation between H<sub>1</sub> and H<sub>3</sub> which were easily distinguished because of their downfield chemical shifts.



**Scheme 3.5** Reagents and conditions: (i) LiAlH<sub>4</sub>, diethyl ether, reflux, 8 h.

Scheme 3.6 shows an alternative approach to the target compound *endo*-(54) using existing chemistry.



**Scheme 3.6** Reagents and conditions: (i) HCl generated *in situ*, 4h, RT, (ii)  $\text{NaBH}_3\text{CN}$ , 40% formaldehyde, acetonitrile, 24 h.

Removal of the Boc protecting group from **endo-(43)** was carried out directly using standard acidic conditions (3M HCl generated *in situ* at 0 °C from ethanol (2.7 ml), ethyl acetate (7.2 ml) and acetyl chloride (2.7 ml)) leading to the quantitative formation of the secondary amine **endo-(58)**. The  $^1\text{H}$  NMR spectrum of **endo-(58)** shows the disappearance of the signal due to the Boc protecting group. The IR spectrum shows an NH stretching signal at  $3290\text{ cm}^{-1}$  indicating the formation of the secondary amine **endo-(58)**. The preparation of **endo-(54)** was then achieved successfully using the method of Borch and Hassid<sup>68</sup> in which **endo-(58)** was treated with 40% aqueous HCHO and  $\text{NaBH}_3\text{CN}$ . The free tertiary amine was then purified by column chromatography to furnish **endo-(54)** in 79% yield.

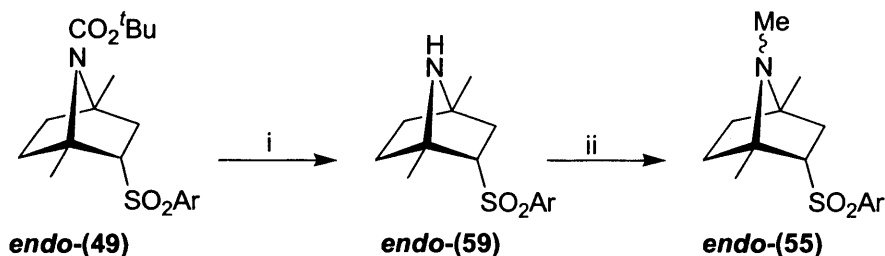
Assignment of protons and coupling constants where applicable were made with the aid of a  $^1\text{H}$  NMR COSY spectrum and homonuclear decoupling experiments (Table 3.3). The inversion barrier of **endo-(54)** was measured successfully at low temperature and the result will be discussed in Chapter 6.



arylsulphonyl orientation. The corresponding signal assigned to H<sub>2</sub> for the other isomer is a dd at 3.28 ppm, consistent with the *exo*- compound.

<i>endo</i> -(49)				<i>exo</i> -(49)			
Protons	Multipl.	J (Hz)	δ (ppm)	Protons	Multipl.	J (Hz)	δ (ppm)
OC(CH <sub>3</sub> ) <sub>3</sub>	s		1.42	OC(CH <sub>3</sub> ) <sub>3</sub>	s		1.48
2 x CH <sub>3</sub>	s		1.73 and 1.55	2 x CH <sub>3</sub>	s		1.96 and 1.62
H <sub>3-endo</sub> , H <sub>5-exo</sub>	m		1.63 – 1.84	H <sub>3-endo</sub> , H <sub>5</sub> , H <sub>6</sub>	m		1.37 – 1.72
H <sub>6-exo</sub> , (H <sub>5-endo</sub> or H <sub>6-endo</sub> )							
H <sub>3-exo</sub>	dd	<i>J</i> <sub>3-exo,3-endo</sub> 12.5 <i>J</i> <sub>2,3-exo</sub> 5.2	2.12	H <sub>3-exo</sub>	br		1.91
aryl CH <sub>3</sub>	s		2.44	aryl CH <sub>3</sub>	s		2.43
H <sub>5-endo</sub> or H <sub>6-endo</sub>	m		2.60				
H <sub>2</sub>	ddd	<i>J</i> <sub>2,3-endo</sub> 11.5 <i>J</i> <sub>2,3-exo</sub> 5.2 <i>J</i> <sub>2,6-exo</sub> 2.1	3.45	H <sub>2</sub>	dd	<i>J</i> <sub>2,3-endo</sub> 12.5 <i>J</i> <sub>2,3-exo</sub> 5.3	3.28
4 x aryl CH	d	<i>J</i> 8.2	7.34 and 7.76	4 x aryl CH	d	<i>J</i> 8.3	7.32 and 7.73

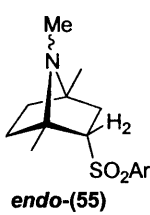
Table 3.4 <sup>1</sup>H NMR spectroscopic data for *endo*-(49) and *exo*-(49).



Scheme 3.7 Reagents and conditions: (i) HCl generated *in situ*, 4h, RT, (ii) MeI, THF, 0 °C (10 min) to RT over 6 h.

*Endo*-(49) was then hydrolyzed to *endo*-(59) in quantitative yield using a similar procedure to that described for *endo*-(58). The <sup>1</sup>H NMR spectrum of *endo*-(59) shows the disappearance of the signal due to the Boc group and has similar chemical shifts to its analogue *endo*-(58). *N*-Methylation of the secondary amine *endo*-(59) employing 1.1 equivalent of MeI in anhydrous THF provided the desired amine *endo*-(55) in good yield (71%) (Scheme 3.7). Assignment of protons and coupling constants where applicable were made with the aid of a <sup>1</sup>H NMR COSY spectrum (Table 3.5).

In addition, the nitrogen inversion barrier for *endo*-(55) was measured successfully at low temperature and the result will be discussed in Chapter 6.

Protons	Multipl.	J (Hz)	$\delta$ (ppm)	Structure
2 x $\text{CH}_3$	s		1.21 and 1.42	 <b>endo-(55)</b>
$\text{H}_{3\text{-endo}}$ , $\text{H}_{5\text{-exo}}$ , $\text{H}_{6\text{-exo}}$ , ( $\text{H}_{5\text{-endo}}$ or $\text{H}_{6\text{-endo}}$ )	m		1.48 – 1.81	
$\text{H}_{3\text{-exo}}$	dd	$J_{3\text{-exo},3\text{-endo}}$ 12.5 $J_{2,3\text{exo}}$ 5.2	2.05	
$\text{NCH}_3$	s		2.08	
aryl $\text{CH}_3$	s		2.44	
$\text{H}_{5\text{-endo}}$ or $\text{H}_{6\text{-endo}}$	m		2.60	
$\text{H}_2$	ddd	$J_{2,3\text{-endo}}$ 10.9 $J_{2,3\text{-exo}}$ 4.7 $J_{2,6\text{-exo}}$ 1.8	3.26	
4 x aryl $\text{CH}$	d	$J$ 8.1	7.33 and 7.75	

**Table 3.5**  $^1\text{H}$  NMR spectroscopic data for *endo*-(55).

Similar methylation of the minor isomers *exo*-(58) and *exo*-(59) with MeI gave the corresponding amines *exo*-(54) and *exo*-(55) respectively. Complete  $^1\text{H}$  NMR data for the free amines *exo*-(54) and *exo*-(55) are summarized in Table 3.6.

Protons	Multipl.	J (Hz)	$\delta$ (ppm)	Protons	Multipl.	J (Hz)	$\delta$ (ppm)
$\text{H}_{5\text{-endo}}$ , $\text{H}_{6\text{-endo}}$	m		1.28	2 x $\text{CH}_3$	s		1.24 and 1.66
$\text{H}_{3\text{-endo}}$	dd	$J_{3\text{-endo},3\text{-exo}}$ 12.6 $J_{2,3\text{-endo}}$ 9.1	1.55	$\text{H}_3$ , $\text{H}_5$ , $\text{H}_6$	m		1.33 – 1.80
$\text{H}_{5\text{-exo}}$ , $\text{H}_{6\text{-exo}}$	m		1.77 – 1.98				
$\text{H}_{3\text{-exo}}$	m		2.12				
$\text{NCH}_3$	s		2.17	$\text{NCH}_3$	s		2.19
aryl $\text{CH}_3$	s		2.44	aryl $\text{CH}_3$	s		2.43
$\text{H}_2$	dd	$J_{2,3\text{-endo}}$ 9.1 $J_{2,3\text{-exo}}$ 5.7	3.04	$\text{H}_2$	br t		3.22
$\text{H}_4$	br t		3.31				
$\text{H}_1$	br d	$J_{4,6\text{-exo}}$ 4.2	3.71				
4 x aryl $\text{CH}$	d	$J$ 8.1	7.32 and 7.75	4 x aryl $\text{CH}$	d	$J$ 8.1	7.32 and 7.73

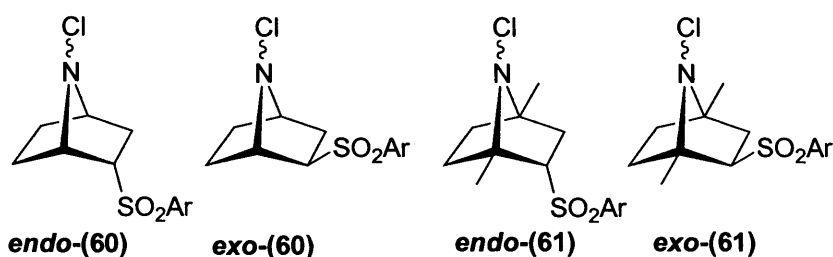
**Table 3.6**  $^1\text{H}$  NMR spectroscopic data for *exo*-(54) and *exo*-(55).

Unfortunately, attempts to measure the inversion barriers of both *exo*-(54) and *exo*-(55) at low and high temperatures were unsuccessful; these results will be discussed in more detail in Chapter 6.

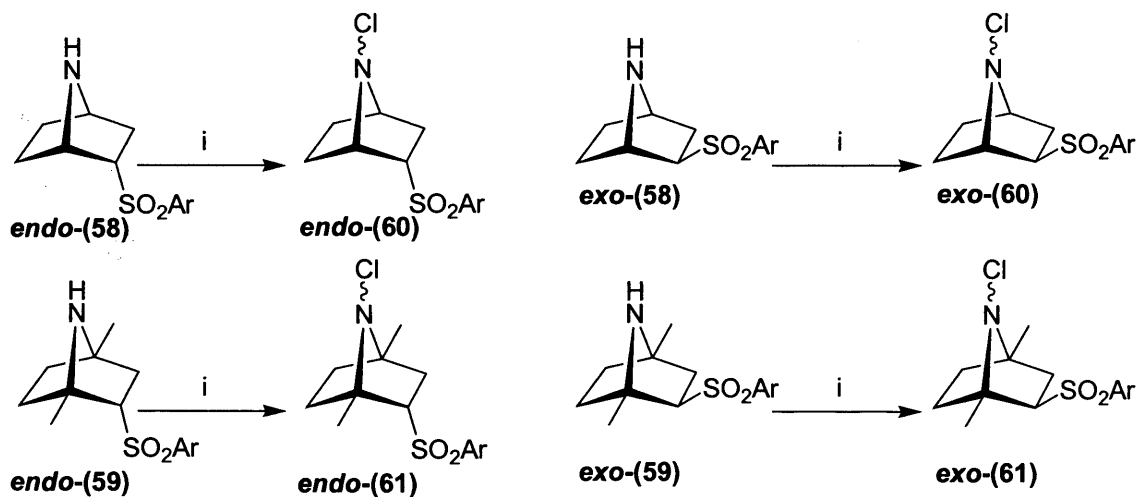
### 3.7 Synthesis of *N*-chloroamine derivatives

The choice of chlorine as the other substituent on nitrogen has important consequences. The inversion barrier is raised due the electronegativity of chlorine and the

presence of lone pairs. Also, due to its ease of removal as chloride ion, it provides a potentially useful substituent for the study of rearrangement reactions taking place at nitrogen.<sup>13,40</sup> In view of these reasons which have been introduced in more detail in Chapter 1 and, bearing in mind the considerable number of *N*-chloroazabicycles available for comparison, the synthesis of a range of *N*-Cl derivatives such as *endo*- and *exo*-(60) and *endo*- and *exo*-(61) was attempted and the synthesis of these compounds will be described in the next section.



The amines *endo*- and *exo*-(58) and *endo*- and *exo*-(59) were chlorinated in essentially quantitative yield using sodium hypochlorite (NaOCl) in dichloromethane at room temperature to furnish the desired chlorinated products *endo*- and *exo*-(60) and *endo*- and *exo*-(61) (Scheme 3.8).



**Scheme 3.8** Reagents and conditions: (i) NaClO<sub>4</sub>, CH<sub>2</sub>Cl<sub>2</sub>, 30 min, RT.

The <sup>1</sup>H NMR spectra clearly show the presence of two invertomeric species in both *endo*-(60) and *endo*-(61) at room temperature. The assignment of the invertomers from the spectra of *endo*-(60) and *endo*-(61) was completed by making comparisons with analogous compounds having similar bicyclic systems. Cristol reported full assignments

of the  $^1\text{H}$  NMR chemical shifts and coupling constants for benzonorbornene and benzonorbornadiene derivatives.<sup>69</sup> Our particular interest in connection with this report was the  $^1\text{H}$  NMR assignments for 5,7-dichlorobenzonorbornene isomers (Figure 3.3). The assignments of the isomeric orientation were made on the basis of the presence or absence of long range coupling for the bridgehead proton. Thus, the *syn* bridgehead proton (with respect to the aryl ring) couples with *endo*  $\text{H}_5$  and  $\text{H}_6$ , but not with the *exo* protons. For the *anti*-bridgehead proton (with respect to the aryl ring) no such coupling is observed. The  $^1\text{H}$  NMR chemical shift of the *exo*-proton of the ethano-bridge (Figure 3.3) is influenced according to the orientated chlorine atom. The  $^1\text{H}$  NMR chemical shift of the *exo*-proton is shifted downfield when Cl is *anti* and highfield when it is *syn* with respect to the aryl ring. On this basis, the invertomer ratios of the *syn*-Cl and *anti*-Cl (with respect to the tosyl-substituted bridge) for the *N*-Cl amines *endo*-(60) and *endo*-(61) were determined using the *exo*-proton chemical shifts of the ethano-bridge ( $\text{H}_2$ ). The invertomer ratios of *syn*- and *anti*-chlorine of *endo*-(60) and *endo*-(61) are 71:29 and 79:21 respectively. Moreover, Table 3.7 shows the  $^1\text{H}$  NMR chemical shifts of the ethano-bridge *exo*-protons having the same trend for similar benzo-derivative ring systems.<sup>23,42</sup>

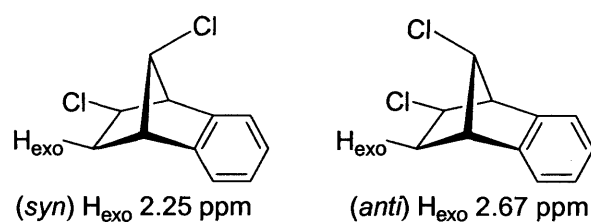


**Figure 3.3**

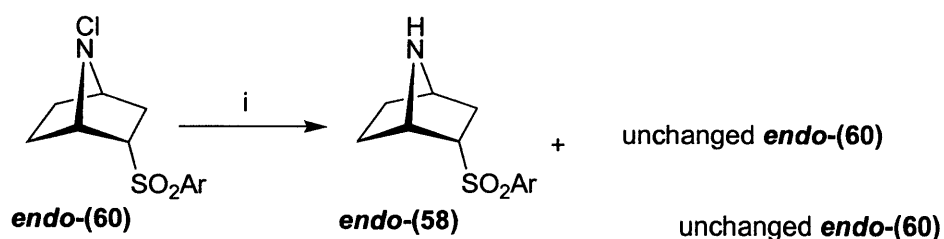
(15)		(14)		<i>endo</i> -(60)		<i>endo</i> -(61)	
$\delta$ (ppm) <i>exo</i> - $\text{H}_5, \text{H}_6$		<i>exo</i> - $\text{H}_5, \text{H}_6$		$\text{H}_2$		$\text{H}_2$	
<i>syn</i>	<i>anti</i> <sup>a</sup>	<i>syn</i>	<i>anti</i> <sup>a</sup>	<i>syn</i>	<i>anti</i> <sup>b</sup>	<i>syn</i>	<i>anti</i> <sup>b</sup>
2.17	2.46	2.00	2.24	3.99	3.48	3.60	3.25

**Table 3.7** a) with respect to the aryl ring. b) with respect to the tosyl group.

Unfortunately, it was not possible to measure the inversion barrier for *endo*-(60). The  $^1\text{H}$  NMR spectrum showed no change over the temperature range +25 – –80 °C. The compound decomposed when heated above 70 °C and showed no coalescence, consistent

with a high inversion barrier for *endo*-(60). High field, 75 MHz,  $^{13}\text{C}$  NMR clearly showed the presence of two invertomeric species in *endo*-(60). An interesting feature of  $^{13}\text{C}$  NMR spectrum was the small frequency separation ( $\Delta\nu$ ) observed between the bridgehead carbon signals and the ethano- carbons arising from each invertomer. This indicated potential for variable temperature coalescence studies, however, at 75 MHz these relative small separations still proved to be large for coalescence to be observed. Simple calculations suggested that with a lower field (such as 15 MHz)  $^{13}\text{C}$  NMR spectrometer (at 60 MHz  $^1\text{H}$  NMR spectrometer) it might be possible to observe temperature-dependent coalescence for *endo*-(60) at temperatures which could be realistically achieved. The difficulties associated with the move to lower field arise from the lower sensitivity which required the use of relatively concentrated samples and long acquisition times. Moreover, it is difficult now a days to find low field NMR spectrometers.

When attempts were made to solvolyse *endo*-(60) using the conditions which had previously been applied successfully to *N*-Cl- derivatives of 7-azabenzonorbornane,<sup>40</sup> no rearrangement products were isolated. The method used involved the treatment of the *N*-chloroamine *endo*-(60) with silver tetrafluoroborate ( $\text{AgBF}_4$ ) in the presence of methanol (1.1 equivalents) and subjected to basic work-up (Scheme 3.9). This afforded mainly the unchanged *endo*-(60) together with a small amount of the dechlorinated parent amine *endo*-(58), presumably formed via a homolytic process.<sup>40</sup>



**Scheme 3.9** Reagents and conditions: (i)  $\text{AgBF}_4$ , 1.1 equiv. MeOH, toluene, 48h.

## **Chapter 4**

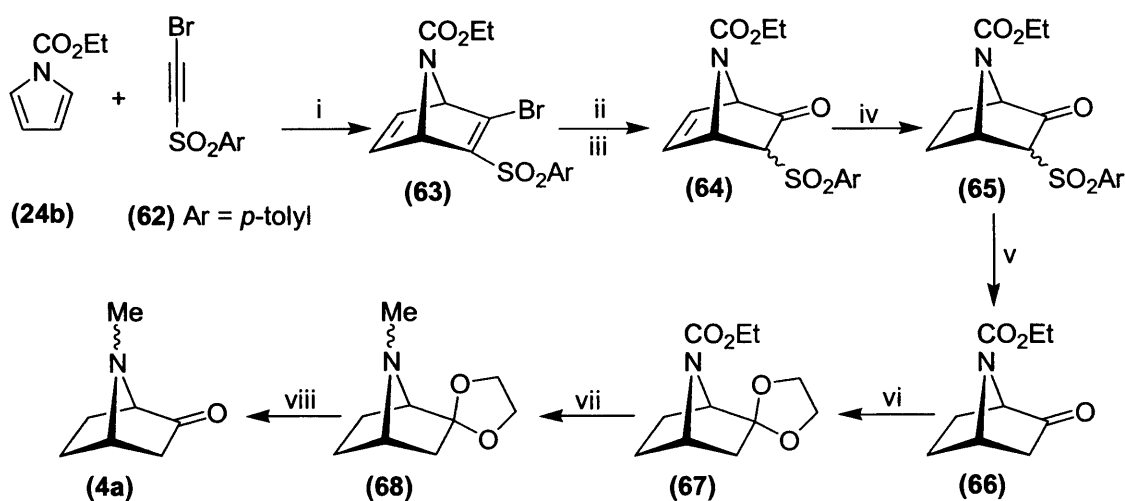
### **Synthesis of 7-azabicyclo[2.2.1]heptan-2-one derivatives**

## Chapter 4

### Synthesis of 7-azabicyclo[2.2.1]heptan-2-one derivatives

#### 4.1 Routes to the synthesis of 7-methyl-7-azabicyclo[2.2.1]heptan-2-one (4a)

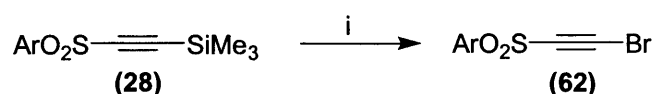
The routes used to synthesize the novel derivative of 2-keto-*N*-methyl-7-azanorbomane (**4a**) are outlined in Scheme 4.1. Some of the intermediates are known with different protecting groups but compounds (**63**) → (**68**) are new. The methods that were used will be illustrated as follows with the references.



**Scheme 4.1** Reagents and conditions: (i) 90 °C, toluene, 48 h; (ii) Et<sub>2</sub>NH, Et<sub>3</sub>N, MeCN; (iii) 10% HCl; (iv) H<sub>2</sub>, Pd/C, CH<sub>3</sub>CN; (v) Al-Hg, MeOH; (vi) HOCH<sub>2</sub>CH<sub>2</sub>OH, (EtO)<sub>3</sub>CH, *p*-TsOH (cat.), toluene; (vii) LiAlH<sub>4</sub>, diethyl ether, reflux, 8 h. (viii) HClO<sub>4</sub>, THF.

#### 4.2 Synthesis of 2-bromoethynyl *p*-tolyl sulfone (62)

The route to the formation of 2-bromoethynyl *p*-tolyl sulfone (**62**) is illustrated in Scheme 4.2, using Trudell's method.<sup>70</sup> The alkyne (**28**) (which was synthesized in chapter 2) was treated in acetone with *N*-bromosuccinimide (NBS) in the presence of AgNO<sub>3</sub> as a catalyst at room temperature for 30 minutes and afforded (**62**) in good yield (73 %). This was purified by column chromatography. The <sup>1</sup>H NMR spectrum of (**62**) was identical to the spectrum reported before.<sup>70</sup>



**Scheme 4.2** Reagents and conditions: (i) NBS, AgNO<sub>3</sub>, acetone, 30 min.

### 4.3 Synthesis of 2-bromo-7-azabicyclo[2.2.1]hept-2,5-diene sulfone (63)

2-Bromoethynyl *p*-tolyl sulfone (**62**) was found to readily undergo a [4+2] cycloaddition reaction with *N*-acylpyrrole derivatives.<sup>70</sup> The reaction of this substituted acetylene derivative (**62**) with the diene *N*-ethoxycarbonyl pyrrole (**24b**) in toluene at 90 °C gave the corresponding cycloadduct (**63**) in 56% yield (Scheme 4.1). The *N*-ethoxycarbonyl derivative (**63**) was first described here and the yield was similar to that reported using *N*-Boc pyrrole.<sup>70</sup>

The <sup>1</sup>H NMR spectrum of (**63**) includes two bridgehead protons H<sub>1</sub> and H<sub>4</sub> appearing at 5.43 and 5.22 ppm. The CH<sub>2</sub> protons on the ethoxy group, the alkene protons (H<sub>5</sub> and H<sub>6</sub>) and the bridgehead protons (H<sub>1</sub> and H<sub>4</sub>) are broad peaks due to restricted rotation about the NC=O bond at room temperature. Finally, the aromatic protons appear at 7.79 and 7.36 ppm as an AA'BB' pattern (J = 8.2 Hz).

### 4.4 Synthesis of 7-azabicyclo[2.2.1]heptan-2-one sulfone derivative (65)

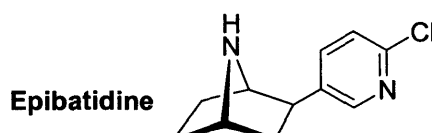
The ketone (**64**) can be readily prepared from the cycloadduct (**63**) by using the method of Trudell.<sup>70</sup> Treatment of cycloadduct (**63**) with 1.1 equivalents of diethylamine in the presence of three equivalents of triethylamine in acetonitrile at room temperature, followed by hydrolysis with 10% HCl at room temperature, gave a mixture of the *exo*- and *endo*-arylsulphonyl derivatives (**64**) in 60% yield (Scheme 4.1).

The <sup>1</sup>H NMR spectrum of (**64**) exhibits signals in agreement with the presence of a mixture of two isomers, the *exo*- and *endo*-tosyl ketones (**64**). The <sup>1</sup>H NMR spectrum was used to establish firmly the ratio of *exo*- and *endo*-tosyl (**64**). The *exo*-tosyl isomer has a singlet assigned to H<sub>3-*endo*</sub> at 3.54 ppm which does not couple to the bridgehead H<sub>1</sub> due to the dihedral angle of 90° between them. On the other hand, the *endo*-tosyl isomer shows a doublet corresponding to H<sub>3-*exo*</sub> at 4.02 ppm which couples to the bridgehead H<sub>1</sub> (J = 3.8 Hz). The ratio of *exo*- and *endo*-tosyl (**64**) was calculated to be 76:24 respectively using <sup>1</sup>H NMR integration.

Hydrogenation of the carbon-carbon double bond of (**64**) over 10% Pd/C (H<sub>2</sub>, 1 atm) in acetonitrile gave an almost quantitative yield (98%) of the corresponding product (**65**) (Scheme 4.1). The <sup>1</sup>H NMR spectrum of (**65**) shows the disappearance of the characteristic alkene protons signals indicating the formation of the saturated ethano-bridge.

#### 4.5 Synthesis of 7-azanorbornanone derivative (66)

The intermediate (66) is the key compound in the synthesis of the target compound (4a) (Scheme 4.1). Removal of the tosyl group of (65) was readily achieved after 2 hours reflux in Al-Hg in 10% aqueous THF affording the corresponding ketone (66) in 54% yield. Trudell *et. al.* reported a 60% yield when employing analogous conditions.<sup>71</sup> The keto-derivative (66) is known as an intermediate precursor of the synthesis of the natural product epibatidine.<sup>72-76</sup>



The <sup>1</sup>H NMR spectrum of the ketone (66) shows a doublet signal at 2.03 ppm which corresponds to H<sub>3-endo</sub> ( $J_{\text{H}_{3\text{-endo}},\text{H}_{3\text{-exo}}} = 17.5$  Hz). The H<sub>3-exo</sub> signal which couples to H<sub>3-endo</sub> and H<sub>4</sub> ( $J = 17.5$  and 5.9 Hz respectively) and appears as a doublet of doublet at 2.49 ppm. The ethano-bridge protons H<sub>5</sub> and H<sub>6</sub> appear at 1.58 – 2.02 ppm. The <sup>13</sup>C NMR spectrum shows a downfield signal at 209.1 ppm corresponding to the ketone carbon. Also, the DEPT experiment shows three CH<sub>2</sub> signals at 24.4, 27.6 and 45.2 ppm indicating the removal of the tosyl group. Moreover, a new measurement of the <sup>15</sup>N chemical shift was made for the ketone (66) (-265.8 ppm) and this result will be discussed later in the <sup>15</sup>N NMR spectroscopic chapter.

With the ketone (66) in hand, a direct reduction of the *N*-ethoxycarbonyl group to the amine (4a) with LiAlH<sub>4</sub> was not possible because of the presence of the keto function. Thus, as shown in Scheme 4.1, the ketone (66) was firstly protected as a 1,3-dioxolane (67) with HOCH<sub>2</sub>CH<sub>2</sub>OH, (EtO)<sub>3</sub>CH and *p*-TsOH.<sup>77</sup> The purity of the resultant oil (67) (93%) was checked by <sup>1</sup>H NMR spectroscopy and judged to be satisfactory for the next step reaction.

The <sup>1</sup>H NMR chemical shift of H<sub>3-exo</sub> of (67) appears as a doublet of doublets of doublets at 2.15 ppm. The 2D COSY experiment shows that H<sub>3-exo</sub> proton is coupled to the H<sub>3-endo</sub> proton ( $J = 13.0$  Hz), and to the adjacent bridgehead H<sub>4</sub> ( $J = 5.4$  Hz). A long range coupling was also observed between the H<sub>3-exo</sub> and H<sub>5-exo</sub> protons ( $J = 2.3$  Hz). The <sup>15</sup>N chemical shift of (67) was measured and found to be -261.8 ppm. This new result will be discussed in the <sup>15</sup>N chemical shifts chapter.

We were then in a position to reduce the *N*-ethoxycarbonyl group of 1,3-dioxolane (**67**) to the corresponding *N*-Me compound (**68**) (Scheme 4.1). This was achieved by reaction of the (**67**) with LiAlH<sub>4</sub> in diethyl ether at reflux to afford (**68**) in good yield (83%). The free amine (**68**) is expected to be volatile thus, it was isolated as the hydrochloride salt.

The <sup>1</sup>H NMR spectrum of the free amine (**68**) shows a singlet signal at 2.27 ppm corresponding to the methyl group. The multiplicities of the H<sub>3-*exo*</sub> and H<sub>3-*endo*</sub> protons were similar to those observed for (**67**). Moreover, the structure of (**68:HCl**) could be inferred from its <sup>1</sup>H NMR spectrum and was confirmed by X-ray crystallographic analysis (Figure 4.1). The *N*-Me group is *anti* to the acetal group which may indicate that the *anti*-configuration is of lower energy than the *syn*-.

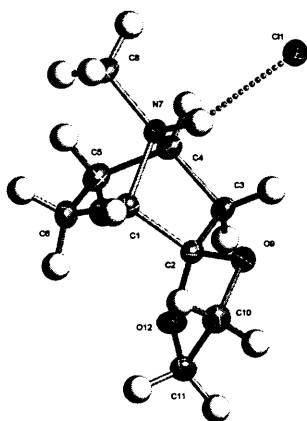


**Figure 4.1** X-Ray crystal structure of (**68:HCl**).

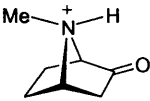
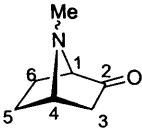
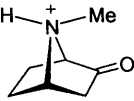
The inversion barrier was measured at low temperature for the free amine (**68**) and the result will be introduced in Chapter 6.

#### 4.6 Synthesis of 7-methylazabicyclo[2.2.1]heptan-2-one (**4a**)

Finally, the 1,3-dioxolane group of (**68**) was removed with 70% perchloric acid to provide the novel ketone (**4a**) in good yield (74%) (Scheme 4.1). The free amine (**4a**) was handled as a salt because of its potential volatility.

The <sup>1</sup>H NMR signals of the protonated form (**4a:HCl**) are downfield from their counterparts in the free amine (**4a**) due to the electron withdrawal by the quaternary nitrogen which is similar to that observed for the secondary and tertiary amine salts reported in Chapter 2. The *N*-Me group in the free amine (**4a**) which is a singlet at 2.33 ppm became a doublet in the protonated form due to its coupling with NH ( $J_{\text{NH},\text{NMe}} = 4.4$

Hz) (2.90 ppm). The quaternization of amine (**4a**) with HCl has yielded two stereoisomeric quaternary salts where the *N*-Me group is *syn* or *anti* to the ketone group. The  $^1\text{H}$  NMR shifts of the *N*-Me group (*syn* or *anti*) are similar to each other indicating that the effect of the ketone group is small. The assignment of the stereoisomeric ratio of (**4a:HCl**) will be discussed in more details in Chapter 6. The  $^{13}\text{C}$  NMR spectrum shows two sets of signals corresponding to the two stereoisomeric quaternary salts of (**4a:HCl**). The assignments of *anti* and *syn* stereoisomers were based again on the  $\gamma$ -effect phenomenon (Chapter 2) (Table 4.1). The assignment of  $\text{C}_5$  and  $\text{C}_6$  is arbitrary, they could be reversed.

	 <b>Major (<i>anti</i>-Me)</b>	 <b>Free amine (<b>4a</b>)</b>	 <b>Minor (<i>syn</i>-Me)</b>
<b>Carbons</b>		<b><math>\delta</math> (ppm)</b>	
$\text{C}_2$	201.4	213.9	202.8
$\text{C}_1$	69.5	70.0	68.4
$\text{C}_4$	63.1	61.3	63.9
$\text{C}_3$	44.5	43.2	38.9
$\text{NCH}_3$	33.7	35.1	33.0
$\text{C}_5$ or $\text{C}_6$	24.2	26.4	26.7
$\text{C}_5$ or $\text{C}_6$	20.2	22.4	21.8

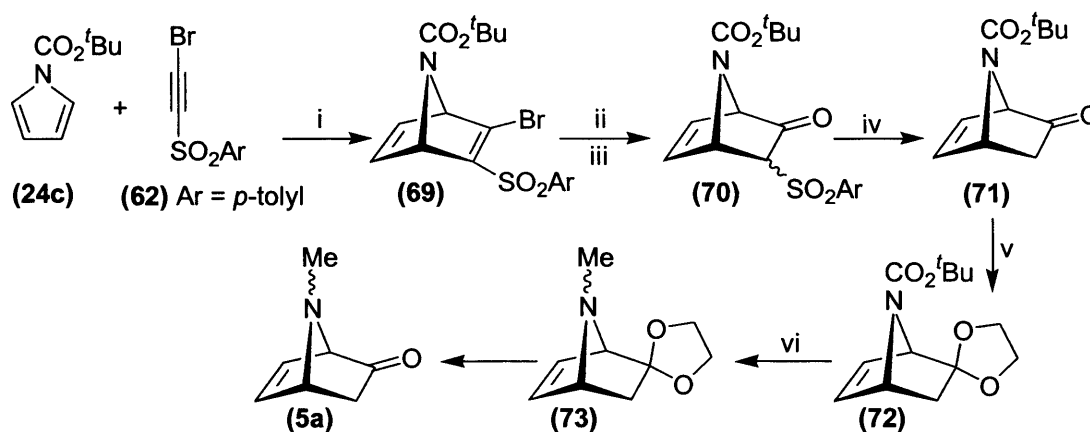
**Table 4.1**  $^{13}\text{C}$  NMR data for free amine (**4a**) and its protonated quaternary salts (**4a:HCl**).

The effect of the ketone group on the  $^1\text{H}$  NMR chemical shifts is obvious when comparison was made between the free amines (**4a**) and (**1a**). The shifts of the bridgehead protons  $\text{H}_1$  and  $\text{H}_4$  in (**4a**) are shifted downfield when compared with (**1a**). Similar observations of downfield shifts were observed when the ethano- and *N*-Me protons in (**4a**) compared with (**1a**). Thus, the effect of the ketone group shifts the  $^1\text{H}$  NMR downfield.

Moreover, the inversion barrier of the free amine (**4a**) was measured at low temperature and the significant result will be compared and discussed with other reported inversion barriers in Chapter 6. The  $^{15}\text{N}$  NMR chemical shift of (**4a:HCl**) was measured and found to be at  $-308.7$  ppm. Only one nitrogen signal was observed.

#### 4.7 Attempted synthesis of 7-methyl-7-azabicyclo[2.2.1]hept-5-en-2-one (5a)

The starting material for our proposed synthesis was the known *N*-protected 7-azabicyclo[2.2.1]hept-2,5-diene (69) which was prepared by Diels-Alder reaction between 2-bromoethynyl *p*-tolyl sulfone (62) and *N*-Boc pyrrole (24c) as described above.<sup>70</sup> *N*-Boc pyrrole was used instead of *N*-ethoxycarbonyl pyrrole (24b) because (24c) is commercially available and no (24b) was available at this stage. Scheme 4.3 summarizes the routes toward the synthesis of the target compound (5a). Unfortunately, the series of reactions could not be completed for the reasons that will follow.



**Scheme 4.3** Reagents and conditions: (i) 90 °C, toluene, 48 h; (ii) Et<sub>2</sub>NH, Et<sub>3</sub>NH, MeCN; (iii) 10% HCl; (iv) SmI<sub>2</sub>, THF-MeOH -78 °C; (v) HOCH<sub>2</sub>CH<sub>2</sub>OH, (EtO)<sub>3</sub>CH, *p*-TsOH (cat.), toluene; (vi) LiAlH<sub>4</sub>, diethyl ether, reflux, 8 h.

Treatment of adduct (69) with 1.1 equivalents of diethylamine in the presence of three equivalents of triethylamine in acetonitrile at room temperature, followed by hydrolysis with 10% HCl at room temperature, afforded the known<sup>70</sup> ketone (70) in 94% yield as a mixture of the *exo*- and *endo*-arylsulphonyl stereoisomers (70) (Scheme 4.3). The ratio of *exo*- and *endo*- isomers (70) (75:35 respectively) was similar to that observed for compound (64). There was no significant influence on the ratio by changing the protecting group from the *N*-ethoxycarbonyl to the Boc group.

#### 4.8 Synthesis of 7-azanorbornenone derivative (71)

The synthesis of the key intermediate (71) was carried out starting from the isomeric mixture of (70) which was pure enough judged by <sup>1</sup>H NMR spectroscopy. Desulfonylation of compound (70) was performed in a similar fashion to that described for (66) using Al-Hg. The resulting yield of the unsaturated ketone (71) after purification by column chromatography was poor (14%) (Scheme 4.3). Vogel reported less than 10%

yield of the corresponding ketone (**71**) using the same methodology.<sup>78</sup> Recently Kozikowski *et. al.* reported that  $\text{SmI}_2$  in THF:MeOH at  $-78^\circ\text{C}$  was employed to desulfonate the unsaturated keto sulfone (**70**).<sup>79</sup> This was reported to give the corresponding unsaturated ketone (**71**) in high yield (90%) although there was no procedure published. Vogel *et. al.* also used this reaction to synthesize (**71**).<sup>75</sup> In their procedure, they managed a best yield of 75%. Following the same conditions that was mentioned by Vogel, we were able to synthesize (**71**) in low yield (24%) after purification by column chromatography (Scheme 4.3). There are some points worth mentioning here.  $\text{SmI}_2$  (0.1M) is commercially available as a suspension in THF. This expensive reagent is highly reactive and reacts with traces of moisture.

The  $^1\text{H}$  NMR spectrum of ketone (**71**) shows two alkene protons  $\text{H}_5$  and  $\text{H}_6$  at 6.73 and 6.42 ppm respectively. The spectrum also shows a doublet of doublets for both  $\text{H}_5$  and  $\text{H}_6$  protons with  $J_{5,6} = 5.5$  Hz,  $J_{4,5} = 2.0$  Hz and  $J_{1,6} = 2.0$  Hz. The  $\text{H}_{3\text{-exo}}$  proton appears as doublet of doublets of doublets at 2.28 ppm. Some broadening was noticed for  $\text{H}_{3\text{-exo}}$  as a result of long-range coupling with  $\text{H}_1$  ( $J_{1,3\text{-exo}} < 1$  Hz) beside the coupling with  $\text{H}_{3\text{-endo}}$  and  $\text{H}_4$  protons ( $J_{3\text{-exo},3\text{-endo}} = 16.0$  Hz and  $J_{3\text{-exo},4} = 3.9$  Hz respectively). An X-ray crystal structure of ketone (**71**) was obtained and this allowed us to investigate the non-planarity of the bridging urethane nitrogen in this system (Chapter 7) (Figure 4.2). The  $^{15}\text{N}$  chemical shift of (**71**) was also measured to be at  $-252.4$  ppm and this new result will be discussed in Chapter 5.

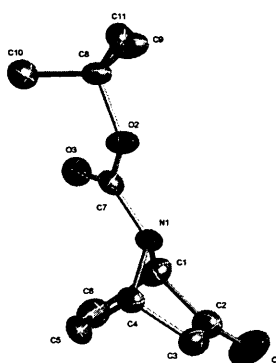
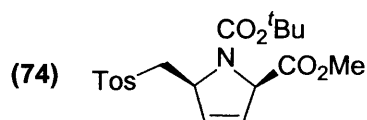


**Figure 4.2** X-Ray crystal structure of (**71**).

A major byproduct isolated in the desulfonylation of ketone (**70**) was subsequently identified as 2,5-disubstituted 3-pyrroline (**74**) and this was a factor in the low yield of the desired product (**71**). The byproduct (**74**) may be derived from the addition of methanol across the ethano-bridge. Vogel *et. al.* reported 2,5-disubstituted 3-pyrroline (**74**) as a

side product when (70) was purified by column chromatography (SiO<sub>2</sub>) using a mixture of dichloromethane:methanol (60:1) as an eluent.<sup>78</sup> The use of methanol as solvent clearly plays an important role in the formation of this byproduct (74). Accurate mass spectroscopic analysis of (74) confirms the molecular weight of the structure (74). A careful analysis of the <sup>1</sup>H NMR analysis of (74) indicates the presence of a mixture of rotamers. Four broad alkene protons signals can be readily distinguished. Two methyl signals due to the Boc group and CO<sub>2</sub>Me appear at 1.40 and 1.38 ppm. The assignment of the Me signals was based on the <sup>1</sup>H NMR integrations. The <sup>13</sup>C NMR spectrum of the rotamers of (74) shows two signals at 170.6 and 170.4 ppm which confirms the formation of the CO<sub>2</sub>Me group. The <sup>13</sup>C NMR signals of the methyl ester group appear at 52.5 and 52.4 ppm, within the correct chemical shift range for this group. The DEPT experiment also shows the presence of two CH<sub>2</sub> carbon signals at 60.7 and 59.1 ppm which are not part of the starting material (70).



Using the small amount of (70) that was in our hands, protection of the ketone using the same procedure described for (67) afforded the unsaturated 1,3-dioxolane (72)<sup>80</sup> in 42% yield (Scheme 4.3). The <sup>13</sup>C NMR spectrum of (72) shows the disappearance of the ketone group carbon which is usually easy to identify from its chemical shift. The alkene carbons, 1,3-dioxolane group and the bridgehead carbons of (72) exhibited a duplication of the <sup>13</sup>C NMR signals due to the slow rotation around the NC=O bond at room temperature. Confirmation of the formation of (72) was obtained from the X-ray crystal structure which is reported here as a new result (Figure 4.3). The non-planarity of the urethane group is obvious from the crystal structure and will be discussed later.

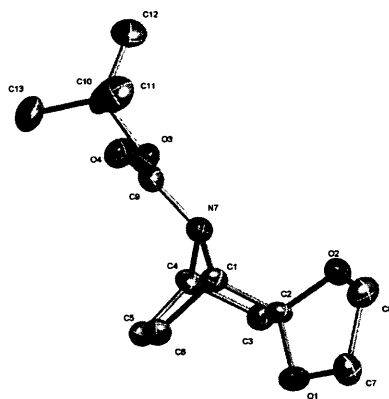
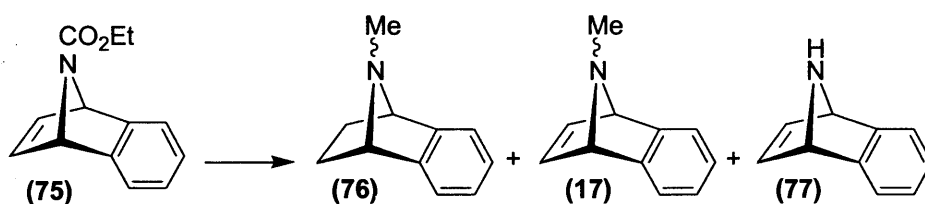
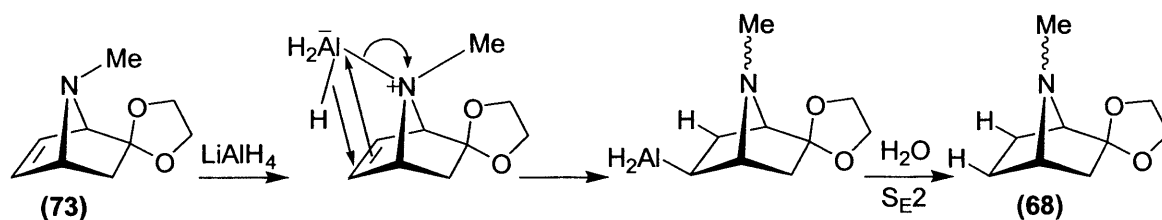


**Figure 4.3** X-Ray crystal structure of (72).

Another limitation of this synthetic route to the amine (**5a**) was the reduction of (72) with  $\text{LiAlH}_4$ . Treatment of (72) with  $\text{LiAlH}_4$  in diethyl ether at reflux afforded a mixture of two products together with unreacted (72). The reaction products were identified as the unsaturated amine (73) (Scheme 4.3) and the saturated amine (68) (Scheme 4.1) which resulted from the reduction of the carbon-carbon double bond of (73). Marchand has reported this unusual reduction of the carbon-carbon double bond in 7-azanorbornane systems with  $\text{LiAlH}_4$ .<sup>81</sup> *N*-Ethoxycarbonyl-7-aza-5,6-benzobicyclo-[2.2.1]hepta-2,3-ene (75) was reduced with  $\text{LiAlH}_4$  to afford three products (76), (17) and (77). Marchand showed that (17) could be an intermediate in the overall reduction of (75) to (76) by performing a separate experiment in which (17) was reduced to (76) using similar conditions.



Moreover, Marchand proposed an intramolecular mechanism for this reduction.<sup>81</sup> An analogous mechanism for the corresponding reduction in our azabicyclic system is shown in Scheme 4.4.



**Scheme 4.4**

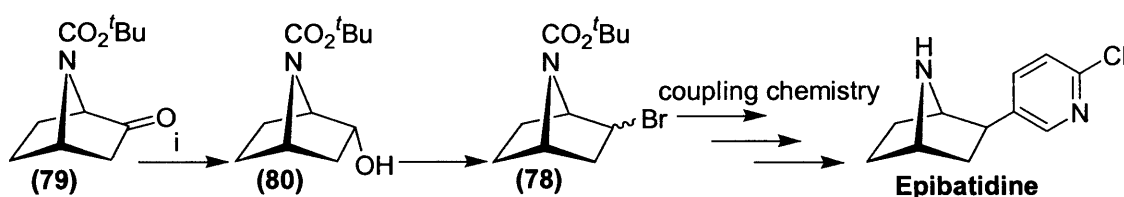
Finally, it was decided that proceeding toward the synthesis of the amine (**5a**) would not be practical as a result of the low yield of the key intermediate (**71**) and the formation of (**68**) in competition with (**73**).

#### 4.9 Attempted synthesis of epibatidine

Epibatidine is an alkaloid featuring the 7-azabicyclo[2.2.1]heptane structure to which is attached in an *exo* orientation a 5-(2-chloropyridyl) substituent. It has been found to be a potent analgesic agent with potency 200 to 500 greater than morphine and it acts at nicotinic receptors.<sup>1,82,83</sup> In contrast to epibatidine, morphine acts at opioid receptors, the more usual site of action for an analgesic.<sup>84</sup>

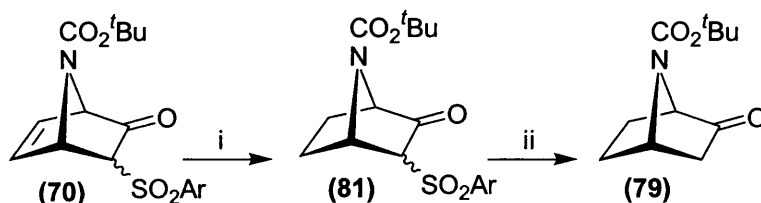
Since the discovery of epibatidine and its biological activity, the challenge of the synthesis of epibatidine and epibatidine analogues has attracted synthetic chemists from laboratories around the world.<sup>85</sup> Many different synthetic strategies have been developed for the preparation of this novel alkaloid based, in principle, on four different methodologies for construction of the azabicyclic system: (1) the [4+2] cycloaddition reaction of *N*-protected pyrroles and activated dienophiles; (2) the intramolecular nucleophilic substitution ring closure of 1,4-cyclohexane derivatives; (3) the [3+2] cycloaddition of nonstabilized azomethine ylide and substituted 6-chloro-3-vinylpyridine; and (4) the ring contraction of the tropinone skeleton via a Favorskii rearrangement.<sup>74</sup>

Work at Leicester on the 2-azabicyclo[2.2.1]heptane system has led to the synthesis of many analogues of epibatidine.<sup>86</sup> Heterocycles such as the chloropyridyl substituents were introduced at the 7-position using Suzuki coupling chemistry. Therefore, our strategy using similar methodology was the synthesis of a halide (bromide) substituted in the 2-position of the 7-azanorbornane system (**78**). Unfortunately, after many attempts, synthesis of the key compound (**78**) could not be achieved. Scheme 4.5 shows our proposed route starting from the known keto derivative of 7-azanorbornane (**79**)<sup>70</sup> and the key steps will be described.



**Scheme 4.5** Reagents and conditions: (i) L-Selectride, THF, -55 °C to RT, 1h.

Synthesis of **(79)** was achieved using similar chemistry to that described for the synthesis of the *N*-ethoxycarbonyl protected compound **(67)**. The double bond of **(74)** was firstly reduced over 10% Pd/C (H<sub>2</sub>, 1atm) in acetonitrile with almost quantitative yield (Scheme 4.6). Desulfonylation of β-keto sulfone **(81)** was carried out employing Al-Hg. This provided the desired ketone **(79)** in good yield (70%) (Scheme 4.6). The yield of the *N*-Boc protected compound **(79)** was higher when compared with the corresponding *N*-ethoxycarbonyl analogue **(66)**. The <sup>1</sup>H and <sup>13</sup>C NMR spectroscopic data were essentially identical to those described for ketone **(66)**. The structure of **(79)** was determined by X-ray crystallography and is reported here for the first time (Figure 4.4). The <sup>15</sup>N NMR chemical shift also was measured for **(79)** and was found to be at -261.4 ppm. This result will be discussed in Chapter 5.



**Scheme 4.6** Reagents and conditions: (i) H<sub>2</sub>, Pd/C in CH<sub>3</sub>CN; (ii) Al-Hg, 10% aqueous THF, 65 °C, 2h.

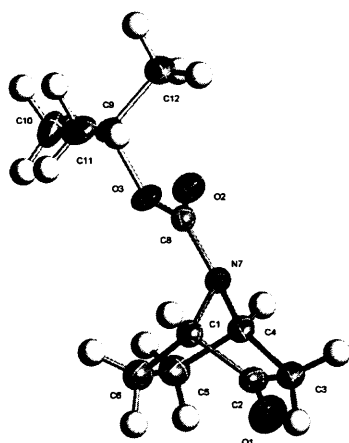
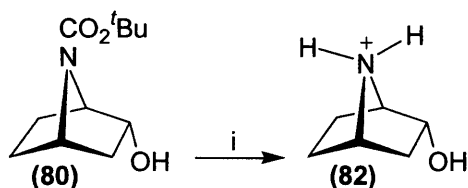


**Figure 4.4** X-Ray crystal structure of (79).

Fletcher *et. al.* reported the reduction of the ketone (79) to the corresponding alcohol (80) with L-selectride (lithium tri-*sec*-butylborohydride).<sup>73</sup> Stereoselective reduction of (79) with the sterically hindered L-selectride in THF at -55 to 0 °C in our hands provided preferentially the *endo* alcohol (80) in good yield (79%) (Scheme 4.5).

The assignment of configuration to the hydroxyl group in (80) is based on the NMR data. The <sup>1</sup>H NMR COSY experiment shows correlation between H<sub>2</sub> and H<sub>1</sub>. This coupling was consistent with the vicinal Karplus angles required by the *endo*-hydroxy stereochemistry. The <sup>1</sup>H NMR chemical shift of H<sub>2</sub> was easily identified at 4.34 ppm because it is bonded to the same carbon that is linked to the hydroxyl group. The H<sub>2</sub> proton appears as broad multiplet as a consequence of restricted rotation about the NC=O bond.

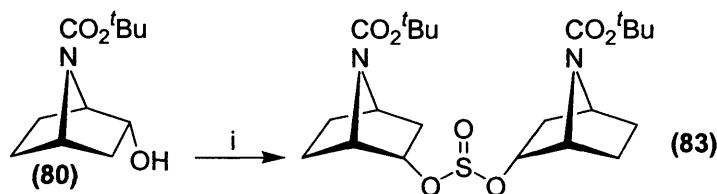
The configuration of the hydroxyl group was confirmed by conversion of (80) to the secondary amine derivative (82) which has been reported by Fletcher<sup>73</sup> who reported no NMR spectroscopic data for (82). Deprotection of the resulting *N*-Boc (80) was performed with HCl (generated *in situ*) to afford the secondary amine which was isolated as the salt (82) (Scheme 4.7).



**Scheme 4.7** Reagents and conditions: (i) 3M HCl (generated *in situ*), 0 °C.

The multiplicity of the H<sub>2</sub> signal was then resolved for **(82)** using homonuclear decoupling experiments. It can be seen from the multiplicity and the coupling constants that the assignment of H<sub>2</sub> is based on the presence of couplings with H<sub>1</sub> ( $J = \sim 4.3$  Hz), H<sub>3-endo</sub> ( $J = 3.3$  Hz) and H<sub>3-exo</sub> ( $J = 9.8$  Hz). H<sub>2</sub> appears at 4.48 ppm as a doublet of doublets of doublets due to these couplings. The couplings of H<sub>3-exo</sub> were also resolved. H<sub>3-exo</sub> appears as a doublet of doublets of doublets of doublets due to its coupling to H<sub>4</sub> ( $J = 5.2$  Hz), H<sub>3-endo</sub> ( $J = 14.1$  Hz), H<sub>2</sub> ( $J = 9.8$  Hz) and by W coupling to H<sub>6-exo</sub> ( $J = 3.0$  Hz).

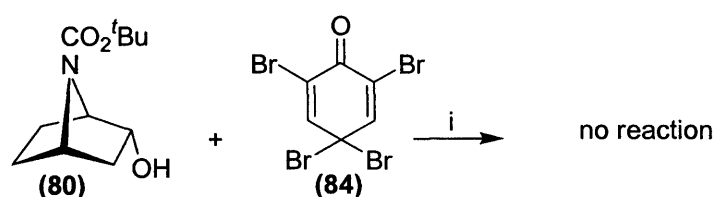
The most common precursors for alkyl halides are the corresponding alcohols; and a variety of procedures have been developed for this transformation. The choice of an appropriate reagent was considered as the *N*-Boc group is acid-sensitive. Therefore, alcohol **(80)** was subjected to different reactions conditions in attempts to synthesize the bromide **(78)**. Firstly, alcohol **(80)** was treated with thionyl bromide in dichloromethane with pyridine (to prevent cleavage of the *N*-Boc protecting group). No indication of **(78)** formation was detected using mass spectrometric and <sup>1</sup>H NMR analysis. A byproduct was instead isolated and was purified using column chromatography. This byproduct was then identified as the dialkyl sulfite **(83)**, isolated in 68% yield (Scheme 4.8). The same compound was obtained when thionyl chloride was used instead, using standard literature procedures. Gerrard *et. al.* reported the isolation of *n*-butyl sulfite when *n*-butanol was treated with thionyl chloride in the presence of pyridine<sup>87</sup> and the formation of **(83)** is thus precedented.



**Scheme 4.8** Reagents and conditions: (i) Br<sub>2</sub>SO or Cl<sub>2</sub>SO, pyridine, CH<sub>2</sub>Cl<sub>2</sub>, 0 °C, 3 h.

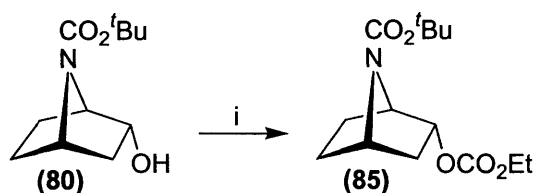
Mass spectrometric analysis confirms the accurate molecular weight of **(83)**. In the <sup>1</sup>H NMR spectrum of **(83)**, the H<sub>2</sub> signal is observed at 4.84 ppm which is shifted downfield compared with the corresponding H<sub>2</sub> (4.34 ppm) in alcohol **(80)**. The chemical shifts of H<sub>1</sub> and H<sub>4</sub> are observed at 4.28 and 4.18 ppm respectively which are in the usual chemical shifts range of the bridgehead protons for the 7-azabicyclic system. A <sup>13</sup>C DEPT spectrum of **(83)** exhibits three CH<sub>2</sub> carbon signals and three CH carbon signals, consistent with assignment of the 7-azabicyclic framework.

Tanaka and Oritani reported a new reagent for transforming alcohols to the corresponding bromides with inversion of configuration under mild and neutral conditions.<sup>88</sup> 2,4,4,6-Tetrabromo-2,5-cyclohexadienone is a brominating agent that convert alcohols to bromides when treated with an equivalent amount of triphenylphosphine (PPh<sub>3</sub>) in dry dichloromethane.<sup>88</sup> This method was applied to the corresponding alcohol (**80**); unfortunately, treatment of alcohol (**80**) with 2,4,4,6-tetrabromo-2,5-cyclohexadienone (**84**) and PPh<sub>3</sub> in dry dichloromethane did not lead to the desired bromo compound (**78**) (Scheme 4.9). Unreacted starting material was recovered in high yield.



**Scheme 4.9** Reagents and conditions: (i) PPh<sub>3</sub>, Dichloromethane, 5 h at RT.

As a result of the unsuccessful synthesis of the bromide (**78**) as described above, an alternative synthetic procedure was attempted. Falck reported the synthesis of alkyl halides from alcohols by modification of the Mitsunobu procedure using lithium salts.<sup>89</sup> There are reported advantages using this procedure such as the mildness of the reaction conditions (giving good to excellent yields) and the inversion of configuration of secondary alcohols. Following the reaction procedure as described,<sup>89</sup> lithium bromide was added to the stirred complex of diethyl azodicarboxylate (DEAD)/PPh<sub>3</sub> followed by the addition of alcohol (**80**). Unfortunately, no (**78**) was obtained. A byproduct was instead isolated as a result of this reaction and was identified as the derivative (**85**) (Scheme 4.10).

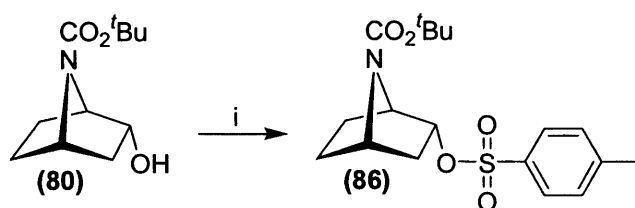


**Scheme 4.10** Reagents and conditions: (i) DEAD, PPh<sub>3</sub>, LiBr, THF, 0 °C to RT.

The compound (**85**) was then purified by column chromatography. Accurate mass spectrometric analysis confirmed the molecular weight of (**85**). The <sup>1</sup>H and <sup>13</sup>C NMR

spectroscopic data also led to the confirmation of structure **(85)**. The  $^1\text{H}$  NMR spectrum shows two broad signals at 4.53 and 4.02 ppm corresponding to  $\text{H}_1$  and  $\text{H}_4$  which are in the normal shifts of 7-azabicyclic bridgehead protons.  $\text{H}_2$  proton signal appears at 4.96 ppm as broad multiplet. The  $^1\text{H}$  NMR integrations prove that the protons of  $\text{OCO}_2\text{CH}_2\text{CH}_3$  group are part of **(85)** structure compared with other protons. The  $^{13}\text{C}$  DEPT spectrum of **(85)** shows three  $\text{CH}_2$  signals at 36.7, 29.1 and 21.8 as part of the 7-azabicyclic skeleton. The  $\text{CH}_2$  carbon signal of  $\text{OCO}_2\text{CH}_2\text{CH}_3$  group is at 64.1 ppm. Two quaternary carbon signals appear at 155.2 and 154.6 ppm corresponding to  $\text{NCO}_2^t\text{Bu}$  and  $\text{OCO}_2\text{Et}$ . The bridgehead carbon signals  $\text{C}_1$  and  $\text{C}_4$  of this system appear at 58.1 and 56.7 ppm.

The attempts so far in this laboratory to directly transform the alcohol **(80)** into the corresponding bromide **(78)** have not been successful. As a consequence, we sought an alternative approach utilizing **(80)**. Since the hydroxyl group in **(80)** could not be replaced easily with a bromine, it was thought that the hydroxyl might be converted to a good leaving group which might be replaced more easily with a bromine ion. One way might make use of protonation, but this was discounted because **(80)** is acid-sensitive due to the presence of the Boc group. Another is the conversion of alcohol to a reactive ester such as a sulfonate. The sulfonate groups (tosylate and mesylate) were selected to be the leaving groups. Firstly, alcohol **(80)** was treated with *p*-toluenesulfonyl chloride to form the corresponding tosylate **(86)** in 54% yield after normal purification using column chromatography (Scheme 4.11).



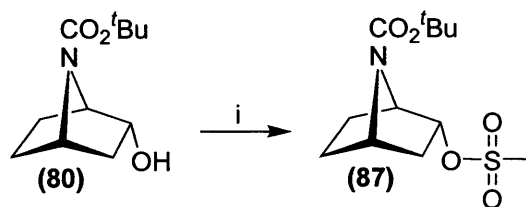
**Scheme 4.11** Reagents and conditions: (i) *p*-TsCl, pyridine, 0 °C to RT, 24 h.

The  $^1\text{H}$  NMR spectrum of tosylate **(86)** shows the bridgehead protons  $\text{H}_1$  and  $\text{H}_4$  at 4.18 and 4.12 ppm respectively. The assignment of  $\text{H}_1$  based on a correlation with  $\text{H}_2$  (4.71 ppm) using  $^1\text{H}$  COSY experiment. In the other hand,  $\text{H}_4$  couples to  $\text{H}_{3\text{-exo}}$  proton (2.16 ppm). The chemical shifts of the aromatic protons of the tosyl group appear at 7.79 ppm (d,  $J = 8.3$  Hz) and 7.36 ppm (d,  $J = 8.3$  Hz). The aryl Me protons appear as singlet at 2.46 ppm. Moreover, the  $^{13}\text{C}$  NMR chemical shifts analysis agrees with the tosylate

**(86)** structure. Three CH<sub>2</sub> carbons signals corresponding to C<sub>3</sub>, C<sub>5</sub> and C<sub>6</sub> appear at 36.7, 29.1 and 21.7 ppm respectively. The assignments were performed with the aid of <sup>1</sup>H-<sup>13</sup>C HMQC experiment. The C<sub>2</sub> signal appears downfield at 78.1 ppm because it is linked to the tosyl group.

With the tosylate **(86)** in hand, treatment of **(86)** with LiBr<sup>90</sup> in dry acetone under nitrogen at room temperature overnight led only to unreacted starting material. The starting material **(86)** was recovered and confirmed by <sup>1</sup>H NMR. The reaction was then performed at reflux.<sup>91</sup> No reaction was detected and the starting material was recovered.

As no reaction occurred with the tosylate **(86)**, alcohol **(80)** was then converted to the corresponding mesylate. Treatment of alcohol **(80)** with methanesulfonyl chloride in NEt<sub>3</sub> at 0 °C to room temperature afforded the mesylate **(87)** (Scheme 4.12).



**Scheme 4.12** Reagents and conditions: (i) CH<sub>3</sub>SO<sub>2</sub>Cl, NEt<sub>3</sub>, 0 °C to RT, 24 h.

The <sup>1</sup>H NMR spectrum of mesylate **(87)** shows a singlet signal at 2.97 ppm corresponding to the Me of the mesylate group. The H<sub>2</sub> signal appears downfield at 4.87 ppm due to its linkage to the same carbon that the mesylate group is bonded to.

The mesylate **(87)** was then treated under similar conditions to those described for the tosylate **(86)**. Unfortunately, there was no evidence for the desired bromide **(78)** and only starting material **(87)** was recovered.

In conclusion, the bromide **(78)** could not be synthesized using the range of reagents and conditions described above. This might be due to the nature of the 7-azabicyclic system. It is considered that this research is worth further exploration but, due to the shortage of time, it could not be completed as part of this investigation.

## **Chapter 5**

### **Nitrogen NMR spectroscopy of 7-azabicyclo[2.2.1]heptane derivatives**

## Chapter 5

### Nitrogen NMR spectroscopy of 7-azabicyclo[2.2.1]heptane derivatives

#### 5.1 Nitrogen NMR spectroscopy

The number of compounds containing nitrogen is enormous, and there are more distinct nitrogen functional groups in organic chemistry than for any other heteroatom. The ability to observe nitrogen NMR directly is a big advantage for chemists and biochemists similarly, but there are barriers on the way.

Nitrogen has two NMR active nuclei ( $^{14}\text{N}$  and  $^{15}\text{N}$ ).  $^{14}\text{N}$  is the major isotope of nitrogen at high natural abundance (99.63%) with a spin quantum number  $I = 1$ . Its signals are usually significantly broadened by quadrupolar interactions, linewidths of up to hundreds Hertz are common, and it is often difficult to recognize the signal above the base line except in simple cases. The  $^{15}\text{N}$  isotope ( $I = 1/2$ ) yields sharp lines and has a large chemical shift range so in that respect it is an easier NMR isotope to deal with than  $^{14}\text{N}$ . However, it suffers from serious disadvantages in that its natural abundance is only 0.37% and its magnetogyric ratio is negative and small resulting in low sensitivity compared to the proton (Table 5.1). These problems can, however, be overcome. Moreover, the  $^{14}\text{N}$  and  $^{15}\text{N}$  chemical shifts are effectively similar to each other. Wong *et al.* reported the  $^{14}\text{N}$  and  $^{15}\text{N}$  chemical shifts of some acyclic tertiary amines and amine hydrochlorides.<sup>92</sup> They found that the resulting  $^{14}\text{N}$  and  $^{15}\text{N}$  chemical shifts usually agree with each other to within 0.5 ppm for the same molecule.

Isotope	N. abundance (%)	Relative sensitivity	Spin
$^1\text{H}$	99.98	1	1/2
$^{13}\text{C}$	1.11	$1.59 \times 10^{-2}$	1/2
$^{15}\text{N}$	0.37	$1.04 \times 10^{-3}$	-1/2

Table 5.1<sup>93</sup>

In order to enhance the measurement of such spectra, it is necessary to use a sensitive high-field Fourier-transform NMR instrument with highly concentrated samples. The slow relaxation of the  $^{15}\text{N}$  nucleus requires exceptionally long spectral acquisition times and further problems arise as a result of the negative magnetogyric ratio ( $\gamma$ ) of the  $^{15}\text{N}$  nucleus, which in turn, result in the nuclear Overhauser effect (nOe) enhancement factors becoming negative, thus causing NMR signals to become more negative with proton decoupling.

However, proton substituents on nitrogen aid relaxation and thus may shorten spectral acquisition. Further improvement can be achieved by the use of paramagnetic relaxation reagents such as tris(acetylacetonato)chromium(III) ( $\text{Cr}(\text{acac})_3$ ). Undesired Overhauser effect can be removed by gated decoupling or addition of ( $\text{Cr}(\text{acac})_3$ ).

Measurement of  $^{15}\text{N}$  chemical shifts can be obtained more easily and quickly using  $^{15}\text{N}$ -enriched samples. However, synthesis of  $^{15}\text{N}$ -enriched sample is not always easy to achieve in practical terms.  $^{15}\text{N}$ -Enriched samples of 7-azabicyclo[2.2.1]heptyl derivatives have been synthesized in the Leicester laboratories.<sup>94</sup> The synthesis of these derivatives required enormous efforts to make compounds enriched to just 2%. Therefore, all the  $^{15}\text{N}$  chemical shifts measurements of our study were performed at natural abundance levels in view of the cost and time that would be involved in producing enriched samples.

## 5.2 Referencing nitrogen NMR spectra

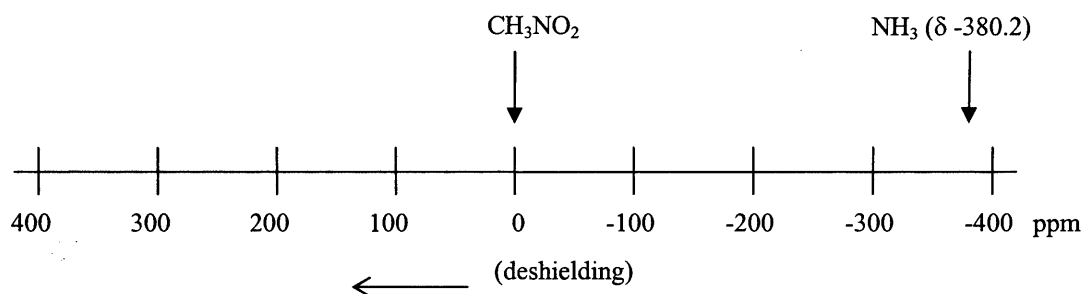
Field and frequency are linked; the favored procedure for measuring chemical shifts is to reference them to an internal frequency standard. For both  $^1\text{H}$  and  $^{13}\text{C}$  NMR, the most suitable standard is tetramethylsilane (TMS), chosen because it is chemically unreactive, soluble in most organic substrates, provides sharp signal and can be easily removed from the sample after use.

For nuclei other than  $^1\text{H}$  and  $^{13}\text{C}$  the choice of a reasonable standard is not so easily determined. The use of an internal standard in  $^{15}\text{N}$  NMR is generally unreliable.<sup>95,96</sup> The  $^{15}\text{N}$  chemical shifts are quite sensitive to molecular interactions, and for any given compound in a variety of solvents, nitrogen shifts can extend a range of more than 10 ppm; this includes obviously the shielding of the internal standard themselves. Another disadvantage of using internal standards is contamination of the sample under examination. There is, however, a way to avoid, at least to some extent, the complexity of internal referencing of nitrogen shielding. The method relies on the use of an external standard which has an obvious advantage since no contamination of the sample is involved. The use of coaxial cylindrical sample/reference tubes diminishes the susceptibility effects and allows the direct measurement of chemical shift difference between the sample and the reference.<sup>95</sup> Neat nitromethane has been widely used because of its high nitrogen concentration per unit volume (18.42 M at 30° C).

Neat nitromethane is gaining ground as the universal external reference for both  $^{14}\text{N}$  and  $^{15}\text{N}$  measurement of nitrogen shielding, as can be inferred from the following comparison:

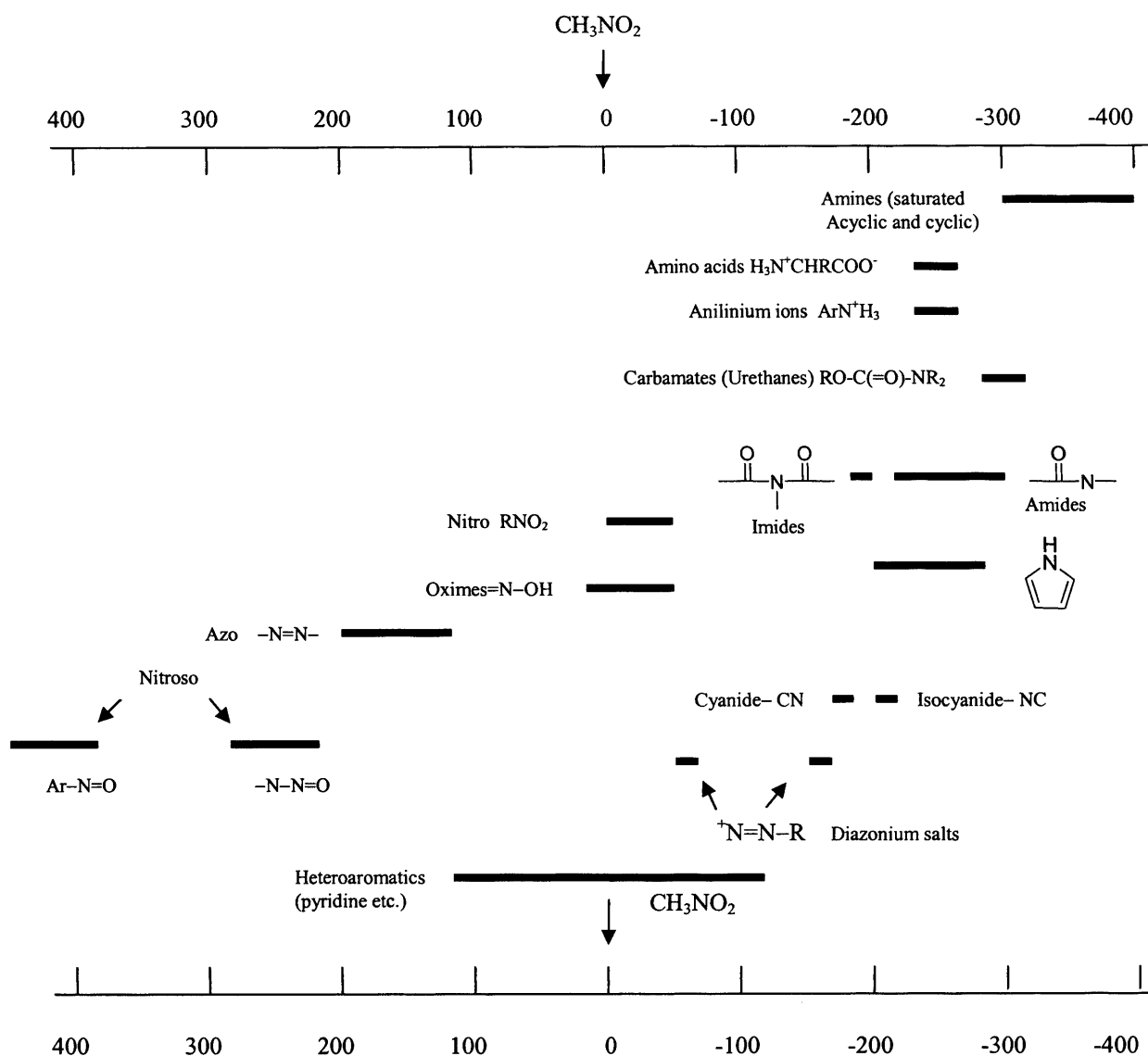
Standard	% of papers where the standard specified was employed <sup>97</sup>
Neat nitromethane	40%
$\text{NH}_4^+$ , in various solutions	15%
$\text{NO}_3^-$ , in various solutions	10%
$\text{HNO}_3$ , in various solutions	10%
Liquid $\text{NH}_3$	10%
Others	15%

Another source of confusion is the problem of the sign conventions used with nitrogen shifts. The plus sign has, at different times, been used to denote either an increasing or decreasing shielding referred to an arbitrary standard. The later system became the accepted usage in  $^1\text{H}$  and  $^{13}\text{C}$  NMR spectroscopy. In the present work neat nitromethane was employed as an external standard and the plus sign refers to the direction of decreasing magnetic field (high frequencies) (Figure 5.1). All of the shifts in this thesis are upfield of the standard and are therefore negative values.



**Figure 5.1**

Figure 5.2 summarizes the nitrogen NMR chemical shielding ranges for some various classes of molecules which are referred to external neat nitromethane.<sup>98</sup> We are in this study interested in 7-azabicyclic derivative carbamates (urethanes) and amines nitrogen NMR chemical shifts.

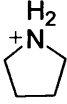
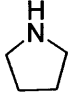
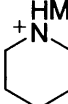
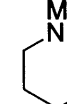


**Figure 5.2**

### 5.3 Influence of protonation on $^{15}\text{N}$ chemical shifts

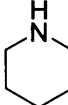
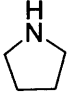
The nitrogen atom of an amine is basic and owes this property to the pair of non-bonding electrons; the reactivity of these electrons causes shifts to be produced if the amine is protonated. The magnitude of the shift depends on several factors including pH, the nature of the counter-ion and the degree of hydrogen bonding lost or gained. Unfortunately, the direction of the shift is not uniform. The protonation of a nitrogen atom within a system of saturated bonds such as alkylamines usually results in weak deshielding (typically *ca.* 10 ppm) while in a conjugated system of double bonds or to an aromatic ring such as pyridine it moves the signal *ca.* 100 ppm upfield.<sup>95</sup> The protonated amines of the parent 7-azanorbornane derivatives in this study play a major part in obtaining nitrogen chemical shifts in view of difficulties measuring shifts for the free

amines. This was considered acceptable in view of the small differences between the shifts of free amines and protonated forms. Table 5.2 shows the  $^{15}\text{N}$  chemical shifts of some selected examples of the free amines and their protonated forms.<sup>95</sup> Slight deshielding was observed as a result of protonation.

Compound					$\text{Me}_2\text{NH}_2^+$	$\text{Me}_2\text{NH}$	$\text{Et}_3\text{NH}_2^+$	$\text{Et}_3\text{NH}$
$^{15}\text{N}$ (ppm)	-333.4	-342.5	-335.3	-340.6	-356.6	-369.5	-322.8	-332.0

**Table 5.2**  $^{15}\text{N}$  chemical shifts of some selected amines.<sup>95</sup>

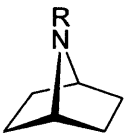
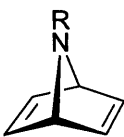
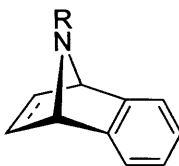
It was noticed in early studies that nitrogen shielding variations can be influenced by the solvent as the influence of protonation.<sup>95,97</sup> The largest differences noticed in nitrogen shielding as a result of solvent effects was about 45 ppm.<sup>97</sup> However, in some types of compound such as amines, the variation of solvents have smaller effects on the nitrogen shielding (just a few ppm), even if both polar or non-polar solvents are used.<sup>95,97</sup> In addition to the solvent effects, the variations of concentration and temperature might have an effect on the nitrogen shielding. Table 5.3 summarizes the  $^{15}\text{N}$  chemical shifts of some selected examples of alkyl amines measured in different solvents and variable concentrations.<sup>95</sup> As a result of these variations, the nitrogen chemical shift comparisons under different conditions might be less valid. Therefore, the experimental conditions for the nitrogen shift measurements were maintained and kept constant as much as possible in this study.

			$\text{Et}_3\text{NH}$
Solvent	$^{15}\text{N}$ (ppm)	$^{15}\text{N}$ (ppm)	$^{15}\text{N}$ (ppm)
cyclohexane	-341.4	-342.4	-331.8
neat liquid	-341.6	-342.5	-332.6
DMSO	-342.4	-341.7	-333.9
MeOH	-342.6	-341.4	-333.1
$\text{H}_2\text{O}$	-340.4	-341.3	-331.2
$\text{CHCl}_3$	-340.6	-340.3	

**Table 5.3**  $^{15}\text{N}$  chemical shifts of some selected amines.<sup>95</sup>

The solvent effects were investigated in this study of some selected 7-azabicyclic compounds such as amines (**1a**) and (**2a**); and the result of using polar or non-polar solvent was that the nitrogen chemical shift variation was *ca.* 1 ppm. Similarly, the concentration effect on the nitrogen shielding was considered in this study. The result of using different concentration of some selected amines (**1a**), (**2a**) and (**3b**) led to only 0.5 ppm difference. We could conclude that neither solvent nor concentration has a big effect on the nitrogen chemical shifts.

#### 5.4 <sup>15</sup>N chemical shifts of urethane derivatives of 7-azabicyclic systems

				
R = CO <sub>2</sub> Et	( <b>42</b> ) -259.5	( <b>38</b> ) -247.3	( <b>26b</b> ) -203.6	ethano- ( <b>30</b> ) <sup>b</sup> -241.0 <sup>55</sup> etheno- ( <b>29</b> ) <sup>b</sup> -208.6 <sup>55</sup>
R = CO <sub>2</sub> <sup>t</sup> Bu	( <b>44</b> ) -257.5	( <b>39</b> ) -248.1	( <b>26c</b> ) -202.6	

**Table 5.4** <sup>15</sup>N chemical shift values for urethanes.<sup>a</sup>

- Measurements at 300K in CDCl<sub>3</sub> in 10 mm NMR tubes (chemical shift values in ppm relative to neat CH<sub>3</sub>NO<sub>2</sub> contained in an internal, coaxial 5 mm tube). Samples at natural abundance.
- Values quoted by Quin *et al.* using a 23% <sup>15</sup>N-enriched sample. These values were recorded as 139.2 and 171.6 ppm respectively relative to liquid ammonia; the <sup>15</sup>N spectra were referenced externally to CH<sub>3</sub>NO<sub>2</sub>, where δ CH<sub>3</sub>NO<sub>2</sub> = 380.2 with liquid ammonia as zero; samples dissolved in CDCl<sub>3</sub>.<sup>55</sup>

##### 5.4.1 *N*-Alkoxy carbonyl-7-Azanorbornane derivatives

The saturated derivatives (**42**) were established as the point of reference (Table 5.4). There are no <sup>15</sup>N data reported in the literature for saturated 7-azanorbornane systems (**42**). The chemical shifts observed for (**42**) are at higher field than any of the unsaturated examples (**38**) and (**26b**) and at higher field than the benzo-derivatives (**29**) and (**30**) which provide the only comparison data for azabicyclic systems from the literature.<sup>55</sup> The <sup>15</sup>N chemical shift of the *N*-ethoxycarbonyl derivatives (**42**) is similar to the shift observed for the *t*-butoxycarbonyl derivatives (**44**) (Δδ = 2.0 ppm) suggesting that the ester alkyl group has only a small effect.

##### 5.4.2 *N*-Alkoxy carbonyl-7-Azanorbornene derivatives

Introduction of a single unsaturated linkage into the 7-azabicyclic framework (**38**) leads to deshielding of the bridging nitrogen when comparison is made with the

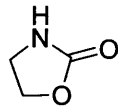
corresponding saturated analogue (**42**) ( $\Delta\delta = 12.2$  ppm) (Table 5.4). Introduction of a benzo group instead of the alkene [compound (**29**)] induces a larger downfield shift ( $\Delta\delta = 18.5$  ppm). The variation of the ester alkyl group at the nitrogen has also a minor effect on the  $^{15}\text{N}$  shifts as noticed for (**42**) and (**44**).

### 5.4.3 *N*-Alkoxy carbonyl-7-Azanorbornadiene derivatives

Introduction of a second double bond into the 7-azabicyclic frameworks (**26b**) leads to a further, much larger downfield shift ( $\Delta\delta = 43.7$  ppm) when comparison is made with the mono-unsaturated analogue (**38**) (Table 5.4). The incorporation of an additional double bond in (**30**) also leads to a substantial shift ( $\Delta\delta = 32.4$  ppm) when comparison is made with (**29**).

The results that can be demonstrated from table 5.4 are as follows: the  $^{15}\text{N}$  chemical shifts of (**26b**) and (**26c**) are over 100 ppm downfield when compared to the values for normal urethanes. A substantial downfield shift is observed on replacing an ethano- bridge with an etheno- bridge (**42**)  $\rightarrow$  (**38**). A larger downfield shift is observed on introducing a second  $\pi$  bond to the system (**42**)  $\rightarrow$  (**26b**). A similar downfield shift occurs on introducing a second  $\pi$ -bond in the benzo-series (**30**  $\rightarrow$  **29**). Thus, introduction of  $\pi$ -bonds leads to downfield shifts and is a cumulative effect in these urethanes.

In addition, comparison with data for normal urethanes shows that these 7-azabicyclic urethanes display  $^{15}\text{N}$  chemical shifts which are significantly downfield from any normal urethanes especially in (**26b**) and (**26c**) (Table 5.5).<sup>99</sup>

	<chem>MeOC(=O)NMe2</chem>	<chem>EtOC(=O)NH2</chem>		
$^{15}\text{N}$ (ppm)	-315.7	-307.6	-305.6	-203.6

**Table 5.5**  $^{15}\text{N}$  chemical shifts of selected urethanes for comparison.<sup>99</sup>

## 5.5 $^{15}\text{N}$ NMR spectra of tertiary amine derivatives of 7-azabicyclic systems (and the derived HCl salts)

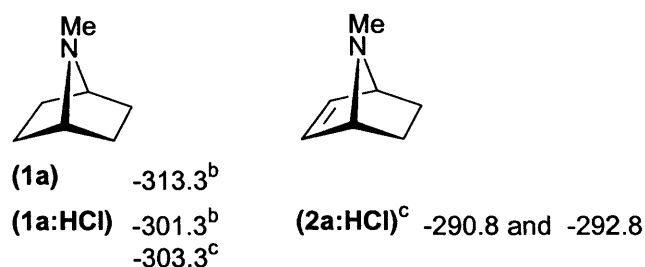


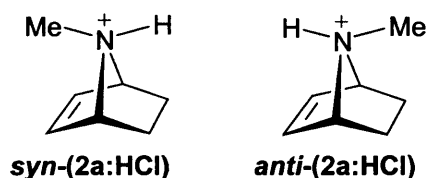
**Table 5.6**  $^{15}\text{N}$  chemical shift values for the free tertiary amine derivatives and HCl salts.<sup>a</sup>

- a. Measurements at 300K in 10 mm NMR tubes (chemical shift values in ppm relative to neat  $\text{CH}_3\text{NO}_2$  contained in an internal, coaxial 5 mm tube). Samples at natural abundance.
- b. Dissolved in  $\text{CDCl}_3$ .
- c. Dissolved in  $\text{CD}_2\text{Cl}_2$ .

The free tertiary amines lack a hydrogen directly attached to nitrogen and this leads to slower relaxation and hence to weaker signals, requiring longer accumulation times and larger samples. The free tertiary amine (**1a**) shows a signal at  $-313.3$  ppm (Table 5.6) which required *ca.* 30,000 scans in order to obtain a reasonable signal to noise (S/N) ratio. The  $^{15}\text{N}$  shift for the mono-unsaturated *N*-methyl free amine (**2a**) shows a very broad signal at room temperature suggesting either that insufficient material was available, that a negative nOe effect was operating (canceling out the signals), or that the process of nitrogen inversion was leading to coalescence of the signals for the two invertomers. However, when the temperature was lowered to  $-10$  °C, no signal appeared. Further work over a broader range of temperature is required to discover whether significantly lower or higher temperatures will lead to sharpening of the signals which is clearly difficult in practical terms. As a result of the difficulties in obtaining  $^{15}\text{N}$  shifts of the free amines (**2**) and (**3**), we then considered  $^{15}\text{N}$  shift measurements of the protonated forms of amines (**1**) – (**3**) and derivatives substituted in the 2-carbon bridge.

The first successful measurements for amines derived from (**1**) – (**3**) were made on amine salts because the protons on nitrogen aid relaxation and thus shorten spectral acquisition. The  $^{15}\text{N}$  chemical shift of (**1a:HCl**) is  $-301.3$  ppm which is downfield ( $\Delta\delta = 12$  ppm) by comparison with the free amine (**1a**) (Table 5.6). Incorporation of a single unit of unsaturation into the framework of (**1a:HCl**) leads to downfield shifts for (**2a:HCl**) ( $\Delta\delta = 12.5$  and  $10.5$  ppm). The observation of two signals for (**2a:HCl**) is explained by the presence of two stereoisomeric quaternary salts in which the methyl group is *syn* or *anti* to the double bond. The  $^{15}\text{N}$  chemical shift difference between the

*syn* and *anti* stereoisomers as can be seen from Table 5.6 is small ( $\Delta\delta = 2$  ppm). Signals due to the major and minor peaks were assigned on the basis of ratio of invertomer derived from  $^1\text{H}$  and  $^{13}\text{C}$  NMR (described in chapter 6). The larger  $^{15}\text{N}$  NMR peak was assigned to the major stereoisomer (*syn* where the *N*-Me *syn* to the double bond), this is because the ratio of *syn* : *anti* is 85 : 15.



The deshielding effect of the extra  $\pi$  bond on the  $^{15}\text{N}$  chemical shift of the tertiary amines (**1a:HCl**) and (**2a:HCl**) is again observed. The  $^{15}\text{N}$  chemical shifts of (**1**) and (**2**) derivatives are over 70 ppm downfield when compared to the values for normal tertiary amines.

## 5.6 $^{15}\text{N}$ NMR spectra of secondary amine derivatives 7-azabicyclic systems (and the derived HCl salts)

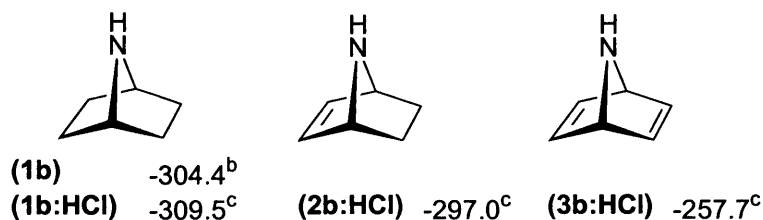


**Table 5.7**  $^{15}\text{N}$  chemical shift values for the free secondary amine derivatives and HCl salts.

- Measurements at 300K in 10 mm NMR tubes (chemical shift values in ppm relative to neat  $\text{CH}_3\text{NO}_2$  contained in an internal, coaxial 5 mm tube). Samples at natural abundance.
- Dissolved in  $\text{CDCl}_3$ .
- Dissolved in MeOH.

The  $^{15}\text{N}$  NMR spectrum for the free secondary amine (**1b**) shows a signal at -304.4 ppm (Table 5.7), slightly downfield of the signal for the HCl salt (in contrast to the situation for the tertiary amines (**1a**) and (**1a:HCl**) where the free amine signal was relatively upfield. No signal was observed for (**2b**) at room temperature. It is not yet clear whether this is because of a negative nOe leading to lower signal intensity as a consequence of  $^1\text{H}$ -decoupling. Thus,  $^{15}\text{N}$  shift measurements of the free secondary amines (**2b**) and (**3b**) were again not possible. Therefore, the availability of the  $^{15}\text{N}$  shift

data for the series of secondary amine salts (**1b**) – (**3b**) allows effective shift comparisons to be made and spectra were all measured in MeOH. The signal for the secondary amine salt (**1b:HCl**) is again shifted downfield when a double bond is introduced in (**2b:HCl**). The downfield increment ( $\Delta\delta = 12.5$  ppm) is of a similar order of magnitude to the earlier observations. The  $^{15}\text{N}$  chemical shift of (**3b:HCl**) also moves further downfield when a second double bond is introduced to the 7-azabicyclic systems. The solubility of these salts (**1b**) – (**3b**) is low in non-polar solvent such as  $\text{CDCl}_3$ , thus MeOH was used instead as the solvent to reach high solubility.

The substantial downfield shifts in these amines become clear when comparison is made with data for other cyclic secondary amines.<sup>97</sup>

### 5.7 $^{15}\text{N}$ shifts of urethane derivatives of 7-azabicyclic systems containing different substituents in the 2-carbon bridges

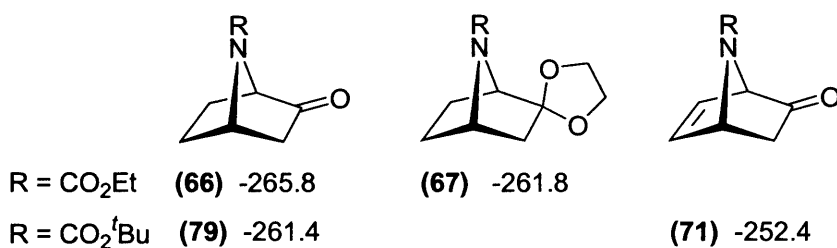


**Table 5.8**  $^{15}\text{N}$  chemical shift values for urethanes with different substituents in the 2-carbon bridges.<sup>a</sup>

- a. Measurements at 300K in  $\text{CDCl}_3$  in 10 mm NMR tubes (chemical shift values in ppm relative to neat  $\text{CH}_3\text{NO}_2$  contained in an internal, coaxial 5 mm tube). Samples at natural abundance.

The chemical shift of the 7-azanorbornane substituted at the 2-carbon bridge by a carbonyl group (**66**) is  $-265.8$  ppm which is upfield compared to the 7-azanorbornane (**42**) ( $\Delta\delta = 6.3$  ppm). As expected, small variations of the nitrogen-protecting group in (**66**) and (**79**) make relatively little difference to the chemical shifts; the  $^{15}\text{N}$  chemical shift of the *t*-butoxycarbonyl derivative (**79**) is similar to that observed for (**66**) ( $\Delta\delta = 4$  ppm), as expected (Table 5.8).

The chemical shift of the protected carbonyl compound, the cyclic acetal (**67**), is very similar to the saturated 7-azanorbornane (**42**) ( $\Delta\delta = 2$  ppm). The incorporation of unsaturation into the 2-carbon bridge in (**71**) leads to a shifted downfield shift ( $\Delta\delta = 9$  ppm), as expected, when compared with the saturated (**66**) (Table 5.8).

## 5.8 $^{15}\text{N}$ shifts of the tertiary amine (HCl salts) derivatives of 7-azabicyclic systems containing different substituents in the 2-carbon bridges

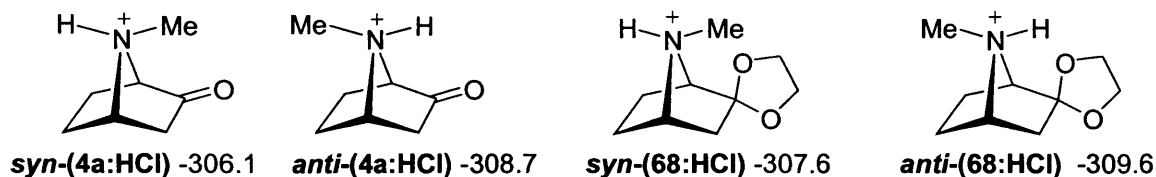


**Table 5.9**  $^{15}\text{N}$  chemical shift values for tertiary amine derivatives (HCl salts).<sup>a</sup>

a. Measurements at 300K in MeOH in 10 mm NMR tubes (chemical shift values in ppm relative to neat  $\text{CH}_3\text{NO}_2$  contained in an internal, coaxial 5 mm tube). Samples at natural abundance.

The chemical shift of the quaternary salt (**4a:HCl**) is shifted to higher field than the quaternary salt (**1a:HCl**) ( $\Delta\delta = 5$  ppm). The observation of the two signals for (**4a:HCl**) is due to the presence of the two stereoisomeric quaternary salts in which the methyl group is *syn* or *anti* to the carbonyl group. The  $^{15}\text{N}$  chemical shifts of the two stereoisomeric acetals (**68:HCl**) are fairly similar to these for (**4a:HCl**) ( $\Delta\delta = 1$  ppm). The  $^{15}\text{N}$  chemical shift difference between the *syn* and *anti* stereoisomers as can be seen from Table 5.9 is small ( $\Delta\delta = 2.6$  ppm for (**4a:HCl**) and  $\Delta\delta = 2$  ppm for (**68:HCl**)). Signals due to the major and minor peaks were assigned for the stereoisomers (**4a:HCl**) and (**68:HCl**) on the basis of the invertomer ratios measured by  $^1\text{H}$  and  $^{13}\text{C}$  NMR spectroscopy (described in chapter 6). The larger  $^{15}\text{N}$  NMR peaks were assigned to the major stereoisomers (*anti* where the *N*-Me *anti* to the ketone or acetal group) (Table 5.9).

There are general observations which can be made when looking at the  $^{15}\text{N}$  results described above.

- The general downfield shift is common to all members of this family of 7-azabicyclo[2.2.1]heptyl systems compared to normal acyclic and mono-cyclic amines.
- The dependence of the deshielding on the degree of unsaturation. The introduction of an extra  $\pi$  bond in the urethane systems (**38**) comparing with data for saturated urethane systems (**42**) affects the  $^{15}\text{N}$  resonance. A downfield increment of ca. 12 ppm is observed on replacing an ethano-bridge with an etheno-bridge (**42**) to (**38**). However, a significant cumulative downfield increment of ca. 56 ppm was observed by introducing two double bonds at the ethano-bridge (**42**) to (**26b**). A similar observation was made for the *t*-butoxycarbonyl-protected analogues. Evidence of a similar trend of  $^{15}\text{N}$  shifts was

observed with the protonated secondary amines **(1b:HCl)**, **(2b:HCl)** and **(3b:HCl)**. Thus, the differences of the  $^{15}\text{N}$  shifts of the urethanes and the secondary amine salts could be considered as an estimate of the  $^{15}\text{N}$  shift differences of some important compounds such as **(2a)** and **(3a)** which were difficult to measure.

- c) Substitution in the 2-carbon bridge **(66)** seems to have a relatively small effect on the  $^{15}\text{N}$  chemical shifts of the saturated urethane **(42)**; and the protonated tertiary amines **(1a:HCl)** and **(4a:HCl)**, but the trend is that the ketone group leads to an upfield shift.
- d) The  $^{15}\text{N}$  chemical shift of the tertiary amine **(1a)** is relatively upfield compared to that of the secondary amine **(1b)**. This is probably explained by the electron donating character of the methyl group at nitrogen ( $\alpha$ -effect).<sup>97</sup> The *N*-Me amine **(1a)** is shifted upfield by 8.9 ppm compared to the secondary amine **(1b)**. Similar observations were reported in 7-azabicyclo[2.2.1]heptyl derivatives<sup>25</sup> and monocyclic<sup>97</sup> amines.
- e) Two  $^{15}\text{N}$  signals were detected for the quaternary salts **(2a:HCl)**, **(4a:HCl)** and **(68:HCl)** due to the presence of two stereoisomeric quaternary salts in which the methyl group is *syn* or *anti* to the double bond or the substituted group at C<sub>2</sub>.

We then decided to investigate the  $^{15}\text{N}$  and  $^{14}\text{N}$  chemical shifts similarity of some selected 7-azabicyclic derivatives;  $^{14}\text{N}$  spectra were expected to be obtained much more easily but signals would, inevitably, be broader than  $^{15}\text{N}$  signals. For all the samples, both  $^{15}\text{N}$  and  $^{14}\text{N}$  spectra were measured under similar experimental conditions. Table 5.10 summarizes the  $^{15}\text{N}$  and  $^{14}\text{N}$  shifts of some selected compounds as comparison data. The comparisons between the results of table 5.10 show that  $^{15}\text{N}$  and  $^{14}\text{N}$  chemical shifts are similar to each other within *ca.* 1 ppm.

	<b>(1a)</b>	<b>(1a:HCl)</b>	<b>(2a:HCl)</b>	<b>(1b)</b>	<b>(1b:HCl)</b>	<b>(3b:HCl)</b>
$^{15}\text{N}$ (ppm) <sup>a</sup>	-313.3	-303.3	-290.8/-292.8	-304.4	-309.5	-257.7
$^{14}\text{N}$ (ppm)	-312.5 ± 2	-304.0 ± 2	-292.1 ± 3	-304.0 ± 1	-308.7 ± 1	-256.5 ± 1

**Table 5.10**

a. Samples at natural abundance.

Therefore, the  $^{15}\text{N}$  chemical shifts of the free tertiary amines (**2a**) and (**3a**) could be estimated using the approximate values described at point (b) above. The  $^{15}\text{N}$  result of the free amine (**1a**) ( $-313.3$  ppm) which required 48 hours accumulation at natural abundance and highly concentrated (ca. 320 mg) sample was used as starting point. The approximate  $^{15}\text{N}$  chemical shifts estimated for the free amines (**2a**) and (**3a**) are  $-301.0 \pm 2$  and  $-256.0 \pm 2$  ppm respectively; this is an attempt to overcome the difficulty in achieving direct measurements of  $^{15}\text{N}$  shifts for (**2a**) and (**3a**); and allow us to use the  $^{14}\text{N}$  chemical shifts. Measurements of the nitrogen shifts of (**2a**) and (**3a**) were performed using  $^{14}\text{N}$  NMR instead. The  $^{14}\text{N}$  chemical shifts of the free amines (**2a**) and (**3a**) are  $-297.0 \pm 3$  and  $-253.0 \pm 3$  ppm respectively. The range between the estimated  $^{15}\text{N}$  shift values and measured  $^{14}\text{N}$  shifts are in agreement (ca. 4 ppm) for (**2a**) and (**3a**). The  $^{14}\text{N}$  shift was also measured for the ketone free amine (**4a**) ( $-319.5 \pm 2$  ppm).

## 5.9 Discussion

The  $^{15}\text{N}$  NMR spectra have been measured successfully for some bridged urethanes and amines at natural abundance. Approximately 35,000 scans were necessary in order to obtain a reasonable signal to noise ratio.

These results show that the incorporation of nitrogen into the bridging position of 7-azabicyclo[2.2.1]heptyl systems leads to significant downfield shifts compared to acyclic and mono-cyclic amines. Table 5.11 demonstrates the reported limits of the chemical shifts recognized earlier for primary, secondary and tertiary amines.<sup>47,97</sup> Some mono-cyclic amines are included for comparison purposes.

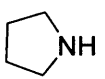
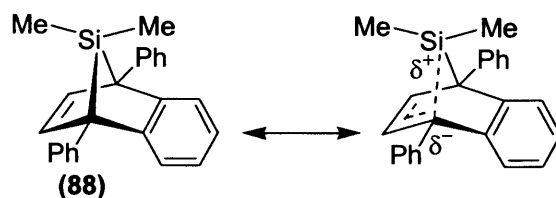
Species	Chemical shift (ppm)
$\text{NH}_2\text{R}$	$-325 \rightarrow -380$
$\text{NHR}_2$	$-300 \rightarrow -370$
$\text{NR}_3$	$-325 \rightarrow -330$
	$-342.5$ ppm
	$-343.5$ ppm
	$-388.7$ ppm

Table 5.11<sup>47,97</sup>

It seems unlikely that CNC angle strain at the 7-position is the reason for this deshielding phenomenon as nitrogen atoms found in 3- and 4-membered rings are significantly shielded relative to other cyclic amines. Further, the degree of deshielding

is dependent on the number of unsaturated bonds present at the two-carbon bridges. The greater the unsaturation in the 7-azabicyclo[2.2.1]heptyl skeleton, the greater the downfield shift of the nitrogen atom at the 7-position.

Sakuri<sup>46</sup> studied the <sup>29</sup>Si NMR chemical shifts of some 7-silanorbornadiene and related systems such as compound (**88**) and found that these systems not only exhibit a <sup>29</sup>Si resonance at very low field, but rather surprisingly, they come out at far lower field than sp<sup>2</sup>-hybridized silicon atom. An enhanced polarization in the ground state of the molecule was suggested as the cause of this deshielding effect.<sup>46</sup> Such polarization should be correlated with  $\sigma$ - $\pi$  conjugation which must be very important in these rigid frameworks.



In another study, Quin<sup>45</sup> observed a similar unusual deshielding effect in <sup>31</sup>P NMR chemical shifts of systems having phosphorus at the 7-position of bicyclo[2.2.1]heptyl systems. Quin supported the idea of ground state polarization which occurs from  $\sigma$ - $\pi$  conjugation.

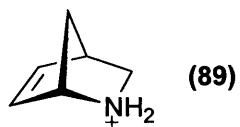
Christl<sup>100</sup> commented on the downfield shift of the carbon atom at the 7-position of norbornene and norbornadiene. The  $\pi^*$  orbital in norbornene is of relatively low energy which causes a  $\sigma$ - $\pi^*$  interaction. This interaction leads to a downfield shift of C<sub>7</sub>. In norbornadiene, the interaction of two double bonds leads to a low-lying  $\pi^*$  orbital and hence a substantial electron-withdrawal from C<sub>7</sub> (Figure 5.3). Christl's idea seems to be more convincing and better explanation than the idea of an enhanced polarization at the ground state put forward by Sakuri and supported by Quin.



**Figure 5.3**

The chemical shift of the <sup>15</sup>N atom in 2-azabicyclo[2.2.1]hept-5-ene hydrochloride (**89**) (-334.6 ppm)<sup>101</sup> showed that the downfield shift was only observed when the

nitrogen was incorporated into the 7-position in of bicyclo[2.2.1]heptyl systems, not in the 2-position.



The deshielding of nitrogen in the 7-azabicyclo[2.2.1]heptyl derivatives suggest that some increased delocalization of the lone-pair of electrons into the bicyclic framework occurs when compared with normal aliphatic and alicyclic amines.

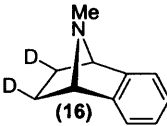
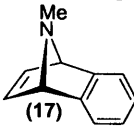
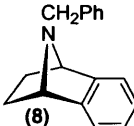
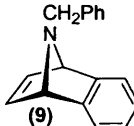
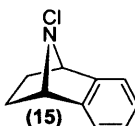
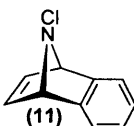
**Chapter 6**  
**Inversion Barriers**

## Chapter 6

### Inversion barriers

#### 6.1 Inversion barriers in 7-azabicyclo[2.2.1]heptyl derivatives

7-Azabicyclo[2.2.1]heptyl derivatives are known to possess high barriers to nitrogen inversion.<sup>2</sup> The predicted C-N-C bond angle for the 7-azabicyclo[2.2.1]heptane structure is relatively similar to that found in azetidines (ca. 95°), but the inversion barriers for the azabicyclic systems are at least 20 kJmol<sup>-1</sup> higher.<sup>1</sup> Therefore, there are other effects than ring strain influencing the inversion barriers. More recently Nelsen *et al.* reported the inversion barrier of the simplest derivative of 7-methyl-7-azanorbornane (**1a**) (57.4 kJmol<sup>-1</sup>) at 25 °C by dynamic <sup>13</sup>C NMR.<sup>3</sup> In another study of inversion barrier at nitrogen, Marchand, *et al.* reported higher inversion barriers when a double bond was introduced to the 7-methyl-7-azanorbornane framework (**2a**).<sup>21</sup> These were calculated from changes in signals due to the vinyl protons (62.1 kJmol<sup>-1</sup>) at 22 °C and the bridgehead protons (57.1 kJmol<sup>-1</sup>) at -10 °C. Moreover, Malpass, *et al.* reported the measurements of the nitrogen inversion barriers for *N*-methyl benzo-derivatives of these ring systems in order to investigate the effects of variations of the 2-carbon bridges on the inversion process.<sup>22</sup> In this work, comparison of  $\Delta G^\ddagger$  values for (**16**) (55.8 kJmol<sup>-1</sup>)<sup>22</sup> and (**17**) (64.6 kJmol<sup>-1</sup>)<sup>22</sup> demonstrated a barrier reduction ( $\Delta\Delta G^\ddagger = 8.8$  kJmol<sup>-1</sup>) as the etheno-bridge was saturated (Table 6.1).

				
	(1a)	(2a)	(3a)	
$\Delta G^\ddagger_{\text{inv}}$ (kJmol <sup>-1</sup> )	57.4 <sup>3</sup>	62.1 <sup>21</sup> (vinyl protons) 57.1 <sup>21</sup> (bridgehead protons)	67.6 <sup>a</sup>	
				
	(16)	(17)	(8)	(9)
$\Delta G^\ddagger_{\text{inv}}$ (kJmol <sup>-1</sup> )	55.8 <sup>22</sup>	64.6 <sup>22</sup>	52.4 <sup>16</sup>	61.9 <sup>16</sup>
				
	(15)	(11)		
$\Delta G^\ddagger_{\text{inv}}$ (kJmol <sup>-1</sup> )	94.8 <sup>23</sup>	98.2 <sup>36</sup>		

**Table 6.1** Nitrogen inversion barriers in 7-azanorbornane derivatives.

a. This work. All values in this table calculated assuming 50:50 invertomer ratio.

Sutherland measured the nitrogen inversion barriers of *N*-benzyl derivatives of the same ring systems.<sup>16</sup> The inversion barrier of the compound with one saturated ethano-bridge (**8**) (52.7 kJmol<sup>-1</sup>) is lower than the unsaturated analogue (**9**) (64.6 kJmol<sup>-1</sup>).<sup>16</sup> In the systems (**16**) and (**8**) another factor that may lower the nitrogen barrier is a simple destabilization of the ground state due to steric interactions between the *N*-Me and *exo*-protons of the ethano- bridge. Malpass, *et al.* studied the effect of the presence of an electronegative atom on the bridging nitrogen on the nitrogen barriers.<sup>23</sup> The fully unsaturated system (**11**)<sup>36</sup> (98.2 kJmol<sup>-1</sup>) possesses a higher barrier than the partly saturated system (**15**)<sup>23</sup> (94.8 kJmol<sup>-1</sup>) but the nitrogen inversion barriers for these systems (**11**) and (**15**) are uniquely high due to the combined effects of the ‘bicyclic’ effect and the electronegative atom on the nitrogen (Table 6.1). Much of this work has been performed using benzo-derivatives since these are slightly easier to synthesize. There are no reported inversion barrier data for the 7-azanorbornadiene system itself. Therefore, one of our interests was to measure the inversion barrier for the 7-methyl-7-azanorbornadiene derivative (**3a**).

In early work, all barriers reported in the literatures were calculated on the basis of 50:50 populations. All the inversion barrier values were calculated in this study on the basis of 50:50 ratios by analogy with the work reported by other groups. However, this is clearly not always the case and this question will be addressed later in this chapter.

## 6.2 7-azanorbornadiene derivatives

The total synthesis and the measurement of inversion barrier of the previously unknown 7-methyl-7-azanorbornadiene (**3a**) were achieved and this provides significant information on the effect of introducing two double bonds into the system. Two alkene signals in the <sup>1</sup>H NMR spectrum of (**3a**) at 25 °C in C<sub>6</sub>D<sub>6</sub> can be observed. The frequency difference separating the signals ( $\Delta\nu$ ) (164.5 Hz) and the coalescence temperature (75 °C) of the alkene signals were determined for (**3a**). The inversion barriers were calculated using the Gutowsky-Holm equation. The inversion barrier of (**3a**) (67.6 kJmol<sup>-1</sup>) is higher than that for the unsaturated 7-azanorbornane (**1a**) (57.4 kJmol<sup>-1</sup>)<sup>3</sup> derivative. It has been noticed that by introducing one double bond to the ethano-bridge, the inversion barrier is raised for (**2a**) (62.1 kJmol<sup>-1</sup>)<sup>21</sup> and similar increment were observed on introducing an etheno-bridge into the benzazanorbornanes (Table 6.1). However, by introducing two double bonds to the system, the inversion barrier is higher (*ca.* 10 kJmol<sup>-1</sup>) than the simple unsaturated 7-azanorbornane (**1a**). The  $\Delta G_{inv}^\ddagger$  difference between (**2a**) and (**3a**) is

5.3 kJmol<sup>-1</sup>. Therefore, introduction of a second double bond into the parent 7-azanorbornane systems increases the nitrogen inversion barrier by a similar increment. Table 6.2 summarizes the incremental differences in  $\Delta G^\ddagger_{\text{inv}}$  affected by the addition of the  $\pi$ -bond for each of the parent systems and the benzo analogues (comparison of average  $\Delta G^\ddagger_{\text{inv}}$ ).

	Parent systems		benzo analogues	
	(1a) → (2a)	(2a) → (3a)	(16) → (17)	(90) → (91)
$\Delta\Delta G^\ddagger_{\text{inv}}$ (kJmol <sup>-1</sup> )	4.9	5.3	8.8	9.2

Table 6.2

Moreover, the inversion barrier of (2a) was measured in this study to try to resolve the two different values for (2a) quoted by Marchand<sup>21</sup> (Table 6.3). The inversion barriers measured for (2a) using the bridgehead and *N*-Me proton signals are 62.3 and 62.0 kJmol<sup>-1</sup> respectively in our work which is similar to one of the values Marchand<sup>21</sup> quoted. The measurement of the inversion barrier using the alkene proton signals was found to be 61.3 kJmol<sup>-1</sup> which is in good agreement and casts doubt on Marchand's second value. Two alkene and bridgehead signals in the <sup>1</sup>H NMR spectrum of (2a) at -11 °C in CD<sub>2</sub>Cl<sub>2</sub> indicated that two diastereoisomeric invertomers were present. Marchand assigned the *syn* configuration (*N*-Me *syn* to C=C) to the major invertomer (86%) in (2a) on the basis of the anticipated antiaromatic electronic interaction between the nitrogen lone pair and the *syn* double bond in the *anti* configuration (*N*-Me *anti* to C=C).<sup>21</sup> Table 6.3 shows the inversion barriers results for the simplest 7-azabicyclic derivatives. The invertomer preferences will be discussed later in this chapter.

			
	(1a)	(2a)	(3a)
$T_c$ (±5 K) <sup>a</sup>		297	348
$\Delta\nu$ (Hz) <sup>a</sup>		30.0	164.5
$\Delta G^\ddagger_{\text{inv}}$ (±0.5kJmol <sup>-1</sup> )	57.4 <sup>3</sup>	57.1/62.1 <sup>21</sup> 62.3 <sup>a</sup>	67.6 <sup>a</sup>

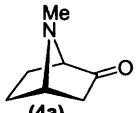
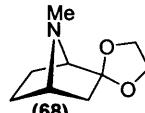
Table 6.3 Nitrogen inversion barriers in 7-azanorbornane derivatives.

a. This work. All values in this table calculated assuming 50:50 invertomer ratio.

### 6.3 Nitrogen inversion barriers of 7-azabicyclo[2.2.1]heptane systems containing different substituent in the 2-carbon bridges

The inversion barrier investigations were extended to include 7-azanorbornane derivatives substituted in the 2-carbon bridges. In relation to this system, a nucleophilic displacement at the C<sub>7</sub> position of a norbornane compound is difficult to achieve. However, when the norbornane is substituted with a carbonyl group at C<sub>2</sub> position, the carbonyl group aids the displacement reaction with complete inversion of configuration at C<sub>7</sub>.<sup>49</sup> This was introduced in more detail in Chapter 1, section 5. Therefore, the inversion barriers will be investigated in the 2-keto-7-azanorbornane derivatives.

From coalescence temperature measurements using variable temperature <sup>1</sup>H NMR experiments on (4a) the barrier for nitrogen inversion was determined. The inversion barrier for the substituted 7-azanorbornane with a carbonyl group at C<sub>2</sub> (4a) (49.2 kJmol<sup>-1</sup>) is lower (8.2 kJmol<sup>-1</sup>) than that for the saturated 7-azanorbornane (1a). Interestingly, the inversion barrier for the protected carbonyl (68) is fairly similar to (4a). Therefore, by introducing the carbonyl group or its protected form to the system, the inversion barriers are significantly lowered (Table 6.4). The low barrier of (4a) caused by the ketone group might be explained by lowering the transition state as the nitrogen electron pair occupies an sp<sup>2</sup> orbital.

			
	(1a)	(4a)	(68)
$\Delta G^\ddagger_{\text{inv}}$ (kJmol <sup>-1</sup> ) <sup>a</sup>	57.4 <sup>2</sup>	49.2 ± 1	47.0 ± 1

**Table 6.4** Nitrogen inversion barriers in 7-azanorbornane derivatives.

a. All values in this table calculated assuming 50:50 invertomer ratio.

It was found that high field <sup>13</sup>C NMR measurements at low temperature could provide both the coalescence temperature and frequency separation under conditions of slow inversion.<sup>3</sup> Therefore, it was possible to measure the inversion barrier for (4a) using <sup>13</sup>C NMR spectra at variable temperatures. Two *N*-Me and C<sub>4</sub> bridgehead carbons were easily distinguished at -60 °C indicating that two diastereoisomeric invertomers were present and the signals coalesced at -26 °C. The inversion barrier measured for (4a) using <sup>13</sup>C NMR was 49.0 ± 1 kJmol<sup>-1</sup> which is in good agreement with the <sup>1</sup>H NMR measurements. The invertomer preferences of (4a) will be discussed later in this chapter.

## 6.4 Nitrogen inversion barriers in 1,4-dimethyl-7-azabicyclo[2.2.1]heptane systems

In view of the influence of the so-called ‘bicyclic effect’ we wished to extend the work to include another compound such as *endo*-(55) where the bridgehead protons are substituted with methyl groups and study the effect of this on the inversion barrier. It was reported that the CNC bond angle was wider for *syn*-(13) than that for *anti*-(12); the angle being 97.3° and 95.7° respectively<sup>37</sup> (introduced in Chapter 1, section 1.5). This was similar to the situation reported in a study of 1,3-disubstituted bicyclo[1.1.1]pentanes where the C<sub>1</sub>-C<sub>3</sub> distances were calculated for a number of derivatives (Table 6.5).<sup>102</sup>



Substituents at position 1 and 3	Distance C <sub>1</sub> -C <sub>3</sub> (Å)
R = H	1.916
R = Me	1.939

Table 6.5

Methyl substituents at the 1 and 3-positions raised the electron density in the carbon bridgehead orbital thus raised the non-bonded C<sub>1</sub>-C<sub>3</sub> distance with respect to the unsubstituted case.<sup>102</sup> The measurement of the inversion barrier was also considered for compound *endo*-(54) as a point of reference.

The inversion barrier for *endo*-(54) was measured at low temperatures using <sup>1</sup>H NMR (49.2 ± 0.5 kJmol<sup>-1</sup>) (Δν = 32.3 Hz and T<sub>c</sub> = -36° C). The addition of the tosyl group to the 7-azabicyclic system reduces the barrier by 8.2 kJmol<sup>-1</sup> when compared with (1a). The reduction of the inversion barrier, from *endo*-(54) to (1a) might be due to electronic factor; rather than steric, since the tosyl group is in the *endo* position. The effect of the substituted methyl groups at the bridgeheads on the inversion barriers was studied earlier in the *N*-Cl 7-azabicyclic derivatives.<sup>23</sup> The inversion barrier measured for *endo*-(55) (46.3 ± 0.5 kJmol<sup>-1</sup>) is lower than the barrier for *endo*-(54) (Table 6.6). This result is in agreement with the relative effects reported earlier in inversion barriers for *N*-Cl compounds.<sup>23</sup>

			
	(1a)	<i>endo</i> -(54)	<i>endo</i> -(55)
		SO <sub>2</sub> Ar	SO <sub>2</sub> Ar
$\Delta G^\ddagger_{\text{inv}}$ (kJmol <sup>-1</sup> ) <sup>a</sup>	57.4 <sup>3</sup>	49.2 ± 0.5	46.3 ± 0.5

**Table 6.6** Nitrogen inversion barriers in 7-azanorbornane derivatives.

a. All values in this table calculated assuming 50:50 invertomer ratio.

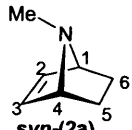
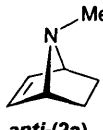
The effect of the bridgehead methyl groups in lowering the inversion barrier, from *endo*-(55) to *endo*-(54), was found to be small ( $\Delta\Delta G^\ddagger_{\text{inv}}$  2.9 kJmol<sup>-1</sup>). This reduction may possibly result from the effect of the two bridgehead methyl groups in raising the electron density in the bridgehead orbitals leading to increase mutual repulsion causing a widening of the CNC bond angle.<sup>23</sup> The widening of the CNC bond angle would explain the reduction of the inversion barrier but the inversion barrier for *endo*-(55) is the lowest recorded value for *N*-Me derivatives of this skeleton to our knowledge. The presence of the SO<sub>2</sub>Ar group has clearly had a very large effect and it would seem reasonable that the additional effects of the methyl groups would be relatively smaller than expected, here. It is certainly smaller than the effect in the *N*-Cl systems studied earlier where the barriers are much higher to start with (because of the ‘bicyclic effect’ and the *N*-Cl substituent). The full effect of bridgehead methyl substituents is therefore observed in these cases.

## 6.5 Invertomer preferences of *N*-Me derivatives

At room temperature in CD<sub>2</sub>Cl<sub>2</sub> solution, the signals due to the alkene (HC=CH) and bridgehead protons (H<sub>1</sub> and H<sub>4</sub>) in the <sup>1</sup>H NMR spectrum of (2a) were broadened by slow inversion on the NMR time scale. On cooling the solution to -17 C°, however, the signals were split into two sets of minor and major signals. The ratio of the two invertomers was determined by direct integration of either the alkene or bridgehead protons. Marchand<sup>21</sup> (as mentioned earlier) assigned the *syn* configuration to be the major invertomer (86%) where the *syn* configuration is defined as that *N*-Me *syn* to the alkene. This assignment is in good agreement with our observation in this study (85:15 *syn* : *anti*) using <sup>1</sup>H NMR spectroscopy.

The <sup>13</sup>C NMR chemical shift for (2a) was also measured at low temperature (-17 C°) and reported here for the first time. The <sup>13</sup>C NMR clearly shows the presence of two invertomeric species in (2a) and the assignments of the configurations were made on the basis of the  $\gamma$ -effect (introduced in Chapter 2, section 2.5.1). Thus, the alkene carbon atom C<sub>2</sub> in *syn*-(2a) was observed to resonate at higher field than the same carbon atom in

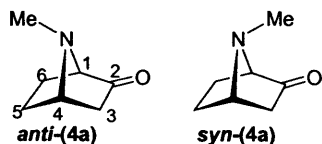
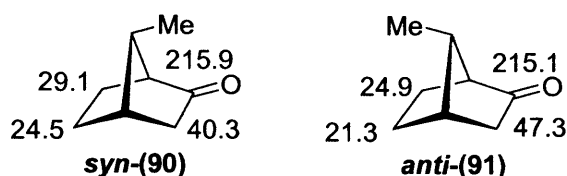
*anti*-(**2a**). Similarly, the ethano-carbon C<sub>6</sub> in *anti*-(**2a**) was observed to resonate at higher field than its counterpart in *syn*-(**2a**) because of the compression shift induced by the eclipsing  $\gamma$ -methyl group. Therefore, the invertomer ratio of this amine (**2a**) was 85:15  $\pm$  1 (*syn:anti*) assigned by <sup>13</sup>C NMR. This result was in good agreement with the result obtained here by <sup>1</sup>H NMR spectroscopy. Table 6.7 shows the <sup>13</sup>C NMR chemical shifts for *syn*-(**2a**) and *anti*-(**2a**) invertomers at low temperature.

		
	<b>syn-(2a)</b>	<b>anti-(2a)</b>
	ppm (major)	ppm (minor)
C <sub>6</sub>	23.7	19.3
NMe	29.9	31.4
C <sub>1</sub>	66.6	64.4
C <sub>2</sub>	130.2	135.6

**Table 6.7** <sup>13</sup>C NMR data for (**2a**). Spectrum was measured at  $-17^{\circ}$  C.

The <sup>1</sup>H NMR spectrum of (**4a**) when recorded at room temperature implied that nitrogen inversion might be rapid on the <sup>1</sup>H NMR timescale. At lower temperatures both <sup>1</sup>H and <sup>13</sup>C NMR showed that two invertomeric species were present in (**4a**). Once again, the assignment of the invertomer ratio from <sup>13</sup>C NMR was facilitated by the application of the  $\gamma$ -effect of carbon substitution.

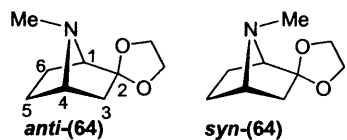
When this analysis was applied to the ethano-carbons (C<sub>5</sub> and C<sub>6</sub>) opposite to the ketone group in (**4a**), it was observed that the major invertomer gave rise to the furthest upfield shifts. So the major invertomer must be that in which the *N*-Me group is *anti* to the ketone group. As the *N*-Me is *anti* to the ketone group, the shift of C<sub>3</sub> which is in the same side of the ketone group is downfield when compared with the minor invertomer *syn*-(**4a**). The ratio of *anti*- and *syn*-(**4a**) was 61:39  $\pm$  1 respectively. The measured invertomer ratio by <sup>13</sup>C NMR was very similar to that measured using <sup>1</sup>H NMR at low temperature (*anti:syn* (62:38) respectively). It should be mentioned that the shift of the ketone carbon (C<sub>2</sub>) is the other way round where the higher field signal corresponds to the *anti* invertomer rather than *syn*. Similar observation was observed in norbornyl derivatives. Roberts *et. al.* reported the <sup>13</sup>C chemical shifts of *syn*-(**90**) and *anti*-(**91**) methyl-2-norbornanone.<sup>43</sup> The ketone carbon in both systems might not experience this effect ( $\gamma$ -effect). Table 6.8 summarizes the <sup>13</sup>C chemical shifts of both invertomers *anti*- and *syn*-(**4a**).



	ppm (major)	ppm (minor)
C <sub>5</sub> , C <sub>6</sub>	20.5, 23.9	24.1, 28.8
NMe	34.5	35.5
C <sub>3</sub>	46.6	37.8
C <sub>4</sub>	61.3	60.6
C <sub>1</sub>	69.6	69.6
C <sub>2</sub>	212.7	218.0

**Table 6.8** <sup>13</sup>C NMR data for (4a). Spectrum was measured at -61° C.

The invertomer preference of the protected carbonyl (64) is heavily weighted toward one major invertomer which was assigned to be the *anti* invertomer (*N*-Me *anti* to the acetal group). The invertomer ratio of *anti*:*syn* is 95:5 measured at low temperature (-68 °C) using <sup>1</sup>H NMR spectra. This ratio was also confirmed using <sup>13</sup>C NMR at the same temperature. Distinguishing between the two invertomers was straightforward, based on the substantial steric interactions between the *N*-Me group and the acetal methylene group but was confirmed by application of the principle of the  $\gamma$ -effect. Table 6.9 shows the obvious <sup>13</sup>C NMR shifts of the two invertomers at low temperature.

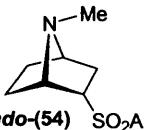
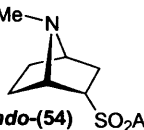


	ppm (major)	ppm (minor)
C <sub>6</sub>	18.7	23.6
C <sub>5</sub>	24.5	28.6
C <sub>3</sub>	44.4	40.1

**Table 6.9** <sup>13</sup>C NMR data for (64). Spectrum was measured at -68° C.

In addition, the invertomer ratios of *endo*-(54) and *endo*-(55) were measured at low temperatures (-61 °C) and (-80 °C) respectively using <sup>1</sup>H and <sup>13</sup>C spectra. The *syn*

Me (with respect to the tosyl group) of *endo*-(54) was assigned as the major invertomer (61%) using  $^1\text{H}$  NMR. The assignment of the invertomer preference of *endo*-(54) was again based on the  $\gamma$ -effect. Table 6.10 shows some selected  $^{13}\text{C}$  chemical shifts of the two invertomers of *endo*-(54). The invertomer ratio measured by  $^{13}\text{C}$  NMR (60:40  $\pm$  1 *syn:anti*) at low temperature was in good agreement with  $^1\text{H}$  NMR. The invertomer ratio for *endo*-(55) (page 95, Table 6.6) was found to be 80:20 measured at low temperature using  $^1\text{H}$  NMR. The major invertomer in this case was assigned to be *syn* invertomer by analogy with that observed for *endo*-(54).

		
	<i>endo</i> -(54)	<i>endo</i> -(54)
	SO <sub>2</sub> Ar	SO <sub>2</sub> Ar
	<b>ppm (major)</b>	<b>ppm (minor)</b>
C <sub>5</sub> , C <sub>6</sub>	25.8, 29.2	20.7, 26.1
C <sub>3</sub>	29.9	32.5
C <sub>2</sub>	63.6	65.3

**Table 6.10**  $^{13}\text{C}$  NMR data for *endo*-(54). Spectrum was measured at  $-61^\circ\text{C}$ .

The relative populations of the invertomers of (2a), (4a), (64), *endo*-(54) and *endo*-(55) were calculated from integration of the low temperature spectra and, together with the equilibrium constants and free energy differences for the inversions from *syn* methyl to *anti* methyl configurations, are shown in Table 6.11.

	(2a)	(4a)	(64)	<i>endo</i> -(54)	<i>endo</i> -(55)
T ( $^\circ\text{C}$ )	-17	-61	-68	-61	-80
<i>anti</i> -Me <sup>a</sup> (%)	15 $\pm$ 1	62 $\pm$ 1	95 $\pm$ 1	39 $\pm$ 1	20 $\pm$ 1
K <sub>eq</sub> <sup>b</sup>	0.18 $\pm$ 0.02	1.60 $\pm$ 0.1	19 $\pm$ 4.5	0.79 $\pm$ 0.01	0.3 $\pm$ 0.02
$\Delta G^{\circ c}$ (kJmol <sup>-1</sup> )	3.6 $\pm$ 0.2	-0.8 $\pm$ 0.1	-5.0 $\pm$ 0.4	1.3 $\pm$ 0.1	1.8 $\pm$ 0.1

**Table 6.11** Invertomer populations, equilibrium constants and free energy difference for the *N*-Me amines (2a), (4a), (64), (54) and (55).

- a. NMe anti with respect to the functional groups (alkene, ketone, acetal or tosyl).
- b. for the equilibrium *syn*-Me  $\leftrightarrow$  *anti*-Me.
- c. free energy change from *syn*-Me to *anti*-Me.

## 6.6 A more refined treatment of $\Delta G_{inv}^\ddagger$ measurements for systems having unequal invertomer populations

Variable temperature  $^1\text{H}$  NMR spectra of (2a) and (4a) were observed and their barriers to nitrogen inversion assigned from coalescence temperature measurements. Since invertomer preferences in both (2a) and (4a) existed it was necessary to use modified calculations in order to take account of the slightly different relative energies of each invertomer (unnecessary in (1a) and (3a) systems because the ratio of invertomers in these systems was 50:50 due to their symmetrical nature). The calculations used provided separate inversion barriers for the *syn*  $\rightarrow$  *anti* and *anti*  $\rightarrow$  *syn* inversion processes and were made as follows: from the equations<sup>103</sup>

$$T = T_{anti} T_{syn} / T_{anti} + T_{syn} \quad \text{and} \quad K_{eq} = T_{anti} / T_{syn}$$

where:  $T$  = population weighted lifetime of the system;  $T_{syn}$ ,  $T_{anti}$  = lifetimes of the *syn* and *anti* invertomers;  $K_{eq}$  = equilibrium constant *syn*  $\leftrightarrow$  *anti*.

The rate constants for the inversions from *syn* to *anti* and vice versa were calculated using the Gutowsky approximation.<sup>104</sup>

$$T = T_{syn} K_{eq} / 1 + K_{eq} = 1 / \pi \delta\nu \sqrt{2}$$

$$k_{syn} = 1 / T_{syn} = K_{eq} \pi \delta\nu \sqrt{2} / 1 + K_{eq}$$

where:  $\delta\nu$  = frequency separation between the signals due to the same proton in the two invertomers;  $k_{syn}$  = rate constant for the inversion *syn*  $\rightarrow$  *anti*.

By using the value of  $k_{syn}$ , obtained above, in the Eyring equation the free energy of activation for the inversion *syn*  $\leftrightarrow$  *anti* may be calculated.

$$\Delta G^\ddagger = 2.303 R T_c (10.319 + \log_{10} T_c - \log_{10} k_{syn})$$

where:  $T_c$  = coalescence temperature for the proton being studied.

The coalescence temperatures, frequency difference and calculated free energies of activation for the system studied are presented in Table 6.12.

Compound <sup>a</sup>	signal	T <sub>c</sub> (°C)	Δν (Hz)	k <sub>syn</sub> <sup>b</sup>	ΔG <sup>‡</sup> <sub>syn→anti</sub> <sup>c</sup> (kJmol <sup>-1</sup> )	k <sub>anti</sub> <sup>b</sup>	ΔG <sup>‡</sup> <sub>anti→syn</sub> <sup>c</sup> (kJmol <sup>-1</sup> )
(2a)	HC=CH	31 ± 5	84.3	57	64.2 ± 1.1	318	59.8 ± 1.0
(4a)	H <sub>1</sub>	-26 ± 5	92.3	252	48.7 ± 1.0	155	49.7 ± 1.0
(64)	H <sub>1</sub>	-45 ± 5	35.4	0.05	49.6 ± 1.1	7.5	60.9 ± 1.2
<i>endo</i> -(54)	H <sub>3-<i>exo</i></sub>	-36 ± 2	32.3	56	49.6 ± 1.1	88	48.7 ± 1.1
<i>endo</i> -(55)	H <sub>2-<i>exo</i></sub>	-51 ± 5	26.2	23	48.0 ± 1.2	93	45.4 ± 1.0

**Table 6.12** Coalescence temperatures, rate constants and free energies of activation for inversion at nitrogen in the *N*-Me amines (2a), (4a), (64), (54) and (55).

- <sup>1</sup>H NMR spectra measured at 400 MHz; samples dissolved in CD<sub>2</sub>Cl<sub>2</sub>.
- rate constants (s<sup>-1</sup>).
- syn*-/*anti*- with respect to the functional groups (alkene, ketone, acetal or tosyl); calculated using equilibrium constants.

In 1989, it was suggested that unsaturation of (1a) does not have an effect on 7-azanorbornane nitrogen inversion barriers.<sup>3</sup> However, comparison of ΔG<sup>‡</sup><sub>anti→syn</sub> value for (2a) with ΔG<sup>‡</sup><sub>inv</sub> of (1a) shows a barrier increment (2.4 kJmol<sup>-1</sup>) as the ethano- bridge is unsaturated. A further incremental rise in the nitrogen inversion barrier (3.4 kJmol<sup>-1</sup>) was observed when the ΔG<sup>‡</sup><sub>syn→anti</sub> value for (2a) was compared with ΔG<sup>‡</sup><sub>inv</sub> for the totally unsaturated (3a). Use of ΔG<sup>‡</sup><sub>syn→anti</sub> and ΔG<sup>‡</sup><sub>anti→syn</sub> values for (2a) is justified here since it provides the best estimate of the energy difference between the two inversion barriers (*N*-Me *syn*- to the double bond) and the corresponding transition states. A significant drop of the nitrogen inversion barrier (7.7 kJmol<sup>-1</sup>) was observed when the ketone group was introduced into the system (4a) (ΔG<sup>‡</sup><sub>anti→syn</sub>, *N*-Me *syn*- to the ketone group) compared with ΔG<sup>‡</sup><sub>inv</sub> of the totally saturated (1a). This implies a similar effect of the C=O group on the T.S. for nitrogen inversion and the T.S. for S<sub>N</sub>2 substitution at the 7-position of 7-azanorbornanes and norbornanes respectively. Thus, the earlier proposal (Chapter 1) of a stabilizing interaction between the p-orbital at the 7-position (in the T.S.) and the carbonyl group receive support.

## 6.7 Protonation experiments

An alternative approach to the investigation of invertomer ratios at rapidly inverting nitrogen centers is to perform a very fast chemical reaction, such as protonation, at the nitrogen atom and thus achieve irreversible conversion of the two amine invertomers into a mixture of stereoisomeric ions. The rate of protonation by strong acids is diffusion-controlled<sup>105</sup> which is considerably faster than the rate of amine inversion and

therefore the ratio of salts produced should reflect directly the thermodynamic amine invertomer ratio.<sup>35,106</sup> This technique has been employed extensively in the conformational analysis of piperidines and piperazines,<sup>35,107,108</sup> amines which possess much lower inversion barriers than those studied here. Marchand<sup>18</sup> used this method and found that the ratio of the kinetically protonated amines was similar to that observed for the free amines obtained by dynamic NMR experiments at low temperatures. A wider study was later done<sup>109</sup> on a series of strained tertiary amines using the so-called kinetic protonation method. However, the invertomer ratios obtained did not always mirror the respective ratios obtained by dynamic <sup>1</sup>H and <sup>13</sup>C NMR experiments. Malpass reported the determination of the invertomer preferences for less-strained 2-azabicyclo[2.2.1]heptyl ring systems using kinetic protonation, where the inversion barriers are rapid on the NMR time scale even at low temperatures.<sup>61</sup> We performed some kinetic protonation studies in order to examine the validity of the method in 7-azanorbomane derivatives and to provide an additional check on the ratios reported earlier in this chapter.

The protonations in the present study were achieved by slow addition of a CDCl<sub>3</sub> solution of selected amines (**4a**), *endo*-(**54**) and *endo*-(**55**) to an excess of rapidly stirred 1:4 trifluoroacetic acid (TFA):CDCl<sub>3</sub> solution at ambient temperature.<sup>21</sup> The crude reaction mixtures were transferred to an NMR tube and the <sup>1</sup>H NMR spectra were measured immediately. The protonated amine solutions were allowed to stand for a week after which time no change in the initially formed ratios was observed. In the case of amine *endo*-(**54**), the protonated sample was evaporated to dryness, 20% of excess of amine was added and the ratio was measured and found to be similar to the ratio recorded previously. This means either that there was no change in the 'kinetic' ratio during the work-up or that the ratio was already thermodynamic and therefore would not change further. On the basis of earlier work,<sup>21,35,106</sup> the first explanation was considered as a working hypothesis.

As a result of protonation, the *N*-Me singlets of (**4a**), *endo*-(**54**) and *endo*-(**55**) at 2.33, 2.25 and 2.08 ppm respectively moved downfield by *ca.* 0.6 ppm. Two *N*-Me signals of *endo*-(**55**) appeared as major and minor doublets (coupled to the *N*-H proton) separated by *ca.* 0.3 ppm allowing easy integration (except (**4a**) where the two *N*-Me signals appeared as broad singlet). Only one doublet signal was observed for *endo*-(**55**).

The ratios of the diastereoisomeric salts of (4a), *endo*-(54) and *endo*-(55) are presented in Table 6.13 along with the free amine invertomer ratios from low temperature <sup>1</sup>H NMR spectroscopy and <sup>13</sup>C NMR spectroscopy, where applicable.

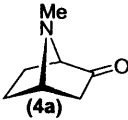
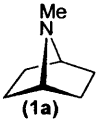
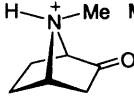
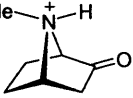
Compound	Free amine ratio	Kinetic protonation
	<i>syn</i> -Me : <i>anti</i> -Me	<i>syn</i> -Me : <i>anti</i> -Me
(4a)	62 : 38	59 : 41
	( <sup>13</sup> C) 62 : 38 ±1	
<i>endo</i> -(54)	61 : 39	80 : 20
	( <sup>13</sup> C) 61 : 39 ±1	
<i>endo</i> -(55)	80 : 20	81 : 19

Table 6.13

To summarize then, the barriers to inversion at nitrogen in the structurally related amines (2a)-(3a) and in other 7-azabicyclic systems studied here have been measured and their values confirm the previous observation that this skeleton leads to unusually high barriers. The high barriers in these compounds are uniformly high due to operation of the 'bicyclic effect'. The barrier is highest when the two-carbon bridges are unsaturated; the saturation of the two-carbon bridges leads to a lowering of the barrier. Further, the effect of the ketone group on the barrier leads to substantial reduction of the barrier compared with the totally saturated 7-azanorbornane. Methyl substituents at the bridgehead positions of the 7-azabicyclic system lead to a lowering of the inversion barrier.

## 6.8 Investigation of correlations between nitrogen inversion barriers and <sup>15</sup>N chemical shifts

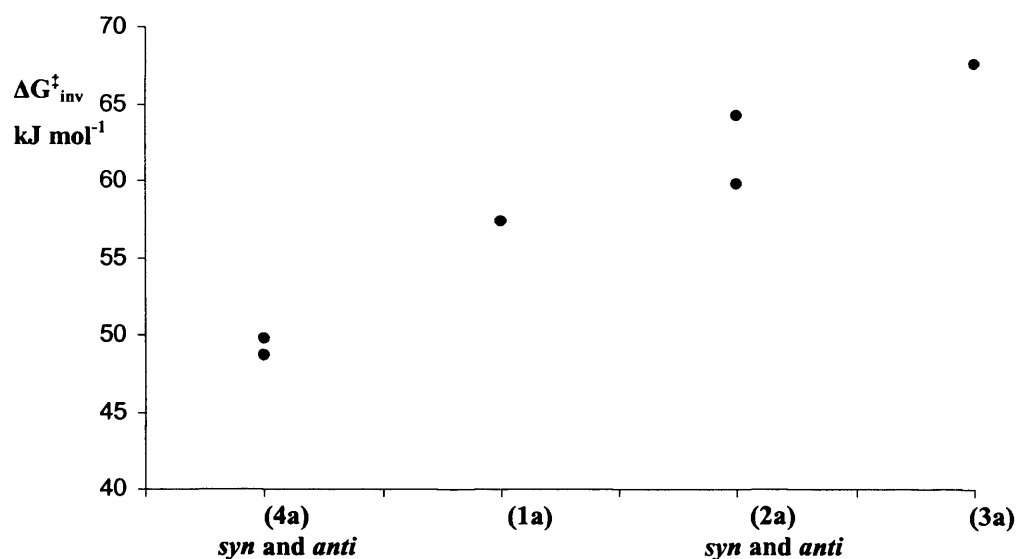
Having measured a wide range of <sup>15</sup>N chemical shifts and nitrogen inversion barrier values, a study of possible correlations between these values will be made. In this study, we expect possible ground state stabilization as a result of delocalizing nitrogen electrons to the bicyclic framework. This will increase  $\Delta G^\ddagger_{inv}$  and delocalization of nitrogen lone pair should also deshield the nitrogen atom. The compounds of interest in this study are 7-methyl-7-azanorbornane derivatives. Table 6.14 summarizes the inversion barriers at nitrogen and the available results of <sup>15</sup>N chemical shifts of compounds of interest.

					
$\Delta G_{inv}^\ddagger$ (kJ mol <sup>-1</sup> )	<i>syn</i> → <i>anti</i> 48.7 <i>anti</i> → <i>syn</i> 49.7	57.4 <sup>2</sup>	<i>syn</i> → <i>anti</i> 64.2 <i>anti</i> → <i>syn</i> 59.8	67.6	
					
<sup>15</sup> N δ ppm	-306.1	-308.7	-301.3	-292.8	-290.8

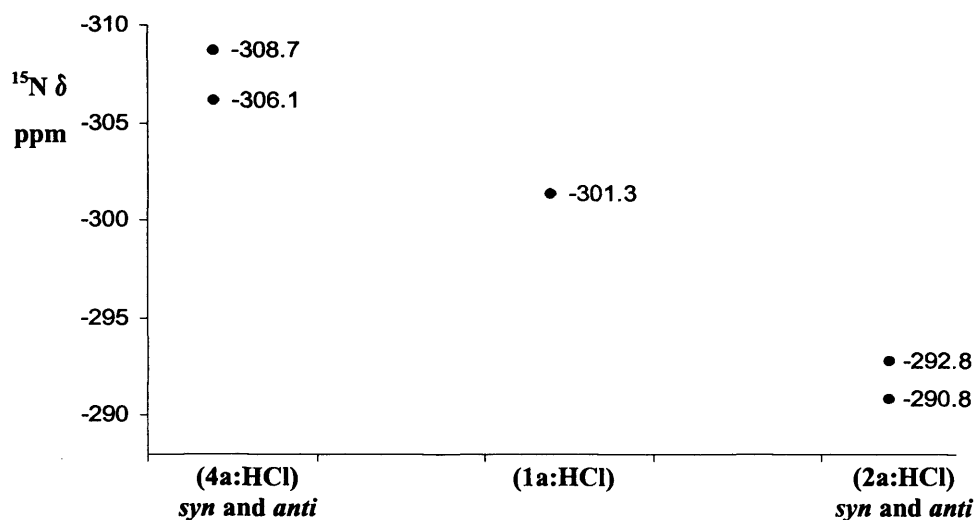
**Table 6.14** <sup>15</sup>N chemical shifts and nitrogen inversion barriers in 7-azanorbomane derivatives.

Figure 6.1 shows the effects of introducing alkene double bonds and the carbonyl group at C<sub>2</sub> on the inversion barriers. There is a clear trend for the inversion barriers as the system is substituted by double bonds and by the carbonyl group. The inversion barriers are lowest in (4a) and highest in (3a). An explanation of these results would be expected if the electron density from the nitrogen is delocalized into the bicyclic framework. Such an effect would stabilize the ground state, thus the energy required to reach the sp<sup>2</sup> transition state, in which the nitrogen lone pair occupies p-orbital would be increased. As a result, the free energy of activation for the nitrogen inversion will be raised. Figure 6.2 shows the <sup>15</sup>N chemical shift values that are a useful tool for probing changes of hybridization in 7-azanorbomane systems. An explanation of these results is that when the electron density is delocalized from the nitrogen, less shielding at nitrogen will be expected. As a result more downfield shifts will be observed as the delocalization increases.

This is observed from Figures 6.1 and 6.2 in which two trends in opposite directions of  $\Delta G_{inv}^\ddagger$  and <sup>15</sup>N chemical shifts were observed. Precise reasons are not understood; and this is empirical.



**Figure 6.1** Nitrogen inversion barriers of 7-azanorbornane derivatives.



**Figure 6.2** <sup>15</sup>N chemical shifts of 7-azanorbornane derivatives

Moreover, to extend this study, the correlations between the inversion barriers and <sup>15</sup>N chemical shifts of compounds of interest were plotted in one diagram. The <sup>15</sup>N chemical shifts of the salts of the parent compounds were used against the inversion barriers (as a result of not having enough <sup>15</sup>N data of the free amines). The monocyclic amine salt (**92:HCl**)<sup>95</sup> was included as a point of reference (Figure 6.3). The trend in figure 6.3 demonstrates good correlations between the inversion barriers and <sup>15</sup>N shifts of the salts. The higher barrier is correlated with the more downfield <sup>15</sup>N shift.

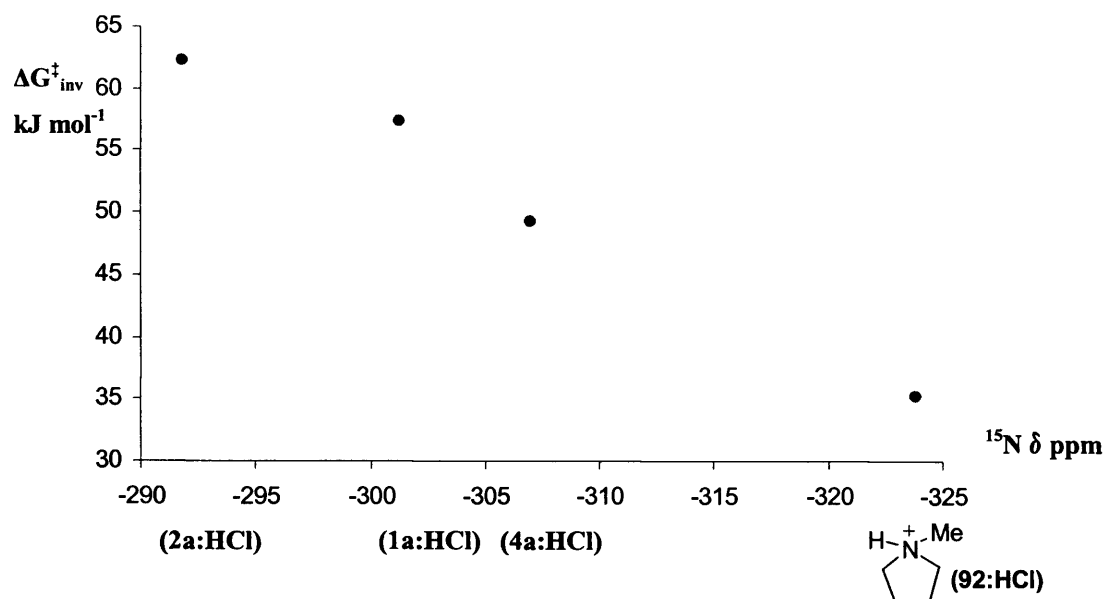


**Figure 6.3**

To extend this relationship with other available data, work done by the Leicester and an Australian group measured the inversion barriers of extended 7-azanorbornane<sup>14</sup> (6a)-(6c) (introduced in Chapter 1, section 1.3.1.a) and the <sup>15</sup>N chemical shifts of the same system (unpublished work). The nitrogen chemical shifts (<sup>15</sup>N and <sup>14</sup>N) of the free amines (1a)-(3a) were used in this correlation with the inversion barriers instead of the salts (Figure 6.4). The mono-cyclic free amine (92)<sup>95</sup> was again included as a point of reference.

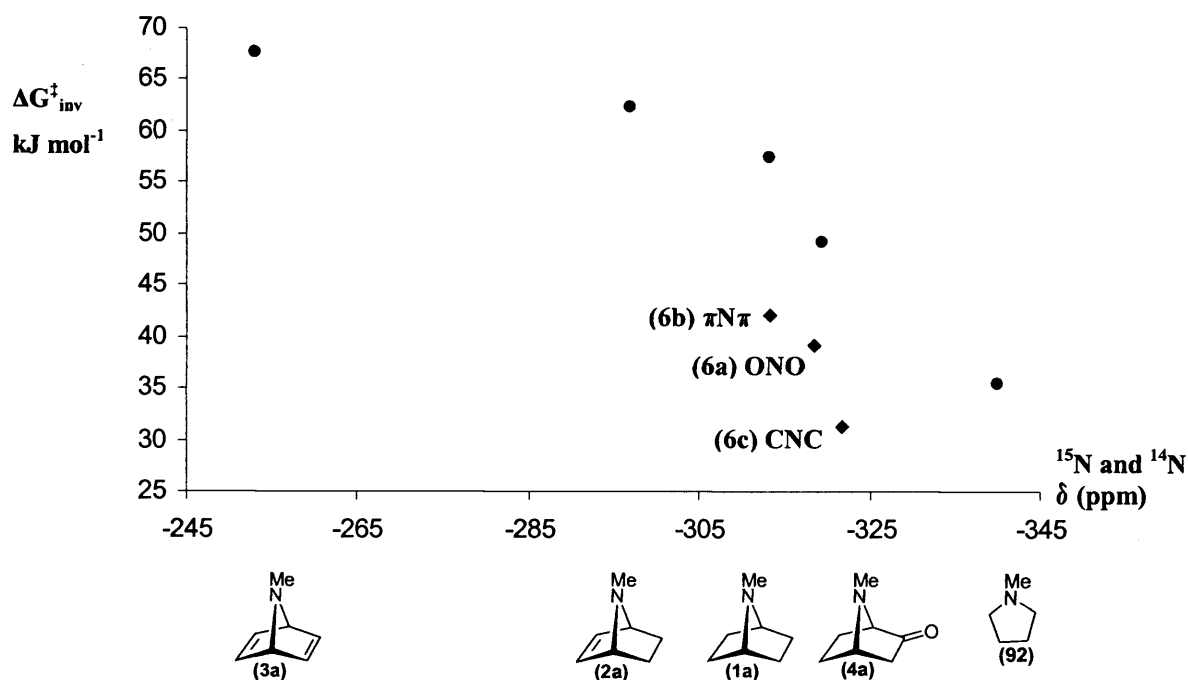


**Figure 6.4**

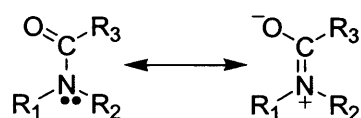
To summarize, there is a correlation between the inversion barriers and nitrogen chemical shifts, the inversion barriers at nitrogen in the 7-azanorbornane systems are almost as high as those in aziridines (where the angle strain is greater). Additional delocalization of electron density from nitrogen into the bicyclic framework is supported by the unusual deshielding of the bridging nitrogen in these systems (in contrast with the substantial shielding of the nitrogen in aziridines). This effect would increase the energy required to achieve the  $sp^2$  transition state, in which the nitrogen lone pair occupies a p-orbital. The increase of the energy would be explained as a result of stabilization of the ground state.

**Chapter 7**  
**Nitrogen-pyramidalization**

## Chapter 7

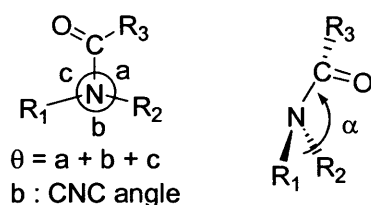
### 7.1 Nitrogen-pyramidalization

The amide bond, which is widely distributed in many natural and synthetic molecules, is considered to be planar in the ground state. Thus, this characteristic often determines the overall structure of these molecules. There are two ways that geometrical transformation, with respect to the amide bond, can occur: (1) through N-C(O) bond rotation and (2) nitrogen inversion. These transitional structures, which are non-planar, are called twisted and pyramidal structures respectively. Amide N-C(O) bonds have double bond character, which is normally interpreted on the basis of a pair of resonance structures (Scheme 7.1).



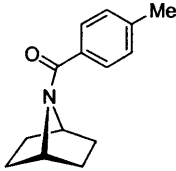
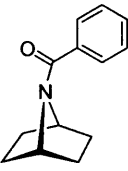
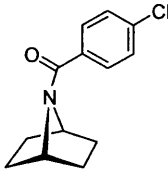
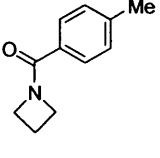
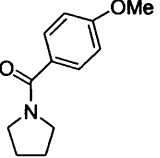
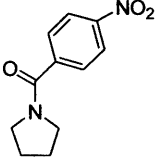
**Scheme 7.1** Resonance structures for planar amides.

On the other hand, several examples of amides and urethanes in which the amide group is not planar have been reported.<sup>26,27</sup> Examples include derivatives of the 7-azabicyclo[2.2.1]heptane where there is a clear reduction in the 'double-bond' character of the amide bridge (Table 7.1). Single-crystal X-ray diffraction structures of a range of amides were determined in order to prove this.<sup>27</sup> The planarity of the amide nitrogen can be represented in terms of two angle parameters: the summation of the three valence angles around the nitrogen atom ( $\theta$ ) and the hinge angle ( $\alpha$ ) of the N-substituent with respect to the plane defined by the nitrogen atom and the adjacent carbon atoms (Figure 7.1). The angle  $\theta$  of the ideal trigonal planar nitrogen atom is  $360^\circ$ . The hinge angle  $\alpha$  is between  $180^\circ$  (pure  $sp^2$ ) and  $125^\circ$  (pure  $sp^3$ ).



**Figure 7.1** Definition of angle parameters.

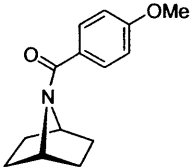
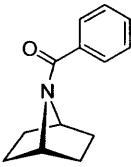
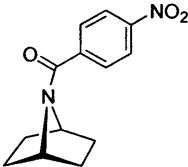
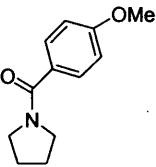
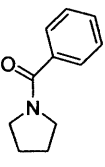
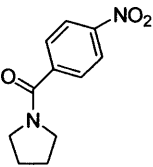
The angle  $\theta$ , of amides derived from the 7-azabicyclo[2.2.1]heptane and also azetidines, show the intermediate character of nitrogen between  $sp^3$  and  $sp^2$ , while the nitrogen atom of pyrrolidine amides is obviously closer to  $sp^2$  in character (Table 7.1).<sup>27</sup>

			
CNC (°)	97.1	97.2	97.6
$\theta$ (°)	346.2	349.5	349.0
$\alpha$ (°)	149.0	153.2	152.4
			
CNC (°)	94.6	111.5	111.6
$\theta$ (°)	354.2	359.2	359.3
$\alpha$ (°)	161.0	171.3	172.5

**Table 7.1** Selected crystal structural data of amides having a cyclic nitrogen.<sup>27</sup>

Rotational barriers with respect to the amide bond,  $\Delta G_{\text{rot}}^{\ddagger}$  (the free energy of activation), were measured to explore the planarity of amides in solution.<sup>27</sup> Rotational barriers about C-N amide bonds in *N*-benzoyl bicyclic and monocyclic amides were evaluated by VT <sup>1</sup>H NMR spectroscopy. The rotational barriers were obtained by a coalescence temperature method. The two bridgehead protons, or the four protons bonded to the carbons adjacent to nitrogen, are non-equivalent when amide rotation is slow enough to discriminate each signal on the NMR time-scale. Therefore, the rate constant  $k$  and  $\Delta G_{\text{rot}}^{\ddagger}$  were calculated from the difference in chemical shift between these two signals, and their coalescence temperatures  $T_c$  (Table 7.2).

The magnitudes of the rotational barriers measured for *N*-benzoyl-7-azanorbornanes were smaller than for the corresponding monocyclic *N*-benzoylpyrrolidines. This decreased rotational barrier in bicyclic amides strongly implies that the double bond character in the N-CO bond is reduced for *N*-benzoyl derivatives of the 7-azanorbornane system. This observation indicates distortion of the amide planarity.

			
$T_c$ (K)	315.5	334.5	343.1
$\Delta G^\ddagger_{rot}$ (kJ mol <sup>-1</sup> )	60.9	63.8	65.1
			
$T_c$ (K)	330.3	352.4	367.7
$\Delta G^\ddagger_{rot}$ (kJmol <sup>-1</sup> )	67.6	70.5	73.0

**Table 7.2** Selected rotational barriers for amides using coalescence temperature method.<sup>27</sup>

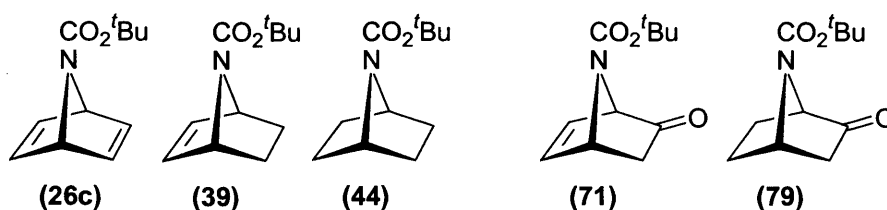
Moreover, the origin of the nitrogen pyramidalization could be associated with the angle strain around the nitrogen atom of 7-azanorbornanes. Thus the relationship between CNC angle and the magnitude of the rotational barrier was investigated.<sup>27</sup> With the crystal or calculated data, no correlation between the CNC angle and the rotational barrier was observed. The CNC angles for the amides of 7-azanorbornane are smaller than those of monocyclic pyrrolidine amides, because of ‘pinching’ of the ring by the ethano bridge. The CNC angles of the azetidine amides are smaller than those of bicyclic amides. However, within a series of compounds bearing a particular skeleton, there is little fluctuation in the CNC angles, despite apparent changes in rotational barriers. Thus, CNC angle alone cannot be used to explain the differences in the rotational barrier and, hence nitrogen pyramidalization.

A reduced CNC angle may be one of the factors influencing nitrogen-pyramidalization, but ‘allylic strain’, i.e. steric repulsion between the bridgehead hydrogens and substituents on the nitrogen of the amide in 7-azanorbornane, may also contribute.<sup>27</sup> This allylic strain can induce twisting about the amide N-C(O) bond. To assess the effect of the bulkiness of the substituents in the amide functional group, there was obtained optimized minimum energy structures of the amides that bear acetyl and formyl groups as *N*-substituents. The minimum-energy structures of *N*-acetyl and *N*-formyl 7-azanorbornanes are nitrogen-pyramidal. Moreover, within the same bicyclic system the calculated rotational barriers increase as the amide substituent changes from benzoyl to acetyl to formyl. This is reasonable, because the electron deficiency of the carbonyl carbon centers increases in this order, leading to enhanced amide resonance, and

also because the steric repulsion described above is reduced as the size of the substituent attached to the carbon atom is decreased. A general trend is that the larger the degree of nitrogen pyramidalization, the larger the twisting of the amide. Thus nitrogen-pyramidalization and twisting of the amide bond are closely inter-related.

Thus, the low rotational barrier of 7-azanorbornane was attributed to the twisting of the N-C(O) bond in addition to nitrogen pyramidalization. In other words, the nitrogen non-planarity, a reflection of the rotational barrier, is determined by the overall structural character of the molecule and not by a single structural parameter.

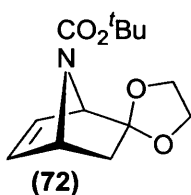
In order to assess the importance of the shape and hybridization of nitrogen in 7-azanorbornane systems more data are highly desirable. In this chapter, we will investigate the relationship between the  $^{15}\text{N}$  shifts and  $\theta$ -angle around the central bridging nitrogen in a range of urethane derivatives of 7-azanorbornane (**26c**), (**39**), (**44**), (**71**) and (**79**). These compounds offered an exceptional opportunity to examine the effect of the saturation, unsaturation or even the substituted ketone group on the nitrogen hybridization. The first measurements of  $^{15}\text{N}$  chemical shifts in these compounds were reported earlier (Chapter 5) and calculated bond angles which were supported by solid state crystal data in some cases were performed in these compounds. The  $^{15}\text{N}$  shifts and the degree of flattening at the urethane group were induced by through-bond effects rather than through-space effects. We hope these results together with the present empirical study reported by Leicester and the Australian group will demonstrate the potential relationship between  $^{15}\text{N}$  shifts and hybridization.



## 7.2 Results and discussion

All the *ab initio* calculations were performed using the PC Spartan Program.<sup>110</sup> Initially, the structures of 7-azabicyclic urethanes were optimized using the default gradient methods at Hartree-Fock (HF) level using the 6-31G\* basis set. The minimum energy structure of 7-azabicyclic urethane (**79**) was found to be substantially pyramidalized (calculated  $\theta$  and  $\alpha$  are  $345.0^\circ$  and  $143.4^\circ$ , respectively). The ground state minimum energy structure of urethane (**71**) is also pyramidalized, but to a smaller degree

as a result of introducing a  $\pi$ -bond into the system (calculated  $\theta$  and  $\alpha$  are  $340.1^\circ$  and  $138.7^\circ$ , respectively). The degree of nitrogen-pyramidalization of the calculated structures is generally in good agreement with the X-ray crystallographic data, the relative order of the magnitudes of pyramidalization of the calculated structures is consistent with that found in X-ray crystallographic data. The  $\theta$ -angle was also calculated for the acetal (**72**) and found to be similar to (**71**). Table 7.3 summarizes the calculated and X-ray crystallographic data of CNC,  $\theta$  and  $\alpha$  angles.



Compound	CNC ( $^\circ$ )	CNC ( $^\circ$ )	$\theta$ ( $^\circ$ )	$\theta$ ( $^\circ$ )	$\alpha$ ( $^\circ$ )	$\alpha$ ( $^\circ$ )	$^{15}\text{N}$ shift (ppm)
	(HF/6-31G*)	(X-ray)	(HF/6-31G*)	(X-ray)	(HF/6-31G*)	(X-ray)	
(79)	98.5	97.7	345.0	341.5	147.2	143.4	-261.4
(72)	96.9	96.4	340.7	337.2			
(71)	97.4	97.4	340.1	336.9	142.1	138.7	-252.4

**Table 7.3** Selected calculated and X-ray crystallographic data of 7-azabicyclic systems.

The highest measured and calculated  $\theta$ -angles are seen for (**79**) (larger  $\theta$  = more planar); (**79**) also has more  $sp^2$  character (more planar) than (**71**) according to the hinge angle ( $\alpha$ ). The higher s-character of the nitrogen in (**79**) is in agreement with higher shielding and the  $^{15}\text{N}$  chemical shift of (**79**) ( $-261.4$  ppm) is upfield when compared with (**71**) ( $-252.4$  ppm). The  $^{15}\text{N}$  shift of (**72**) was difficult to achieve because of the low yield step synthesis and all the  $^{15}\text{N}$  measurements were performed at the natural abundance of nitrogen.

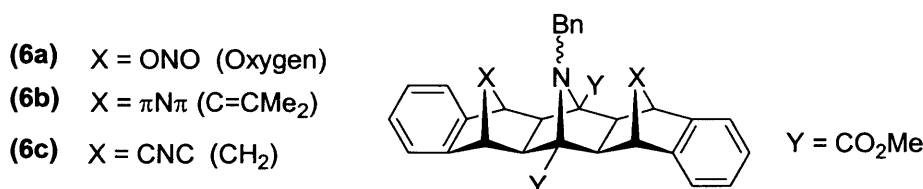
This study was extended to include urethanes (**26c**), (**39**) and (**44**) and the  $\alpha$ - and  $\theta$ -angles were calculated as part of this investigation. Furthermore, we optimized two possible conformation structures of (**39**) where the N-C(O) bond is *syn* or *anti* with respect to the alkene bridge. In this case (**39**), the *syn* conformer is lower in energy than the *anti* conformer (HF/6-31G\* optimized structure), so we focused on the *syn* conformer. Table 7.4 shows the calculated results of the CNC bond angle,  $\theta$  and  $\alpha$  angles for 7-azabicyclic derivatives (**26c**), (**39**) and (**44**).

Compound	CNC (°) (HF/6-31G*)	$\theta$ (°) (HF/6-31G*)	$\alpha$ (°) (HF/6-31G*)	$^{15}\text{N}$ shift (ppm)
(26c)	95.1	336.6	139.3	-202.6
(39)	96.7	339.6	141.8	-248.1
(44)	97.8	344.9	147.2	-257.5

**Table 7.4** Calculated data of 7-azabicyclic derivatives.

Table 7.4 illustrates the effect of the incorporation of double bonds on the  $\theta$ -angle. The highest calculated  $\theta$ -angle was found in the saturated symmetrical urethane (44) which also had the largest  $\alpha$ -angle. The  $\theta$ -angle was reduced when one double bond was introduced into the system as in (39) (less planar than (44)); and the  $\theta$ -angle was reduced further as a result of the second double bond (26c). Again, the consequence of the increasing planarity as in (44) is associated with an upfield  $^{15}\text{N}$  shift (-257.5 ppm). The  $^{15}\text{N}$  shifts of (39) and (26c) are -248.1 and -202.6 ppm respectively. The large  $\alpha$ -angle of (44) indicates that (44) has more  $\text{sp}^2$  character (upfield shift) compared with the unsaturated symmetrical (26c) (smaller  $\alpha$ -angle = more  $\text{sp}^3$  character, downfield shift).

In relation to nitrogen-pyramidalization investigations, work done by a joint Leicester and Australian group (unpublished work) reported a correlation study between the  $^{15}\text{N}$  chemical shifts and the degree of flattening in the tertiary amino-[3]polynorborene systems induced by through-space interactions. This empirical study was the first successful attempt to examine Nelsen's proposal regarding the potential relationship between the  $^{15}\text{N}$  shifts and hybridization.<sup>111</sup> Table 7.5 demonstrates the relationship of  $^{15}\text{N}$  shifts and  $\theta$  degree of some selected examples having identical flanking bridges. The relative correlation is that the upfield shifts of  $^{15}\text{N}$  are associated with the degree of flattening at nitrogen (greater s-character in the N-C bonds and greater p-character in the lone pair).



Linear polynorborenes	$^{15}\text{N}$ shift (ppm)	$\theta$ (AM1)	$\theta$ (X-ray)
CNC (6c)	-321.8	348.5	348.4
ONO (6a)	-318.4	336.0	337.2
$\pi\text{N}\pi$ (6b)	-313.2	336.5	

**Table 7.5**  $^{15}\text{N}$  chemical shifts and  $\theta$ -angles for XNX.

Given the correlations above, it was anticipated that changes of shape and hybridization in the parent systems of 7-azanorbornane (**1a**)-(**3a**) would also correlate with nitrogen NMR shifts. The CNC bond angles and  $\theta$ -angles were optimized for the free amines (**1a**)-(**3a**) and (**4a**) using the default gradient methods at HF level (6-31G\*) since it is difficult to obtain solid state crystal data; however, it was possible in some cases of the salt forms. Table 7.6 lists the calculated CNC bond angles and  $\theta$ -angles beside the measured nitrogen shifts of the free amines (**1a**)-(**3a**) and (**4a**).

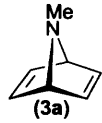
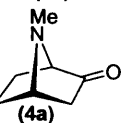
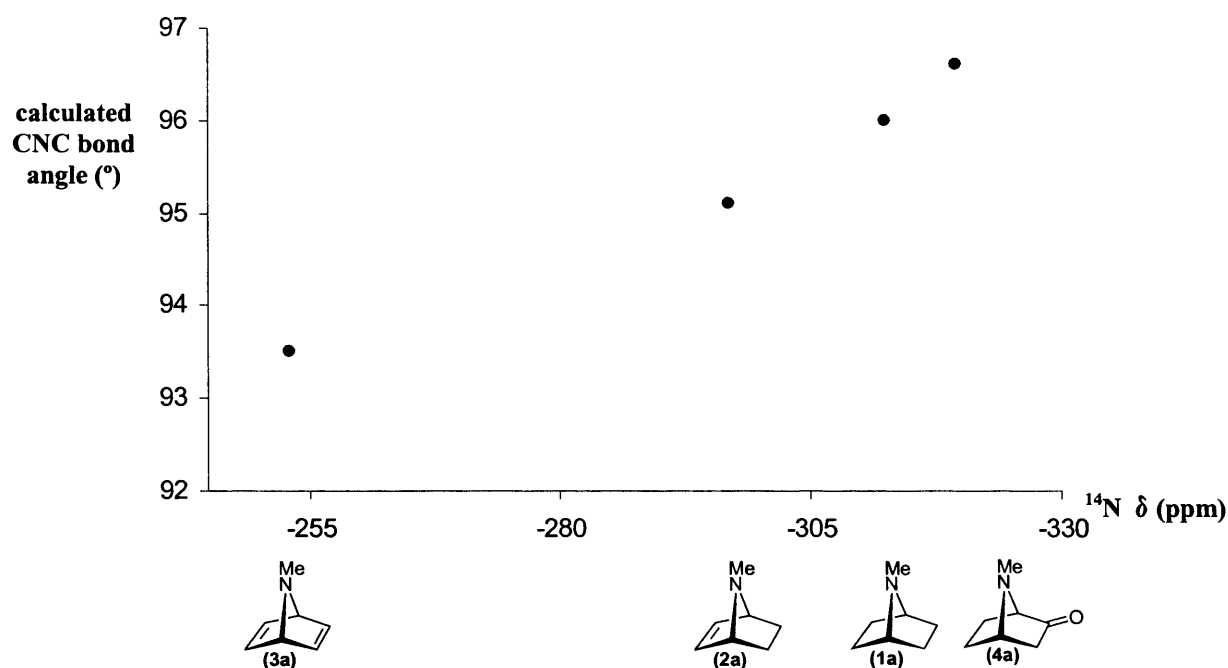
	CNC ( $^{\circ}$ ) (HF/6-31G*)	$\theta$ ( $^{\circ}$ ) (HF/6-31G*)	Nitrogen $\delta$ (ppm)	
			$^{15}\text{N}$	$^{14}\text{N}$
 ( <b>3a</b> )	93.5	327.5		-253.0
 ( <b>2a</b> )	95.1	328.0		-297.0
 ( <b>1a</b> )	96.0	329.9	-313.3	-312.5
 ( <b>4a</b> )	96.6	330.6		-319.5

Table 7.6

The calculated CNC bond angle for the free amine (**1a**) was in good agreement with the measured CNC bond angle ( $95.5^{\circ}$ ) for its salt form (**1a:HCl**) from the crystallographic X-ray data. A similar observation was made in the case of the acetal (**68:HCl**). The calculated CNC bond angle for the free amine (**68**) is  $96.1^{\circ}$  which is similar to the data obtained from X-ray ( $95.6^{\circ}$ ) of (**68:HCl**). Therefore, the protonation of the free amine in this system appears not to have a large effect on the CNC bond angle.

Figure 7.2 shows a good correlation between the calculated CNC bond angles and the nitrogen NMR chemical shifts for the tertiary amines (**1a**) – (**4a**). The low downfield nitrogen NMR shift of (**3a**) is associated with the more CNC angle strain. On the other hand, the highfield nitrogen shift is associated with the less CNC angle strain (**4a**).



**Figure 7.2**

To summarize, firstly, the planarity of the urethane group of the 7-azabicyclo[2.2.1]heptane in the solid, solution and calculated gas-phase structures was assessed. The downfield reduction experiment of the  $^{15}\text{N}$  shifts, as compared with those of monocyclic and acyclic urethanes, suggested that 7-azabicyclo[2.2.1]heptane are nonplanar. The magnitude of the  $^{15}\text{N}$  shift in solution is a reflection of the nonplanarity. The  $^{15}\text{N}$  shift is associated with the  $\theta$ - and  $\alpha$ -angle. The more downfield  $^{15}\text{N}$  shift is associated with the large  $\alpha$ -angle. Thus, the nonplanarity of the urethanes of 7-azabicyclo[2.2.1]heptane is a reasonable result of the delocalization of the nitrogen lone pair to the bicyclic framework, which reduces the availability of the lone pair electrons to take part in amide (urethane) resonance. Secondly, there is good correlation between the CNC bond angle and the nitrogen NMR shift for the free amines. The low downfield nitrogen NMR shift is associated with the more CNC angle strain. The lack of correlation between the  $\theta$ -angle and nitrogen NMR shift necessitated the use of the CNC bond angle for the free amines as they chemically differ from the urethanes.

### 7.3 Overall summary and conclusions

The total synthesis of the secondary and tertiary amines of the parent 7-azabicyclo[2.2.1]heptane system was achieved successfully. The *N*-protected key intermediates of the parent 7-azabicyclo[2.2.1]heptane system were synthesized as a part

of this study. The work was extended to include the synthesis of the analogues having a carbonyl group introduced into the 2 position of the parent 7-azabicyclo[2.2.1]heptane system and a successful synthesis of the novel 7-methyl-7-azabicyclo[2.2.1]heptan-2-one was achieved. On the other hand, the synthesis of the unsaturated *N*-Me derivative of the 7-azabicyclo[2.2.1]heptan-2-one system (the -hept-2-one-5-ene) was difficult to achieve. The *N*-protected key intermediates of the saturated and unsaturated ketone derivatives were also used as part of this study. The novel 1,4-dimethyl derivatives (bridgehead methyl groups) of the 7-azabicyclo[2.2.1]heptane system were synthesized.

The inversion barriers in the title compounds are uniquely high due to the operation of the 'bicyclic effect'. The inversion barriers in the novel *N*-Me derivative of the 7-azabicyclo[2.2.1]hepta-2,5-diene ring system is the highest as a result of the two-double bonds introduced to the system. Saturation of the etheno-bridges leads to a lowering of the barrier; the barrier for the mono-unsaturated derivative is in-between. This might be consistent with the idea of ground state stabilization as a result of the delocalization of the nitrogen lone pair to the bicyclic framework. Strong support for this proposal was provided by nitrogen NMR chemical shift studies of the title compounds. A good correlation was seen between the nitrogen inversion barriers and nitrogen NMR chemical shifts. The high barrier is associated with the more downfield nitrogen NMR shift. The introduction of a carbonyl group at the C2 position in the 7-azanorbornyl ring system is consistent with stabilization of the transition state for nitrogen inversion by the carbonyl leading to a lower nitrogen inversion barrier. This parallels the observation of a substantial increase in the rate of nucleophilic displacement ( $S_N2$ ) at the C7 position of norbornane derivatives when carbonyl substituents are introduced into the 2-carbon bridge; the stabilization of the transition state in this case parallels the effect observed in our azanorbornane studies. The effect of the methyl substituents at the bridgehead position on the inversion barrier leads to a lowering of the inversion barrier. The low inversion barrier is consistent with the wider than usual CNC bond angle which is probably resulted from increasing the electron density in the bridgehead orbitals leading to increase mutual repulsion.

Nitrogen NMR chemical shifts were measured successfully for the title compounds at natural abundance. The nitrogen NMR shifts were used in this study as a probe of nitrogen hybridization. The deshielding of nitrogen in the 7-azabicyclo[2.2.1]heptane ring system is consistent with increased delocalization of the nitrogen lone pair. The large downfield shifts of nitrogen are associated with the

unsaturated bridges of the 7-azabicyclo[2.2.1]hepta-2,5-diene system. The presence of the unsaturated bridges lead to deshielding compared with the saturated 7-azabicyclo[2.2.1]heptane system. This observation was noticed in both the urethanes and amines derivatives of the 7-azabicyclic system. The incorporation of a carbonyl group at the C2 position in the 7-azanorbornyl ring system leads to high field nitrogen shifts in both urethanes and amines derivatives. Increased planarity at nitrogen correlated with upfield nitrogen NMR shifts.

**Chapter 8**  
**Experimental**

## Chapter 8

### Experimental Section

This chapter contains the experimental procedures and spectroscopic data for each experiment. Where experiments were repeated the most successful is recorded. The NMR spectra were recorded at 250 MHz using a Bruker ARX 250 spectrometer, at 300 MHz using a Bruker ARX 250 spectrometer, or at 400 MHz using a Bruker ARX 400 spectrometer. Chemical shifts are expressed in ppm ( $\delta$ ) relative to an internal standard tetramethylsilane (TMS). All spectra were obtained in  $\text{CDCl}_3$  with TMS unless stated otherwise. Signal characteristics are described using standard abbreviations: s (singlet), d (doublet), dd (doublet of doublets), t (triplet), m (multiplet), br (broad). Signal multiplicities in  $^{13}\text{C}$  NMR were determined by DEPT experiments.

$^{15}\text{N}$  and  $^{14}\text{N}$  NMR spectra were recorded on a Bruker ARX 400 spectrometer at 40 and 29 MHz respectively.  $^{15}\text{N}$  NMR spectra were recorded at natural abundance in  $\text{CDCl}_3$  in 10 mm tubes and referenced to neat nitromethane using the methods that described by Harris.<sup>112</sup> Any variations of solvent or conditions are mentioned in the text.

Temperature measurements on the NMR instruments used for the VT work were found to be accurate to within  $\pm 1$  K over the range used.

IR spectra were recorded on a Perkin Elmer FT universal ATR spectrometer as solid or oily. Band intensities are described as follows: s (strong), m (medium), w (weak). Accurate mass measurements were measured on a Kratos Concept 1H Sector mass spectrometer and were obtained using ionization by fast atom bombardment. Mass spectra were determined in units of mass relative to charge ( $m/z$ ). Routine mass spectra were measured on a Micromass Quattro L.C. Triple Quadrupole spectrometer and were obtained using ionization by electrospray.

Removal of solvent under reduced pressure was carried out using a Buchi rotary evaporator followed by removal of final traces of volatile materials using a high vacuum pump unless stated otherwise.

All reactions were carried out in oven-dried glassware under nitrogen (or argon where noted) using solvents distilled by standard methods.

Flash chromatography was carried out using silica gel (60) manufactured by Fisher. Thin layer chromatography was conducted on standard commercial aluminium sheets pre-coated with 0.2 mm layer of silica gel (Merck Kieselgel 60-254). The Aldrich Chemical Company, Sigma or Lancaster supplied the reagents used.

### Synthesis of *p*-tolyl-2-(trimethylsilyl)ethynyl sulfone (**28**)<sup>51</sup>

$\text{Me}_3\text{Si}-\equiv-\text{SO}_2\text{C}_6\text{H}_4\text{CH}_3$  In a flame-dried, 500 ml three-necked round-bottomed flask fitted with a nitrogen inlet was placed *p*-toluenesulfonyl chloride (14.1 g; 0.074 mol) and anhydrous dichloromethane (120 ml) was added. To the resulting solution was added powdered aluminium chloride (9.9 g; 0.074 mol). The resulting dark brown solution was maintained at room temperature for 30 minutes, then slowly transferred by cannula (30 min) under nitrogen to an ice-cold solution of bis(trimethylsilyl)acetylene (**27**) (11.5 g; 0.067 mol) in anhydrous dichloromethane (60 ml). The colour of the solution changed from colourless to red then to dark red. The reaction mixture was allowed to warm to room temperature and stirred for 24 h. The mixture was hydrolyzed by pouring it into slurry of 20% HCl (100 ml) with crushed ice (100 g). The organic layer was separated, washed twice with water (100 ml) and dried over anhydrous  $\text{Na}_2\text{SO}_4$ . The solvent was removed in a rotary evaporator to furnish a dark brown solid which was recrystallized from light petroleum ether (bp 40-60 °C) to yield 8.6 g (75%) of *p*-tolyl-2-(trimethylsilyl)ethynyl sulfone (**28**) as white crystals, mp 80-81 °C (lit.<sup>40</sup> 81-82 °C).

<sup>1</sup>H NMR (250 MHz,  $\text{CDCl}_3$ )  $\delta$ : 7.89 (d,  $J = 8.4$  Hz, 2H, 2 x aryl  $\text{CH}$ ), 7.37 (d,  $J = 8.4$  Hz, 2H, 2 x aryl  $\text{CH}$ ), 2.47 (s, 3H), 0.22 (s, 9H).

<sup>13</sup>C NMR (75 MHz,  $\text{CDCl}_3$ )  $\delta$ : 145.6, 138.7 (2 x Aryl C), 130.2, 127.8 (4 x Aryl  $\text{CH}$ ), 101.6, 98.6, 22.0 (Aryl  $\text{CH}_3$ ), -0.9 ( $\text{Si}(\text{CH}_3)_3$ ).

Literature data:

<sup>1</sup>H NMR of (**28**) ( $\text{CDCl}_3$ )  $\delta$ : 7.91 (d,  $J = 9$  Hz, 2H, 2 x aryl  $\text{CH}$ ), 7.40 (d,  $J = 9$  Hz, 2H, 2 x aryl  $\text{CH}$ ), 2.48 (s, 3H), 0.22 (s, 9H).<sup>51</sup>

### Synthesis of 1-ethynesulfonyl-4-methylbenzene (*p*-tolyl ethynyl sulfone) (**25**)<sup>51,52</sup>

$\text{H}-\equiv-\text{SO}_2\text{C}_6\text{H}_4\text{CH}_3$  The trimethylsilyl group was removed by hydrolysis. Two methods (a) and (b) were used to synthesize (**25**). There were some disadvantages for using method (a) such as the low yields, sometimes incomplete hydrolysis and formation of a side product. To avoid these problems, the alternative method (b) was used for the removal of TMS group in this synthesis as (**25**) could be obtained more directly and in a higher degree of purity.

**Method a.**<sup>40</sup> A solution of (**28**) (8.5 g; 0.034 mol) in methanol (100 ml) was placed in a 500 ml three-necked round-bottomed flask fitted with a thermometer and a 250 ml addition funnel. The mixture was stirred for 30 min. In the addition funnel was placed 120 ml of an aqueous solution of potassium carbonate ( $6.2 \times 10^{-3}$  M) and potassium

bicarbonate ( $6.2 \times 10^{-3}$  M). This buffer solution was added at a rate to maintain the reaction temperature at 30 °C. The mixture was diluted with water (150 ml) and extracted with chloroform (4 x 100 ml). The combined organic layer were washed with water (4 x 100 ml), brine (2 x 100 ml) and dried over anhydrous  $\text{Na}_2\text{SO}_4$ . The solvent was removed under reduced pressure to leave (**25**) as a creamy white solid (6.1 g, 72%); mp 75-77 °C (lit.<sup>40</sup> 74-75 °C).

$^1\text{H}$  NMR (250 MHz,  $\text{CDCl}_3$ )  $\delta$ : 7.90 (d,  $J = 8.4$  Hz, 2H, 2 x aryl  $\text{CH}$ ), 7.40 (d,  $J = 8.4$ , Hz, 2H, 2 x aryl  $\text{CH}$ ), 3.47 (s, 1H), 2.48 (s, 3H, aryl  $\text{CH}_3$ ).

$^{13}\text{C}$  NMR (75 MHz,  $\text{CDCl}_3$ )  $\delta$ : 146.1, 137.8, 130.1, 127.7, 81.2, 80.4, 21.8.

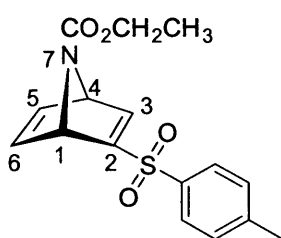
Literature data:

$^1\text{H}$  NMR of (**25**) ( $\text{CDCl}_3$ )  $\delta$ : 7.88 (d,  $J = 8.5$  Hz, 2H, 2 x aryl  $\text{CH}$ ), 7.38 (dd,  $J = 8.5, 0.6$  Hz, 2H, 2 x aryl  $\text{CH}$ ), 3.52 (s, 1H), 2.47 (s, 3H).<sup>51</sup>

$^{13}\text{C}$  NMR (75 MHz,  $\text{CDCl}_3$ )  $\delta$ : 145.9, 137.7, 130.0, 127.8, 81.1, 80.4, 21.8.<sup>113</sup>

**Method b.**<sup>52</sup> A solution of *p*-tolyl-2-(trimethylsilyl)ethynyl sulfone (**28**) (15.0 g; 0.059 mol) in 95% ethanol (300 ml) was cooled with stirring to 0 °C. A chilled solution of sodium fluoride (NaF) (7.4 g, 0.176 mol) dissolved in water (115 ml) was added dropwise to the reaction mixture. The ice bath was removed, and the reaction mixture was left to stir as it rose to room temperature for 4 h. The organic residue was then extracted with dichloromethane (3 x 80 ml), the extract was dried over anhydrous  $\text{MgSO}_4$  and the solvent was removed. The yield was 13.1 g (87%) of (**25**) as a brown solid which was sufficiently pure for the next reaction.

### Synthesis of 2-(toluene-4-sulfonyl)-7-azabicyclo[2.2.1]hepta-2,5-diene-7-carboxylic acid ethyl ester (**23b**)<sup>53</sup>



Based on the procedure of Muchowski,<sup>41</sup> a stirred solution of *p*-tolyl ethynyl sulfone (**25**) (2.3 g; 0.013 mol) in *N*-ethoxycarbonylpyrrole (**24b**) (3.6 g; 0.026 mol) was heated in an inert atmosphere (nitrogen) at 80-85 °C for 48 h. The reaction mixture was separated by column chromatography. Elution with

1:9 diethyl ether:petroleum (bp 40-60 °C) removed the excess *N*-ethoxycarbonylpyrrole (**24b**) which was recycled. The product was eluted with 4:6 diethyl ether:petroleum (bp 40-60 °C) to yield (**23b**) (3.1 g, 74%) as a pale yellow oil which, under cooling, became a brown solid (mp 103 – 104 °C);  $R_f$  0.27 (1:1 diethyl ether:petroleum (bp 40-60 °C)).

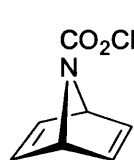
$^1\text{H}$  NMR (250 MHz,  $\text{CDCl}_3$ )  $\delta$ : 7.74 (d,  $J = 8.3$  Hz, 2H, 2 x aryl  $\text{CH}$ ), 7.60 (br d,  $J_{3,4} = 1.9$  Hz, 1H,  $\text{H}_3$ ), 7.36 (d,  $J = 8.3$  Hz, 2H, 2 x aryl  $\text{CH}$ ), 6.95 (br s, 1H,  $\text{H}_6$ ), 6.90 (br dd,  $J_{5,6} = 5.2$  Hz,  $J_{4,5} = 2.4$  Hz, 1H,  $\text{H}_5$ ), 5.43 (br s, 1H,  $\text{H}_4$ ), 5.23 (br s, 1H,  $\text{H}_1$ ), 3.97 (br, 2H,  $\text{OCH}_2\text{CH}_3$ ), 2.44 (s, 3H, aryl  $\text{CH}_3$ ), 1.09 (br s, 3H,  $\text{CH}_2\text{CH}_3$ ).

$^{13}\text{C}$  NMR (63 MHz,  $\text{CDCl}_3$ )  $\delta$ : 159.4 ( $\text{C}_2$ ), 154.9 ( $\text{C}=\text{O}$ ), 152.9 ( $\text{C}_3$ ), 145.3 (aryl C), 143.4 ( $\text{C}_6$ ), 142.1 ( $\text{C}_5$ ), 135.9 (aryl C), 130.4, 128.4 (4 x aryl  $\text{CH}$ ), 68.1 ( $\text{C}_4$ ), 66.9 ( $\text{C}_1$ ), 62.3 ( $\text{OCH}_2\text{CH}_3$ ), 22.0 (aryl  $\text{CH}_3$ ), 14.6 ( $\text{OCH}_2\text{CH}_3$ ).

MS  $m/z$ : 320 ( $\text{MH}^+$ ).  $\text{C}_{16}\text{H}_{18}\text{NO}_4\text{S}$  [ $\text{MH}^+$ ] calculated 320.09566; observed 320.09559.

$\nu_{\text{max}}$ : 1715s, 1596w, 1372m, 1314s, 1253s, 1148s, 1085s, 1017m, 816m, 719m, 666s.

### Synthesis of 7-azabicyclo[2.2.1]hepta-2,5-diene-7-carboxylic acid ethyl ester (26b)



Based on the procedure of Vogel,<sup>7</sup> 7-azanorborndiene derivative (**23b**) (6.9 g; 0.022 mol) was dissolved in anhydrous  $\text{CH}_3\text{OH}$  (45 ml) and THF (45 ml) (1:1) and then disodium hydrogen phosphate (12.3 g; 0.087 mol) was added to the solution under argon. The resulting slurry was cooled to  $-78$  °C. In the course of 1 h, 11.7 g of freshly prepared 6% sodium amalgam was added in several portions with vigorous stirring. The resulting suspension was stirred for 4 h at  $-78$  °C, then water (10 ml) was added and the reaction mixture was filtered through Celite. The mixture was extracted with dichloromethane (3 x 50 ml). The combined organic phase was dried over anhydrous  $\text{MgSO}_4$  and the solvent was removed *in vacuo* to give the crude product which was purified by flash column chromatography (2% diethyl ether-petroleum (bp 40-60 °C)). The first compound to be eluted was (**26b**), isolated as a colourless oil (0.810 g, 23%):  $R_f$  0.36 (1:1 diethyl ether:petroleum (bp 40-60 °C)).

$^1\text{H}$  NMR (300 MHz,  $\text{CDCl}_3$ )  $\delta$ : 6.99 (br d,  $J = 11.5$  Hz, 4H,  $\text{H}_2$ ,  $\text{H}_3$ ,  $\text{H}_5$ ,  $\text{H}_6$ ), 5.25 (br s, 2H,  $\text{H}_1$ ,  $\text{H}_4$ ), 4.07 (q,  $J = 7.1$  Hz, 2H,  $\text{OCH}_2\text{CH}_3$ ), 1.21 (t,  $J = 7.1$  Hz, 3H,  $\text{OCH}_2\text{CH}_3$ ).

$^{13}\text{C}$  NMR (75 MHz,  $\text{CDCl}_3$ )  $\delta$ : 155.1 ( $\text{C}=\text{O}$ ), 144.5, 143.7 ( $\text{C}_2$ ,  $\text{C}_3$ ,  $\text{C}_5$ ,  $\text{C}_6$ ), 66.2 ( $\text{C}_1$ ,  $\text{C}_4$ ), 61.4 ( $\text{OCH}_2\text{CH}_3$ ), 14.6 ( $\text{OCH}_2\text{CH}_3$ ).

$^{15}\text{N}$  NMR (40 MHz,  $\text{CDCl}_3$ )  $\delta$ :  $-203.6$ .

EI: 165 ( $\text{M}^+$ ).  $\text{C}_9\text{H}_{11}\text{NO}_2$  [ $\text{M}^+$ ] calculated 165.07898; observed 165.07896.

$\nu_{\text{max}}$ : 1703s, 1372m, 1251s, 1092s, 845m, 667m.

### Synthesis of 7-methyl-7-azabicyclo[2.2.1]hepta-2,5-diene (**3a**)



Following the procedure of Marchand,<sup>5</sup> (**26b**) (0.124 g;  $7.51 \times 10^{-4}$  mol) was dissolved in anhydrous toluene (3 ml). To the resulting solution was added a solution of diisobutylaluminum hydride in toluene (2.34 ml;  $2.34 \times 10^{-3}$  mol). After stirring for 4 hr at room temperature, an additional 0.5 ml ( $5.1 \times 10^{-4}$  mol) of the toluene solution of diisobutylaluminum hydride was added. After stirring for an additional 4 hr at room temperature, the reaction was quenched with excess methanol until precipitation of aluminium methoxide was complete. The reaction mixture was then filtered and combined with an equal volume of a saturated solution of picric acid in 95% ethanol to precipitate *N*-methyl-7-azanorbornene picrate. Unfortunately, no precipitated crystals of *N*-methyl-7-azanorbornene picrate were formed. The solution then was basified with 2M NaOH and extracted 3 times with  $\text{CFCl}_3$ . The organic layer was dried over anhydrous  $\text{MgSO}_4$ , concentrated and transferred to a 5 mm NMR tube with 0.5 ml of  $\text{CDCl}_3$ . The product was identified by characteristic signals in the NMR spectra but the yield was low of (**3a**) [11% based on a known volume of an internal reference (dichloromethane) which was added to the mixture].

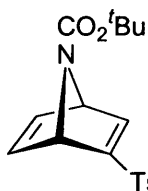
$^1\text{H}$  NMR (400 MHz,  $\text{C}_6\text{D}_6$ )  $\delta$ : 7.00 (br s, 2H), 6.29 (br s, 2H), 3.94 (br s, 2H,  $\text{H}_1$ ,  $\text{H}_4$ ), 2.04 (s, 3H,  $\text{NCH}_3$ ).

$^{13}\text{C}$  NMR (100 MHz,  $\text{C}_6\text{D}_6$ )  $\delta$ : 144.6, 139.4 ( $\text{C}_2$ ,  $\text{C}_3$ ,  $\text{C}_5$ ,  $\text{C}_6$ ), 72.2 ( $\text{C}_1$ ,  $\text{C}_4$ ), 36.2 ( $\text{N-CH}_3$ ).

$^{14}\text{N}$  NMR (40 MHz,  $\text{CDCl}_3$ )  $\delta$ :  $-253.0 \pm 1$ .

MS  $m/z$ : 108 ( $\text{MH}^+$ ).  $\text{C}_7\text{H}_{10}\text{N}$  [ $\text{MH}^+$ ] calculated 108.08132; observed 108.08136.

### Synthesis of 2-(toluene-4-sulfonyl)-7-azabicyclo[2.2.1]hepta-2,5-diene-7-carboxylic acid *tert*-butyl ester (**23c**)<sup>57</sup>



This compound was prepared using a similar method to that used to prepare (**23b**). *N-tert*-butoxycarbonylpyrrole (**24c**) (12.07 g; 0.072 mol) was used for the cycloaddition reaction instead; (**25**) (6.5 g; 0.036 mol). The compound (**23c**) (8.8 g; 70% as a pale yellow oil) was purified by column chromatography (silica and 4:6 diethyl ether:petroleum (bp 40-60 °C)):  $R_f$  0.72 (1:1 diethyl ether:petroleum (bp 40-60 °C)), mp 95-96 °C (lit.<sup>42</sup> 96-97 °C).

$^1\text{H}$  NMR (300 MHz,  $\text{CDCl}_3$ )  $\delta$ : 7.76 (d,  $J = 8.3$  Hz, 2H, 2 x aryl  $\text{CH}$ ), 7.58 (br s, 1H,  $\text{H}_3$ ), 7.36 (d,  $J = 8.3$  Hz, 2H, 2 x aryl  $\text{CH}$ ), 6.95 (br s, 1H,  $\text{H}_6$ ), 6.90 (br dd,  $J_{5,6} = 5.3$

Hz,  $J_{4,5} = 2.5$  Hz, 1H, H<sub>5</sub>), 5.39 (br s, 1H, H<sub>4</sub>), 5.18 (br s, 1H, H<sub>1</sub>), 2.49 (s, 3H, aryl CH<sub>3</sub>), 1.28 (br s, 9H, OC(CH<sub>3</sub>)<sub>3</sub>).

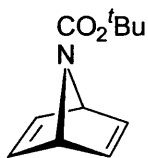
<sup>13</sup>C NMR (75 MHz, CDCl<sub>3</sub>)  $\delta$ : 159.0 (C<sub>2</sub>), 153.9 (C=O), 152.6 (C<sub>3</sub>), 144.9 (aryl C), 143.1 (C<sub>6</sub>), 141.5 (C<sub>5</sub>), 135.7 (aryl C), 130.0, 128.1 (4 x aryl CH), 81.4 (OC(CH<sub>3</sub>)<sub>3</sub>), 67.7 (C<sub>4</sub>), 66.9 (C<sub>1</sub>), 27.9 (OC(CH<sub>3</sub>)<sub>3</sub>), 21.7 (aryl CH<sub>3</sub>).

MS  $m/z$ : 348 (MH<sup>+</sup>). C<sub>18</sub>H<sub>22</sub>NO<sub>4</sub>S [MH<sup>+</sup>] calculated 348.12696; observed 348.12692.

$\nu_{\max}$ : 1703s, 1586w, 1312s, 1257m, 1147s, 1085s, 1017m, 810m, 719m, 666s.

Anal. Calcd for C<sub>18</sub>H<sub>21</sub>NO<sub>4</sub>S: C, 62.23; H, 6.09; N, 4.03. Found: C, 62.33; H, 6.02; N, 4.13.

### Synthesis of 7-azabicyclo[2.2.1]hepta-2,5-diene-7-carboxylic acid *tert*-butyl ester (26c)<sup>114</sup>



This compound was prepared using a similar method to that used to prepare (26b). The crude product was purified by flash column chromatography (2% diethyl ether:petroleum (bp 40-60 °C)). The first compound to be eluted was (26c), isolated as a colourless oil (0.576 g; 19%): R<sub>f</sub> 0.59 (1:1 diethyl ether:petroleum (bp 40-60 °C)).

<sup>1</sup>H NMR (300 MHz, CDCl<sub>3</sub>)  $\delta$ : 6.98 (br d,  $J = 12.7$  Hz, 4H, H<sub>2</sub>, H<sub>3</sub>, H<sub>5</sub>, H<sub>6</sub>), 5.18 (br s, 2H, H<sub>1</sub>, H<sub>4</sub>), 1.41 (s, 9H, OC(CH<sub>3</sub>)<sub>3</sub>).

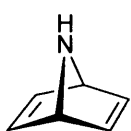
<sup>13</sup>C NMR (75 MHz, CDCl<sub>3</sub>)  $\delta$ : 154.6 (C=O), 144.5, 143.6 (C<sub>2</sub>, C<sub>3</sub>, C<sub>5</sub>, C<sub>6</sub>), 80.3 (OC(CH<sub>3</sub>)<sub>3</sub>), 66.7, 66.1 (C<sub>1</sub>, C<sub>4</sub>), 28.2 (OC(CH<sub>3</sub>)<sub>3</sub>).

<sup>15</sup>N NMR (40 MHz, CDCl<sub>3</sub>)  $\delta$ : -202.6.

MS  $m/z$ : 194 (MH<sup>+</sup>). C<sub>11</sub>H<sub>16</sub>NO<sub>2</sub> [MH<sup>+</sup>] calculated 194.11810; observed 194.11806.

$\nu_{\max}$ : 1736s, 1477w, 1367s, 1252m, 1150s, 846m, 668m.

### Synthesis of 7-azabicyclo[2.2.1]hepta-2,5-diene (3b)<sup>7</sup>



To a stirred solution of (26c) (0.150 g; 7.76 x 10<sup>-4</sup> mol) in 4 ml of dichloromethane and at 0 °C was added drop-wise 2 ml of saturated MeOH with HCl. After 2 minutes, the solvent was removed under reduced pressure at 0 °C to give (3b) as a white solid HCl salt (0.092 g; equivalent to 0.067 g, 93% as free amine). The hydrochloride salt of (3b) was dissolved in water (3 ml) and the solution then was basified with 2M NaOH and extracted 3 times with CFCl<sub>3</sub>. The organic layer

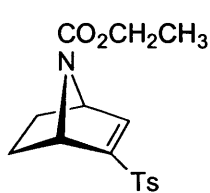
was dried over anhydrous MgSO<sub>4</sub>, concentrated and transferred to a 5 mm NMR tube with 0.5 ml of CDCl<sub>3</sub>.

<sup>1</sup>H NMR (300 MHz, CDCl<sub>3</sub>) δ: 7.04 – 7.02 (m, 4H, H<sub>2</sub>, H<sub>3</sub>, H<sub>5</sub>, H<sub>6</sub>), 4.73 (br s, 2H, H<sub>1</sub>, H<sub>4</sub>), 1.68 (br s, NH).

<sup>13</sup>C NMR (100 MHz, CDCl<sub>3</sub>) δ: 145.9 (C<sub>2</sub>, C<sub>3</sub>, C<sub>5</sub>, C<sub>6</sub>), 66.7 (C<sub>1</sub>, C<sub>4</sub>).

<sup>15</sup>N NMR (40 MHz, MeOH) δ: –257.7 (as HCl salt).

### Synthesis of 2-(toluene-4-sulfonyl)-7-azabicyclo[2.2.1]hept-2-ene-7-carboxylic acid ethyl ester (36)



Based on the procedure of Vogel,<sup>4</sup> compound (**23b**) (0.157 g; 4.92 x 10<sup>-4</sup> mol) was placed in a 25 ml reaction vessel and dissolved in anhydrous acetonitrile (5 ml) and 0.050 g of palladium/charcoal (Pd/C) catalyst was added to the solution. Hydrogen (17 ml, 7.57 x 10<sup>-4</sup> mol)

was passed into the reaction flask by using hydrogenation apparatus and the reaction mixture was stirred at room temperature. The catalyst was removed by filtration over Celite, and the solvent was evaporated on a rotary evaporator to give 0.146 g (93%) of (**36**) as brown oil.

<sup>1</sup>H NMR (250 MHz, CDCl<sub>3</sub>): δ 7.66 (d, *J* = 8 Hz, 2H, 2 x aryl CH), 7.29 (d, *J* = 8 Hz, 2H, 2 x aryl CH), 7.04 (d, *J* = 2 Hz, 1H, H<sub>3</sub>), 4.89 (br s, 1H, H<sub>1</sub>), 4.84 (d, *J* = 3.2 Hz, 1H, H<sub>4</sub>), 3.91 (br q, *J* = 7.1 Hz, 2H, OCH<sub>2</sub>), 2.44 (s, 3H, aryl CH<sub>3</sub>), 2.08 – 1.94 (m, 2H, H<sub>5-*exo*</sub>, H<sub>6-*exo*</sub>), 1.40 – 1.26 (m, 2H, H<sub>5-*endo*</sub>, H<sub>6-*endo*</sub>), 1.04 (br s\*, 3H, CH<sub>2</sub>CH<sub>3</sub>).

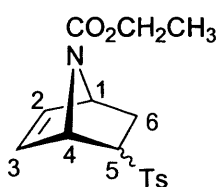
<sup>13</sup>C NMR (75 MHz, CDCl<sub>3</sub>) δ: 155.4 (C=O), 148.9 (C<sub>2</sub>), 144.9 (aryl C), 143.5 (C<sub>3</sub>), 136.6 (aryl C), 130.0, 127.9 (4 x aryl CH), 61.7 (OCH<sub>2</sub>CH<sub>3</sub>), 61.7 (C<sub>4</sub>), 60.5 (C<sub>1</sub>), 25.0, 24.2, (C<sub>5</sub>, C<sub>6</sub>), 21.7 (aryl CH<sub>3</sub>), 14.2 (OCH<sub>2</sub>CH<sub>3</sub>).

MS *m/z*: 322 (MH<sup>+</sup>). C<sub>16</sub>H<sub>20</sub>NO<sub>4</sub>S [MH<sup>+</sup>] calculated 322.11131; observed 322.11124.

*v*<sub>max</sub>: 1710s, 1595w, 1371m, 1317s, 1278s, 1150s, 1092m, 813m, 673s.

\* as a result of the slow rotation around the NC=O bond.

### Synthesis of 5-(toluene-4-sulfonyl)-7-azabicyclo[2.2.1]hept-2-ene-7-carboxylic acid ethyl ester (37)



Compound (**23b**) (0.281 g; 8.8 x 10<sup>-4</sup> mol) was placed in a 25 ml reaction vessel and dissolved in 5 ml of methanol. NaBH<sub>4</sub> (0.017 g, 4.4 x 10<sup>-4</sup>) was added to the reaction mixture at room temperature and

stirred for 1 hr. The mixture was extracted with dichloromethane (10 ml), and the extract was washed with water (3 x 10 ml), dried over anhydrous Na<sub>2</sub>SO<sub>4</sub>, filtered, and concentrated under vacuum. The crude yield of **(37)** was 0.271 g, 96% and the product was pure enough (by <sup>1</sup>H NMR) to be used for the next step without further purification. The crude residue gave a mixture of *endo*-**(37)** and *exo*-**(37)** (7:3 respectively) as a pale yellow oil.

The signals corresponding to the minor (*exo*-tosyl) isomer are shown in italics.

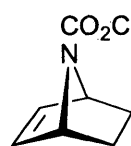
<sup>1</sup>H NMR (300 MHz, CDCl<sub>3</sub>) δ: 7.74 (d, *J* = 8.3 Hz, 2H, 2 x aryl CH), 7.37 (d, *J* = 8.3 Hz, 2H, 2 x aryl CH), 6.53 (dd, *J* = 2.2 Hz, *J* = 5.8 Hz, 1H), 6.43 (dd, *J* = 1.9 Hz, *J* = 5.8 Hz, 1H) (H<sub>2</sub> and H<sub>3</sub>), 6.32 (br d, 1H, H<sub>2</sub> or H<sub>3</sub>), 5.06, 4.82 (2 x br s, 4H, H<sub>1</sub>, H<sub>4</sub>, *H*<sub>1</sub>, *H*<sub>4</sub>), 4.11 (q, *J* = 7.1 Hz, 2H, OCH<sub>2</sub>CH<sub>3</sub>), 3.76 – 3.70 (m, 1H, H<sub>5-*exo*</sub>), 3.04 (br dd, *J*<sub>5-*endo*,6-*exo*</sub> = 4.2 Hz, *J*<sub>5-*endo*,6-*endo*</sub> = 8.2 Hz, 1H, H<sub>5-*endo*</sub>), 2.46 (s, 3H, aryl CH<sub>3</sub>), 2.25 (ddd, *J*<sub>1,6-*exo*</sub> = 4.2 Hz, *J*<sub>5-*exo*,6-*exo*</sub> = 9.1 Hz, *J*<sub>6-*exo*,6-*endo*</sub> = 12.1 Hz, 1H, H<sub>6-*exo*</sub>), 1.68 (dd, *J*<sub>5-*exo*,6-*endo*</sub> = 4.2 Hz, *J*<sub>6-*exo*,6-*endo*</sub> = 12.1 Hz, 1H, H<sub>6-*endo*</sub>), 1.19 (t, *J* = 7.1 Hz, 3H, OCH<sub>2</sub>CH<sub>3</sub>).

<sup>13</sup>C NMR (75 MHz, CDCl<sub>3</sub>) δ: 153.7, 153.3 (C=O), 143.9, 143.8 (aryl C), 136.0, 130.6 (C<sub>2</sub>, C<sub>3</sub>), 135.9 (aryl C), 129.1, 126.9 (4 x aryl CH), 61.5 (C<sub>5</sub>), 60.8, 60.5 (OCH<sub>2</sub>CH<sub>3</sub>), 60.0, 58.3 (C<sub>1</sub>, C<sub>4</sub>), 28.0 (C<sub>6</sub>), 20.6 (aryl CH<sub>3</sub>), 13.4, (OCH<sub>2</sub>CH<sub>3</sub>).

MS <sup>m/z</sup>: 322 (MH<sup>+</sup>). C<sub>16</sub>H<sub>20</sub>NO<sub>4</sub>S [MH<sup>+</sup>] calculated 322.11131; observed 322.11139.

*v*<sub>max</sub>: 1745s, 1710m, 1596w, 1473m, 1409m, 1372m, 1308s, 1184m, 1145s, 1085m, 947m, 737s, 660m.

### Synthesis of 7-azabicyclo[2.2.1]hept-2-ene-7-carboxylic acid ethyl ester (**38**)<sup>6</sup>



**Method a:** compound **(36)** (0.605 g; 1.88 x 10<sup>-3</sup> mol) was dissolved in anhydrous CH<sub>3</sub>OH (4 ml) and THF (8 ml) (1:2) and then disodium hydrogen phosphate (1.7 g; 7.53 x 10<sup>-3</sup> mol) was added under argon. The resulting slurry was cooled to -78 °C. In the course of 1 h, 1.03 g of 6% sodium amalgam (freshly prepared) was added in several portions with vigorous stirring. The resulting suspension was stirred under argon for 4 h at -78 °C, then distilled water (10 ml) was added and the reaction mixture was filtered through Celite. The mixture was extracted with 50 ml dichloromethane three times. The combined organic phase was dried over anhydrous MgSO<sub>4</sub> and the solvent was removed under reduced pressure to give crude product. The crude product could not be purified by flash column chromatography.

**Method b:** Following the procedure of Hodgson,<sup>66</sup> Compound **(37)** (0.271 g;  $8.44 \times 10^{-4}$  mol) was dissolved in anhydrous CH<sub>3</sub>OH (4 ml) and THF (4 ml) (1:1) and then disodium hydrogen phosphate (1.16 g;  $8.15 \times 10^{-4}$  mol) was added to the solution under argon. The resulting slurry was cooled to -10 °C. Freshly prepared sodium amalgam (6%; 2.71g) was added with vigorous stirring. The resulting suspension was stirred at -10 °C for 30 mins. and was warmed to 25 °C over 3 h, then distilled water (10 ml) was added and the reaction mixture was filtered through Celite. The mixture was extracted with dichloromethane (3 x 25 ml). The combined organic phase was dried over anhydrous MgSO<sub>4</sub> and the solvent was removed under reduced pressure to give the crude product which was subjected to flash column chromatography. Elution with 2% diethyl ether and petroleum (bp 40-60 °C) gave **(38)** (0.057 g, 44% yield) as a colourless liquid: R<sub>f</sub> 0.50 (1:1 diethyl ether:petroleum (bp 40-60 °C)).

<sup>1</sup>H NMR (300 MHz, CDCl<sub>3</sub>): δ 6.23 (br s, 2H, H<sub>2</sub>, H<sub>3</sub>), 4.73 (br s, 2H, H<sub>1</sub>, H<sub>4</sub>), 4.07 (q, *J* = 7.1 Hz, 2H, OCH<sub>2</sub>), 1.86 (br d, *J* = 7.7 Hz, 2H, H<sub>5-exo</sub>, H<sub>6-exo</sub>), 1.22 (t, *J* = 7.1 Hz, 3H, CH<sub>2</sub>CH<sub>3</sub>) 1.12 (d, *J* = 7.7 Hz, 2H, H<sub>5-endo</sub>, H<sub>6-endo</sub>).

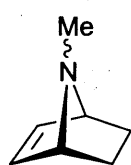
<sup>13</sup>C NMR (75 MHz, CDCl<sub>3</sub>): δ 155.6 (C=O), 134.7 (C<sub>2</sub>, C<sub>3</sub>), 61.1 (O-CH<sub>2</sub> CH<sub>3</sub>), 59.5 (C<sub>1</sub>, C<sub>4</sub>), 23.9 (C<sub>5</sub>, C<sub>6</sub>), 14.6 (OCH<sub>2</sub>CH<sub>3</sub>).

<sup>15</sup>N NMR (40 MHz, CDCl<sub>3</sub>) δ: -247.3.

EI: 167 (M<sup>+</sup>). C<sub>9</sub>H<sub>13</sub>NO<sub>2</sub> [M<sup>+</sup>] calculated 167.09463; observed 167.09458.

ν<sub>max</sub>: 1712s, 1373m, 1278s, 1175w, 1079s, 863m, 704s.

### Synthesis of 7-methyl-7-azabicyclo[2.2.1]hept-2-ene (**2a**)<sup>21</sup>



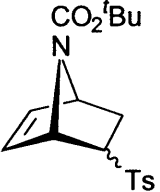
A solution of **(38)** (0.196 g;  $1.17 \times 10^{-3}$  mol) in 10 ml of anhydrous diethyl ether was added to a stirring suspension of LAH 0.18 g;  $4.69 \times 10^{-3}$  mol) in anhydrous diethyl ether (20 ml) under nitrogen. The reaction mixture was refluxed for 8 h, and quenched with 0.5 ml of distilled water, 0.5 ml of 10% NaOH, and 1.5 ml of distilled water. The reaction mixture was then filtered through a pad of Celite and washed with ether. The ether solutions were combined and dried over MgSO<sub>2</sub>, and **(2a:HCl)** was precipitated by bubbling HCl through the solution, yielding 0.143 g as salt (0.107 g, 84% as free amine **(2a)**). The **(2a:HCl)** was dissolved in distilled water then basified with 2M NaOH and extracted 3 times with CFCl<sub>3</sub> to obtain the free amine **(2a)**. The organic layer was dried over anhydrous MgSO<sub>4</sub>, concentrated and transferred to a 5 mm NMR tube with 0.5 ml of CDCl<sub>3</sub>.

$^1\text{H}$  NMR (300 MHz,  $\text{CDCl}_3$ )  $\delta$ : 5.92 (br s, 2H,  $\text{H}_2$ ,  $\text{H}_3$ ), 3.69 (br s, 2H,  $\text{H}_1$ ,  $\text{H}_4$ ), 2.05 (s, 3H,  $\text{NCH}_3$ ), 1.81 (br d,  $J = 7.1$  Hz, 2H,  $\text{H}_{5\text{-exo}}$ ,  $\text{H}_{6\text{-exo}}$ ), 0.97 (d,  $J = 7.1$  Hz, 2H,  $\text{H}_{5\text{-endo}}$ ,  $\text{H}_{6\text{-endo}}$ ).

$^{13}\text{C}$  NMR (75 MHz,  $\text{CDCl}_3$ )  $\delta$ : 130.3 ( $\text{C}_2$ ,  $\text{C}_3$ ), 66.4 ( $\text{C}_1$ ,  $\text{C}_4$ ), 34.6 ( $\text{NCH}_3$ ), 24.7 ( $\text{C}_5$ ,  $\text{C}_6$ ).

$^{14}\text{N}$  NMR (40 MHz,  $\text{CDCl}_3$ )  $\delta$ :  $-297.0 \pm 2$  ppm.

### Synthesis of 5-(toluene-4-sulfonyl)-7-azabicyclo[2.2.1]hept-2-ene-7-carboxylic acid *tert*-butyl ester (**40**)<sup>53</sup>

 This compound was prepared using a similar method to that used to prepare (**23c**). The crude yield was 2.7 g (95%) of (**40**) which was pure enough ( $^1\text{H}$  NMR) to be used directly for the next reaction. The crude residue gave a mixture of *endo*-(**40**) and *exo*-(**40**) as pale yellow oil (7:3 respectively).

The signals corresponding to the minor (*exo*-tosyl) isomer are shown in italics.

$^1\text{H}$  NMR (300 MHz,  $\text{CDCl}_3$ )  $\delta$ : 7.74 (d,  $J = 8.3$  Hz, 2H, 2 x aryl  $\text{CH}$ ), 7.34 (d,  $J = 8.3$  Hz, 2H, 2 x aryl  $\text{CH}$ ), 6.52 (dd,  $J = 2.0$  Hz,  $J = 5.8$  Hz, 1H), 6.41 (dd,  $J = 1.8$  Hz,  $J = 5.8$  Hz, 1H)  $\text{H}_2$  and  $\text{H}_3$ , 6.33 (br s, 1H,  $\text{H}_2$  or  $\text{H}_3$ ), 4.98, 4.75 (2 x br s, 4H,  $\text{H}_1$ ,  $\text{H}_4$ ,  $\text{H}_1$ ,  $\text{H}_4$ ), 3.75 – 3.70 (m, 1H,  $\text{H}_{5\text{-exo}}$ ), 3.02 (br dd,  $J_{5\text{-endo},6\text{-exo}} = 4.0$  Hz,  $J_{5\text{-endo},6\text{-endo}} = 8.0$  Hz, 1H  $\text{H}_{5\text{-endo}}$ ), 2.45 (s, 3H, aryl  $\text{CH}_3$ ), 2.29 – 2.20 (m, 1H,  $\text{H}_{6\text{-exo}}$ ), 1.66 (br d,  $J = 4.4$  Hz, 1H,  $\text{H}_{6\text{-endo}}$ ), 1.38 (s, 9H,  $\text{OC}(\text{CH}_3)_3$ ).

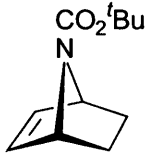
$^{13}\text{C}$  NMR (75 MHz,  $\text{CDCl}_3$ )  $\delta$ : 154.2 ( $\text{C}=\text{O}$ ), 144.9, 137.0 (2 x aryl C), 131.6 ( $\text{C}_2$ ,  $\text{C}_3$ ), 130.1, 128.0 (2 x aryl  $\text{CH}$ ), 81.0 ( $\text{OC}(\text{CH}_3)_3$ ), 62.4 ( $\text{C}_5$ ), 61.1 ( $\text{C}_1$ ,  $\text{C}_4$ ), 28.9 ( $\text{C}_6$ ), 28.1, ( $\text{OC}(\text{CH}_3)_3$ ), 21.6 (aryl  $\text{CH}_3$ ).

MS  $m/z$ : 350 ( $\text{MH}^+$ ).  $\text{C}_{18}\text{H}_{24}\text{NO}_4\text{S}$  [ $\text{MH}^+$ ] calculated 350.14261; observed 350.14259.

$\nu_{\text{max}}$ : 1710s, 1594w, 1336s, 1286s, 1143s, 1089s, 818m, 741m, 660s.

Anal. Calcd for  $\text{C}_{18}\text{H}_{23}\text{NO}_4\text{S}$ : C, 61.92; H, 6.64; N, 4.01. Found: C, 61.81; H, 6.61; N, 3.97.

### Synthesis of 7-aza-bicyclo[2.2.1]hept-2-ene-7-carboxylic acid *tert*-butyl ester (**39**)<sup>64</sup>

 This compound was prepared using a similar method to that used to prepare (**36**) (Method b). The yield of (**39**) was 33% after column chromatography:  $R_f$  0.57 (1:1 diethyl ether:petroleum (bp 40-60 °C)).

$^1\text{H}$  NMR (300 MHz,  $\text{CDCl}_3$ ):  $\delta$  6.22 (br s, 2H,  $\text{H}_2$ ,  $\text{H}_3$ ), 4.65 (br s, 2H,  $\text{H}_1$ ,  $\text{H}_4$ ), 1.86 (br d,  $J = 8.8$  Hz, 2H,  $\text{H}_{5\text{-exo}}$ ,  $\text{H}_{6\text{-exo}}$ ), 1.42 (s, 9H,  $\text{OC}(\text{CH}_3)_3$ ) 1.10 (d,  $J = 7.8$  Hz, 2H,  $\text{H}_{5\text{-endo}}$ ,  $\text{H}_{6\text{-endo}}$ ).

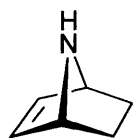
$^{13}\text{C}$  NMR (75 MHz,  $\text{CDCl}_3$ ):  $\delta$  155.2 (C=O), 134.8 ( $\text{C}_3$ ,  $\text{C}_3$ ), 79.7, ( $\text{OC}(\text{CH}_3)_3$ ) 59.6 ( $\text{C}_1$ ,  $\text{C}_4$ ), 28.2 ( $\text{OC}(\text{CH}_3)_3$ ), 23.8 ( $\text{C}_5$ ,  $\text{C}_6$ ).

$^{15}\text{N}$  NMR (40 MHz,  $\text{CDCl}_3$ )  $\delta$ : -248.1.

MS  $m/z$ : 196 ( $\text{MH}^+$ ).  $\text{C}_{11}\text{H}_{18}\text{NO}_2$  [ $\text{MH}^+$ ] calculated 196.13375; observed 196.13380.

$\nu_{\text{max}}$ : 1699s, 1478w, 1354s, 1284m, 1157s, 1077m, 881m, 703m.

### Synthesis of 7-azabicyclo[2.2.1]hept-2,3-ene (2b)<sup>21</sup>



To a stirred solution of (39) (0.259 g;  $1.33 \times 10^{-3}$  mol) in ethyl acetate (5 ml) was added drop-wise 3M HCl (5 ml, at 0 °C) formed *in situ* from the reaction of ethanol (2.7 ml), ethyl acetate (7.2 ml) and acetyl chloride (2.7 ml). The mixture was allowed to warm to room temperature with continuance of the stirring overnight. The reaction mixture was then evaporated under reduced pressure. The residue (2b:HCl) (0.172 g; 0.124 g, 99% as free amine) was dissolved in 3 ml distilled water, basified with 2M NaOH and extracted with  $\text{CFCl}_3$  (3 x 5 ml). The organic layers were combined, dried over anhydrous  $\text{MgSO}_4$ , concentrated and transferred to a 5 mm NMR tube with 0.5 ml of  $\text{CDCl}_3$ .

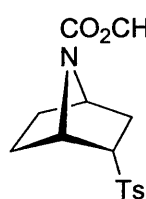
$^1\text{H}$  NMR (300 MHz,  $\text{CDCl}_3$ )  $\delta$ : 6.16 (br s, 2H,  $\text{H}_2$ ,  $\text{H}_3$ ), 4.06 (br s, 2H,  $\text{H}_1$ ,  $\text{H}_4$ ), 1.92 (br s, 1H,  $\text{NH}$ ), 1.71 – 1.65 (m, 2H,  $\text{H}_{5\text{-exo}}$ ,  $\text{H}_{6\text{-exo}}$ ), 0.95 (dd,  $J_{5\text{-endo},6\text{-exo}} = 3.8$  Hz,  $J_{5\text{-endo},5\text{-exo}} = 11.2$ , 2H,  $\text{H}_{5\text{-endo}}$ ,  $\text{H}_{6\text{-endo}}$ ).

$^{13}\text{C}$  NMR (75 MHz,  $\text{CDCl}_3$ )  $\delta$ : 136.0 ( $\text{C}_2$ ,  $\text{C}_3$ ), 58.8 ( $\text{C}_1$ ,  $\text{C}_4$ ), 26.6 ( $\text{C}_5$ ,  $\text{C}_6$ ).

$^{15}\text{N}$  NMR (40 MHz, MeOH)  $\delta$ : -297.0 (as HCl salt).

MS  $m/z$ : 96 ( $\text{MH}^+$ ).  $\text{C}_6\text{H}_{10}\text{N}$  [ $\text{MH}^+$ ] calculated 96.08132; observed 96.08140.

### Synthesis of 2-(toluene-4-sulfonyl)-7-azabicyclo[2.2.1]heptane-7-carboxylic acid ethyl ester *endo*-(41)



Compound (23b) ( $0.650$  g;  $2.04 \times 10^{-3}$  mol) was dissolved in anhydrous acetonitrile (15 ml) and hydrogenated over palladium/charcoal (Pd/C) using a balloon of hydrogen. The reaction vessel was purged first with nitrogen and then carefully with hydrogen. The reaction mixture was stirred vigorously at room temperature for 7h. After the addition was complete, the

catalyst was removed by filtration through Celite and the solvent was evaporated *in vacuo* to give the saturated **endo-(41)** (0.645 g, 98%):  $R_f$  0.35 (1:1 diethyl ether:petroleum (bp 40-60 °C)).

$^1\text{H}$  NMR (300 MHz,  $\text{CDCl}_3$ )  $\delta$ : 7.76 (d,  $J = 8.2$  Hz, 2H, 2 x aryl  $\text{CH}$ ), 7.36 (d,  $J = 8.2$  Hz, 2H, 2 x aryl  $\text{CH}$ ), 4.43 (br t,  $J = 4.3$  Hz, 1H,  $\text{H}_1$ ), 4.34 (br t,  $J = 4.7$  Hz, 1H,  $\text{H}_4$ ), 4.08 (q,  $J = 7.1$  Hz, 2H,  $\text{OCH}_2\text{CH}_3$ ), 3.59 – 3.52 (m, 1H,  $\text{H}_2$ ), 2.60 – 2.51 (m, 1H,  $\text{H}_{6\text{-endo}}$ ), 2.9 – 1.85 (m, 3H,  $\text{H}_{3\text{-exo}}$ ,  $\text{H}_{3\text{-endo}}$ ,  $\text{H}_{5\text{-exo}}$ ), 1.81 – 1.65 (m, 2H, ( $\text{H}_{5\text{-endo}}$ ,  $\text{H}_{6\text{-exo}}$ ), 1.22 (t,  $J = 7.1$  Hz, 3H,  $\text{OCH}_2\text{CH}_3$ ).

$^{13}\text{C}$  NMR (75 MHz,  $\text{CDCl}_3$ )  $\delta$ : 155.2 (C=O), 144.9, 137.2 (2 x aryl C), 130.1, 127.8 (4 x aryl  $\text{CH}$ ), 64.6 ( $\text{C}_2$ ), 61.5 ( $\text{OCH}_2\text{CH}_3$ ), 58.0, 57.6 ( $\text{C}_1$ ,  $\text{C}_4$ ), 32.3 ( $\text{C}_3$ ), 29.3 ( $\text{C}_5$ ), 24.8 ( $\text{C}_6$ ), 21.6 (aryl  $\text{CH}_3$ ), 14.5, ( $\text{OCH}_2\text{CH}_3$ ).

MS  $m/z$ : 324 ( $\text{MH}^+$ ).  $\text{C}_{16}\text{H}_{22}\text{NO}_4\text{S}$  [ $\text{MH}^+$ ] calculated 324.12696; observed 324.12702.

$\nu_{\text{max}}$ : 1701s, 1596w, 1301s, 1249m, 1253w, 1144s, 1086s, 815m, 723m, 666s.

### Synthesis of 7-azabicyclo[2.2.1]heptane-7-carboxylic acid ethyl ester (**42**)<sup>3</sup>

  $\text{CO}_2\text{CH}_2\text{CH}_3$  This compound was prepared using a similar method to that used to prepare (**38**) (Method b). The yield of (**42**) was 50% after column chromatography:  $R_f$  0.77 (1:1 diethyl ether:petroleum (bp 40-60 °C)).

$^1\text{H}$  NMR (300 MHz,  $\text{CDCl}_3$ )  $\delta$ : 4.28 – 4.24 (m, 2H,  $\text{H}_1$ ,  $\text{H}_4$ ), 4.11 (q,  $J = 7.1$  Hz, 2H,  $\text{OCH}_2\text{CH}_3$ ), 1.79 – 1.75 (m, 4H,  $\text{H}_{2\text{-exo}}$ ,  $\text{H}_{3\text{-exo}}$ ,  $\text{H}_{5\text{-exo}}$ ,  $\text{H}_{6\text{-exo}}$ ), 1.41 (br d,  $J = 7.1$  Hz, 4H,  $\text{H}_{2\text{-endo}}$ ,  $\text{H}_{3\text{-endo}}$ ,  $\text{H}_{5\text{-endo}}$ ,  $\text{H}_{6\text{-endo}}$ ), 1.25 (t,  $J = 7.1$  Hz, 3H,  $\text{OCH}_2\text{CH}_3$ ).

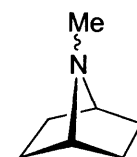
$^{13}\text{C}$  NMR (75 MHz,  $\text{CDCl}_3$ )  $\delta$ : 156.0 (C=O), 60.9 (O- $\text{CH}_2$   $\text{CH}_3$ ), 56.0 ( $\text{C}_1$ ,  $\text{C}_4$ ), 29.6 ( $\text{C}_2$ ,  $\text{C}_3$ ,  $\text{C}_5$ ,  $\text{C}_6$ ), 14.6 ( $\text{OCH}_2\text{CH}_3$ ).

$^{15}\text{N}$  NMR (40 MHz,  $\text{CDCl}_3$ )  $\delta$ : -259.5.

EI: 169 ( $\text{M}^+$ ).  $\text{C}_9\text{H}_{15}\text{NO}_2$  [ $\text{M}^+$ ] calculated 169.11028; observed 169.11027.

$\nu_{\text{max}}$ : 1698s, 1373m, 1312s, 1259m, 1152s, 1096s, 902m, 778m.

### Synthesis of 7-methyl-7-azabicyclo[2.2.1]heptane (**1a**)<sup>3</sup>

 A solution of (**42**) (0.205 g;  $1.21 \times 10^{-3}$  mol) in 5 ml of anhydrous diethyl ether was added to a stirring suspension of LAH (0.18 g;  $4.85 \times 10^{-3}$  mol) in 10 ml of anhydrous diethyl ether under nitrogen. The reaction mixture was refluxed for 8 h, and quenched with 0.5 ml of distilled water, 0.5 ml of 10% NaOH, and 1.5 ml of distilled water. The reaction mixture was then filtered through a

pad of Celite and washed with ether. The ether solutions were combined and dried over MgSO<sub>4</sub>, and (**1a:HCl**) was precipitated by bubbling HCl through the solution, yielding the HCl salt (0.169 g; 0.127 g, 95% as free amine). The (**1a:HCl**) was dissolved in distilled water then basified with 2M NaOH and extracted 3 times with CFC<sub>3</sub>. The organic layer was dried over anhydrous MgSO<sub>4</sub>, concentrated and transferred to a 5 mm NMR tube with 0.5 ml of CDCl<sub>3</sub>.

<sup>1</sup>H NMR (300 MHz, CDCl<sub>3</sub>) δ: 3.19 – 3.16 (m, 2H, H<sub>1</sub>, H<sub>4</sub>), 2.24 (s, 3H, NCH<sub>3</sub>),  
<sup>1</sup>H NMR (300 MHz, CDCl<sub>3</sub>) δ: 3.19 – 3.16 (m, 2H, H<sub>1</sub>, H<sub>4</sub>), 2.24 (s, 3H, NCH<sub>3</sub>),

1.77 (br d, *J* = 7.1 Hz, 4H, H<sub>2-*exo*</sub>, H<sub>3-*exo*</sub>, H<sub>5-*exo*</sub>, H<sub>6-*exo*</sub>), 1.27 (br d, *J* = 7.1 Hz, 4H, H<sub>2-*endo*</sub>, H<sub>3-*endo*</sub>, H<sub>5-*endo*</sub>, H<sub>6-*endo*</sub>).  
<sup>13</sup>C NMR (75 MHz, CDCl<sub>3</sub>) δ: 61.2 (C<sub>1</sub>, C<sub>4</sub>), 34.8 (NCH<sub>3</sub>) 28.6 (br, C<sub>2</sub>, C<sub>3</sub>, C<sub>5</sub>, C<sub>6</sub>).

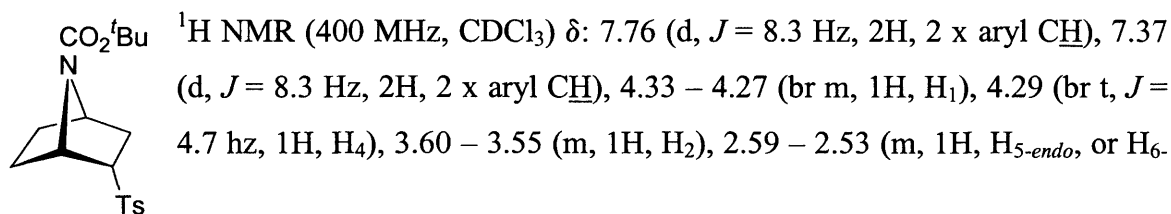
<sup>15</sup>N NMR (40.5 MHz, CDCl<sub>3</sub>) δ: –313.3 ppm.

EI: 111 (M<sup>+</sup>). C<sub>7</sub>H<sub>13</sub>N [M<sup>+</sup>] calculated 111.10480; observed 111.10485.

### Synthesis of 2-(toluene-4-sulfonyl)-7-azabicyclo[2.2.1]heptane-7-carboxylic acid *tert*-butyl ester (**43**)<sup>53</sup>

A mixture of the two stereoisomers of compound (**40**) (0.842 g; 2.41 x 10<sup>-3</sup> mol) was dissolved in anhydrous acetonitrile (15 ml) and hydrogenated over Pd/C using a balloon of hydrogen. The reaction vessel was purged first with nitrogen and then carefully with hydrogen. The reaction mixture was stirred vigorously at room temperature for 7h. After the addition was complete, the catalyst was removed by filtration through Celite and the solvent was evaporated *in vacuo* to give the saturated mixtures of *endo*- and *exo*- tosyl (**43**) (0.821 g, 97%). The mixture was used directly for the de-tosylation reaction step. Separation of the mixture of isomers was necessary for some reactions below and details are summarised below. The mixture was chromatographed on silica gel. Elution with diethyl ether-petroleum (bp 40-60 °C) (20:80) gave first *endo*-(**43**) (0.640 g, 80%) as white solid: R<sub>f</sub> 0.32 (diethyl ether-petroleum (bp 40-60 °C), 1:1). *exo*-(**43**) was eluted with 25:75 of diethyl ether-petroleum (bp 40-60 °C) to gave 0.165 g (20%) as white solid: R<sub>f</sub> 0.15 (1:1 diethyl ether:petroleum (bp 40-60 °C)), mp 114-115 °C.

#### *endo*-(**43**) isomer



*endo*), 2.45 (s, 3H, aryl  $\underline{\text{CH}}_3$ ), 2.09 – 2.01 (m, 1H,  $\text{H}_{3\text{-exo}}$ ), 1.95 (dd,  $J_{2,3\text{-endo}} = 5.7$  Hz,  $J_{3\text{-exo},3\text{-endo}} = 12.6$  Hz, 1H,  $\text{H}_{3\text{-endo}}$ ), 1.92 – 1.86 (m, 1H,  $\text{H}_{5\text{-exo}}$ ), 1.78 – 1.64 (m, 2H,  $\text{H}_{6\text{-exo}}$ , ( $\text{H}_{5\text{-endo}}$ , or  $\text{H}_{6\text{-endo}}$ )), 1.41 (s, 9H,  $\text{OC}(\underline{\text{CH}}_3)_3$ ).

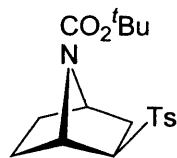
$^{13}\text{C}$  NMR (75 MHz,  $\text{CDCl}_3$ )  $\delta$ : 154.8 (C=O), 144.8, 137.2 (2 x aryl C), 130.1, 127.8 (4 x aryl  $\underline{\text{CH}}$ ), 80.5 ( $\text{OC}(\underline{\text{CH}}_3)_3$ ), 64.6 ( $\text{C}_2$ ), 58.0, 57.6 ( $\text{C}_1$ ,  $\text{C}_4$ ), 32.1 ( $\text{C}_3$ ), 29.2 ( $\text{C}_5$  or  $\text{C}_6$ ), 28.2, ( $\text{OC}(\underline{\text{CH}}_3)_3$ ), 24.7 ( $\text{C}_5$  or  $\text{C}_6$ ), 21.6 (aryl  $\underline{\text{C}}\text{H}_3$ ).

MS  $m/z$ : 352 ( $\text{MH}^+$ ).  $\text{C}_{18}\text{H}_{26}\text{NO}_4\text{S}$  [ $\text{MH}^+$ ] calculated 352.15826; observed 352.15817.

$\nu_{\text{max}}$ : 1699s, 1345s, 1300m, 1253w, 1141s, 1084s, 819m, 719m, 675s.

Anal. Calcd for  $\text{C}_{18}\text{H}_{25}\text{NO}_4\text{S}$ : C, 61.57; H, 7.18; N, 3.99. Found: C, 61.64; H, 6.98; N, 3.55.

#### *exo*-(43) isomer



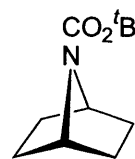
$^1\text{H}$  NMR (300 MHz,  $\text{CDCl}_3$ )  $\delta$ : 7.79 (d,  $J = 8.0$  Hz, 2H, 2 x aryl  $\underline{\text{CH}}$ ), 7.34 (d,  $J = 8.0$  Hz, 2H, 2 x aryl  $\underline{\text{CH}}$ ), 4.55 (br d,  $J_{1,6\text{-exo}} = 2.8$  Hz, 1H,  $\text{H}_1$ ), 4.25 (br s, 1H,  $\text{H}_4$ ), 3.21 (dd,  $J_{2,3\text{-endo}} = 8.8$  Hz,  $J_{2,3\text{-exo}} = 5.5$  Hz, 1H,  $\text{H}_2$ ), 2.43 (s, 3H, aryl  $\underline{\text{CH}}_3$ ), 2.21 (br s, 1H,  $\text{H}_{5\text{-endo}}$ , or  $\text{H}_{6\text{-endo}}$ ), 1.84 – 1.42 (br m, 5H,  $\text{H}_{3\text{-exo}}$ ,  $\text{H}_{3\text{-endo}}$ ,  $\text{H}_{5\text{-exo}}$ ,  $\text{H}_{6\text{-exo}}$ , ( $\text{H}_{5\text{-endo}}$ , or  $\text{H}_{6\text{-endo}}$ )), 1.41 (br s, 9H,  $\text{OC}(\underline{\text{CH}}_3)_3$ ).

$^{13}\text{C}$  NMR (75 MHz,  $\text{CDCl}_3$ )  $\delta$ : 153.7 (C=O), 144.6, 134.6 (2 x aryl C), 129.7, 129.2 (4 x aryl  $\underline{\text{CH}}$ ), 79.9 ( $\text{OC}(\underline{\text{CH}}_3)_3$ ), 67.3 ( $\text{C}_2$ ), 57.1 ( $\text{C}_4$ ), 55.1 ( $\text{C}_1$ ), 32.9, 30.3, 29.0 ( $\text{C}_3$ ,  $\text{C}_5$ ,  $\text{C}_6$ ), 28.2, ( $\text{OC}(\underline{\text{CH}}_3)_3$ ), 21.6 (aryl  $\underline{\text{C}}\text{H}_3$ ).

MS  $m/z$ : 352 ( $\text{MH}^+$ ).  $\text{C}_{18}\text{H}_{26}\text{NO}_4\text{S}$  [ $\text{MH}^+$ ] calculated 352.15826; observed 352.15836.

$\nu_{\text{max}}$ : 1701s, 1345s, 1300m, 1253w, 1141s, 1084m, 819m, 719m, 675s.

#### Synthesis of 7-azabicyclo[2.2.1]heptane-7-carboxylic acid *tert*-butyl ester (44)<sup>115</sup>



This compound was prepared using a similar method to that used to prepare (41) (Method b). The yield of (44) was 55% after column chromatography as a light yellow oil:  $R_f$  0.75 (1:1 diethyl ether:petroleum (bp 40-60 °C)).

$^1\text{H}$  NMR (300 MHz,  $\text{CDCl}_3$ )  $\delta$ : 4.20 – 4.16 (m, 2H,  $\text{H}_1$ ,  $\text{H}_4$ ), 1.78 – 1.74 (m, 4H,  $\text{H}_{2\text{-exo}}$ ,  $\text{H}_{3\text{-exo}}$ ,  $\text{H}_{5\text{-exo}}$ ,  $\text{H}_{6\text{-exo}}$ ), 1.45 (s, 9H,  $\text{OC}(\underline{\text{CH}}_3)_3$ ), 1.34 (br d,  $J = 7.0$  Hz, 4H,  $\text{H}_{2\text{-endo}}$ ,  $\text{H}_{3\text{-endo}}$ ,  $\text{H}_{5\text{-endo}}$ ,  $\text{H}_{6\text{-endo}}$ ).

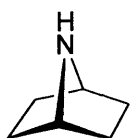
$^{13}\text{C}$  NMR (75 MHz,  $\text{CDCl}_3$ )  $\delta$ : 155.7 (C=O), 79.2 ( $\text{OC}(\underline{\text{CH}}_3)_3$ ), 56.1 ( $\text{C}_1$ ,  $\text{C}_4$ ), 29.6 ( $\text{C}_2$ ,  $\text{C}_3$ ,  $\text{C}_5$ ,  $\text{C}_6$ ), 28.3 ( $\text{OC}(\underline{\text{CH}}_3)_3$ ).

$^{15}\text{N}$  NMR (40 MHz,  $\text{CDCl}_3$ )  $\delta$ : -257.5.

MS  $m/z$ : 198 ( $MH^+$ ).  $C_{11}H_{20}NO_2$  [ $MH^+$ ] calculated 198.14940; observed 198.14960.

$\nu_{max}$ : 1697s, 1354s, 1317m, 1183w, 1144s, 1088m, 903m, 776w.

### Synthesis of 7-aza-bicyclo[2.2.1]heptane (**1b**)<sup>3</sup>



Amine (**1b**) was prepared using a similar method to that used to prepare (**2b**). To a stirred solution of (**44**) (0.83 g;  $4.19 \times 10^{-3}$  mol) in 8 ml ethyl acetate was added drop-wise 3M HCl (10 ml, at 0 °C) formed *in situ* from the reaction of ethanol (2.7 ml), ethyl acetate (7.2 ml) and acetyl chloride (2.7 ml). The mixture was allowed to warm to room temperature with continued stirring overnight. The reaction mixture was then evaporated under reduced pressure. The residue (**1b:HCl**) (0.552 g; 0.401 g, 99% as free amine) was dissolved in 5 ml distilled water and basified with 2M NaOH and extracted with  $CFCl_3$  (3 x 8 ml). The organic layers were combined, dried over anhydrous  $MgSO_4$ , concentrated and transferred to a 5 mm NMR tube with 0.5 ml of  $CDCl_3$ .

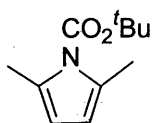
$^1H$  NMR (300 MHz,  $CDCl_3$ )  $\delta$ : 3.63 (br s, 2H,  $H_1$ ,  $H_4$ ), 1.56 (br d,  $J = 6.9$  Hz, 4H,  $H_{2-exo}$ ,  $H_{3-exo}$ ,  $H_{5-exo}$ ,  $H_{6-exo}$ ), 1.35 (br d,  $J = 6.9$  Hz, 4H,  $H_{2-endo}$ ,  $H_{3-endo}$ ,  $H_{5-endo}$ ,  $H_{6-endo}$ ).

$^{13}C$  NMR (75 MHz,  $CDCl_3$ )  $\delta$ : 56.1 ( $C_1$ ,  $C_4$ ), 30.2 ( $C_2$ ,  $C_3$ ,  $C_5$ ,  $C_6$ ).

$^{15}N$  NMR (40 MHz,  $CDCl_3$ )  $\delta$ :  $-304.4 \pm 0.5$ .

MS  $m/z$ : 98 ( $MH^+$ ).  $C_6H_{12}N$  [ $MH^+$ ] calculated 98.09697; observed 98.09703.

### Synthesis of *N*-(*tert*-butoxycarbonyl)-2,5-dimethylpyrrole (**46**)<sup>65</sup>

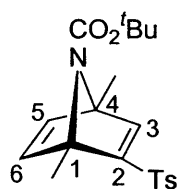


Based on the procedure of Hodgson,<sup>66</sup> DMAP (0.501 g;  $4.1 \times 10^{-3}$  mol) was added to a stirred solution of 2,5-dimethylpyrrole (0.696 g;  $7.32 \times 10^{-3}$  mol) and  $Boc_2O$  (1.82 g;  $8.34 \times 10^{-3}$  mol) in anhydrous acetonitrile (15 ml) and the reaction was stirred at 25 °C under argon atmosphere for 24 h. The solvent was removed at reduced pressure. Column chromatography on silica, eluting with 2% diethyl ether:petrol (bp 40-60 °C) gave the pyrrole derivative (**46**) as a colourless oil (0.81 g, 57%):  $R_f$  57 (1:1 diethyl ether:petrol (bp 40-60 °C)).

$^1H$  NMR (300 MHz,  $CDCl_3$ )  $\delta$ : 5.67 (s, 2H,  $H_3$ ,  $H_4$ ), 2.28 (s, 6H, 2 x  $CH_3$ ), 1.49 (s, 9H,  $OC(CH_3)_3$ ).

$^{13}C$  NMR (75 MHz,  $CDCl_3$ )  $\delta$ : 149.5 ( $C=O$ ), 130.1 ( $C_2$ ,  $C_5$ ), 109.2 ( $C_3$ ,  $C_4$ ), 82.0 ( $OC(CH_3)_3$ ), 27.0 ( $OC(CH_3)_3$ ), 15.5 (2 x  $CH_3$ ).

**Synthesis of 1,4-dimethyl-2-(toluene-4-sulfonyl)-7-azabicyclo[2.2.1]hepta-2,5-diene-7-carboxylic acid *tert*-butyl ester (47)**



Based on the procedure of Muchowski,<sup>53</sup> *N*-(*tert*-butoxycarbonyl)-2,5-dimethylpyrrole (**46**) (0.411 g;  $2.11 \times 10^{-3}$  mol) was added to a stirred solution of *p*-tolyl ethynyl sulfone (**25**) (0.190 g;  $1.06 \times 10^{-3}$  mol) in 5 ml toluene and heated in an inert atmosphere (nitrogen) at 80-85 °C. After 48 h the black oil was cooled to room temperature, the solvent was removed, then the crude material was purified on silica gel. Elution with 2:98 diethyl ether:petrol (bp 40-60 °C) removed the excess of pyrrole derivative (**46**) which was recycled. The product (**47**) (0.282 g, 72%) was eluted with 1:4 diethyl ether:petrol (bp 40-60 °C) as a yellow solid:  $R_f$  0.36 (1:1 diethyl ether:petrol (bp 40-60 °C)), mp 98-99 °C.

$^1\text{H}$  NMR (300 MHz,  $\text{CDCl}_3$ )  $\delta$ : 7.72 (d,  $J = 8.1$  Hz, 2H, 2 x aryl  $\underline{\text{CH}}$ ), 7.50 (s, 1H,  $\text{H}_3$ ), 7.33 (d,  $J = 8.1$  Hz, 2H, 2 x aryl  $\underline{\text{CH}}$ ), 6.71 (d,  $J_{5,6} = 5.3$  Hz, 1H,  $\text{H}_5$  or  $\text{H}_6$ ), 6.60 (d,  $J_{5,6} = 5.3$  Hz, 1H,  $\text{H}_5$  or  $\text{H}_6$ ), 2.44 (s, 3H, aryl  $\underline{\text{CH}_3}$ ), 1.97, 1.84 (s, 6H, 2 x  $\underline{\text{CH}_3}$ ), 1.33 (s, 9H,  $\text{OC}(\underline{\text{CH}_3})_3$ ).

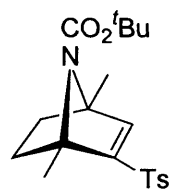
$^{13}\text{C}$  NMR (75 MHz,  $\text{CDCl}_3$ )  $\delta$ : 160.4 ( $\text{C}_2$ ), 159.3 ( $\text{C}_3$ ), 154.5 ( $\text{C}=\text{O}$ ), 149.0, 146.7 ( $\text{C}_5$ ,  $\text{C}_6$ ), 144.6, 136.3 (2 x aryl C), 129.8, 128.1 (4 x aryl  $\underline{\text{CH}}$ ), 81.4 ( $\text{OC}(\underline{\text{CH}_3})_3$ ), 76.8, 76.5 ( $\text{C}_1$ ,  $\text{C}_4$ ), 28.1 ( $\text{OC}(\underline{\text{CH}_3})_3$ ), 21.6 (aryl  $\underline{\text{CH}_3}$ ), 17.2, 16.1 (2 x  $\underline{\text{CH}_3}$ ).

MS  $m/z$ : 376 ( $\text{MH}^+$ ).  $\text{C}_{20}\text{H}_{26}\text{NO}_4\text{S}$  [ $\text{MH}^+$ ] calculated 376.15826; observed 376.15818.

$\nu_{\text{max}}$ : 1705s, 1597w, 1314s, 1252m, 1145s, 1085s, 813m, 730m, 664s.

Anal. Calcd for  $\text{C}_{20}\text{H}_{25}\text{NO}_4\text{S}$ : C, 64.03; H, 6.72; N, 3.73. Found: C, 63.98; H, 6.60; N, 3.66.

**Synthesis of 1,4-dimethyl-2-(toluene-4-sulfonyl)-7-azabicyclo[2.2.1]hept-2-ene-7-carboxylic acid *tert*-butyl ester (50)**



Compound (**47**) (0.85 g;  $2.27 \times 10^{-3}$  mol) was placed in a 50 ml reaction vessel and dissolved in anhydrous acetonitrile (10 ml) and 0.1 g of palladium/charcoal (Pd/C) catalyst was added to the solution. The reaction vessel was purged first with nitrogen and then carefully with hydrogen. Hydrogen gas was passed into the reaction flask by using a balloon and the reaction mixture was stirred at room temperature under hydrogen for 30 minutes. The catalyst was removed by filtration over Celite, and the solvent was evaporated on a rotary evaporator

to give 0.835 g (97%) of **(50)** as brown oil:  $R_f$  0.39 (1:1 diethyl ether:petrol (bp 40-60 °C)), mp 107-108 °C.

$^1\text{H}$  NMR (300 MHz,  $\text{CDCl}_3$ )  $\delta$ : 7.76 (d,  $J = 8.0$  Hz, 2H, 2 x aryl  $\underline{\text{CH}}$ ), 7.33 (d,  $J = 8.0$  Hz, 2H, 2 x aryl  $\underline{\text{CH}}$ ), 6.95 (s, 1H,  $\text{H}_3$ ), 2.43 (s, 3H, aryl  $\underline{\text{CH}_3}$ ), 1.81, 1.71 (s, 6H, 2 x  $\underline{\text{CH}_3}$ ), 1.89 – 1.37 (m, 4H,  $\text{H}_5$ ,  $\text{H}_6$ ), 1.30 (s, 9H,  $\text{OC}(\underline{\text{CH}_3})_3$ ).

$^{13}\text{C}$  NMR (75 MHz,  $\text{CDCl}_3$ )  $\delta$ : 155.1 (C=O), 155.0 ( $\text{C}_3$ ), 149.2 ( $\text{C}_2$ ), 144.5, 137.4 (2 x aryl C), 129.8, 128.0 (4 x aryl  $\underline{\text{CH}}$ ), 80.5 ( $\text{OC}(\underline{\text{CH}_3})_3$ ), 71.5, 70.4 ( $\text{C}_1$ ,  $\text{C}_4$ ), 34.6, 33.4 ( $\text{C}_5$ ,  $\text{C}_6$ ), 28.1 ( $\text{OC}(\underline{\text{CH}_3})_3$ ), 21.6 (aryl  $\underline{\text{CH}_3}$ ), 19.3, 18.0 (2 x  $\underline{\text{CH}_3}$ ).

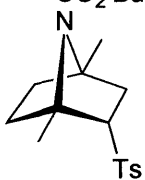
MS  $m/z$ : 378 ( $\text{MH}^+$ ).  $\text{C}_{20}\text{H}_{28}\text{NO}_4\text{S}$  [ $\text{MH}^+$ ] calculated 378.17391; observed 378.17397.

$\nu_{\text{max}}$ : 1698s, 1597w, 1336s, 1289s, 1252m, 1143s, 1086s, 815m, 720m, 687s, 657s.

### Synthesis of 1,4-dimethyl-2-(toluene-4-sulfonyl)-7-azabicyclo[2.2.1]heptane-7-carboxylic acid *tert*-butyl ester (**49**)

Compound **(50)** (0.3 g;  $7.95 \times 10^{-4}$  mol) was placed in a 25 ml reaction vessel and dissolved in 10 ml of methanol.  $\text{NaBH}_4$  (0.216 g;  $5.7 \times 10^{-3}$  mol) was added to the reaction mixture at room temperature and stirred for 1 hr. The mixture was extracted with dichloromethane (3 x 10 ml), and the dichloromethane solution was washed three times with 10 ml portions of water, dried over anhydrous  $\text{Na}_2\text{SO}_4$ , filtered, and concentrated under vacuum. The crude residue gave a mixture of *endo*-**(49)** and *exo*-**(49)** as a pale yellow oil (~ 7:3 respectively). The mixture was chromatographed on silica gel. Elution with 15:75 diethyl ether:petroleum (bp 40-60 °C) gave first *exo*-**(49)** (0.068 g, 23%) as a pale yellow oil:  $R_f$  0.54 (1:1 diethyl ether:petroleum (bp 40-60 °C)). *endo*-**(49)** was then eluted with 1:4 diethyl ether:petroleum (bp 40-60 °C) to gave 0.19 g (64%) as a pale yellow oil:  $R_f$  0.28 (1:1 diethyl ether:petroleum (bp 40-60 °C)).

#### *endo*-**(49)** isomer

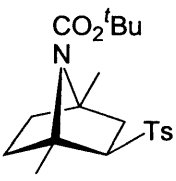
  $^1\text{H}$  NMR (300 MHz,  $\text{CDCl}_3$ )  $\delta$ : 7.76 (d,  $J = 8.2$  Hz, 2H, 2 x aryl  $\underline{\text{CH}}$ ), 7.34 (d,  $J = 8.2$  Hz, 2H, 2 x aryl  $\underline{\text{CH}}$ ), 3.45 (ddd,  $J_{2,3\text{-exo}} = 11.5$  Hz,  $J_{2,3\text{-endo}} = 5.2$  Hz,  $J_{2,6\text{-exo}} = 2.1$  Hz, 1H,  $\text{H}_2$ ), 2.63 – 2.55 (m, 1H,  $\text{H}_{5\text{-endo}}$ , or  $\text{H}_{6\text{-endo}}$ ), 2.44 (s, 3H, aryl  $\underline{\text{CH}_3}$ ), 2.12 (dd,  $J_{3\text{-exo},3\text{-endo}} = 12.5$  Hz,  $J_{2,3\text{-exo}} = 5.2$  Hz, 1H,  $\text{H}_{3\text{-exo}}$ ), 1.84 – 1.63 (m, 4H,  $\text{H}_{3\text{-endo}}$ ,  $\text{H}_{5\text{-exo}}$ ,  $\text{H}_{6\text{-exo}}$ , ( $\text{H}_{5\text{-endo}}$ , or  $\text{H}_{6\text{-endo}}$ )), 1.73, 1.55 (s, 6H, 2 x  $\underline{\text{CH}_3}$ ), 1.42 (s, 9H,  $\text{OC}(\underline{\text{CH}_3})_3$ ).

$^{13}\text{C}$  NMR (75 MHz,  $\text{CDCl}_3$ )  $\delta$ : 155.6 (C=O), 144.6, 138.0 (2 x aryl C), 129.9, 128.0 (4 x aryl  $\underline{\text{CH}}$ ), 80.3 ( $\text{OC}(\underline{\text{CH}_3})_3$ ), 70.0, 67.1 ( $\text{C}_1$ ,  $\text{C}_4$ ), 68.7 ( $\text{C}_2$ ), 41.0 ( $\text{C}_3$ ), 36.3, 32.6 ( $\text{C}_5$ ,  $\text{C}_6$ ), 28.4, ( $\text{OC}(\underline{\text{CH}_3})_3$ ), 22.0, 21.9 (2 x  $\underline{\text{CH}_3}$ ), 21.6 (aryl  $\underline{\text{CH}_3}$ ).

MS  $m/z$ : 380 ( $\text{MH}^+$ ).  $\text{C}_{20}\text{H}_{30}\text{NO}_4\text{S}$  [ $\text{MH}^+$ ] calculated 380.18956; observed 380.18949.

$\nu_{\text{max}}$ : 1694s, 1597w, 1366m, 1301s, 1138s, 1084s, 1054m, 815m, 727m, 666s.

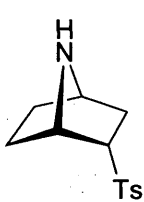
### *exo*-(49) isomer

  $^1\text{H}$  NMR (300 MHz,  $\text{CDCl}_3$ )  $\delta$ : 7.73 (d,  $J = 8.3$  Hz, 2H, 2 x aryl  $\underline{\text{CH}}$ ), 7.32 (d,  $J = 8.3$  Hz, 2H, 2 x aryl  $\underline{\text{CH}}$ ), 3.28 (dd,  $J_{2,3\text{-endo}} = 12.5$  Hz,  $J_{2,3\text{-exo}} = 5.3$  Hz, 1H,  $\text{H}_2$ ), 2.43 (s, 3H, aryl  $\underline{\text{CH}_3}$ ), 1.91 (br dd,  $J = 6.6$  Hz,  $J = 2.2$  Hz, 1H,  $\text{H}_{3\text{-exo}}$ ), 1.72 – 1.37 (m, 5H,  $\text{H}_{3\text{-endo}}$ ,  $\text{H}_5$ ,  $\text{H}_6$ ), 1.96, 1.62 (s, 6H, 2 x  $\underline{\text{CH}_3}$ ), 1.48 (s, 9H,  $\text{OC}(\underline{\text{CH}_3})_3$ ).

$^{13}\text{C}$  NMR (75 MHz,  $\text{CDCl}_3$ )  $\delta$ : 154.2 (C=O), 144.3, 136.4 (2 x aryl C), 129.7, 128.6 (4 x aryl  $\underline{\text{CH}}$ ), 79.8 ( $\text{OC}(\underline{\text{CH}_3})_3$ ), 69.7 ( $\text{C}_2$ ), 68.4, 64.8 ( $\text{C}_1$ ,  $\text{C}_4$ ), 41.1 ( $\text{C}_3$ ), 40.5, 36.1 ( $\text{C}_5$ ,  $\text{C}_6$ ), 28.5, ( $\text{OC}(\underline{\text{CH}_3})_3$ ), 21.6 (aryl  $\underline{\text{CH}_3}$ ), 21.1, 20.5 (2 x  $\text{CH}_3$ ).

MS  $m/z$ : 380 ( $\text{MH}^+$ ).  $\text{C}_{20}\text{H}_{30}\text{NO}_4\text{S}$  [ $\text{MH}^+$ ] calculated 380.18956; observed 380.18947.

### Synthesis of 2-(toluene-4-sulfonyl)-7-azabicyclo[2.2.1]heptane *endo*-(58)

 This amine *endo*-(58) was prepared using a similar method to that described for (2b). *Endo*-(43) (0.125 g,  $3.56 \times 10^{-4}$  mol) gave *endo*-(58) (0.088 g, 99%) as a brown solid after the normal work-up.

$^1\text{H}$  NMR (300 MHz,  $\text{CDCl}_3$ )  $\delta$ : 7.76 (d,  $J = 8.1$  Hz, 2H, 2 x aryl  $\underline{\text{CH}}$ ), 7.34 (d,  $J = 8.1$  Hz, 2H, 2 x aryl  $\underline{\text{CH}}$ ), 3.82 – 3.81 (m, 2H,  $\text{H}_1$ ,  $\text{H}_4$ ), 3.48 – 3.41 (m, 1H,  $\text{H}_2$ ), 2.56 – 2.48 (m, 1H,  $\text{H}_{5\text{-endo}}$ , or  $\text{H}_{6\text{-endo}}$ ), 2.45 (s, 3H, aryl  $\underline{\text{CH}_3}$ ), 1.96 (br, 1H,  $\underline{\text{NH}}$ ), 1.94 – 1.50 (m, 5H,  $\text{H}_{3\text{-exo}}$ ,  $\text{H}_{3\text{-endo}}$ ,  $\text{H}_{5\text{-exo}}$ ,  $\text{H}_{6\text{-exo}}$ , ( $\text{H}_{5\text{-endo}}$ , or  $\text{H}_{6\text{-endo}}$ )).

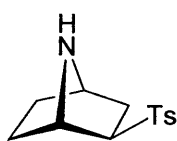
$^{13}\text{C}$  NMR (75 MHz,  $\text{CDCl}_3$ )  $\delta$ : 144.5, 137.8 (2 x aryl C), 130.0, 127.8 (4 x aryl  $\underline{\text{CH}}$ ), 66.4 ( $\text{C}_2$ ), 58.7, 57.8 ( $\text{C}_1$ ,  $\text{C}_4$ ), 32.8, 29.8, 25.3 ( $\text{C}_3$ ,  $\text{C}_5$ ,  $\text{C}_6$ ), 21.6 (aryl  $\underline{\text{CH}_3}$ ).

MS  $m/z$ : 252 ( $\text{MH}^+$ ).  $\text{C}_{13}\text{H}_{18}\text{NO}_2\text{S}$  [ $\text{MH}^+$ ] calculated 252.10583; observed 252.10588.

$\nu_{\text{max}}$ : 3290w, 1596w, 1279s, 1136s, 1083s, 911m, 810s, 719s, 662s.

Anal. Calcd for  $\text{C}_{13}\text{H}_{17}\text{NO}_2\text{S}$ : C, 62.12; H, 6.82; N, 5.57. Found: C, 62.05; H, 6.93; N, 5.51.

### Synthesis of 2-(toluene-4-sulfonyl)-7-azabicyclo[2.2.1]heptane *exo*-(58)

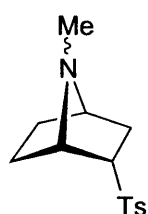


This amine *exo*-(58) was prepared using a similar method to that was described for *endo*-(58). *exo*-(43) (0.017 g,  $6.09 \times 10^{-5}$  mol) gave *exo*-(58) (0.018 g, 95%) as brown solid after the normal work-up.

$^1\text{H}$  NMR (300 MHz,  $\text{CDCl}_3$ )  $\delta$ : 7.77 (d,  $J = 8.1$  Hz, 2H, 2 x aryl  $\text{CH}$ ), 7.37 (d,  $J = 8.1$  Hz, 2H, 2 x aryl  $\text{CH}$ ), 3.95 (br d,  $J_{1,6\text{-exo}} = 3.9$  Hz, 1H,  $\text{H}_1$ ), 3.79 (br t,  $J = 4.1$  Hz, 1H,  $\text{H}_4$ ), 3.20 (dd,  $J_{2,3\text{-endo}} = 8.5$  Hz,  $J_{2,3\text{-exo}} = 5.2$  Hz, 1H,  $\text{H}_2$ ), 2.46 (s, 3H, aryl  $\text{CH}_3$ ), 2.28 (br s, 1H,  $\text{NH}$ ), 2.06 – 1.98 (m, 1H,  $\text{H}_{3\text{-exo}}$ ), 1.78 (dd,  $J_{3\text{-exo},3\text{-endo}} = 13.3$  Hz,  $J_{2,3\text{-endo}} = 8.5$  Hz, 1H,  $\text{H}_{3\text{-endo}}$ ), 1.71 – 1.69 (m, 2H,  $\text{H}_{5\text{-exo}}$ ,  $\text{H}_{6\text{-exo}}$ ), 1.27 – 1.15 (m, 2H,  $\text{H}_{5\text{-endo}}$ ,  $\text{H}_{6\text{-endo}}$ ).

$^{13}\text{C}$  NMR (75 MHz,  $\text{CDCl}_3$ )  $\delta$ : 144.6, 135.5 (2 x aryl C), 130.0, 128.4 (4 x aryl  $\text{CH}$ ), 66.8 ( $\text{C}_2$ ), 58.2 ( $\text{C}_1$ ), 56.0 ( $\text{C}_4$ ), 34.2 ( $\text{C}_3$ ), 29.0, 28.5 ( $\text{C}_5$ ,  $\text{C}_6$ ), 21.7 (aryl  $\text{CH}_3$ ).

### Synthesis of 7-methyl-2-(toluene-4-sulfonyl)-7-azabicyclo[2.2.1]heptane *endo*-(54)



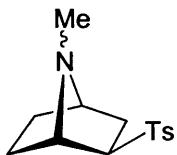
Based on the general methylation procedure of Borch and Hassid,<sup>68</sup> the secondary amine *endo*-(58) (0.023 g,  $9.16 \times 10^{-5}$  mol) was dissolved in 5 ml acetonitrile and the solution was added to a 25 ml flask charged with sodium cyanoborohydride ( $\text{NaBH}_3\text{CN}$ ) (0.013 g,  $2.01 \times 10^{-4}$  mol) and 40% formaldehyde solution (13 mL,  $4.58 \times 10^{-4}$  mol). The reaction mixture was stirred overnight then diethyl ether was added and the flask contents were washed with acid (0.6 M HCl; 3 x 5 ml). The aqueous acid layers were made basic (2M NaOH, 20 ml) and the basic aqueous layer then extracted with dichloromethane (3 x 30 ml). The combined organic phases were dried over anhydrous  $\text{Na}_2\text{SO}_4$  and evaporated under reduced pressure to give crude *endo*-(54) which was chromatographed (3:2 diethylether:petrol (bp 40-60 °C), saturated with  $\text{NH}_3$ ) yielding *endo*-(54) (0.019 g, 79%):  $R_f$  0.12 (diethyl ether, saturated with  $\text{NH}_3$ ).

$^1\text{H}$  NMR (300 MHz,  $\text{CDCl}_3$ )  $\delta$ : 7.76 (d,  $J = 8.1$  Hz, 2H, 2 x aryl  $\text{CH}$ ), 7.34 (d,  $J = 8.1$  Hz, 2H, 2 x aryl  $\text{CH}$ ), 3.63 – 3.55 (m, 1H,  $\text{H}_2$ ), 3.44 (br t,  $J = 4.3$  Hz, 1H,  $\text{H}_1$ ), 3.32 (br t,  $J = 4.6$  Hz, 1H,  $\text{H}_4$ ), 2.51 – 2.46 (m, 1H,  $\text{H}_{5\text{-endo}}$ , or  $\text{H}_{6\text{-endo}}$ ), 2.44 (s, 3H, aryl  $\text{CH}_3$ ), 2.25 (s, 3H,  $\text{NCH}_3$ ), 2.07 – 1.97 (m, 1H,  $\text{H}_{3\text{-exo}}$ ), 1.87 (dd,  $J_{3\text{-exo},3\text{-endo}} = 12.6$  Hz,  $J_{2,3\text{-endo}} = 5.6$  Hz, 1H,  $\text{H}_{3\text{-endo}}$ ), 1.80 – 1.72 (m, 1H,  $\text{H}_{6\text{-exo}}$ ), 1.62 – 1.54 (m, 1H, ( $\text{H}_{5\text{-endo}}$ , or  $\text{H}_{6\text{-endo}}$ )),  $\text{H}_{5\text{-exo}}$  overlapped with  $\text{H}_{3\text{-endo}}$ .

$^{13}\text{C}$  NMR (75 MHz,  $\text{CDCl}_3$ )  $\delta$ : 144.4, 138.1 (2 x aryl C), 129.9, 127.7 (4 x aryl  $\text{CH}$ ), 64.7 ( $\text{C}_2$ ), 63.6 ( $\text{C}_1$ ), 62.5 ( $\text{C}_4$ ), 34.2 ( $\text{NCH}_3$ ), 30.7 ( $\text{C}_3$ ), 28.1, 23.4 ( $\text{C}_5$ ,  $\text{C}_6$ ), 21.6 (aryl  $\text{CH}_3$ ).

MS  $m/z$ : 266 ( $MH^+$ ).  $C_{14}H_{20}NO_2S$  [ $MH^+$ ] calculated 266.12148; observed 266.12152.

### Synthesis of 7-methyl-2-(toluene-4-sulfonyl)-7-azabicyclo[2.2.1]heptane *exo*-(54)



A solution of *endo*-(58) (0.027 g,  $1.08 \times 10^{-4}$  mol) in 3 ml anhydrous THF under nitrogen was treated with methyl iodide ( $CH_3I$ ) (0.02 g,  $1.29 \times 10^{-4}$  mol) and the reaction mixture was stirred for 10 minutes at 0 °C. The reaction mixture was warmed to room temperature and stirred for 6 h under nitrogen. The reaction mixture was made basic with the addition of 2M NaOH and extracted with dichloromethane (3 x 5 ml). The combined extracts were washed with saturated  $NaHCO_3$ , dried over  $Na_2SO_4$  and concentrated *in vacuo*. Flash chromatography ( $SiO_2$ , 60% diethyl ether:petrol(bp 40-60 °C), saturated with  $NH_3$ ) afforded *exo*-(54) (0.019 g, 68%) as a white solid:  $R_f$  0.20 (diethyl ether, saturated with  $NH_3$ ), mp 58-59 °C.

$^1H$  NMR (300 MHz,  $CDCl_3$ )  $\delta$ : 7.75 (d,  $J = 8.1$  Hz, 2H, 2 x aryl  $\underline{CH}$ ), 7.32 (d,  $J = 8.1$  Hz, 2H, 2 x aryl  $\underline{CH}$ ), 3.71 (d,  $J_{1,6-exo} = 4.2$  Hz, 1H,  $H_1$ ), 3.31 (br t,  $J = 4.3$  Hz, 1H,  $H_4$ ), 3.04 (dd,  $J_{2,3-endo} = 9.1$  Hz,  $J_{2,3-exo} = 5.7$  Hz, 1H,  $H_2$ ), 2.44 (s, 3H, aryl  $\underline{CH_3}$ ), 2.17 (s, 3H,  $N\underline{CH_3}$ ), 2.15 – 2.10 (m, 1H,  $H_{3-exo}$ ), 1.98 – 1.77 (m, 2H,  $H_{5-exo}$ ,  $H_{6-exo}$ ), 1.55 (dd,  $J_{3-endo,3-exo} = 12.6$  Hz,  $J_{2,3-endo} = 9.1$  Hz, 1H,  $H_{3-endo}$ ), 1.33 – 1.23 (m, 2H,  $H_{5-endo}$ ,  $H_{6-endo}$ ).

$^{13}C$  NMR (75 MHz,  $CDCl_3$ )  $\delta$ : 144.2, 136.2 (2 x aryl C), 129.6, 128.7 (4 x aryl  $\underline{CH}$ ), 68.3 ( $C_2$ ), 62.6 ( $C_1$ ), 61.0 ( $C_4$ ), 34.2 ( $N\underline{CH_3}$ ) 33.8 ( $C_3$ ), 26.6, 25.3 ( $C_5$ ,  $C_6$ ), 21.6 (aryl  $\underline{CH_3}$ ).

MS  $m/z$ : 266 ( $MH^+$ ).  $C_{14}H_{20}NO_2S$  [ $MH^+$ ] calculated 266.12148; observed 266.12140.

$\nu_{max}$ : 2959m, 1598w, 1278s, 1129s, 1087s, 1019m, 880m, 810s, 732s, 695m.

### Synthesis of 1,4-dimethyl-2-(toluene-4-sulfonyl)-7-azabicyclo[2.2.1]heptane *endo*-(59)



This amine was prepared using a similar method to that used to prepare (2b). To a stirred solution of *endo*-(49) (0.02 g,  $5.27 \times 10^{-5}$  mol) in 2 ml ethyl acetate was added drop-wise 3M HCl (3 ml, at 0 °C) formed *in situ* from the reaction of ethanol (2.7 ml), ethyl acetate (7.2 ml) and acetyl chloride (2.7 ml). The mixture was allowed to warm to room temperature with continuance of the stirring overnight. The reaction mixture was then evaporated under reduced pressure. The residue was dissolved in 3 ml distilled water, basified with 2M NaOH and extracted with dichloromethane (3 x 3 ml). The organic layers were

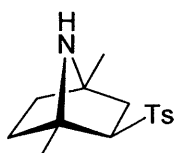
combined, dried over anhydrous  $\text{MgSO}_4$  and the solvent was removed *in vacuo* to give **endo-(59)** (0.013 g, 93%) as a brown solid.

$^1\text{H}$  NMR (300 MHz,  $\text{CDCl}_3$ )  $\delta$ : 7.76 (d,  $J = 8.2$  Hz, 2H, 2 x aryl  $\text{CH}$ ), 7.33 (d,  $J = 8.2$  Hz, 2H, 2 x aryl  $\text{CH}$ ), 3.26 (ddd,  $J_{2,3\text{-exo}} = 11.5$  Hz,  $J_{2,3\text{-endo}} = 5.3$  Hz,  $J_{2,6\text{-exo}} = 2.1$  Hz, 1H,  $\text{H}_2$ ), 2.68 (m, 1H,  $\text{H}_{5\text{-endo}}$ , or  $\text{H}_{6\text{-endo}}$ ), 2.44 (s, 3H, aryl  $\text{CH}_3$ ), 2.13 (dd,  $J_{3\text{-exo},3\text{-endo}} = 12.2$  Hz,  $J_{2,3\text{exo}} = 5.3$  Hz, 1H,  $\text{H}_{3\text{-exo}}$ ), 1.90 – 1.82 (m, 2H,  $\text{H}_{5\text{-exo}}$ ,  $\text{H}_{6\text{-exo}}$ ), 1.73 – 1.53 (m, 2H,  $\text{H}_{3\text{-endo}}$ , ( $\text{H}_{5\text{-endo}}$ , or  $\text{H}_{6\text{-endo}}$ )), 1.47, 1.32 (s, 6H, 2 x  $\text{CH}_3$ ).

$^{13}\text{C}$  NMR (75 MHz,  $\text{CDCl}_3$ )  $\delta$ : 143.4, 137.3 (2 x aryl C), 128.9, 126.9 (4 x aryl  $\text{CH}$ ), 70.3 ( $\text{C}_2$ ), 67.0, 62.9 ( $\text{C}_1$ ,  $\text{C}_4$ ), 40.7 ( $\text{C}_3$ ), 36.5, 32.5 ( $\text{C}_5$ ,  $\text{C}_6$ ), 20.6 (aryl  $\text{CH}_3$ ), 20.5, 20.1 (2 x  $\text{CH}_3$ ).

MS  $m/z$ : 280 ( $\text{MH}^+$ ).  $\text{C}_{15}\text{H}_{22}\text{NO}_2\text{S}$  [ $\text{MH}^+$ ] calculated 280.13713; observed 280.13716.

#### Synthesis of 1,4-dimethyl-2-(toluene-4-sulfonyl)-7-azabicyclo[2.2.1]heptane *exo*-(59)



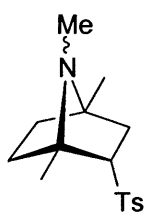
This amine **exo-(59)** was prepared using a similar method to that was described for **endo-(59)**. **exo-(49)** (0.05 g,  $1.32 \times 10^{-4}$  mol) gave **exo-(59)** (0.034 g, 94%) as brown solid after the normal work-up.

$^1\text{H}$  NMR (300 MHz,  $\text{CDCl}_3$ )  $\delta$ : 7.72 (d,  $J = 8.2$  Hz, 2H, 2 x aryl  $\text{CH}$ ), 7.34 (d,  $J = 8.2$  Hz, 2H, 2 x aryl  $\text{CH}$ ), 3.41 (dd,  $J_{2,3\text{-endo}} = 8.3$  Hz,  $J_{2,3\text{-exo}} = 6.1$  Hz, 1H,  $\text{H}_2$ ), 2.44 (s, 3H, aryl  $\text{CH}_3$ ), 2.23 (br s, 1H,  $\text{NH}$ ), 1.80 – 1.35 (m, 6H,  $\text{H}_3$ ,  $\text{H}_5$ ,  $\text{H}_6$ ), 1.71, 1.38 (s, 6H, 2 x  $\text{CH}_3$ ).

$^{13}\text{C}$  NMR (75 MHz,  $\text{CDCl}_3$ )  $\delta$ : 144.4, 136.6 (2 x aryl C), 129.8, 128.2 (4 x aryl  $\text{CH}$ ), 69.9 ( $\text{C}_2$ ), 67.5, 62.9 ( $\text{C}_1$ ,  $\text{C}_4$ ), 43.8, 40.0, 36.3 ( $\text{C}_3$ ,  $\text{C}_5$ ,  $\text{C}_6$ ), 21.6 (aryl  $\text{CH}_3$ ), 20.6, 19.4 (2 x  $\text{CH}_3$ ).

MS  $m/z$ : 280 ( $\text{MH}^+$ ).  $\text{C}_{15}\text{H}_{22}\text{NO}_2\text{S}$  [ $\text{MH}^+$ ] calculated 280.13713; observed 280.13721.

#### Synthesis of 1,4,7-trimethyl-2-(toluene-4-sulfonyl)-7-azabicyclo[2.2.1]heptane *endo*-(55)



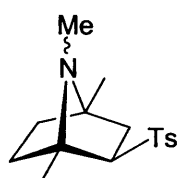
This amine **endo-(55)** was prepared using a similar method to that was described for **exo-(54)**. **Endo-(59)** (0.016 g,  $5.73 \times 10^{-5}$  mol) gave **endo-(55)** (0.012 g, 71%) as a brown solid:  $R_f$  0.15 (diethyl ether, saturated with  $\text{NH}_3$ ).

$^1\text{H}$  NMR (300 MHz,  $\text{CDCl}_3$ )  $\delta$ : 7.75 (d,  $J = 8.1$  Hz, 2H, 2 x aryl  $\text{CH}$ ), 7.33 (d,  $J = 8.1$  Hz, 2H, 2 x aryl  $\text{CH}$ ), 3.26 (ddd,  $J_{2,3\text{-exo}} = 10.9$  Hz,  $J_{2,3\text{-endo}} = 4.7$  Hz,  $J_{2,6\text{-exo}} = 1.8$  Hz, 1H,  $\text{H}_2$ ), 2.63 – 2.56 (m, 1H,  $\text{H}_{5\text{-endo}}$ , or  $\text{H}_{6\text{-endo}}$ ), 2.44 (s, 3H, aryl  $\text{CH}_3$ ), 2.08 (s, 3H,  $\text{NCH}_3$ ), 2.05 (dd,  $J_{3\text{-exo},3\text{-endo}} = 12.5$  Hz,  $J_{2,3\text{exo}} = 5.2$  Hz, 1H,  $\text{H}_{3\text{-exo}}$ ), 1.81 – 1.48 (m, 4H,  $\text{H}_{3\text{-endo}}$ ,  $\text{H}_{5\text{-exo}}$ ,  $\text{H}_{6\text{-exo}}$ , ( $\text{H}_{5\text{-endo}}$ , or  $\text{H}_{6\text{-endo}}$ )), 1.42, 1.21 (s, 6H, 2 x  $\text{CH}_3$ ).

$^{13}\text{C}$  NMR (75 MHz,  $\text{CDCl}_3$ )  $\delta$ : 144.3, 138.7 (2 x aryl C), 129.9, 127.8 (4 x aryl  $\text{CH}$ ), 68.9 ( $\text{C}_2$ ), 70.1, 65.9 ( $\text{C}_1$ ,  $\text{C}_4$ ), 38.3, 35.1, 30.8 ( $\text{C}_3$ ,  $\text{C}_5$ ,  $\text{C}_6$ ), 27.9 ( $\text{NCH}_3$ ), 21.6 (aryl  $\text{CH}_3$ ), 19.6, 19.2 (2 x  $\text{CH}_3$ ).

MS  $m/z$ : 294 ( $\text{MH}^+$ ).  $\text{C}_{16}\text{H}_{24}\text{NO}_2\text{S}$  [ $\text{MH}^+$ ] calculated 294.15278; observed 294.15270.

### Synthesis of 1,4,7-trimethyl-2-(toluene-4-sulfonyl)-7-azabicyclo[2.2.1]heptane *exo*-(55)



This amine *exo*-(55) was prepared using a similar method to that described for *endo*-(55). *Exo*-(59) (0.024 g,  $8.6 \times 10^{-3}$  mol) gave *exo*-(55) (0.015 g, 60%) as a brown solid after the normal work-up:  $R_f$  0.20 (diethyl ether, saturated with  $\text{NH}_3$ ), mp 101-102 °C.

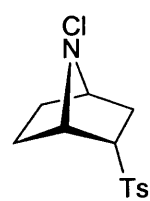
$^1\text{H}$  NMR (300 MHz,  $\text{CDCl}_3$ )  $\delta$ : 7.73 (d,  $J = 8.1$  Hz, 2H, 2 x aryl  $\text{CH}$ ), 7.32 (d,  $J = 8.1$  Hz, 2H, 2 x aryl  $\text{CH}$ ), 3.22 (br t, 1H,  $\text{H}_2$ ), 2.43 (s, 3H, aryl  $\text{CH}_3$ ), 2.19 (s, 3H,  $\text{NCH}_3$ ), 1.80 – 1.33 (m, 6H,  $\text{H}_3$ ,  $\text{H}_5$ ,  $\text{H}_6$ ), 1.66, 1.24 (s, 6H, 2 x  $\text{CH}_3$ ).

$^{13}\text{C}$  NMR (75 MHz,  $\text{CDCl}_3$ )  $\delta$ : 144.0, 137.2 (2 x aryl C), 129.6, 128.3 (4 x aryl  $\text{CH}$ ), 69.9 ( $\text{C}_2$ ), 70.1, 65.1 ( $\text{C}_1$ ,  $\text{C}_4$ ), 40.5, 38.4, 33.6 ( $\text{C}_3$ ,  $\text{C}_5$ ,  $\text{C}_6$ ), 29.1 ( $\text{NCH}_3$ ), 21.6 (aryl  $\text{CH}_3$ ), 18.8, 17.2 (2 x  $\text{CH}_3$ ).

MS  $m/z$ : 294 ( $\text{MH}^+$ ).  $\text{C}_{16}\text{H}_{24}\text{NO}_2\text{S}$  [ $\text{MH}^+$ ] calculated 294.15278; observed 294.15285.

$\nu_{\text{max}}$ : 1598w, 1450w, 1378m, 1316m, 1278s, 1142s, 1085s, 1046w, 821m, 746m, 674s.

### Synthesis of 7-chloro-2-(toluene-4-sulfonyl)-7-azabicyclo[2.2.1]heptane *endo*-(60)



A solution of the secondary amine *endo*-(58) (0.032 g,  $1.27 \times 10^{-4}$  mol) in 3 ml dichloromethane was treated with 5% aqueous sodium hypochlorite ( $\text{NaClO}$ ) (4 ml) and stirred for 30 minutes at room temperature. The dichloromethane layer was separated and the aqueous layer extracted with dichloromethane (3 x 5 ml). The combined organic solutions were dried over anhydrous

MgSO<sub>4</sub> and the solvent was removed under reduced pressure to give a brown solid of **endo-(60)** (0.035 g, 97%).

**endo-tosyl** (two invertomers signals at room temperature).

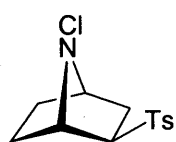
Duplicated signals were observed due to two invertomers at room temperature, the signals corresponding to the minor invertomer where the *N*-Cl is *anti* to the tosyl group are shown in italics.

<sup>1</sup>H NMR (300 MHz, CDCl<sub>3</sub>) δ: 7.72, 7.66 (d, *J* = 8.2 Hz, 4H, 4 x aryl CH), 7.30 (d, *J* = 8.2 Hz, 2H, 2 x aryl CH), 4.09 – 3.96 (m, 1H, H<sub>2</sub>), 3.78 (br t, *J* = 4.2 Hz, 1H, H<sub>1</sub>), 3.70 – 3.65 (m, 3H, H<sub>4</sub>, H<sub>1</sub>, H<sub>4</sub>), 3.51 – 3.44 (m, 1H, H<sub>2</sub>), 2.61 – 2.45 (m, 2H, (H<sub>5-endo</sub> or H<sub>6-endo</sub>), (H<sub>5-endo</sub> or H<sub>6-endo</sub>), 2.39, 2.38 (s, 6H, 2 x aryl CH<sub>3</sub>), 2.35 – 2.25 (m, 1H, H<sub>3-exo</sub>), 2.18 – 2.08 (m, 2H, H<sub>5-exo</sub>, H<sub>6-exo</sub>), 2.02 (dd, *J*<sub>3-endo,3-exo</sub> = 13.0 Hz, *J*<sub>2,3-endo</sub> = 5.3 Hz, 1H, H<sub>3-endo</sub>), 1.92 – 1.58 (m, 6H, H<sub>3-endo</sub>, H<sub>3-exo</sub>, (H<sub>5-endo</sub>, or H<sub>6-endo</sub>), H<sub>5-exo</sub>, H<sub>6-exo</sub>, (H<sub>5-endo</sub>, or H<sub>6-endo</sub>)).

<sup>13</sup>C NMR (75 MHz, CDCl<sub>3</sub>) δ: 144.0, 143.8, 136.9, 135.7 (2 x aryl C), 129.1, (126.8, 126.7), (4 x aryl CH), 68.0 (C<sub>2</sub>), 63.7, 60.8 (C<sub>1</sub>, C<sub>4</sub>), 29.9, 28.8 (C<sub>3</sub>), 27.0, 25.8, 21.5, 21.3 (C<sub>5</sub>, C<sub>6</sub>), 20.6 (aryl CH<sub>3</sub>).

MS <sup>m/z</sup>: 286 (MH<sup>+</sup>). C<sub>13</sub>H<sub>17</sub>NO<sub>2</sub>ClS [MH<sup>+</sup>] calculated 286.06685; observed 286.06690.

### Synthesis of 7-chloro-2-(toluene-4-sulfonyl)-7-azabicyclo[2.2.1]heptane *exo*-(60)



This amine was prepared using a similar method to that was described for **endo-(60)**. **Exo-(58)** (0.014 g, 5.57 x 10<sup>-5</sup> mol) gave **exo-(60)** (0.015 g, 94%) as a brown solid after the normal work-up, mp 110-111 °C.

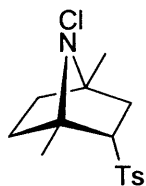
<sup>1</sup>H NMR (300 MHz, CDCl<sub>3</sub>) δ: 7.70 (d, *J* = 8.3 Hz, 2H, 2 x aryl CH), 7.29 (d, *J* = 8.3 Hz, 2H, 2 x aryl CH), 3.98 (d, *J*<sub>1,6-exo</sub> = 4.7 Hz, 1H, H<sub>1</sub>), 3.62 (br t, *J* = 4.6 Hz, 1H, H<sub>4</sub>), 3.10 (dd, *J*<sub>2,3-endo</sub> = 10.4 Hz, *J*<sub>2,3-exo</sub> = 5.5 Hz, 1H, H<sub>2</sub>), 2.39 (s, 3H, aryl CH<sub>3</sub>), 2.29 – 2.15 (m, 1H, H<sub>6-exo</sub>), 2.15 – 2.04 (m, 2H, H<sub>3-exo</sub>, H<sub>5-exo</sub>), 1.67 (dd, *J*<sub>3-exo,3-endo</sub> = 12.8 Hz, *J*<sub>2,3-endo</sub> = 10.4 Hz, 1H, H<sub>3-endo</sub>), 1.47 – 1.36 (m, 2H, H<sub>5-endo</sub>, H<sub>6-endo</sub>).

<sup>13</sup>C NMR (75 MHz, CDCl<sub>3</sub>) δ: 143.8, 133.9 (2 x aryl C), 128.8, 128.0 (4 x aryl CH), 67.2 (C<sub>1</sub>), 66.0 (C<sub>4</sub>), 64.5 (C<sub>2</sub>), 29.7 (C<sub>3</sub>), 26.9, 25.8 (C<sub>5</sub>, C<sub>6</sub>), 20.7 (aryl CH<sub>3</sub>).

MS <sup>m/z</sup>: 286 (MH<sup>+</sup>). C<sub>13</sub>H<sub>17</sub>NO<sub>2</sub>ClS [MH<sup>+</sup>] calculated 286.06685; observed 286.06684.

$\nu_{\max}$ : 1597w, 1451w, 1301m, 1261s, 1131s, 1084s, 1087s, 1018s, 886w, 799s, 723s, 657m.

**Synthesis of 7-chloro-1,4-dimethyl-2-(toluene-4-sulfonyl)-7-azabicyclo[2.2.1]heptane *endo*-(61)**



This amine *endo*-(61) was prepared using a similar method to that was described for *endo*-(60). *Endo*-(59) (0.017 g,  $6.09 \times 10^{-5}$  mol) gave *endo*-(61) (0.018 g, 95%) as brown solid after the normal work-up.

Duplicated signals were observed due to two invertomers at room temperature, the signals corresponding to the minor invertomer where the *N*-Cl is *anti* to the tosyl group are shown in italics.

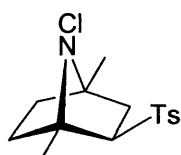
$^1\text{H}$  NMR (300 MHz,  $\text{CDCl}_3$ )  $\delta$ : 7.77 (d,  $J = 8.2$  Hz, 2H, 2 x aryl  $\underline{\text{CH}}$ ), 7.35 (d,  $J = 8.2$  Hz, 2H, 2 x aryl  $\underline{\text{CH}}$ ), 3.60 (ddd,  $J_{2,3\text{-exo}} = 11.4$  Hz,  $J_{2,3\text{-endo}} = 5.3$  Hz,  $J_{2,6\text{-exo}} = 2.2$  Hz, 1H,  $\text{H}_2$ ), 3.25 (ddd,  $J_{2,3\text{-exo}} = 11.3$  Hz,  $J_{2,3\text{-endo}} = 5.6$  Hz,  $J_{2,6\text{-exo}} = 1.8$  Hz, 1H,  $\text{H}_2$ ), 2.77 – 2.66 (m, 1H,  $\text{H}_{5\text{-endo}}$ , or  $\text{H}_{6\text{-endo}}$ ), 2.45 (s, 3H, aryl  $\underline{\text{CH}_3}$ ), 2.18 (dd,  $J_{3\text{-exo},3\text{-endo}} = 13.0$  Hz,  $J_{2,3\text{-endo}} = 5.3$  Hz, 1H,  $\text{H}_{3\text{-endo}}$ ), 2.10 – 1.87 (m, 3H,  $\text{H}_{3\text{-exo}}$ ,  $\text{H}_{5\text{-exo}}$ ,  $\text{H}_{6\text{-exo}}$ ), 1.69 – 1.61 (m, 1H, ( $\text{H}_{5\text{-endo}}$ , or  $\text{H}_{6\text{-endo}}$ )), 1.51, *1.48*, *1.33*, 1.31 (s, 12H, 4 x  $\underline{\text{CH}_3}$ ).

$^{13}\text{C}$  NMR (75 MHz,  $\text{CDCl}_3$ )  $\delta$ : (143.9, 143.6), 137.3 (2 x aryl C), 129.0, (*127.1*, 126.9), (4 x aryl  $\underline{\text{CH}}$ ), 74.8, 74.1, *71.4*, 70.8 ( $\text{C}_1$ ,  $\text{C}_4$ ), 68.3, *64.6* ( $\text{C}_2$ ), 37.6, *35.5*, *34.0*, 31.5, 28.8, 27.4 ( $\text{C}_3$ ,  $\text{C}_5$ ,  $\text{C}_6$ ), 20.6 (aryl  $\underline{\text{CH}_3}$ ), 19.1, 18.6 (2 x  $\underline{\text{CH}_3}$ ).

MS  $m/z$ : 314 ( $\text{MH}^+$ ).  $\text{C}_{15}\text{H}_{21}\text{NO}_2\text{ClS}$  [ $\text{MH}^+$ ] calculated 314.09815; observed 314.09819.

$\nu_{\text{max}}$ : 1597w, 1447w, 1377m, 1303s, 1276s, 1143s, 1085s, 1018m, 811s, 704s, 662s.

**Synthesis of 7-chloro-1,4-dimethyl-2-(toluene-4-sulfonyl)-7-azabicyclo[2.2.1]heptane *exo*-(61)**



This amine *exo*-(61) was prepared using a similar method to that was described for *endo*-(60). *Exo*-(59) (0.017 g,  $6.09 \times 10^{-5}$  mol) gave *exo*-(61) (0.018 g, 95%) as brown solid after the normal work-up.

$^1\text{H}$  NMR (300 MHz,  $\text{CDCl}_3$ )  $\delta$ : 7.67 (d,  $J = 8.2$  Hz, 2H, 2 x aryl  $\underline{\text{CH}}$ ), 7.27 (d,  $J = 8.2$  Hz, 2H, 2 x aryl  $\underline{\text{CH}}$ ), 3.21 (dd,  $J_{2,3\text{-endo}} = 10.1$  Hz,  $J_{2,3\text{-exo}} = 6.8$  Hz, 1H,  $\text{H}_2$ ), 2.37 (s, 3H, aryl  $\underline{\text{CH}_3}$ ), 1.99 – 1.38 (m, 6H,  $\text{H}_3$ ,  $\text{H}_5$ ,  $\text{H}_6$ ), 1.67, 1.28 (s, 6H, 2 x  $\underline{\text{CH}_3}$ ).

$^{13}\text{C}$  NMR (75 MHz,  $\text{CDCl}_3$ )  $\delta$ : 143.5, 135.0 (2 x aryl C), 128.8, 127.6 (4 x aryl  $\underline{\text{CH}}$ ), 74.0, 70.1 ( $\text{C}_1$ ,  $\text{C}_4$ ), 64.8 ( $\text{C}_2$ ), 37.1, 36.1, 33.1 ( $\text{C}_3$ ,  $\text{C}_5$ ,  $\text{C}_6$ ), 20.6 (aryl  $\underline{\text{CH}_3}$ ), 18.0, 16.3 (2 x  $\underline{\text{CH}_3}$ ).

MS  $m/z$ : 314 ( $MH^+$ ).  $C_{15}H_{21}NO_2ClS$  [ $MH^+$ ] calculated 314.09815; observed 314.09823.

$\nu_{max}$ : 1597m, 1450m, 1379m, 1321m, 1279s, 1137s, 1084s, 1018m, 810s, 737s, 705s, 667s.

### Synthesis of 1-(2-bromo-ethynylsulfonyl)-4-methyl-benzene (**62**)<sup>70</sup>

$Br-C\equiv C-SO_2C_6H_4CH_3$  Following the procedure of Trudell,<sup>70</sup> *p*-tolyl-2-(trimethylsilyl)ethynyl sulfone (**25**) (10.55 g; 0.042 mol) was placed in 50 ml three-necked round-bottomed flask in 50 ml acetone. To the stirred solution of (**25**) was added silver nitrate (0.71 g;  $4.18 \times 10^{-3}$  mol) followed by the addition of *N*-bromosuccinimide (NBS) (8.2 g;  $4.6 \times 10^{-2}$  mol) in one portion. The mixture was stirred at 25 °C for 30 min. The resulting precipitate was filtered and washed with 5 ml chloroform. The solvent was removed under reduced pressure and the crude product was subjected to column chromatography (1:5 ethyl acetate:hexane) to give (**62**) (7.84 g, 73%,  $R_f$ : 0.23) as a light yellow solid.

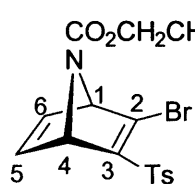
$^1H$  NMR (300 MHz,  $CDCl_3$ )  $\delta$ : 7.87 (d,  $J = 8.3$  Hz, 2H, aryl  $\underline{CH}$ ), 7.37 (d,  $J = 8.3$  Hz, 2H, aryl  $\underline{CH}$ ), 2.45 (s, 3H, aryl  $\underline{CH}_3$ ).

$^{13}C$  NMR (75 MHz,  $CDCl_3$ ):  $\delta$  149.9 (aryl C), 138.0 (aryl C), 130.1 (2 x aryl CH), 127.6 (2 x aryl CH), 78.0 (C-Br), 61.3 (C-S), 21.7 (aryl- $\underline{CH}_3$ ).

Literature data:

$^1H$  NMR (300 MHz,  $CDCl_3$ )  $\delta$ : 7.86 (d,  $J = 8.4$  Hz, 2H, aryl  $\underline{CH}$ ), 7.36 (d,  $J = 8.4$  Hz, 2H, aryl  $\underline{CH}$ ), 2.45 (s, 3H, aryl  $\underline{CH}_3$ ).<sup>70</sup>

### Synthesis of 2-bromo-3-(toluene-4-sulfonyl)-7-azabicyclo[2.2.1]hepta-5,6-diene-7-carboxylic acid ethyl ester (**63**)



Following the procedure of Trudell,<sup>70</sup> a stirred solution of 2-bromoethynyl *p*-tolyl sulfone (**62**) (0.604 g;  $2.33 \times 10^{-3}$  mol) and *N*-ethoxycarbonylpyrrole (**24b**) (0.65 g;  $4.65 \times 10^{-3}$  mol) in 2 ml toluene was heated in an inert atmosphere (nitrogen) at 90 °C for 48 h. The

reaction mixture was separated by column chromatography. Elution with diethyl ether-petroleum (5:95) removed the excess *N*-ethoxycarbonylpyrrole which was recycled (**24b**). The product (**63**) was eluted with 1:9 diethyl ether:petroleum (bp 40-60 °C) as a white solid material (0.52 g, 56%):  $R_f$  0.63 (1:1 diethyl ether:petroleum (bp 40-60 °C)), mp 121-122 °C.

$^1\text{H}$  NMR (300 MHz,  $\text{CDCl}_3$ )  $\delta$ : 7.79 (d,  $J = 8.2$  Hz, 2H, 2 x aryl  $\text{CH}$ ), 7.36 (d,  $J = 8.2$  Hz, 2H, aryl  $\text{CH}$ ), 7.00 – 6.96 (br m, 2H,  $\text{H}_5$ ,  $\text{H}_6$ ), 5.43, 5.22 (br s, 2H,  $\text{H}_1$ ,  $\text{H}_4$ ), 4.07 – 3.93 (br m, 2H,  $\text{OCH}_2\text{CH}_3$ ), 2.45 (s, 3H, aryl  $\text{CH}_3$ ), 1.14 (t,  $J = 7.2$  Hz, 3H,  $\text{OCH}_2\text{CH}_3$ ).

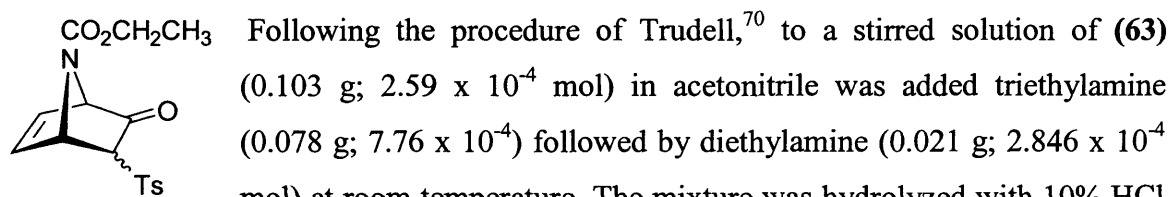
$^{13}\text{C}$  NMR (75 MHz,  $\text{CDCl}_3$ )  $\delta$ : 154.3 (C=O), 150.4 ( $\text{C}_3$ ), 145.3 (2 x aryl C), 143.0, 139.7 ( $\text{C}_5$ ,  $\text{C}_6$ ), 136.0 (2 x aryl C), 130.0, 127.8 (4 x aryl  $\text{CH}$ ), 75.3, 69.3 ( $\text{C}_1$ ,  $\text{C}_4$ ), 62.3 ( $\text{OCH}_2\text{CH}_3$ ), 21.7 (aryl  $\text{CH}_3$ ), 14.3 ( $\text{OCH}_2\text{CH}_3$ ),  $\text{C}_2$  not resolved.

MS  $m/z$ : 398 ( $\text{MH}^+$ ).  $\text{C}_{16}\text{H}_{17}\text{NO}_4$   $^{79}\text{BrS}$  [ $\text{MH}^+$ ] calculated 398.00617; observed 398.00614.

$\nu_{\text{max}}$ : 1704s, 1573m, 1372m, 1315s, 1259m, 1150s, 1016s, 815m, 672s.

Anal. Calcd for  $\text{C}_{16}\text{H}_{16}\text{NO}_4\text{BrS}$ : C, 48.40; H, 4.10; N, 3.50. Found: C, 48.33; H, 4.03; N, 3.45.

### Synthesis of 2-oxo-3-(toluene-4-sulfonyl)-7-azabicyclo[2.2.1]hept-5,6-ene-7-carboxylic acid ethyl ester (64)



at room temperature to give the crude product which was extracted with 20 ml dichloromethane three times. The combined organic phase was dried anhydrous  $\text{MgSO}_4$  and the solvent was removed under reduced pressure to give crude product. The crude product was subjected to column chromatography (3:7 diethyl ether:petroleum (bp 40-60  $^\circ\text{C}$ )) to give (64) (0.052 g, 60%) as a light yellow solid. The ratio of *endo*- to *exo*- tosyl isomers was (24:76).

The signals corresponding to the minor (*endo*-tosyl) isomer are shown in italics.

$^1\text{H}$  NMR (300 MHz,  $\text{CDCl}_3$ )  $\delta$ : 7.81 (d,  $J = 8.2$  Hz, 2H, 2 x aryl  $\text{CH}$ ), 7.77 (d,  $J = 8.2$  Hz, 2H, aryl  $\text{CH}$ ), 7.38 (d,  $J = 8.2$  Hz, 2H, 2 x aryl  $\text{CH}$ ), 7.33 (d,  $J = 8.2$  Hz, 2H, aryl  $\text{CH}$ ), 6.99 (dd,  $J_{5,6} = 5.7$  Hz,  $J_{4,5} = 2.1$  Hz, 1H,  $\text{H}_5$ ), 6.76 (dd,  $J_{5,6} = 5.5$  Hz,  $J_{4,5} = 1.9$  Hz, 1H,  $\text{H}_5$ ), 6.57 (br s, 1H,  $\text{H}_6$ ), 6.49 (dd,  $J_{5,6} = 5.7$  Hz,  $J_{1,6} = 2.7$  Hz, 1H,  $\text{H}_6$ ), 5.55 (br s, 1H,  $\text{H}_4$ ), 5.28 (br s, 1H,  $\text{H}_4$ ), 4.77 (br s, 1H,  $\text{H}_1$ ), 4.67 (br s, 1H,  $\text{H}_1$ ), 4.13 (br q,  $J = 7.1$  Hz, 2H,  $\text{OCH}_2\text{CH}_3$ ), 4.02 (d,  $J_{3\text{-exo},4} = 3.8$  Hz, 1H,  $\text{H}_{3\text{-exo}}$ ), 3.54 (s, 1H,  $\text{H}_{3\text{-endo}}$ ), 2.44 (s, 3H, aryl  $\text{CH}_3$ ), 1.24 (br t,  $J = 7.1$  Hz, 3H,  $\text{OCH}_2\text{CH}_3$ ).

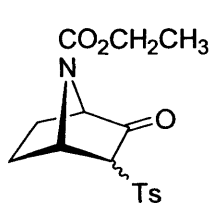
$^{13}\text{C}$  NMR (75 MHz,  $\text{CDCl}_3$ )  $\delta$ : 192.1, 191.9 ( $\text{C}_2$ ), 154.3, 154.1 (C=O), 145.5 (2 x aryl C), 142.8 (br,  $\text{C}_5$ ), 139.9 ( $\text{C}_5$ ), 135.8, 135.0 (2 x aryl C), 133.8, (br,  $\text{C}_6$ ), 130.0, 129.7,

129.3, 128.6 (4 x aryl  $\underline{\text{C}}\text{H}$ ), 68.6, 66.9 ( $\text{C}_1$ ), 66.3, 66.0 ( $\text{C}_3$ ), 62.7, 62.3 ( $\text{O}\underline{\text{C}}\text{H}_2\text{CH}_3$ ), 62.0, 61.1 ( $\text{C}_4$ ), 21.7 (aryl  $\underline{\text{C}}\text{H}_3$ ), 14.4 ( $\text{O}\underline{\text{C}}\text{H}_2\text{CH}_3$ ).

MS  $m/z$ : 336 ( $\text{MH}^+$ ).  $\text{C}_{16}\text{H}_{18}\text{NO}_5\text{S}$  [ $\text{MH}^+$ ] calculated 336.09057; observed 336.09064.

$\nu_{\text{max}}$ : 1769m, 1709s, 1596w, 1376m, 1321s, 1268s, 1148s, 1083s, 813m, 777m, 659s.

### Synthesis of 2-oxo-3-(toluene-4-sulfonyl)-7-azabicyclo[2.2.1]heptane-7-carboxylic acid ethyl ester (65)



The mixture of compounds (64) (1.632 g;  $4.87 \times 10^{-3}$  mol) was dissolved in anhydrous acetonitrile (25 ml) and hydrogenated over Pd/C using a balloon of hydrogen. The reaction vessel was purged first with nitrogen and then carefully with hydrogen. The reaction mixture was stirred vigorously at room temperature overnight. After the addition was complete, the catalyst was removed by filtration through Celite and the solvent was evaporated *in vacuo* to give the saturated mixture of *endo*- and *exo*- tosyl (65) (1.603 g, 98%) as brown oil. The mixture was used directly for the detosylation reaction step.

The signals corresponding to the minor (*endo*-tosyl) isomer are shown in italics.

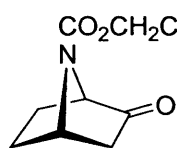
$^1\text{H}$  NMR (300 MHz,  $\text{CDCl}_3$ )  $\delta$ : 7.87 (d,  $J = 8.2$  Hz, 2H, 2 x aryl  $\underline{\text{C}}\text{H}$ ), 7.77 (d,  $J = 8.2$  Hz, 2H, aryl  $\underline{\text{C}}\text{H}$ ), 7.39 (d,  $J = 8.2$  Hz, 2H, 2 x aryl  $\underline{\text{C}}\text{H}$ ), 7.34 (d,  $J = 8.2$  Hz, 2H, aryl  $\underline{\text{C}}\text{H}$ ), 5.08 (br s, 1H,  $\text{H}_4$ ), 4.97 (br t,  $J = 4.6$  Hz, 1H,  $\text{H}_4$ ), 4.41 (br d,  $J = 6.1$  Hz, 1H,  $\text{H}_1$ ), 4.36 (br s, 1H,  $\text{H}_1$ ), 4.12 (br q,  $J = 7.1$  Hz, 2H,  $\text{O}\underline{\text{C}}\text{H}_2\text{CH}_3$ ), 3.59 (s, 1H,  $\text{H}_{3\text{-endo}}$ ), 2.69 – 2.60 (m, 1H, ( $\text{H}_{5\text{-endo}}$  or  $\text{H}_{6\text{-endo}}$ )), 2.44 (s, 3H, aryl  $\underline{\text{C}}\text{H}_3$ ), 2.25 – 2.16 (m, 1H,  $\text{H}_{6\text{-exo}}$ ), 2.05 – 1.97 (m, 4H,  $\text{H}_{5\text{-exo}}$ ,  $\text{H}_{6\text{-exo}}$ ,  $\text{H}_{5\text{-exo}}$ , ( $\text{H}_{5\text{-endo}}$  or  $\text{H}_{6\text{-endo}}$ )), 1.65 (br dd, 2H,  $\text{H}_{5\text{-endo}}$ ,  $\text{H}_{6\text{-endo}}$ ), 1.24 (br t, 3H,  $\text{O}\underline{\text{C}}\text{H}_2\text{CH}_3$ ), ( $\text{H}_{3\text{-exo}}$  not resolved).

$^{13}\text{C}$  NMR (75 MHz,  $\text{CDCl}_3$ )  $\delta$ : 197.4, 196.8 ( $\text{C}_2$ ), 154.8, 154.0 ( $\text{C}=\text{O}$ ), 145.5, 135.3 (2 x aryl C), 130.0, 129.8, 129.2, 128.8 (8 x aryl  $\underline{\text{C}}\text{H}$ ), 74.5, 72.9 ( $\text{C}_3$ ), 64.8, 62.8 ( $\text{C}_1$ ), 62.4, 62.0 ( $\text{O}\underline{\text{C}}\text{H}_2\text{CH}_3$ ), 58.5, 57.7 ( $\text{C}_4$ ), 28.0, 24.9, 24.5 ( $\text{C}_5$ ,  $\text{C}_6$ ), 21.7 (aryl  $\underline{\text{C}}\text{H}_3$ ), 14.5 ( $\text{O}\underline{\text{C}}\text{H}_2\text{CH}_3$ ).

MS  $m/z$ : 338 ( $\text{MH}^+$ ).  $\text{C}_{16}\text{H}_{20}\text{NO}_5\text{S}$  [ $\text{MH}^+$ ] calculated 338.10622; observed 338.10612.

$\nu_{\text{max}}$ : 1770m, 1703s, 1596w, 1378m, 1321s, 1304s, 1183m, 1146s, 1077s, 813m, 725m, 674s.

### Synthesis of 2-oxo-7-aza-bicyclo[2.2.1]heptane-7-carboxylic acid ethyl ester (66)



The keto-sulfone (**65**) (1.151g;  $3.41 \times 10^{-3}$  mol) was dissolved in 70 ml of 10% aqueous THF, and the mixture was placed in a reaction vessel equipped with a stirrer. Aluminum amalgam (10 g-atoms of aluminum/mole of compound) was then freshly prepared as follows. Aluminum foil was cut into square pieces approximately 1 cm x 1 cm and immersed, all at once, into a 5% aqueous solution of mercuric chloride ( $\text{HgCl}_2$ ) for 20 sec. The pieces were rinsed with absolute MeOH and then with diethyl ether and introduced directly into the reaction vessel. The reaction mixture was heated at 65 °C for 2h after the addition of the amalgam. The reaction mixture was then filtered through Celite and the filtered solid was washed with THF. The filtrate was concentrated to remove most of the THF, then diethyl ether was added. The organic layer was separated from the water, dried over anhydrous sodium sulphate, and the solvent removed *in vacuo* to give the ketone (**66**). The crude product (0.71 g) was chromatographed on silica gel. Elution with 1:9 diethyl ether-petroleum (bp 40-60 °C) gave 0.332 g (54%) of (**66**) as a pale oil:  $R_f$  0.45 (1:1 diethyl ether:petroleum (bp 40-60 °C)).

$^1\text{H}$  NMR (300 MHz,  $\text{CDCl}_3$ )  $\delta$ : 4.63 (br t,  $J = 4.7$  Hz, 1H,  $\text{H}_4$ ), 4.32 (br d,  $J = 4.9$  Hz, 1H,  $\text{H}_1$ ), 4.15 (q,  $J = 7.1$  Hz, 2H,  $\text{OCH}_2\text{CH}_3$ ), 2.49 (dd,  $J_{3\text{-exo},3\text{-endo}} = 17.5$  Hz,  $J_{3\text{-exo},4} = 5.9$  Hz, 1H,  $\text{H}_{3\text{-exo}}$ ), 2.03 (d,  $J_{3\text{-exo},3\text{-endo}} = 17.5$  Hz, 1H,  $\text{H}_{3\text{-endo}}$ ), 2.02 – 1.58 (m, 4H,  $\text{H}_{5\text{-exo}}$ ,  $\text{H}_{6\text{-exo}}$ ,  $\text{H}_{5\text{-endo}}$ ,  $\text{H}_{6\text{-endo}}$ ), 1.26 (t,  $J = 7.1$  Hz, 3H,  $\text{OCH}_2\text{CH}_3$ ).

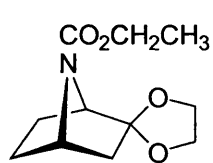
$^{13}\text{C}$  NMR (75 MHz,  $\text{CDCl}_3$ )  $\delta$ : 209.1 ( $\text{C}_2$ ), 155.1 ( $\text{C}=\text{O}$ ), 63.6 ( $\text{C}_1$ ), 61.7 ( $\text{OCH}_2\text{CH}_3$ ), 56.0 ( $\text{C}_4$ ), 45.2 ( $\text{C}_3$ ), 27.6, 24.4 ( $\text{C}_5$ ,  $\text{C}_6$ ), 14.5 ( $\text{OCH}_2\text{CH}_3$ ).

$^{15}\text{N}$  NMR (40 MHz,  $\text{CDCl}_3$ )  $\delta$ : -265.8.

MS  $m/z$ : 184 ( $\text{MH}^+$ ).  $\text{C}_9\text{H}_{14}\text{NO}_3$  [ $\text{MH}^+$ ] calculated 184.09737; observed 184.09736.

$\nu_{\text{max}}$ : 1761s, 1701s, 1403m, 1304m, 1143m, 1095s, 1007w, 781m.

### Synthesis of 2-(1,3-dioxolan-2-yl)-7-azabicyclo[2.2.1]heptane-7-carboxylic acid ethyl ester (67)



Compound (**66**) (0.374g;  $2.04 \times 10^{-3}$  mol) was dissolved in 8 ml anhydrous toluene. Ethylene glycol ( $\text{CH}_2\text{OH}$ )<sub>2</sub> (0.145 g,  $2.33 \times 10^{-3}$  mol), triethyl orthoformate ( $\text{HC}(\text{OEt})_3$ ) (0.148 g,  $9.98 \times 10^{-4}$  mol) and *p*-toluenesulfonic acid (anhydrous,  $1.02 \times 10^{-4}$  mol) were added to the solution of (**66**) under nitrogen. The reaction mixture was heated at 55° C for 4h until the reaction went to completion as judged by TLC. The reaction mixture was cooled and poured into

saturated NaHCO<sub>3</sub> (25 ml). The mixture was extracted with dichloromethane (3 x 25 ml) and washed with water and brine (3 x 25 ml). The dichloromethane portion was dried over anhydrous MgSO<sub>4</sub>/Na<sub>2</sub>CO<sub>3</sub> (1:1) and filtered, and the solvent removed on a rotary evaporator. The purity of the resultant oil (**67**) (0.431 g, 93%) was checked by <sup>1</sup>H NMR spectroscopy and judged to be satisfactory for the next step reaction: R<sub>f</sub> 0.25 (1:1 diethyl ether:petroleum (bp 40-60 °C)).

<sup>1</sup>H NMR (300 MHz, CDCl<sub>3</sub>) δ: 4.29 (br t, *J* = 4.8 Hz, 1H, H<sub>4</sub>), 4.12 (br q, *J* = 7.1 Hz, 2H, OCH<sub>2</sub>CH<sub>3</sub>), 4.03 – 3.85 (m, 5H, H<sub>1</sub>, OCH<sub>2</sub>CH<sub>2</sub>O), 2.15 (ddd, *J*<sub>3-*exo*,3-*endo*</sub> = 13.0 Hz, *J*<sub>3-*exo*,4</sub> = 5.4 Hz, *J*<sub>3-*exo*,5-*exo*</sub> = 2.3 Hz, 1H, H<sub>3-*exo*</sub>), 1.96 – 1.88 (m, 1H, (H<sub>5-*endo*</sub> or H<sub>6-*endo*</sub>)), 1.80 – 1.68 (m, 2H, H<sub>5-*exo*</sub>, H<sub>6-*exo*</sub>), 1.62 (d, *J*<sub>3-*exo*,3-*endo*</sub> = 13.0 Hz, 1H, H<sub>3-*endo*</sub>), 1.53 – 1.46 (m, 1H, (H<sub>5-*endo*</sub> or H<sub>6-*endo*</sub>)), 1.25 (t, *J* = 7.1 Hz, 3H, OCH<sub>2</sub>CH<sub>3</sub>).

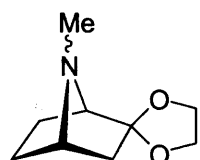
<sup>13</sup>C NMR (75 MHz, CDCl<sub>3</sub>) δ: 155.9 (C=O), 114.3 (C<sub>2</sub>), 65.1, 64.2 (OCH<sub>2</sub>CH<sub>2</sub>O), 61.1, (C<sub>1</sub>), 61.1 (OCH<sub>2</sub>CH<sub>3</sub>), 56.1 (C<sub>4</sub>), 43.4, (C<sub>3</sub>), 28.3, 22.4 (C<sub>5</sub>, C<sub>6</sub>), 14.6 (OCH<sub>2</sub>CH<sub>3</sub>).

<sup>15</sup>N NMR (40 MHz, CDCl<sub>3</sub>) δ: -261.8.

MS <sup>m/z</sup>: 228 (MH<sup>+</sup>). C<sub>11</sub>H<sub>18</sub>NO<sub>4</sub> [MH<sup>+</sup>] calculated 228.12358; observed 228.12365.

*v*<sub>max</sub>: 1698s, 1401w, 1376m, 1329m, 1081s, 1019m, 947w, 776w, 663w.

### Synthesis of 2-(1,3-dioxolan-2-yl)-7-methyl-7-azabicyclo[2.2.1]heptane (**68**)



A solution of compound (**67**) (0.365 g; 1.61 x 10<sup>-3</sup> mol) in 10 ml of anhydrous diethyl ether was added to a stirring suspension of LAH (0.26 g; 6.91 x 10<sup>-3</sup> mol) in 10 ml of anhydrous diethyl ether under nitrogen. The reaction mixture was refluxed for 8 h, and quenched with 0.5 ml of distilled water, 0.5 ml of 10% NaOH, and 1.5 ml of distilled water. The reaction mixture was then filtered through a pad of Celite and washed with ether. The ether solutions were combined and dried over MgSO<sub>2</sub>, and (**68:HCl**) was precipitated by bubbling HCl through the solution, yielding 0.273 g as salt (0.225 g, 83% as free amine). The (**68:HCl**) was dissolved in distilled water then basified with 2M NaOH and extracted 3 times with CFCl<sub>3</sub>. The organic layer was dried over anhydrous MgSO<sub>4</sub>, concentrated and transferred to a 5 mm NMR tube with 0.5 ml of CDCl<sub>3</sub>.

<sup>1</sup>H NMR (300 MHz, CDCl<sub>3</sub>) δ: 3.98 – 3.80 (m, 4H, OCH<sub>2</sub>CH<sub>2</sub>O), 3.24 (br t, *J* = 4.4 Hz, 1H, H<sub>4</sub>), 3.04 (br d, *J*<sub>1,6-*exo*</sub> = 4.6 Hz, 1H, H<sub>1</sub>), 2.27 (s, 3H, NCH<sub>3</sub>), 2.07 (ddd, *J*<sub>3-*exo*,3-*endo*</sub> = 12.7 Hz, *J*<sub>3-*exo*,4</sub> = 5.1 Hz, *J*<sub>3-*exo*,5-*exo*</sub> = 2.2 Hz, 1H, H<sub>3-*exo*</sub>), 1.88 – 1.68 (m, 3H,

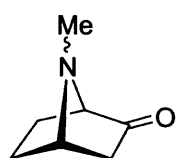
H<sub>5-exo</sub>, H<sub>6-exo</sub>, H<sub>6-endo</sub>), 1.47 (d,  $J_{3-exo,3-endo} = 12.8$  Hz, 1H, H<sub>3-endo</sub>), 1.42 – 1.37 (m, 1H, (H<sub>5-endo</sub>)).

<sup>13</sup>C NMR (75 MHz, CDCl<sub>3</sub>)  $\delta$ : 114.7 (C<sub>2</sub>), 67.1, (C<sub>1</sub>), 64.5, 64.0 (OCH<sub>2</sub>CH<sub>2</sub>O), 61.3 (C<sub>4</sub>), 44.4 (C<sub>3</sub>), 35.1 (NCH<sub>3</sub>), 25.1 (C<sub>5</sub>), 19.3 (C<sub>6</sub>).

MS <sup>m/z</sup>: 170 (MH<sup>+</sup>). C<sub>9</sub>H<sub>16</sub>NO<sub>2</sub> [MH<sup>+</sup>] calculated 170.11810; observed 170.11816.

$\nu_{max}$ : 3386w, 2921, 1716s, 1454m, 1225s, 1094s, 1015s, 873w, 724s.

### Synthesis of 7-methyl-7-azabicyclo[2.2.1]heptan-2-one (4a)



To 1.5 ml of THF containing 1.2 ml of 70% aqueous perchloric acid (HClO<sub>4</sub>) was added 0.105 g (6.21 x 10<sup>-4</sup> mol) of ketal (**68**) dissolved in 3 ml THF without purification. The resulting oily suspension became homogeneous after standing at room temperature for 10 min. After remaining at room temperature for 3 h the solution was diluted with 10 ml water and extracted 3 times with 30 ml of dichloromethane. The combined extracts were dried over anhydrous MgSO<sub>4</sub> and the solvent was removed *in vacuo*. The resulting HCl salt of (**4a**) (0.073 g; 0.057 g, 74% as free base) was treated with 2M NaOH and extracted with 3 x 5 ml of CFC<sub>3</sub>. The organic layer was dried over anhydrous MgSO<sub>4</sub>, concentrated and transferred to a 5 mm NMR tube with 0.5 ml of CDCl<sub>3</sub>.

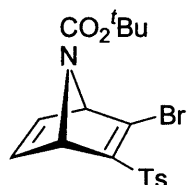
<sup>1</sup>H NMR (300 MHz, CDCl<sub>3</sub>)  $\delta$ : 3.57 (br t,  $J = 4.5$  Hz, 1H, H<sub>4</sub>), 3.28 (br d,  $J_{1,6-exo} = 4.5$  Hz, 1H, H<sub>1</sub>), 2.39 (ddd,  $J_{3-exo,3-endo} = 17.7$  Hz,  $J_{3-exo,4} = 5.4$  Hz,  $J_{3-exo,5-exo} = 1.3$  Hz, 1H, H<sub>3-exo</sub>), 2.33 (s, 3H, NCH<sub>3</sub>), 2.08 – 2.01 (m, 2H, H<sub>5-exo</sub>, H<sub>6-exo</sub>), 1.86 (d,  $J_{3-exo,3-endo} = 17.7$  Hz, 1H, H<sub>3-endo</sub>), 1.59 – 1.49 (m, 2H, (H<sub>5-endo</sub>, H<sub>6-endo</sub>)).

<sup>13</sup>C NMR (75 MHz, CDCl<sub>3</sub>)  $\delta$ : 213.9 (C<sub>2</sub>), 70.0, (C<sub>1</sub>), 61.3 (C<sub>4</sub>), 43.2 (C<sub>3</sub>), 35.1 (NCH<sub>3</sub>), 26.4, 22.4 (C<sub>5</sub>, C<sub>6</sub>).

<sup>14</sup>N NMR (40 MHz, CDCl<sub>3</sub>)  $\delta$ : -319.5  $\pm$  1.

MS <sup>m/z</sup>: 126 (MH<sup>+</sup>). C<sub>7</sub>H<sub>12</sub>NO [MH<sup>+</sup>] calculated 126.09189; observed 126.09185.

### Synthesis of 2-Bromo-3-(toluene-4-sulfonyl)-7-azabicyclo[2.2.1]hept-5,6-ene-7-carboxylic acid *tert*-butyl ester (**69**)<sup>70</sup>



This compound was prepared using a similar method to that used to prepare (**63**). *N*-*tert*-butoxycarbonylpyrrole (**24c**) (6.47 g; 0.038 mol) was used for the cycloaddition reaction instead; (**62**) (5.01 g; 0.019 mol). The product (**69**) (5.17 g; 63% as a pale yellow oil) was purified by

column chromatography (silica and 3:7 diethyl ether and petroleum (bp 40-60 °C)): R<sub>f</sub> 0.46 (1:1 diethyl ether:petroleum (bp 40-60 °C)).

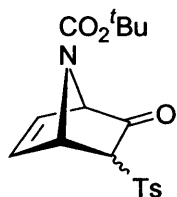
<sup>1</sup>H NMR (300 MHz, CDCl<sub>3</sub>) δ: 7.80 (d, *J* = 8.0 Hz, 2H, 2 x aryl CH), 7.35 (d, *J* = 8.0 Hz, 2H, aryl CH), 6.96 (br s, 2H, H<sub>5</sub>, H<sub>6</sub>), 5.37, 5.15 (br s, 2H, H<sub>1</sub>, H<sub>4</sub>), 2.44 (s, 3H, aryl CH<sub>3</sub>), 1.31 (s, 9H, OC(CH<sub>3</sub>)<sub>3</sub>).

<sup>13</sup>C NMR (75 MHz, CDCl<sub>3</sub>) δ: 153.7 (C=O), 150.1 (C<sub>3</sub>), 145.2 (2 x aryl C), 143.0, 139.6 (C<sub>5</sub>, C<sub>6</sub>), 136.2 (2 x aryl C), 130.0, 127.9 (4 x aryl CH), 81.9 (OC(CH<sub>3</sub>)<sub>3</sub>), 75.6, 69.6 (C<sub>1</sub>, C<sub>4</sub>), 27.9 (OC(CH<sub>3</sub>)<sub>3</sub>), 21.7 (aryl CH<sub>3</sub>), C<sub>2</sub> not resolved.

MS <sup>m/z</sup>: 426 (MH<sup>+</sup>). C<sub>18</sub>H<sub>21</sub>NO<sub>4</sub><sup>79</sup>BrS [MH<sup>+</sup>] calculated 426.03747; observed 426.03738.

*v*<sub>max</sub>: 1713s, 1580w, 1368m, 1322s, 1255m, 1150s, 1086s, 814m, 731s, 672s.

### Synthesis of 2-oxo-3-(toluene-4-sulfonyl)-7-azabicyclo[2.2.1]hept-5,6-ene-7-carboxylic acid *tert*-butyl ester (70)<sup>70</sup>



This compound (70) was prepared using a similar method to that described to synthesise (64), starting from (69) (1.4 g; 3.29 x 10<sup>-3</sup> mol).

The mixture of *endo*- and *exo*- tosyl (69) was obtained as a pale yellow oil (1.1 g, 94%) and was pure enough to be used for the next step as judged by <sup>1</sup>H NMR spectroscopy.

The signals corresponding to the minor (*endo*-tosyl) isomer are shown in italics.

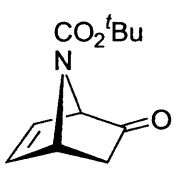
<sup>1</sup>H NMR (300 MHz, CDCl<sub>3</sub>) δ: 7.76 (d, *J* = 8.2 Hz, 2H, aryl CH), 7.38 (d, *J* = 8.2 Hz, 2H, 2 x aryl CH), 7.32 (d, *J* = 8.2 Hz, 2H, aryl CH), 6.95 (m, 1H, H<sub>5</sub>), 6.77 (br d, *J* = 4.1 Hz, 1H, H<sub>5</sub>), 6.55 (br s, 1H, H<sub>6</sub>), 6.47 (dd, *J*<sub>5,6</sub> = 5.5 Hz, *J*<sub>1,6</sub> = 2.1 Hz, 1H, H<sub>6</sub>), 5.43 (br s, 1H, H<sub>4</sub>), 5.17 (br s, 1H, H<sub>4</sub>), 4.70 (br s, 1H, H<sub>1</sub>), 4.57 (br s, 1H, H<sub>1</sub>), 4.02 (d, *J*<sub>3-*exo*,4</sub> = 3.7 Hz, 1H, H<sub>3-*exo*</sub>), 3.57 (s, 1H, H<sub>3-*endo*</sub>), 2.45, 2.43 (s, 3H, aryl CH<sub>3</sub>), 1.41 (s, 9H, OC(CH<sub>3</sub>)<sub>3</sub>).

<sup>13</sup>C NMR (75 MHz, CDCl<sub>3</sub>) δ: 190.4, 190.3 (C<sub>2</sub>), 151.6 151.4 (C=O), 143.8 (2 x aryl C), 141.1, 138.0 (C<sub>5</sub>, C<sub>6</sub>), 133.2 (2 x aryl C), 128.1, 127.9, 127.5, 126.7 (8 x aryl CH), 80.7, 80.0 (OC(CH<sub>3</sub>)<sub>3</sub>), 67.0 (C<sub>3</sub>), 65.4, 64.5 (C<sub>4</sub>), 60.2, 59.3 (C<sub>1</sub>), 26.2 (OC(CH<sub>3</sub>)<sub>3</sub>), 19.8 (aryl CH<sub>3</sub>).

MS <sup>m/z</sup>: 364 (MH<sup>+</sup>). C<sub>18</sub>H<sub>22</sub>NO<sub>5</sub>S [MH<sup>+</sup>] calculated 364.12187; observed 364.12194.

*v*<sub>max</sub>: 1770s, 1709s, 1596w, 1368m, 1321s, 1280m, 1148s, 1083s, 870m, 731m, 683s.

**Synthesis of 2-oxo-7-azabicyclo[2.2.1]hept-5,6-ene-7-carboxylic acid *tert*-butyl ester (71)<sup>70</sup>**

 Keto sulfone (**70**) (0.23 g,  $6.33 \times 10^{-4}$  mol) was dissolved in anhydrous THF-MeOH (3:1, 4ml) and cooled to  $-78^\circ\text{C}$  under argon. The solution was then transferred using cannula to a solution of  $\text{SmI}_2$  (0.1 M) in THF (17 ml) cooled at  $-78^\circ\text{C}$  under argon. The resultant brown mixture was stirred for 10 min and then warmed to room temperature. The reaction mixture was poured into a saturated aqueous solution of  $\text{K}_2\text{CO}_3$ . The aqueous phase was extracted 3 times with dichloromethane; the combined extracts were dried over anhydrous  $\text{MgSO}_4$  and concentrated *in vacuo*. The resultant residue was purified by flash chromatography (1:9 diethyl ether:petroleum (bp  $40\text{-}60^\circ\text{C}$ )) affording (**71**) (0.031 g, 24%) as a colourless oil:  $R_f$  0.42 (1:1 diethyl ether:petroleum (bp  $40\text{-}60^\circ\text{C}$ )).

$^1\text{H}$  NMR (300 MHz,  $\text{CDCl}_3$ )  $\delta$ : 6.73 (dd,  $J_{5,6} = 5.5$  Hz,  $J_{4,5} = 2.0$  Hz, 1H,  $\text{H}_5$ ), 6.42 (br dd,  $J_{5,6} = 5.5$  Hz,  $J_{1,6} = 2.0$  Hz, 1H,  $\text{H}_6$ ), 5.05 (br s, 1H,  $\text{H}_4$ ), 4.54 (br s, 1H,  $\text{H}_1$ ), 2.28 (ddd,  $J_{3\text{-exo},3\text{-endo}} = 16.0$  Hz,  $J_{3\text{-exo},4} = 3.9$  Hz,  $J_{1,3\text{-exo}} = 0.7$  Hz, 1H,  $\text{H}_{3\text{-exo}}$ ), 1.91 (d,  $J_{3\text{-exo},3\text{-endo}} = 16.0$  Hz, 1H,  $\text{H}_{3\text{-endo}}$ ), 1.44 (s, 9H,  $\text{OC}(\text{CH}_3)_3$ ).

$^{13}\text{C}$  NMR (75 MHz,  $\text{CDCl}_3$ )  $\delta$ : 205.2 ( $\text{C}_2$ ), 155.0 ( $\text{C}=\text{O}$ ), 142.9 ( $\text{C}_5$ ), 130.5 ( $\text{C}_6$ ), 81.4 ( $\text{OC}(\text{CH}_3)_3$ ), 68.2 ( $\text{C}_1$ ), 60.0 ( $\text{C}_4$ ), 35.8 ( $\text{C}_3$ ), 28.1 ( $\text{OC}(\text{CH}_3)_3$ ).

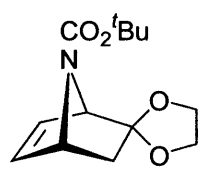
$^{15}\text{N}$  NMR (40 MHz,  $\text{CDCl}_3$ )  $\delta$ :  $-252.4$ .

MS  $m/z$ : 210 ( $\text{MH}^+$ ).  $\text{C}_{11}\text{H}_{16}\text{NO}_3$  [ $\text{MH}^+$ ] calculated 210.11302; observed 210.11308.

$\nu_{\text{max}}$ : 1754s, 1696s, 1475w, 1350s, 1286s, 1255s, 1164s, 1124s, 950m, 876m, 804s.

Anal. Calcd for  $\text{C}_{11}\text{H}_{15}\text{NO}_3$ : C, 63.14; H, 7.23; N, 6.69. Found: C, 63.23; H, 7.10; N, 6.61.

**Synthesis of 2-(1,3-dioxolan-2-yl)-7-azabicyclo[2.2.1]hept-5,6-ene-7-carboxylic acid *tert*-butyl ester (72)<sup>80</sup>**

 Compound (**72**) was prepared according to the procedure described for (**67**), starting from (**71**) (0.18 g;  $8.61 \times 10^{-4}$  mol): (**72**) (0.092 g, 42%) was purified by flash chromatography (15:85 diethyl ether:petroleum (bp  $40\text{-}60^\circ\text{C}$ )) as brown solid:  $R_f$  0.31 (1:1 diethyl ether:petroleum (bp  $40\text{-}60^\circ\text{C}$ )), mp  $114\text{-}116^\circ\text{C}$ .

$^1\text{H}$  NMR (300 MHz,  $\text{CDCl}_3$ )  $\delta$ : 6.37 (br, 2H,  $\text{H}_5$ ,  $\text{H}_6$ ), 4.65 (br s, 1H,  $\text{H}_4$ ), 4.24 (br, 1H,  $\text{H}_1$ ), 4.02 – 3.78 (m, 4H,  $\text{OCH}_2\text{CH}_2\text{O}$ ), 2.12 (br dd,  $J_{3\text{-exo},3\text{-endo}} = 11.7$  Hz,  $J_{3\text{-exo},4} = 3.0$  Hz, 1H,  $\text{H}_{3\text{-exo}}$ ), 1.47 (d,  $J_{3\text{-exo},3\text{-endo}} = 12.1$  Hz, 1H,  $\text{H}_{3\text{-endo}}$ ), 1.35 (s, 9H,  $\text{OC}(\text{CH}_3)_3$ ).

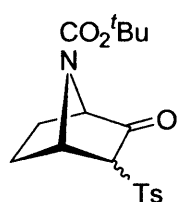
There is a signal duplication because of slow N-CO rotation; the minor rotamer signal is shown in italics.

$^{13}\text{C}$  NMR (75 MHz,  $\text{CDCl}_3$ )  $\delta$ : 155.5 (C=O), 139.4, *138.8*, *134.4*, 132.7 ( $\text{C}_5$ ,  $\text{C}_6$ ), 114.4 ( $\text{C}_2$ ), 80.2 ( $\text{OC}(\text{CH}_3)_3$ ), 65.2, *64.4* ( $\text{OCH}_2\text{CH}_2\text{O}$ ), *60.6*, *59.9* ( $\text{C}_4$ ), 40.0, *39.0* ( $\text{C}_3$ ), 28.2 ( $\text{OC}(\text{CH}_3)_3$ ).

MS  $m/z$ : 254 ( $\text{MH}^+$ ).  $\text{C}_{13}\text{H}_{20}\text{NO}_4$  [ $\text{MH}^+$ ] calculated 254.13923; observed 254.13927.

$\nu_{\text{max}}$ : 1693s, 1479w, 1354s, 1280m, 1152m, 1054s, 1003m, 943m, 802m, 720ms.

### Synthesis of 2-oxo-3-(toluene-4-sulfonyl)-7-aza-bicyclo[2.2.1]heptane-7-carboxylic acid tert-butyl ester (**81**)<sup>70</sup>



Compound (**81**) was prepared using a similar method to that described for (**65**), starting from (**70**) (1.09 g;  $3.01 \times 10^{-3}$  mol). The saturated mixture of *endo*- and *exo*- tosyl (**70**) (29:71 respectively) was obtained as a pale yellow oil (1.1 g, 96%) and was pure enough to be used for the next step

as judged by  $^1\text{H}$  NMR spectroscopy.

The signals corresponding to the minor (*endo*-tosyl) isomer are shown in italics.

$^1\text{H}$  NMR (300 MHz,  $\text{CDCl}_3$ )  $\delta$ : 7.86 (d,  $J = 8.2$  Hz, 2H, 2 x aryl  $\text{CH}$ ), 7.77 (d,  $J = 8.2$  Hz, 2H, aryl  $\text{CH}$ ), 7.39 (d,  $J = 8.2$  Hz, 2H, 2 x aryl  $\text{CH}$ ), 7.33 (d,  $J = 8.2$  Hz, 2H, aryl  $\text{CH}$ ), 4.95 (br s, 1H,  $\text{H}_4$ ), *4.86* (br t, 1H,  $\text{H}_4$ ), 4.33 (br d,  $J = 6.0$  Hz, 1H,  $\text{H}_1$ ), 4.26 (br s, 1H,  $\text{H}_1$ ), *4.06* (br d,  $J = 5.2$  Hz, 1H,  $\text{H}_{3\text{-exo}}$ ), 3.63 (s, 1H,  $\text{H}_{3\text{-endo}}$ ), 2.65 – 2.56 (m, 1H, ( $\text{H}_{5\text{-endo}}$  or  $\text{H}_{6\text{-endo}}$ )), 2.46 (s, 3H, aryl  $\text{CH}_3$ ), 2.43 (s, 3H, aryl  $\text{CH}_3$ ), 2.24 – 2.14 (m, 1H,  $\text{H}_{6\text{-exo}}$ ), 2.00 – 1.85 (m, 3H,  $\text{H}_{6\text{-exo}}$ ,  $\text{H}_{5\text{-exo}}$ , ( $\text{H}_{5\text{-endo}}$  or  $\text{H}_{6\text{-endo}}$ )), 1.70 – 1.59 (m, 2H,  $\text{H}_{5\text{-endo}}$ ,  $\text{H}_{5\text{-exo}}$ ), 1.43 (s, 9H,  $\text{OC}(\text{CH}_3)_3$ ), 1.42 (s, 9H,  $\text{OC}(\text{CH}_3)_3$ ).

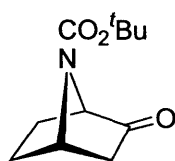
$^{13}\text{C}$  NMR (75 MHz,  $\text{CDCl}_3$ )  $\delta$ : 195.7, 195.1 ( $\text{C}_2$ ), *152.1*, 151.2 (C=O), *143.7*, 143.5 *134.8*, 133.6 (4 x aryl C), *128.1*, 127.9, 127.3, *126.9* (8 x aryl  $\text{CH}$ ), 80.1 ( $\text{OC}(\text{CH}_3)_3$ ), 79.3 ( $\text{OC}(\text{CH}_3)_3$ ), 72.7, *71.0* ( $\text{C}_3$ ), *63.1*, 61.2 ( $\text{C}_1$ ), *56.6*, *55.9* ( $\text{C}_4$ ), 26.4 ( $\text{OC}(\text{CH}_3)_3$ ), 26.1, 22.7 ( $\text{C}_5$ ,  $\text{C}_6$ ).

MS  $m/z$ : 366 ( $\text{MH}^+$ ).  $\text{C}_{18}\text{H}_{24}\text{NO}_5\text{S}$  [ $\text{MH}^+$ ] calculated 366.13752; observed 366.13751.

$\nu_{\text{max}}$ : 1777m, 1708s, 1595w, 1341s, 1304s, 1183m, 1145s, 1075m, 810m, 674s.

Anal. Calcd for C<sub>18</sub>H<sub>23</sub>NO<sub>5</sub>S: C, 59.16; H, 6.34; N, 3.83. Found: C, 58.92; H, 6.27; N, 3.78.

### Synthesis of 2-oxo-7-aza-bicyclo[2.2.1]heptane-7-carboxylic acid *tert*-butyl ester (79)<sup>72</sup>



Ketone (79) was prepared using a similar method to that described for (66), starting from (81) (1.02 g; 2.81 x 10<sup>-3</sup> mol). The ketone (79) was obtained as a colourless oil (0.411 g; 70%): R<sub>f</sub> 0.41 (1:1 diethyl ether:petroleum (bp 40-60 °C)).

<sup>1</sup>H NMR (300 MHz, CDCl<sub>3</sub>) δ: 4.49 (br t, *J* = 4.3 Hz, 1H, H<sub>4</sub>), 4.18 (br d, *J* = 4.9 Hz, 1H, H<sub>1</sub>), 2.40 (dd, *J*<sub>3-exo,3-endo</sub> = 17.5 Hz, *J*<sub>3-exo,4</sub> = 5.2 Hz, 1H, H<sub>3-exo</sub>), 1.93 (d, *J*<sub>3-exo,3-endo</sub> = 17.5 Hz, 1H, H<sub>3-endo</sub>), 1.96 – 1.84 (m, 2H, H<sub>5-exo</sub>, H<sub>6-exo</sub>), 1.63 – 1.44 (m, 2H, H<sub>5-endo</sub>, H<sub>6-endo</sub>), 1.38 (OC(CH<sub>3</sub>)<sub>3</sub>).

<sup>13</sup>C NMR (75 MHz, CDCl<sub>3</sub>) δ: 209.6 (C<sub>2</sub>), 155.1 (C=O), 80.8 (OC(CH<sub>3</sub>)<sub>3</sub>), 63.9 (C<sub>1</sub>), 56.0 (C<sub>4</sub>), 45.2 (C<sub>3</sub>), 28.2 (OC(CH<sub>3</sub>)<sub>3</sub>), 27.5, 24.4 (C<sub>5</sub>, C<sub>6</sub>).

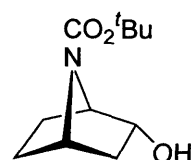
<sup>15</sup>N NMR (40 MHz, CDCl<sub>3</sub>) δ: -261.4.

MS <sup>m/z</sup>: 212 (MH<sup>+</sup>). C<sub>11</sub>H<sub>18</sub>NO<sub>3</sub> [MH<sup>+</sup>] calculated 212.12867; observed 212.12874.

*v*<sub>max</sub>: 1764s, 1695s, 1361s, 1258m, 1145s, 1098m, 781m.

Anal. Calcd for C<sub>11</sub>H<sub>17</sub>NO<sub>3</sub>: C, 62.54; H, 8.11; N, 6.63. Found: C, 62.69; H, 8.19; N, 6.61.

### Synthesis of 2-hydroxy-7-azabicyclo[2.2.1]heptane-7-carboxylic acid *tert*-butyl ester (80)<sup>73</sup>



To a stirred solution of ketone (79) (0.12 g; 5.69 x 10<sup>-4</sup> mol) in anhydrous THF (5 ml) at -55 °C under nitrogen was added *L*-Selectride (0.68 ml of 1.0 M solution in THF, 6.82 x 10<sup>-4</sup> mol) drop-wise. After the addition, the mixture was allowed to warm to room temperature and stirred for a further 30 min. After this time the solution was cooled to 0 °C and EtOH (1 ml) was added, followed by saturated aqueous NH<sub>4</sub>Cl solution (1 ml). The reaction mixture was allowed to achieve room temperature and then partitioned between dichloromethane (3 x 15 ml) and water (15 ml). The combined organic layers were washed with brine (50 ml), dried over anhydrous Na<sub>2</sub>SO<sub>4</sub>, and evaporated *in vacuo*. The residual oil was chromatographed

on silica, eluting with 3:7 diethyl ether:petroleum (bp 40-60 °C) to afford *endo*-alcohol (**80**) (0.095 g, 79%) as a colourless oil:  $R_f$  0.61 (diethyl ether).

$^1\text{H}$  NMR (300 MHz,  $\text{CDCl}_3$ )  $\delta$ : 4.36 – 4.30 (m, 1H,  $\text{H}_2$ ), 4.12 (br, 2H,  $\text{H}_1$ ,  $\text{H}_4$ ), 2.35 (br, 1H, OH), 2.26 – 1.49 (m, 5H,  $\text{H}_{3\text{-exo}}$ ,  $\text{H}_5$ ,  $\text{H}_6$ ), 1.44 (s, 9H,  $\text{OC}(\text{CH}_3)_3$ ), 1.06 (dd,  $J_{3\text{-endo},3\text{-exo}} = 12.7$  Hz,  $J_{2,3\text{-endo}} = 3.4$  Hz, 1H,  $\text{H}_{3\text{-endo}}$ ).

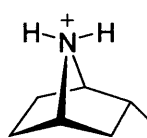
$^{13}\text{C}$  NMR (75 MHz,  $\text{CDCl}_3$ )  $\delta$ : 155.7 (C=O), 79.7 ( $\text{OC}(\text{CH}_3)_3$ ), 78.8 ( $\text{C}_2$ ), 60.0, 57.3 ( $\text{C}_1$ ,  $\text{C}_4$ ), 39.2 ( $\text{C}_3$ ), 29.8, 20.7 ( $\text{C}_5$ ,  $\text{C}_6$ ), 28.3 ( $\text{OC}(\text{CH}_3)_3$ ).

MS  $m/z$ : 214 ( $\text{MH}^+$ ).  $\text{C}_{11}\text{H}_{20}\text{NO}_3$  [ $\text{MH}^+$ ] calculated 214.14432; observed 214.14426.

$\nu_{\text{max}}$ : 3382m, 1666s, 1368s, 1309m, 1158s, 1104s, 1049m, 997w, 900m, 765m.

Anal. Calcd for  $\text{C}_{11}\text{H}_{19}\text{NO}_3$ : C, 61.95; H, 8.98; N, 6.57. Found: C, 62.02; H, 9.04; N, 6.61.

### Synthesis of 7-aza-bicyclo[2.2.1]heptan-2-ol (**82:HCl**)<sup>73</sup>



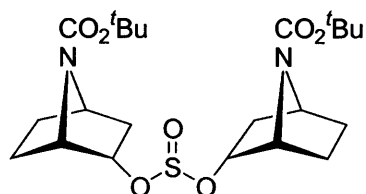
Amine (**82:HCl**) was prepared using a similar method to that used to prepare (**2b**). To a stirred solution of alcohol (**80**) (0.015 g;  $7.04 \times 10^{-5}$  mol) in 2 ml ethyl acetate was added drop-wise 3M HCl (4 ml, at 0 °C) formed *in situ* from the reaction of ethanol (2.7 ml), ethyl acetate (7.2 ml) and acetyl chloride (2.7 ml). The mixture was allowed to warm to room temperature with continued stirring for 2 h. The reaction mixture was then evaporated under reduced pressure. The yield of the residue (**82:HCl**) was 0.01 g (0.0075 g, 96% as free amine).

$^1\text{H}$  NMR (400 MHz, MeOD)  $\delta$ : 4.48 – 4.42 (m, 1H,  $\text{H}_2$ ), 4.14 (br t,  $J = 5.1$  Hz, 1H,  $\text{H}_4$ ), 4.08 (br t,  $J = 4.5$  Hz, 1H,  $\text{H}_1$ ), 2.49 – 2.41 (m, 1H,  $\text{H}_{6\text{-exo}}$ ), 2.34 (dddd,  $J_{3\text{-exo},3\text{-endo}} = 13.4$  Hz,  $J_{2,3\text{-exo}} = 10.1$  Hz,  $J_{3\text{-exo},4} = 5.2$  Hz,  $J_{3\text{-exo},6\text{-exo}} = 3.0$  Hz, 1H,  $\text{H}_{3\text{-exo}}$ ), 2.03 – 1.92 (m, 1H,  $\text{H}_{5\text{-exo}}$ ), 1.87 – 1.78 (m, 2H,  $\text{H}_{5\text{-endo}}$ ,  $\text{H}_{6\text{-exo}}$ ) 1.38 (dd,  $J_{3\text{-endo},3\text{-exo}} = 13.7$  Hz,  $J_{2,3\text{-endo}} = 3.4$  Hz, 1H,  $\text{H}_{3\text{-endo}}$ ).

$^{13}\text{C}$  NMR (100 MHz, MeOD)  $\delta$ : 67.4 ( $\text{C}_2$ ), 61.2 ( $\text{C}_1$ ), 59.7 ( $\text{C}_4$ ), 35.9 ( $\text{C}_3$ ), 26.8, 18.1 ( $\text{C}_5$ ,  $\text{C}_6$ ).

MS  $m/z$ : 114 ( $\text{MH}^+$ ).  $\text{C}_6\text{H}_{12}\text{NO}$  [ $\text{MH}^+$ ] calculated 114.09189; observed 114.09195.

### Synthesis of di-7-aza-bicyclo[2.2.1]heptane-7-carboxylic acid tert-butyl ester sulfite (**83**)



To a stirred solution of alcohol (**80**) (0.218 g;  $1.02 \times 10^{-3}$  mol) and pyridine (0.73 g,  $9.2 \times 10^{-3}$  mol) in 8 ml of

anhydrous dichloromethane was added thionyl bromide (SOBr<sub>2</sub>) (0.85 g, 4.09 x 10<sup>-3</sup> mol) drop-wise at 0 °C under nitrogen. The reaction mixture was stirred for 3 h at 0 °C and then washed with brine (3 x 5 ml). The organic layer was separated, dried over anhydrous MgSO<sub>4</sub> and concentrated. The crude residue was chromatographed on silica, eluting with 1:4 diethyl ether:petroleum (bp 40-60 °C) to afford (**83**) (0.2 g, 68%) as a yellow solid: R<sub>f</sub> 0.38 (1:1 diethyl ether:petroleum (bp 40-60 °C)), mp 89-90 °C.

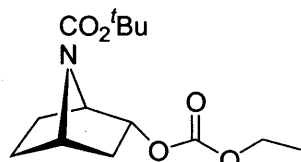
<sup>1</sup>H NMR (300 MHz, CDCl<sub>3</sub>) δ: 4.86 – 4.83 (m, 1H, H<sub>2</sub>), 4.28 (br s, 1H, H<sub>1</sub>), 4.18 (br s, 1H, H<sub>4</sub>), 2.32 – 2.22 (m, 1H, H<sub>3-exo</sub>), 2.12 – 2.01 (m, 1H, H<sub>6-endo</sub>), 1.87 – 1.66 (m, 2H, H<sub>5-exo</sub>, H<sub>6-exo</sub>), 1.57 – 1.49 (m, 1H, H<sub>5-endo</sub>), 1.45 (s, 9H, OC(CH<sub>3</sub>)<sub>3</sub>), 1.38 – 1.23 (m, 1H, H<sub>3-endo</sub>).

<sup>13</sup>C NMR (75 MHz, CDCl<sub>3</sub>) δ: 155.1 (C=O), 80.2 (OC(CH<sub>3</sub>)<sub>3</sub>), 71.4 (C<sub>2</sub>), 58.9 (C<sub>1</sub>), 56.7 (C<sub>4</sub>), 37.6 (C<sub>3</sub>), 29.3 (C<sub>6</sub>), 28.2 (OC(CH<sub>3</sub>)<sub>3</sub>), 21.8 (C<sub>5</sub>).

MS <sup>m/z</sup>: 473 (MH<sup>+</sup>). C<sub>22</sub>H<sub>37</sub>N<sub>2</sub>O<sub>7</sub>S [MH<sup>+</sup>] calculated 473.23215; observed 473.23202.

$\nu_{\max}$ : 1692s, 1359s, 1306m, 1255w, 1159s, 1104s, 1012m, 961m, 904w, 853m, 749m.

### Synthesis of 2-ethoxycarbonyloxy-7-aza-bicyclo[2.2.1]heptane-7-carboxylic acid tert-butyl ester (**85**)



Diethyl azodicarboxylate (DEAD) (0.192 g; 1.10 x 10<sup>-3</sup> mol) was added dropwise with stirring to a 0 °C solution of triphenylphosphine (PPh<sub>3</sub>) (0.295 g; 1.13 x 10<sup>-3</sup> mol) in dry THF (3 ml) under argon. After 20 min, the lithium bromide (0.195 g; 2.25 x 10<sup>-3</sup> mol) was added to solution followed by the alcohol (**80**) (0.048 g; 2.25 x 10<sup>-4</sup>) dissolved in a minimum volume of dry THF. The mixture was stirred at room temperature overnight, then the solvent was removed. The residue was poured into water and extracted twice with dichloromethane (4 ml). The combined extracts were washed with brine, dried over anhydrous MgSO<sub>4</sub>, and evaporated. The crude residue was chromatographed on silica, eluting with 5:95 diethyl ether:petroleum (bp 40-60 °C) to afford (**85**) (0.038 g, 61%) as a colourless oil: R<sub>f</sub> 0.57 (1:1 diethyl ether:petroleum (bp 40-60 °C)).

<sup>1</sup>H NMR (300 MHz, C<sub>6</sub>D<sub>6</sub>) δ: 5.00 – 4.94 (m, 1H, H<sub>2</sub>), 4.54 (br s, 1H, H<sub>1</sub>) 4.03 (br s, 1H, H<sub>4</sub>), 3.88 (q, *J* = 7.1 Hz, 2H, OCH<sub>2</sub>CH<sub>3</sub>), 2.05 (dddd, *J*<sub>3-exo,3-endo</sub> = 12.7 Hz, *J*<sub>2,3-exo</sub> = 10.2 Hz, *J*<sub>3-exo,4</sub> = 5.2 Hz, *J*<sub>3-exo,5-exo</sub> = 2.3 Hz, 1H, H<sub>3-exo</sub>), 1.94 – 1.87 (m, 1H, H<sub>6-endo</sub>), 1.58

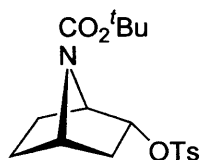
– 1.49 (m, 2H, H<sub>5-exo</sub>, H<sub>6-exo</sub>), 1.37 (s, 9H, OC(CH<sub>3</sub>)<sub>3</sub>), 1.16 – 1.49 (m, 1H, H<sub>5-endo</sub>), 0.99 (dd,  $J_{3-endo,3-exo} = 13.2$  Hz,  $J_{3-endo,2} = 3.2$  Hz, 1H, H<sub>3-endo</sub>), 0.92 (t,  $J = 7.1$  Hz, 3H, OCH<sub>2</sub>CH<sub>3</sub>).

<sup>13</sup>C NMR (75 MHz, C<sub>6</sub>D<sub>6</sub>) δ: 155.2, 154.6 (2 x C=O), 80.0 (OC(CH<sub>3</sub>)<sub>3</sub>), 75.6 (C<sub>2</sub>), 65.8 (OCH<sub>2</sub>CH<sub>3</sub>), 58.1 (C<sub>1</sub>), 56.7 (C<sub>4</sub>), 36.7 (C<sub>3</sub>), 29.1 (C<sub>6</sub>), 28.2 (OC(CH<sub>3</sub>)<sub>3</sub>), 21.8 (C<sub>5</sub>), 14.2 (OCH<sub>2</sub>CH<sub>3</sub>).

MS  $m/z$ : 473 (MH<sup>+</sup>). C<sub>22</sub>H<sub>37</sub>N<sub>2</sub>O<sub>7</sub>S [MH<sup>+</sup>] calculated 286.16545; observed 286.16554.

$\nu_{max}$ : 1745s, 1701s, 1451w, 1365s, 1306m, 1250s, 1160s, 1097m, 1016s, 790m.

### Synthesis of 2-(toluene-4-sulfonyloxy)-7-aza-bicyclo[2.2.1]heptane-7-carboxylic acid tert-butyl ester (**86**)



In accordance with the general procedure of Kabalka,<sup>116</sup> alcohol (**80**) (0.059 g;  $2.77 \times 10^{-4}$  mol) was dissolved in 3 ml of pyridine and cooled to 0 °C. To this solution, *p*-toluenesulfonyl chloride (0.079 g;  $4.15 \times 10^{-4}$ ) was added. After 10 min of stirring at 0 °C, the mixture was kept for 24 h at room temperature. The mixture was then poured into water, extracted twice with 4 ml of dichloromethane and dried over anhydrous Na<sub>2</sub>SO<sub>4</sub>. Removal of the solvent by rotary evaporation and chromatography of the resulting residue on silica gel eluting with 15:85 diethyl ether:petroleum (bp 40-60 °C) gav the tosylate (**86**) (0.055 g; 54%) as a colourless oil: R<sub>f</sub> 0.56 (15:85 diethyl ether:petroleum (bp 40-60 °C)).

<sup>1</sup>H NMR (300 MHz, CDCl<sub>3</sub>) δ: 7.79 (d,  $J = 8.2$  Hz, 2H, 2 x aryl CH), 7.36 (d,  $J = 8.2$  Hz, 2H, 2 x aryl CH), 4.74 – 4.69 (m, 1H, H<sub>2</sub>), 4.18 (br t,  $J = 4.7$  Hz, 1H, H<sub>1</sub>) 4.12 (br t,  $J = 4.9$  Hz, 1H, H<sub>4</sub>), 2.46 (s, 3H, aryl CH<sub>3</sub>), 2.21 – 2.11 (m, 1H, H<sub>3-exo</sub>), 2.07 – 1.99 (m, 1H, H<sub>5-endo</sub> or H<sub>6-endo</sub>), 1.84 – 1.72 (m, 1H, H<sub>5-exo</sub>), 1.67 – 1.61 (m, 1H, H<sub>6-exo</sub>), 1.54 – 1.47 (m, 1H, H<sub>5-endo</sub> or H<sub>6-endo</sub>), 1.42 (s, 9H, OC(CH<sub>3</sub>)<sub>3</sub>), 1.29 (dd,  $J_{3-endo,3-exo} = 13.5$  Hz,  $J_{3-endo,2} = 2.8$  Hz, 1H, H<sub>3-endo</sub>).

<sup>13</sup>C NMR (100 MHz, CDCl<sub>3</sub>) δ: 155.0 (C=O), 145.1, 133.3 (2 x aryl C), 130.0, 127.9 (4 x aryl CH), 80.2 (OC(CH<sub>3</sub>)<sub>3</sub>), 78.1 (C<sub>2</sub>), 65.8 (OCH<sub>2</sub>CH<sub>3</sub>), 58.4 (C<sub>1</sub>), 56.6 (C<sub>4</sub>), 36.7 (C<sub>3</sub>), 29.1 (C<sub>6</sub>), 28.2 (OC(CH<sub>3</sub>)<sub>3</sub>), 21.7 (C<sub>5</sub>), 21.6 (aryl CH<sub>3</sub>).

MS  $m/z$ : 473 (MH<sup>+</sup>). C<sub>22</sub>H<sub>37</sub>N<sub>2</sub>O<sub>7</sub>S [MH<sup>+</sup>] calculated 368.15317; observed 368.15310.

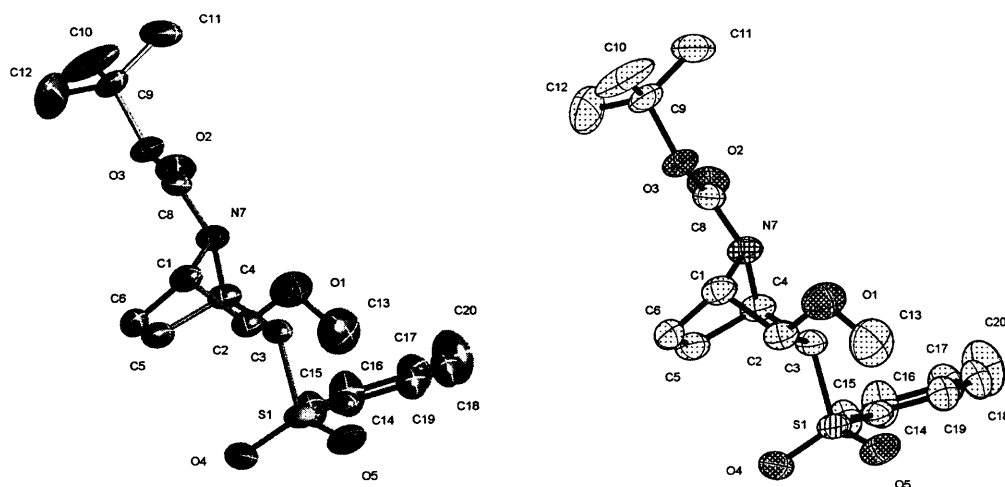
### **Molecular modeling**

Molecular models were determined using the Spartan Pro program; equilibrium geometries were calculated with the Hartree-Fock, 6-31G\* method.

**Appendix**  
**Crystal structure data**

## Appendix

### Crystal structure data

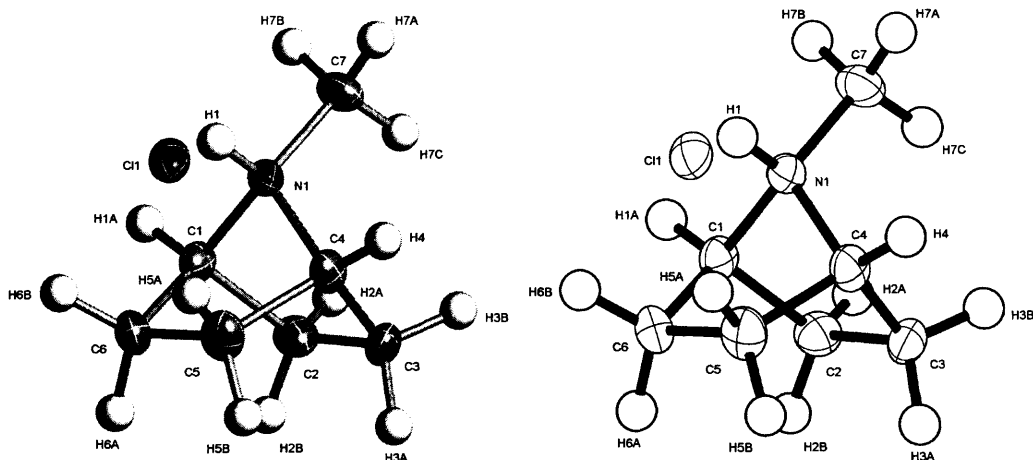


Figures show the atom label scheme and 50% displacement ellipsoids.

Crystal data and structure refinement for (34).

Identification code	05049	
Empirical formula	C <sub>19</sub> H <sub>25</sub> N O <sub>5</sub> S	
Formula weight	379.46	
Temperature	150(2) K	
Wavelength	0.71073 Å	
Crystal system	Triclinic	
Space group	P-1	
Unit cell dimensions	a = 11.529(3) Å	∠ = 71.656(3)°.
	b = 12.204(3) Å	∠ = 79.609(4)°.
	c = 14.965(3) Å	∠ = 79.105(4)°.
Volume	1946.0(7) Å <sup>3</sup>	
Z	4	
Density (calculated)	1.295 Mg/m <sup>3</sup>	
Absorption coefficient	0.195 mm <sup>-1</sup>	
F(000)	808	
Crystal size	0.35 x 0.18 x 0.16 mm <sup>3</sup>	
Theta range for data collection	1.45 to 25.00°.	
Index ranges	-13 ≤ h ≤ 13, -14 ≤ k ≤ 14, -17 ≤ l ≤ 17	

Reflections collected	14004
Independent reflections	6787 [R(int) = 0.0201]
Completeness to theta = 25.00°	99.0 %
Absorption correction	Empirical
Max. and min. transmission	0.98 and 0.81
Refinement method	Full-matrix least-squares on F <sup>2</sup>
Data / restraints / parameters	6787 / 0 / 479
Goodness-of-fit on F <sup>2</sup>	1.034
Final R indices [I > 2sigma(I)]	R1 = 0.0558, wR2 = 0.1448
R indices (all data)	R1 = 0.0656, wR2 = 0.1512
Largest diff. peak and hole	0.572 and -0.585 e.Å <sup>-3</sup>

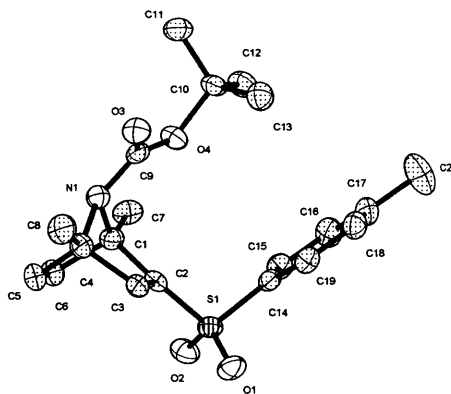
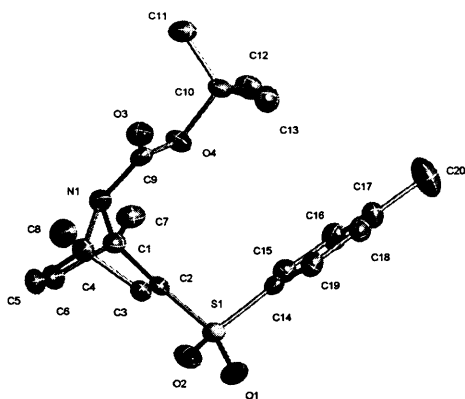


Figures show 50% displacement ellipsoids. Shown are the cation and the anion (Cl).

Crystal data and structure refinement for **(1a:HCl)**.

Identification code	06077	
Empirical formula	C <sub>7</sub> H <sub>14</sub> Cl N	
Formula weight	147.64	
Temperature	150(2) K	
Wavelength	0.71073 Å	
Crystal system	Monoclinic	
Space group	P2(1)	
Unit cell dimensions	a = 6.2225(12) Å	∠ = 90°.
	b = 9.8524(19) Å	∠ = 111.561(3)°.
	c = 6.8523(14) Å	∠ = 90°.
Volume	390.70(13) Å <sup>3</sup>	
Z	2	
Density (calculated)	1.255 Mg/m <sup>3</sup>	
Absorption coefficient	0.403 mm <sup>-1</sup>	
F(000)	160	
Crystal size	0.29 x 0.24 x 0.15 mm <sup>3</sup>	
Theta range for data collection	3.52 to 25.97°.	
Index ranges	-7 ≤ h ≤ 7, -12 ≤ k ≤ 12, -8 ≤ l ≤ 8	
Reflections collected	2988	
Independent reflections	1498 [R(int) = 0.0257]	
Completeness to theta = 25.97°	99.6 %	
Absorption correction	Empirical	

Max. and min. transmission	0.962 and 0.801
Refinement method	Full-matrix least-squares on F <sup>2</sup>
Data / restraints / parameters	1498 / 1 / 84
Goodness-of-fit on F <sup>2</sup>	1.061
Final R indices [I>2sigma(I)]	R1 = 0.0261, wR2 = 0.0689
R indices (all data)	R1 = 0.0266, wR2 = 0.0691
Absolute structure parameter	0.07(6)
Largest diff. peak and hole	0.180 and -0.177 e.Å <sup>-3</sup>

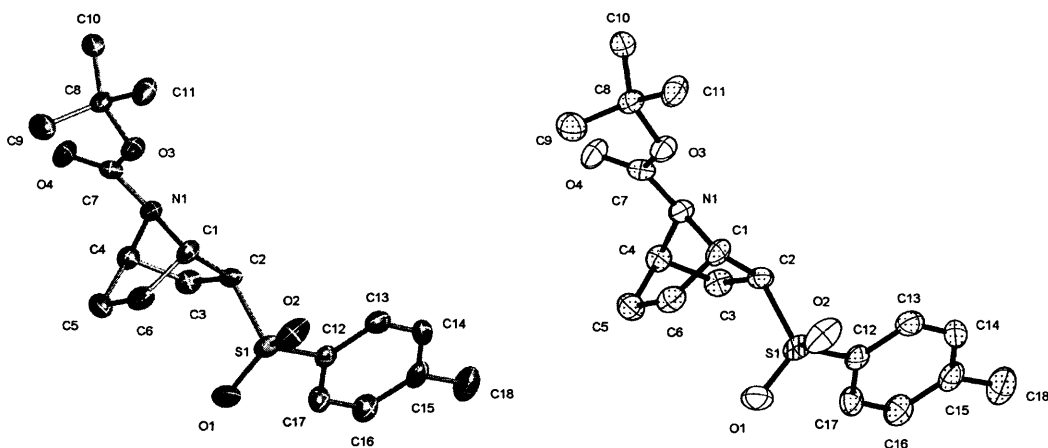


Figures show 50% displacement ellipsoids. The hydrogen atoms have been omitted for clarity.

Crystal data and structure refinement for (47).

Identification code	06022	
Empirical formula	C <sub>20</sub> H <sub>25</sub> N O <sub>4</sub> S	
Formula weight	375.47	
Temperature	150(2) K	
Wavelength	0.71073 Å	
Crystal system	Monoclinic	
Space group	P2(1)/c	
Unit cell dimensions	a = 11.441(2) Å	∠ = 90°.
	b = 18.389(3) Å	∠ = 97.010(3)°.
	c = 9.5772(17) Å	∠ = 90°.
Volume	1999.9(6) Å <sup>3</sup>	
Z	4	
Density (calculated)	1.247 Mg/m <sup>3</sup>	
Absorption coefficient	0.185 mm <sup>-1</sup>	
F(000)	800	
Crystal size	0.35 x 0.23 x 0.20 mm <sup>3</sup>	
Theta range for data collection	1.79 to 25.00°.	
Index ranges	-13 ≤ h ≤ 13, -21 ≤ k ≤ 21, -11 ≤ l ≤ 11	
Reflections collected	14304	
Independent reflections	3529 [R(int) = 0.0346]	
Completeness to theta = 25.00°	100.0 %	
Absorption correction	Empirical	

Max. and min. transmission	0.983 and 0.796
Refinement method	Full-matrix least-squares on F <sup>2</sup>
Data / restraints / parameters	3529 / 0 / 241
Goodness-of-fit on F <sup>2</sup>	1.031
Final R indices [I>2sigma(I)]	R1 = 0.0400, wR2 = 0.0990
R indices (all data)	R1 = 0.0479, wR2 = 0.1030
Largest diff. peak and hole	0.334 and -0.246 e.Å <sup>-3</sup>

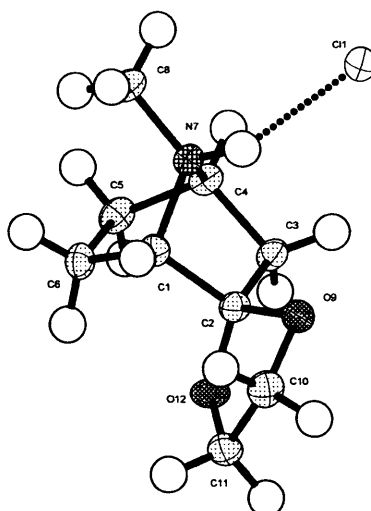
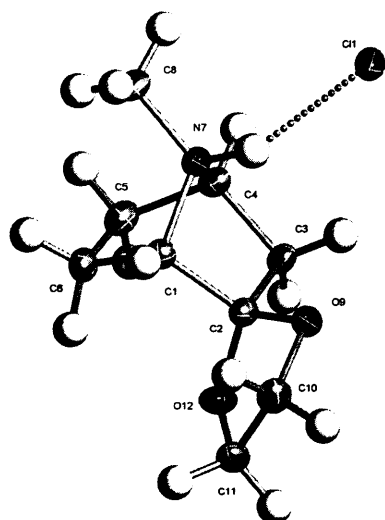


Figures show 50% displacement ellipsoids. The hydrogen atoms have been omitted for clarity.

Crystal data and structure refinement for *endo*-(39).

Identification code	06016	
Empirical formula	C <sub>18</sub> H <sub>25</sub> N O <sub>4</sub> S	
Formula weight	351.45	
Temperature	150(2) K	
Wavelength	0.71073 Å	
Crystal system	Orthorhombic	
Space group	P2(1)2(1)2(1)	
Unit cell dimensions	a = 5.7708(10) Å	∠ = 90°.
	b = 11.602(2) Å	∠ = 90°.
	c = 26.919(5) Å	∠ = 90°.
Volume	1802.3(6) Å <sup>3</sup>	
Z	4	
Density (calculated)	1.295 Mg/m <sup>3</sup>	
Absorption coefficient	0.201 mm <sup>-1</sup>	
F(000)	752	
Crystal size	0.22 x 0.14 x 0.07 mm <sup>3</sup>	
Theta range for data collection	1.91 to 25.00°.	
Index ranges	-6 ≤ h ≤ 6, -13 ≤ k ≤ 13, -32 ≤ l ≤ 32	
Reflections collected	13020	
Independent reflections	3168 [R(int) = 0.0768]	
Completeness to theta = 25.00°	99.9 %	
Absorption correction	Empirical	

Max. and min. transmission	0.981 and 0.663
Refinement method	Full-matrix least-squares on F <sup>2</sup>
Data / restraints / parameters	3168 / 0 / 222
Goodness-of-fit on F <sup>2</sup>	0.984
Final R indices [I>2sigma(I)]	R1 = 0.0536, wR2 = 0.0816
R indices (all data)	R1 = 0.0741, wR2 = 0.0869
Absolute structure parameter	0.30(11)
Largest diff. peak and hole	0.254 and -0.256 e.Å <sup>-3</sup>

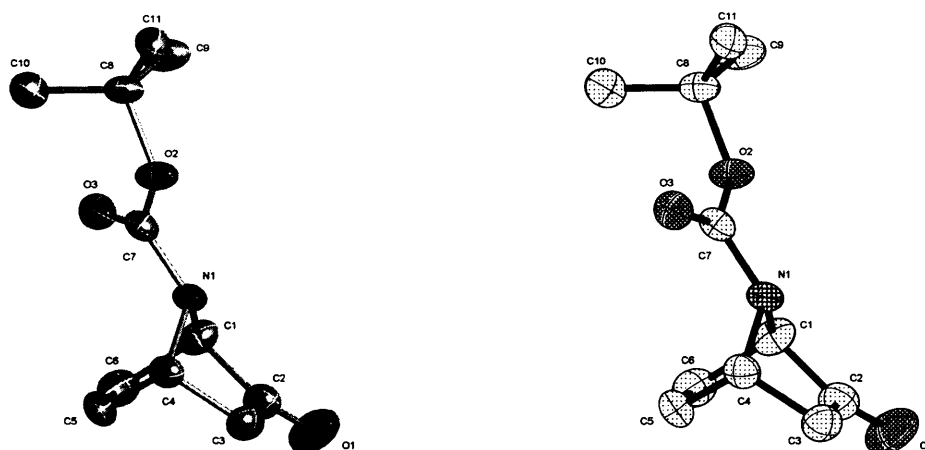


Figures show the molecular structure with 50% displacement ellipsoids.

Crystal data and structure refinement for **(68:HCl)**.

Identification code	04157	
Empirical formula	C <sub>9</sub> H <sub>16</sub> Cl N O <sub>2</sub>	
Formula weight	205.68	
Temperature	150(2) K	
Wavelength	0.71073 Å	
Crystal system	Orthorhombic	
Space group	Pbca	
Unit cell dimensions	a = 8.5642(16) Å	∠ = 90°.
	b = 11.879(2) Å	∠ = 90°.
	c = 19.417(4) Å	∠ = 90°.
Volume	1975.3(7) Å <sup>3</sup>	
Z	8	
Density (calculated)	1.383 Mg/m <sup>3</sup>	
Absorption coefficient	0.355 mm <sup>-1</sup>	
F(000)	880	
Crystal size	0.36 x 0.21 x 0.19 mm <sup>3</sup>	
Theta range for data collection	2.10 to 25.00°.	
Index ranges	-10 ≤ h ≤ 10, -14 ≤ k ≤ 14, -23 ≤ l ≤ 23	
Reflections collected	13042	
Independent reflections	1738 [R(int) = 0.0675]	
Completeness to theta = 25.00°	100.0 %	

Absorption correction	None
Refinement method	Full-matrix least-squares on F <sup>2</sup>
Data / restraints / parameters	1738 / 0 / 119
Goodness-of-fit on F <sup>2</sup>	1.078
Final R indices [I>2sigma(I)]	R1 = 0.0329, wR2 = 0.0867
R indices (all data)	R1 = 0.0359, wR2 = 0.0886
Largest diff. peak and hole	0.296 and -0.211 e.Å <sup>-3</sup>

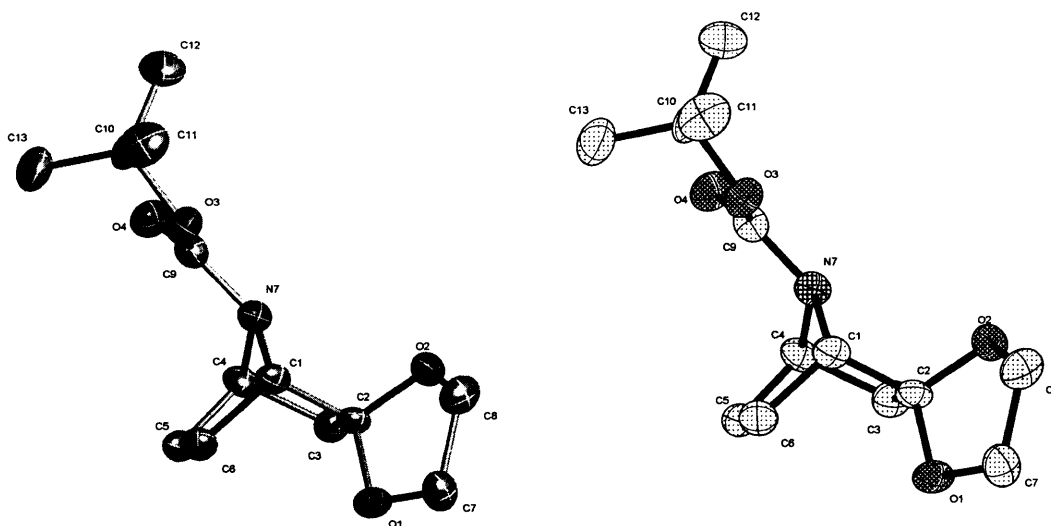


Figures show 50% displacement ellipsoids. The hydrogen atoms have been omitted for clarity.

Crystal data and structure refinement for (71).

Identification code	05125	
Empirical formula	C <sub>11</sub> H <sub>15</sub> N O <sub>3</sub>	
Formula weight	209.24	
Temperature	150(2) K	
Wavelength	0.71073 Å	
Crystal system	Monoclinic	
Space group	Cc	
Unit cell dimensions	a = 19.264(7) Å	∠ = 90°.
	b = 5.718(2) Å	∠ = 112.165(6)°.
	c = 10.900(4) Å	∠ = 90°.
Volume	1112.0(7) Å <sup>3</sup>	
Z	4	
Density (calculated)	1.250 Mg/m <sup>3</sup>	
Absorption coefficient	0.091 mm <sup>-1</sup>	
F(000)	448	
Crystal size	0.23 x 0.11 x 0.04 mm <sup>3</sup>	
Theta range for data collection	2.28 to 24.99°.	
Index ranges	-22 ≤ h ≤ 22, -6 ≤ k ≤ 6, -12 ≤ l ≤ 12	
Reflections collected	3807	
Independent reflections	1908 [R(int) = 0.0833]	

Completeness to theta = 24.99°	99.9 %
Absorption correction	None
Refinement method	Full-matrix least-squares on F <sup>2</sup>
Data / restraints / parameters	1908 / 2 / 139
Goodness-of-fit on F <sup>2</sup>	0.974
Final R indices [I>2sigma(I)]	R1 = 0.0596, wR2 = 0.1026
R indices (all data)	R1 = 0.0854, wR2 = 0.1125
Absolute structure parameter	-1(2)
Largest diff. peak and hole	0.148 and -0.158 e.Å <sup>-3</sup>



Figures show the atom label scheme and 50% displacement ellipsoids. H atoms are omitted for clarity.

Crystal data and structure refinement for (72).

Identification code	05020	
Empirical formula	C <sub>13</sub> H <sub>19</sub> N O <sub>4</sub>	
Formula weight	253.29	
Temperature	150(2) K	
Wavelength	0.71073 Å	
Crystal system	Monoclinic	
Space group	C2/c	
Unit cell dimensions	a = 37.918(18) Å	∠ = 90°.
	b = 5.968(3) Å	∠ = 101.148(13)°.
	c = 11.659(5) Å	∠ = 90°.
Volume	2589(2) Å <sup>3</sup>	
Z	8	
Density (calculated)	1.300 Mg/m <sup>3</sup>	
Absorption coefficient	0.096 mm <sup>-1</sup>	
F(000)	1088	
Crystal size	0.34 x 0.24 x 0.05 mm <sup>3</sup>	
Theta range for data collection	2.19 to 25.00°.	
Index ranges	-44 ≤ h ≤ 44, -7 ≤ k ≤ 7, -13 ≤ l ≤ 13	
Reflections collected	8605	
Independent reflections	2265 [R(int) = 0.1843]	

Completeness to theta = 25.00°	99.5 %
Absorption correction	None
Refinement method	Full-matrix least-squares on F <sup>2</sup>
Data / restraints / parameters	2265 / 0 / 166
Goodness-of-fit on F <sup>2</sup>	1.100
Final R indices [I>2sigma(I)]	R1 = 0.0987, wR2 = 0.2042
R indices (all data)	R1 = 0.1647, wR2 = 0.2333
Largest diff. peak and hole	0.264 and -0.236 e.Å <sup>-3</sup>

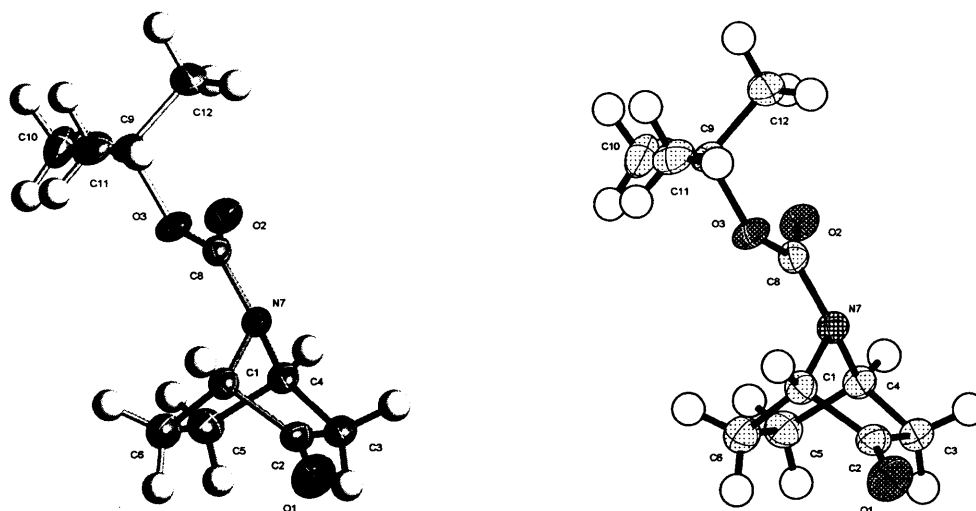


Figure shows the atom label scheme and 50% displacement ellipsoids.

Crystal data and structure refinement for (79).

Identification code	04168	
Empirical formula	C <sub>11</sub> H <sub>17</sub> N O <sub>3</sub>	
Formula weight	211.26	
Temperature	150(2) K	
Wavelength	0.71073 Å	
Crystal system	Monoclinic	
Space group	P2(1)/n	
Unit cell dimensions	a = 13.512(2) Å	∠ = 90°.
	b = 5.7961(11) Å	∠ = 91.472(4)°.
	c = 14.427(3) Å	∠ = 90°.
Volume	1129.5(4) Å <sup>3</sup>	
Z	4	
Density (calculated)	1.242 Mg/m <sup>3</sup>	
Absorption coefficient	0.090 mm <sup>-1</sup>	
F(000)	456	
Crystal size	0.30 x 0.13 x 0.09 mm <sup>3</sup>	
Theta range for data collection	2.04 to 25.00°.	
Index ranges	-16 ≤ h ≤ 15, -6 ≤ k ≤ 6, -16 ≤ l ≤ 17	
Reflections collected	7710	
Independent reflections	1978 [R(int) = 0.0972]	
Completeness to theta = 25.00°	99.9 %	

Absorption correction	None
Refinement method	Full-matrix least-squares on F <sup>2</sup>
Data / restraints / parameters	1978 / 0 / 139
Goodness-of-fit on F <sup>2</sup>	0.985
Final R indices [I > 2σ(I)]	R1 = 0.0613, wR2 = 0.1272
R indices (all data)	R1 = 0.1052, wR2 = 0.1420
Largest diff. peak and hole	0.569 and -0.168 e.Å <sup>-3</sup>

## References

## References

1. Spande, T. F.; Garraffo, H. M.; Edwards, M. W.; Yeh, H. J. C.; Pannell, L.; Daly, J. *W. J. Am. Chem. Soc.* **1992**, *114*, 3475-3478.
2. Lehn, J. M. *Chem. Forsch.* **1970**, *15*, 311-377.
3. Nelsen, S. F.; Ippoliti, J. T.; Frigo, T. B.; Petillo, P. A. *J. Am. Chem. Soc.* **1989**, *111*, 1776-1781.
4. Altenbach, H.; Cnosta, D.; Martin, H.; Mayer, B.; Muller, M.; Vogel, E. *Chem. Ber.* **1991**, *124*, 791-801.
5. Nelsen, S. F.; Blackstock, S. C.; Steffek, D. J.; Cunkle, G. T.; Kurtzweil, M. L. *J. Am. Chem. Soc.* **1988**, *110*, 6149-6153.
6. Marchand, A. P.; Allen, R. W. *J. Org. Chem.* **1975**, *40*, 2551-2552.
7. Altenbach, H.; Blech, B.; Vogel, E. *Angew. Chem. Suppl.* **1982**, 1614-1621.
8. Rauk, A.; Allen, L.C.; Mislow, K. *Angew. Chem. Int. Edn.* **1970**, *9*, 400.
9. Kessler, M. *Angew. Chem. Int. Edn.* **1970**, *9*, 219.
10. Lambert, J. B.; Topics in Stereochemistry, Eds., Allinger, N. L. and Eliel, E. L., Wiley Interscience, New York, **1971**, 6, 19.
11. Davies, J. W.; Malpass, J. R.; Fawcett, J.; Prouse, L. J. S.; Lindsay, R.; Russell, D. *R. J. Chem. Soc. Chem. Commun.* **1986**, 1135-1137.
12. Forni, A.; Moretti, I.; Torre, G.; Brukner, S.; Malpezzi, L.; Di Silvestro, G. *J. Chem. Soc. Perkin. Trans. II*, **1984**, 791-797.
13. Davies, J. W.; Durrant, M. L.; Naylor, A.; Malpass, J. R. *Tetrahedron*, **1995**, *51*, 8655-8664.
14. Malpass, J. R.; Butler, D. N.; Johnston, M. R.; Hammond, M. L. A.; Warrenner, R. *N. Org. Lett.* **2000**, *2*, 725-728.
15. Bushweller, C. H.; Brown, J. H.; DiMeglio, C.M.; Gribble, G. W.; Eaton, J. T.; LeHoullier, C. S.; Olson, E. R. *J. Org. Chem.* **1995**, *60*, 268-271.
16. Deloughry, W. J.; Sutherland, I. O. *J. Chem. Soc. Chem. Commun.* **1971**, 1104-1105.
17. Kincaid, J. F.; Henriques, F. C.; Jr. *J. Am. Chem. Soc.* **1940**, *62*, 1474-1477.
18. Brois, S. J. *J. Am. Chem. Soc.* **1968**, *90*, 508-509.
19. Malpass, J. R.; Tweddle, N. J. *J. Chem. Soc., Perkin Trans. II*, **1978**, 120-127.
20. Chiang, J. F.; Wilcox, C. F.; Jr.; Bauer, S. H. *J. Am. Chem. Soc.* **1968**, *90*, 3149-3157.

21. Marchand, A. P.; Allen, R. W. *Tetrahedron Lett.* **1977**, 619-622.
22. Davies, J. W.; Durrant, M. L.; Walker, M. P.; Belkacemi, D.; Malpass, J. R. *Tetrahedron* **1992**, *48*, 861-884.
23. Davies, J. W.; Durrant, M. L.; Walker, M. P.; Malpass, J. R. *Tetrahedron* **1992**, *48*, 4379-4398.
24. Davies, J. W.; Malpass, J. R. *Tetrahedron Lett.* **1985**, *26*, 4537-4538.
25. Belkacemi, D.; Davies, J. W.; Malpass, J. R.; Naylor, A.; Smith, C. R. *Tetrahedron* **1992**, *48*, 10161-10176.
26. Ohwada, T.; Achiwa, T.; Okamoto, I.; Shudo, K. *Tetrahedron Letters*, **1998**, *39*, 865-868.
27. Otani, Y.; Nagae, O.; Naruse, Y.; Inagaki, S.; Ohno, M.; Yamaguchi, K.; Yamamoto, G.; Uchiyama, M.; Ohwada, T. *J. Am. Chem. Soc.* **2003**, *125*, 15191-15199.
28. Anet, F. A. L.; Yavari, I. *J. Am. Chem. Soc.* **1977**, *99*, 2794-2796.
29. Anet, F. A. L.; Yavari, I. *Tetrahedron Lett.* **1977**, 3207-3210.
30. Nelsen, S. F.; Wiseman, G. R. *J. Am. Chem. Soc.* **1976**, *98*, 1842-1850.
31. Riddell, F. G.; Turner, E. S.; Boyd, A. *Tetrahedron* **1979**, *35*, 259-261.
32. Allerhand, A.; Gutowsky, H. S.; Jonas, J.; Meinzer, R. A. *J. Am. Chem. Soc.* **1966**, *88*, 3185-3194.
33. Shanan-Atidi, H.; Bar-Eli, K. *J. Phys. Chem.* **1970**, *74*, 961-963.
34. Van Deursen, F. W.; Philips-Duphar, N. V. *Org. Magn. Reson.* **1971**, *3*, 221-242.
35. Crowley, P. J.; Robinson, M. J. T.; Ward, M. G. *Tetrahedron* **1977**, *33*, 915-925.
36. Rautenstrauch, V. *J. Chem. Soc. Chem. Commun.* **1969**, 1122-1123.
37. Davies, J. W.; Malpass, J. R.; Fawcett, J.; Prouse, L. J. S.; Lindsay, R.; Russell, D. *R. J. Chem. Soc. Chem. Commun.* **1986**, 1135-1137.
38. Davies, J. W.; Malpass, J. R.; Moss, R. E. *Tetrahedron Lett.* **1985**, *26*, 4533-4536.
39. Nelsen, S. F.; Gannett, P. M. *J. Am. Chem. Soc.* **1982**, *104*, 5292-5297.
40. Durrant, M. L.; Malpass, J. R. *Tetrahedron*, **1995**, *51*, 7063-7076.
41. Gribble, G. W.; Easton, N. R.; Jr.; Eaton, J. T. *Tetrahedron Lett.* **1970**, *11*, 1075-1078.
42. Malpass, J. R.; Walker, M. P. *J. Chem. Soc. Chem. Commun.* **1979**, 585-586.
43. Grutzner, J. B.; Jaukelat, M.; Dence, J. B.; Smith, R. A.; Roberts, J. D. *J. Am. Chem. Soc.* **1970**, *92*, 7107-7120.
44. Nguyen, T. T. T.; Delseth, C.; Kintzinger, J. P.; Carrupt, P. A.; Vogel, P.

*Tetrahedron* **1980**, *36*, 2793-2797.

45. a) Quin, L. D.; Mesch, K. A. *J. Chem. Soc. Chem. Commun.* **1980**, 959-961.  
b) Quin, L. D.; Kaster, K. C.; Kisalus, J. C.; Mesch, K. A. *J. Am. Chem. Soc.* **1984**, *106*, 7021-7032.
46. Sakuri, H.; Nakadaira, Y.; Koyama, T.; Sakaba, H. *Chem. Lett.* **1983**, 213-216.
47. Martin, G. J.; Martin, M. L.; Gouesnard, J. P. *<sup>15</sup>N NMR Spectroscopy*, Springer-Verlag, Berlin, **1981**.
48. Jenkins, M. N.; Nash, J. J.; Morrison, H. *Tetrahedron Letters*, **2002**, *43*, 3773-3775.
49. Nash, J. J.; Waugh, T.; Morrison, H. *Tetrahedron Letters*, **1998**, *39*, 6449-6452.
50. Belostotskii, A. M.; Gottlieb, H. E.; Shokhen, M. *J. Org. Chem.* **2002**, *67*, 9257-9266.
51. Waykole, L.; Paquette, L. A. *Org. Syn.* **1988**, *67*, 149-156.
52. Eisch, J. J.; Shafii, B.; Odom, J. D.; Rheingold, A. L. *J. Am. Chem. Soc.* **1990**, *112*, 1847-1853.
53. Leung-Toung, R.; Liu, Y.; Muchowski, J. M.; Wu, Y. *J. Org. Chem.* **1998**, *63*, 3235-3250.
54. Ciamician, G.; Dennstedt, M. *Chem. Ber.* **1882**, *15*, 2597.
55. Quin, L. D.; Kaster, K. C.; Marsi, B. G.; Miller, J. A. *J. Org. Chem.* **1986**, *51*, 3724-3726.
56. a. Stothers, J. B.; "Carbon-13 NMR spectroscopy", Academic Press, New York, **1972**.  
b. Levy, G. C.; Lichter, R. L.; Nelson, G. L.; "Carbon-13 Nuclear Magnetic Resonance Spectroscopy", Wiley, New York, **1980**.
57. Leung-Toung, R.; Liu, Y.; Muchowski, J. M.; Wu, Y. *Tetrahedron Letters*, **1994**, *35*, 1639-1642.
58. Hodgson, D. M.; Maxwell, C. R.; Wisedale, R.; Matthews, I. R.; Carpenter, K. J.; Dickenson, A. H.; Wonnacott, S. *J. Chem. Soc., Perkin Trans.* **2001**, *1*, 3150-3158.
59. Carroll, F. I.; Liang, F.; Navarro, H. A.; Brieady, L. E.; Abraham, P.; Damaj, M. I.; Martin, B. *J. Me. Chem.* **2001**, *44*, 2229-2237.
60. Hodgson, D. M.; Maxwell, C. R.; Miles, T. J.; Paruch, E.; Matthews, I. R.; Witherington, J. *Tetrahedron*, **2004**, *60*, 3611-3624.
61. Belkacemi, D.; Malpass, J. R. *Tetrahedron*, **1993**, *49*, 9105-9116.
62. Fraser, R. R.; Swingle, R. B. *Can. J. Chem.* **1970**, *48*, 2065-2074.
63. Braun, J. V.; Schwarz, K. *Ann.* **1930**, *481*, 56-68.

64. Dolci, L.; Dolle, F.; Valette, H.; Vaufrey, F.; Fuseau, C.; Bottlaender, M.; Crouzel, C. *Bioorg. Med. Chem.* **1999**, *7*, 467-479.
65. Kaiser, H.; Muchowski, J. M. *J. Org. Chem.* **1984**, *49*, 4203-4209.
66. Hodgson, D. M.; Bebbington, W. P.; Willis, P. *Org. Biomol. Chem.* **2003**, *1*, 3787-3798.
67. Pouchert, C. J.; Behnke, J. *The Aldrich Library of <sup>13</sup>C and <sup>1</sup>H FT NMR Spectra*, 1 ed. **1993**, Vol. 1, p. 72.
68. Borch, R. F.; Hassid, A. I. *J. Org. Chem.* **1972**, *37*, 1673-1674.
69. Cristol, S. J.; Nachtigall, G. W. *J. Org. Chem.* **1967**, *32*, 3738-3743.
70. Zhang, C.; Ballay II, C. J.; Trudell, M. L. *J. Chem. Soc., Perkin Trans.* **1999**, *1*, 675-676.
71. Pavri, N. P.; Trudell, M. L. *Tetrahedron Lett.* **1997**, *38*, 7993-7996.
72. Fletcher, S. R.; Baker, R.; Chambers, M. S.; Hobbs, S. C.; Mitchell, P. J. *J. Chem. Soc. Chem. Commun.* **1993**, *15*, 1216-1218.
73. Fletcher, S. R.; Baker, R.; Chambers, M. S.; Herbert, R. H.; Hobbs, S. C.; Thomas, S. R.; Verrier, H. M.; Watt, A. P.; Ball, R. G. *J. Org. Chem.* **1994**, *59*, 1771-1778.
74. Chunming, Z.; Trudell, M. L. *J. Org. Chem.* **1996**, *61*, 7189-7191.
75. Moreno-Vargas, A. J.; Vogel, P. *Tetrahedron: Asymmetry*, **2003**, *14*, 3173-3176.
76. Kimura, H.; Fujiwara, T.; Katoh, T.; Nishide, K.; Kajimoto, T.; Node, M. *Chem. Pharm. Bull.* **2006**, *54*, 399-402.
77. Koreeda, M.; Brown, L. *J. Org. Chem.* **1983**, *48*, 2122-2124.
78. Moreno-Vargas, A. J.; Schutz, C.; Scopelliti, R.; Vogel, P. *J. Org. Chem.* **2003**, *68*, 5632-5640.
79. Wei, Z.; Petukhov, P. A.; Xiao, Y.; Tuckmantel, W.; George, C.; Kellar, K. J.; Kozikowski, A. P. *J. Med. Chem.* **2003**, *46*, 921-924.
80. Wei, Z.; George, C.; Kozikowski, A. P. *Tetrahedron Lett.* **2003**, *44*, 3847-3850.
81. Marchand, A. P.; Allen, R. W. *Tetrahedron Lett.* **1975**, 67-70.
82. Li, T.; Qian, C.; Eckman, J.; Huang, D. F.; Shen, T. Y. *Bioorg. Med. Chem. Lett.* **1993**, *3*, 2759-2764.
83. Badio, B.; Garraffo, H. M.; Spande, T. F.; Daly, J. W. *Med. Chem. Res.* **1994**, *4*, 440-448.
84. Rang, H. P.; Dale, M. M.; Ritter, J. M. *Pharmacology*; 4 ed.; Churchill Livingstone: London, **1999**.
85. For a review see: Szánty, C.; Kardos-Balogh, Z.; Szánty, C.; *The Alkaloids*,

- Academic Press: New York, **1995**; Vol. 46, p 95.
86. Malpass, J. R.; White, R. *J. Org. Chem.* **2004**, *69*, 5328-5334.
  87. Frazer, M. J.; Gerrard, W.; Machell, G.; Shepherd, B. D. *Chem. Ind.* **1954**, 931-932.
  88. Tanaka, A.; Oritani, T. *Tetrahedron Lett*, **1997**, *38*, 1955-1955.
  89. Manna, S.; Falck, J. R. *Synthetic Communications*, **1985**, *15*, 663-668.
  90. Mondal, M.; Argade, P. *Tetrahedron Lett*, **2004**, *45*, 5693-5695.
  91. Jung, J.; Kache, R.; Vines, K. K.; Zheng, Y.; Bijoy, P.; Valluri, M.; Avery, M. A. *J. Org. Chem.* **2004**, *69*, 9269-9284.
  92. Wong, T. C; Collazo, L. R.; Guziec, F. S. *Tetrahedron*, **1995**, *51*, 649-656.
  93. Williams, D. H.; Fleming, I. *Spectroscopic Methods in Organic Chemistry*, McGraw-Hill, London, **1980**.
  94. Belkacemi, D. Ph.D. thesis, University of Leicester, **1991**.
  95. Witanowski, M.; Stefaniak, L.; Webb, G. A. *Nitrogen NMR Spectroscopy in Annual Reports on NMR Spectroscopy; Vol. 11B*, Academic Press, London, **1981**.
  96. Martin, M. L.; Martin, G. J.; Gouesnard, J. P. *NMR Basic Principles and Progress*. **1981**, *18*, 1.
  97. Witanowski, M.; Stefaniak, L.; Webb, G. A. *Nitrogen NMR Spectroscopy in Annual Reports on NMR Spectroscopy; Vol 18*, Academic Press, London, **1986**.
  98. Witanowski, M.; Stefaniak, L.; Webb, G. A. *Nitrogen NMR Spectroscopy in Annual Reports on NMR Spectroscopy; Vol 18*, Academic Press, London, **1986**, p. 234.
  99. Witanowski, M.; Stefaniak, L.; Webb, G. A. *Nitrogen NMR Spectroscopy in Annual Reports on NMR Spectroscopy; Vol. 11B*, Academic Press, London, **1981**, p. 232.
  100. Christl, M.; Herbert, R. *Org. Magn. Reson.* **1979**, *12*, 150-152.
  101. Davies, J. W. Ph.D. thesis, University of Leicester, **1985**.
  102. Wiberg, K. B. *Tetrahedron Lett.* **1985**, *26*, 599-602.
  103. Jackman, L. M.; Sternhell, S. *Applications of Nuclear Magnetic Resonance Spectroscopy*, Pergamon Press, Oxford, 2<sup>nd</sup> edn., **1969**, 334-336.
  104. Bovey, F. A. *Nuclear Magnetic Resonance Spectroscopy*, Academic Press, New York, **1972**.
  105. Eigen, M. *Angew. Chem. Internat. Edn.* **1964**, *3*, 1.
  106. Mckenna, J. *Tetrahedron*, **1974**, *30*, 1555-1562.

107. Blazejewski, J. C.; Cantacuzene, D.; Wakselman, C. *Tetrahedron Lett.* **1975**, 363-366.
108. Crowley, P. J.; Robinson, M. J. T.; Ward, M. G. *J. Chem. Soc. Chem. Commun.* **1974**, 825-826.
109. Durrant, M. L. Ph.D. thesis, University of Leicester, **1982**.
110. Pc Spartan Pro Ab-Initio Program: (Pc/x86) 6.0.6, Aug 16, 2000.
111. Nelsen, S. F.; Hollinsed, W. C. *J. Org. Chem.* **1980**, *45*, 3609-3613.
112. Harris, R. K.; Becker, E. D.; Cabral De Menezes, S. M.; Goodfellow, R.; Granger, P. *Pure Appl. Chem.* **2001**, *73*, 1795-1818.
113. Chen, Z.; Trudell, M. L. *Synthetic Communications*, **1994**, *21*, 3149-3155.
114. Hodgson, D. M.; Bebbington, W. P.; Willis, P. *Chem. Commun.* **2001**, 889-890.
115. Davis, C. R.; Johnson, R. O.; Cialdella, J. I.; Liggett, W. F.; Mizesak, S. A.; Marshall, V. P. *J. Org. Chem.* **1997**, *62*, 2244-2251.
116. Kabalka, G. W.; Varma, M.; Varma, R. S. *J. Org. Chem.* **1986**, *51*, 2386-2388.